



HAL
open science

Towards new approaches for the generation of phosphorus based radical: synthetic and mechanistic investigations

Giovanni Fausti

► **To cite this version:**

Giovanni Fausti. Towards new approaches for the generation of phosphorus based radical: synthetic and mechanistic investigations. Organic chemistry. Normandie Université, 2017. English. NNT: 2017NORMC271 . tel-01893162

HAL Id: tel-01893162

<https://theses.hal.science/tel-01893162>

Submitted on 11 Oct 2018

HAL is a multi-disciplinary open access archive for the deposit and dissemination of scientific research documents, whether they are published or not. The documents may come from teaching and research institutions in France or abroad, or from public or private research centers.

L'archive ouverte pluridisciplinaire **HAL**, est destinée au dépôt et à la diffusion de documents scientifiques de niveau recherche, publiés ou non, émanant des établissements d'enseignement et de recherche français ou étrangers, des laboratoires publics ou privés.



Normandie Université

THÈSE

Pour obtenir le diplôme de doctorat

Spécialité CHIMIE

Préparé au sein de l'Université de Caen Normandie

Towards new approaches for the generation of phosphorus based radical : synthetic and mechanistic investigations

Présentée et soutenue par
Giovanni FAUSTI

**Thèse soutenue publiquement le 24/07/2017
devant le jury composé de**

M. PHILIPPE BELMONT	Professeur des universités, UNIVERSITE PARIS 5 UNIVERSITE PARIS DESC	Rapporteur du jury
Mme GHENWA BOUHADIR	Maître de conférences HDR, UNIVERSITE TOULOUSE 3 PAUL SABATIER	Rapporteur du jury
Mme ISABELLE GILLAIZEAU	Professeur des universités, UNIVERSITE ORLEANS	Président du jury
M. SAMI LADHDAR	Chargé de recherche, UNIVERSITE CAEN NORMANDIE	Membre du jury
Mme ANNIE-CLAUDE GAUMONT	Professeur des universités, UNIVERSITE CAEN NORMANDIE	Directeur de thèse

Thèse dirigée par ANNIE-CLAUDE GAUMONT, Laboratoire de chimie moléculaire et thio-organique (Caen)



UNIVERSITÉ
CAEN
NORMANDIE



Normande de Chimie



TABLE OF CONTENTS

List of tables.....	4
List of figures.....	5
List of schemes.....	7
List of abbreviations.....	11
Abstract.....	13
Acknowledgements.....	14
Chapter 1: General Introduction.....	16
1.1: Phosphorus nomenclature.....	16
1.2: Synthesis of organophosphorus compounds.....	18
1.3: Markovnikov's rule.....	19
1.4: Hydrophosphination.....	21
1.4.1: Metal-catalyzed hydrophosphination.....	22
1.4.2: Organocatalyzed hydrophosphination.....	25
1.5: Visible light photoredox catalysis.....	28
1.5.1: Theoretical background.....	28
1.5.2: The Jablonski diagram.....	32
1.5.3: Selected examples of photoredox catalyzed reactions.....	33
1.5.4: Metal-free photocatalysts.....	37
1.5.5: Acridinium salt as photocatalyst.....	38
1.5.6: Eosin Y as photocatalyst.....	43
1.5.7: Carbon-phosphorus bond forming photocatalyzed	45
reactions.....	
1.6: Goal of the thesis.....	54
Chapter 2: Visible light mediated hydrophosphinylation reaction.....	56
2.1: General context.....	56
2.2: Anti-Markovnikov alkene functionalizations.....	56
2.2.1: Alkenes as challenging substrates.....	56
2.3: Hydrophosphinylation reaction with phosphinic acid	64
derivatives.....	
2.3.1: Hypophosphorus derivatives.....	64
2.3.2: Hydrophosphinylation reaction.....	66
2.3.3: Metal-catalyzed hydrophosphinylation.....	67
2.3.4: Triethylborane and radical initiators-assisted	68
hydrophosphinylation.....	
2.4: Results and discussion.....	71
2.4.1: Our photocatalytic approach.....	71
2.4.2: Optimization studies.....	72
2.4.3: Scope and limitations of the hydrophosphinylation	74
reaction.....	
2.4.4: Mechanistic studies.....	77
2.5: Conclusions.....	86
2.6: Material and methods.....	87
2.6.1: General.....	87
2.6.2: EPR-ST, Fluorescence and Laser Flash Photolysis	88

experiments.....	89
2.7: Anti-Markovnikov hydrophosphinylation reaction.....	89
2.7.1: General procedure.....	89
Chapter 3: Generation of Phosphinoyl Radicals through EDA complexes and their Reactivity towards Unactivated Alkenes.....	103
3.1: Background.....	103
3.2: Theoretical background for electron-donor acceptor (EDA) complexes.....	109
3.2.1: General scenario.....	109
3.2.2: Photogeneration of radical donor-acceptor (EDA) species and related contributions.....	111
3.3: The phosphonoyl radical and hydrophosphinylation reaction.....	115
3.3.1: General overview.....	115
3.4: Results and discussion.....	118
3.4.1: Mechanistic investigations.....	118
3.4.2: Optimization studies.....	124
3.4.3: Mechanistic proposal for the photocatalytic approach.....	127
3.5: Conclusions.....	129
3.6: Material and methods.....	130
3.6.1: General.....	130
3.7: Hydrophosphinylation reaction products.....	132
3.7.1: General procedure.....	132
Chapter 4: Photocatalyzed Annulation Reaction for the Formation of Phosphorylated Oxindoles.....	143
4.1: Background.....	143
4.2: Oxindoles, cyclic isatin derivatives frameworks.....	146
4.2.1: Bioactive pharmaceutical compounds.....	146
4.2.2: Synthetic pathways to access to C-3 functionalized oxindoles from isatin derivatives.....	149
4.2.3: Synthetic pathways to access to C-3 functionalized oxindoles from <i>N</i> -acrylamides.....	151
4.2.3.1: Metal-catalyzed annulation reaction.....	151
4.2.3.2: Metal-free photoinduced annulation reaction.....	154
4.3: Results and discussion.....	161
4.3.1: Mechanistic studies.....	164
4.4: Conclusions.....	166
4.5: Material and methods.....	167
4.5.1: General.....	167
4.6: Annulation reaction to form phosphorylated oxindoles.....	168
4.6.1: General procedure.....	168
General conclusions.....	179

LIST OF TABLES

Table 2.1: Identification of the optimal reaction conditions.....	73
Table 2.2: Scope and limitations of visible light mediated hydrophosphinylation...	74
Table 3.1: Different meanings of electron-donor (D) and electron-acceptor (A).....	111
Table 3.2: Optimization studies for the hydrophosphinylation of alkenes <i>via</i> EDA-complexes activation	125
Table 3.3: Scope and limitations of hydrophosphinylation reaction.....	127
Table 4.1: Identification of the optimal reaction conditions.....	162
Table 4.2: Scope and limitations of the photocatalyzed annulation reaction of <i>N</i> -arylacrylamides with secondary phosphine oxides.....	164

LIST OF FIGURES AND CHARTS

Figure 1.1: Energy diagram related to the addition of H–X to alkenes.....	21
Figure 1.2: Proposed transition-state for thiourea-catalyzed hydrophosphination of nitroalkenes.....	27
Figure 1.3: The solar spectrum.....	29
Figure 1.4: Graphic illustration of the electron multiplicity of the excited state after light excitation.....	30
Figure 1.5: Common organic and inorganic more common oxidants and their oxidizing capabilities (in MeCN vs. SCE).....	31
Figure 1.6: The Jablonski diagram and possible scenarios with absorption, fluorescence, internal conversion, intersystem crossing and phosphorescence.....	32
Figure 1.7: Most commonly used metal-based photoredox catalysts.....	34
Figure 1.8: The X-ray structure shows the dihedral perpendicular angle between acridinium and mesityl moieties; HOMO and LUMO calculated by DFT method at B3LYP/6-31G (taken from ref. [46]).....	40
Figure 2.1: Hypophosphorus derivatives as versatile substrates for the synthesis of a variety of organophosphorus derivatives.....	66
Figure 2.2: Different examples of phosphorylated drugs containing hypophosphorus acid derivatives.....	67
Figure 2.3: Selected photooxidant for our hydrophosphinylation reaction.....	72
Figure 2.4: ¹ H-NMR spectrum showed the formation of only <i>anti</i> -Markovnikov or b-adduct.....	76
Figure 2.5: ¹ H-NMR spectrum showed that traces of a bis-adduct were formed by hydrophosphonylation reaction.....	77
Figure 2.6: Different pathways of reactivity between excited state (M [*]) of a molecule and a quencher (Q).....	78
Figure 2.7: Fluorescence spectra (λ _{Ex} = 430 nm) of acetonitrile solutions of <i>N</i> -methyl-9-mesityl acridinium photocatalyst ([Mes-Acr] = 5 × 10 ⁻⁶ M) containing increasing concentrations of iodonium triflate at 20°C.....	78
Figure 2.8: Stern-Volmer quenching constant for the reaction of the excited state of Mes-Acr with diphenyliodonium triflate in MeCN.	79
Figure 2.9: Photolysis of acetonitrile solutions of the photocatalyst with diphenyliodonium 73 upon irradiation (LED @ λ _{max} = 420 nm; from t = 0 to 540 s)	80
Figure 2.10: EPR spin-trapping spectra resulting upon irradiation (λ = 420 nm) of a solution of acridinium salt (Mes-Acr) and diphenyliodonium 73 in the presence of PBN I in <i>tert</i> -butylbenzene at room temperature.....	81
Figure 2.11: EPR spin-trapping spectra resulting upon irradiation (λ = 420 nm) of acridinium Mes-Acr /diphenyliodonium 73 solution in the presence of butyl phosphinate 58b and PBN I in toluene at room temperature.....	82
Figure 2.12: ¹ H-NMR spectrum showed the formation of benzaldehyde 76 and traces of benzoic acid 77	82
Figure 2.13: General mechanism for oxidative photoredox reactions.....	84
Figure 3.1: Bond Dissociation Energy (BDE) of most common organophosphorus compounds.....	104

Figure 3.2: Graphic illustration of phosphorus based radicals with high pyrimidalization.....	105
Figure 3.3: Formation of phosphinoyl radical <i>via</i> different activation modes.....	106
Figure 3.4: a) 4- <i>N,N</i> -trimethylaniline in solution exhibits any colour, it means any absorption below 380 nm. b) <i>N,N</i> -trimethylamine and diaryliodonium salt mixed in DCM. c) Diaryliodonium salt in DCM.	119
Figure 3.5: UV-Vis absorption spectrum of 4- <i>N,N</i> -trimethylaniline (4- <i>N,N</i> -TMA, black), 4- <i>N,N</i> -trimethylaniline and diphenyliodonium (red) and diphenyliodonium (Iod, blue) (spectrum taken from ref. [30]).	120
Figure 3.6: EDA-complex structures of three possible interactions between $\text{Ph}_2\text{I}^+/\text{Ph}_2\text{P}(\text{O})\text{H}$	120
Figure 3.7: UV-Vis spectra of different EDA-complexes calculated by TP-DFT....	122
Figure 3.8: ROESY-NMR spectrum of an equimolar mixture of SPO and Ph_2I^+ in dichloromethane at -15 °C.	123
Figure 3.9: EPR-spin trapping spectra for the reaction between diphenyliodonium triflate 73 and diphenylphosphine oxide 46a in the presence of PBN I in <i>tert</i> -butylbenzene at room temperature.....	124
Figure 3.10: EPR-spin trapping spectra for the reaction between diphenyliodonium triflate 73 and excess of diphenylphosphine oxide 46a in the presence of PBN I	125
Figure 4.1: Isatin or 1H-indole-2,3-dione.....	144
Figure 4.2: General structure of oxindoles (indolin-2-one).....	147
Figure 4.3: Some examples of bioactive molecules possessing 2-oxindole moiety (red).....	148
Figure 4.4: Motif of general structure (102); GW5074 (103), potent inhibitor of neurodegeneration.	149
Figure 4.5: Esermethole (R = Me) is an intermediate of the synthesis of Physostigmine (R= CONHMe), reversible natural alkaloid cholinesterase inhibitor.....	153
Chart 1.1: Nomenclature of trivalent (P(III)) organophosphorus compounds.....	18
Chart 1.2: Nomenclature of trivalent (P(V)) organophosphorus compounds.....	19
Chart 1.3: Electrochemical and photophysical properties of the excited states of some common metal-free photocatalysts.....	38
Chart 2.1: Oxidation potentials measured in MeCN vs. SCE of various functionalized alkenes.....	57
Chart 2.2: Comparison of some reduction potentials to some common alkene oxidation potentials.....	59

LIST OF SCHEMES

Scheme 1.1: <i>i)</i> Synthesis of <i>P</i> -stereogenic phosphines using menthylphosphinite borane diastereoisomers. <i>ii)</i> Alkylation reaction of resolved <i>tert</i> -butylphenylphosphine borane. <i>iii)</i> Pt-catalyzed asymmetric hydrophosphination..	19
Scheme 1.2: Mechanisms for the formation of Markovnikov and <i>anti</i> -Markovnikov adducts.	21
Scheme 1.3: <i>i)</i> Microwave-, <i>ii)</i> radical initiator- and <i>iii)</i> UV-induced hydrophosphination reaction.....	22
Scheme 1.4: Nickel catalyzed asymmetric hydrophosphination of methacrylonitrile.....	23
Scheme 1.5: Proposed catalytic cycle for Nickel-catalyzed hydrophosphination of nitriles.	24
Scheme 1.6: Iron-catalyzed hydrophosphination of alkenes with secondary phosphines.....	24
Scheme 1.7: Proposed mechanism for the iron-catalyzed Markovnikov hydrophosphination of styrenes.....	25
Scheme 1.8: Organocatalytic asymmetric hydrophosphination of nitroalkenes with diphenyl phosphine.....	26
Scheme 1.9: Asymmetric organocatalytic hydrophosphination of α,β -unsaturated aldehydes with diphenyl phosphine.	27
Scheme 1.10: Proposed catalytic cycle for asymmetric organocatalytic hydrophosphination of α,β -unsaturated aldehydes with diphenyl phosphine.....	27
Scheme 1.11: [2 + 2] photocatalyzed cycloaddition of enones.....	34
Scheme 1.12: Direct photocatalyzed α -alkylation of aldehydes.....	35
Scheme 1.13: Direct asymmetric alkylation of aldehydes by merging photocatalysis and organocatalysis in the presence of [Ru]-based photocatalyst.....	36
Scheme 1.14: Photocatalyzed bromination of different functionalized arenes.	40
Scheme 1.15: Photocatalytic bromination of functionalized arenes with the acridinium salt as photocatalyst.....	41
Scheme 1.16: Photocatalyzed intramolecular hydroalkoxylation of alkenols.....	42
Scheme 1.17: Proposed mechanism for the intramolecular hydroalkoxylation..	42
Scheme 1.18: Acid-base behavior of eosin Y.....	43
Scheme 1.19: Eosin Y-catalyzed direct C–H arylation of heteroarenes.....	44
Scheme 1.20: Proposed mechanism for the direct eosin Y-catalyzed direct C–H arylation of heteroarenes.....	45
Scheme 1.21: Photoinduced hydrophosphinylation of alkenes in the absence of photocatalyst.....	46
Scheme 1.22: Oxidative phosphorylation of <i>N</i> -aryl-tetrahydroisoquinilones in the presence of diethyl phosphite and metal-based polypyridyl complexes.....	47
Scheme 1.23: Plausible mechanism for the oxidative phosphorylation of <i>N</i> -aryl-tetrahydroisoquinilones with diethyl phosphite and metal-based polypyridyl complexes.....	47
Scheme 1.24: Nickel-catalyzed phosphorylation of aryl iodides with secondary phosphine oxides.....	48
Scheme 1.25: Proposed dual catalytic mechanism for the phosphorylation of aryl iodides with secondary phosphine oxides.	48
Scheme 1.26: Gold-based oxidative P-arylation of H-phosphonate with	49

aryldiazonium salts under photoredox conditions.....	50
Scheme 1.27: Photocatalytic C–Br activation with Rhodamine 6G as photocatalyst and DIPEA as sacrificial electron donor; phosphonylated active pharmaceutical compounds: bromazepam (<i>left</i>) and nicergoline (<i>right</i>).....	51
Scheme 1.28: Proposed mechanism for the photocatalytic aryl phosphonates forming reaction <i>via</i> C–Br activation.....	52
Scheme 1.29: Metal-free visible light mediated photocatalyzed hydrophosphinylation of unactivated alkenes.....	53
Scheme 1.30: Plausible mechanism for the hydrophosphinylation of unactivated alkenes with secondary phosphine oxides.	54
Scheme 1.31: Visible light mediated hydrophosphinylation of alkenes employing ethyl and butyl phosphinates.....	54
Scheme 1.32: Charge-transfer complex based photoinduced hydrophosphinylation of alkenes with secondary phosphine oxides.....	55
Scheme 1.33: Visible light mediated phosphorylation of <i>N</i> -arylacrylamides with secondary phosphine oxides.....	57
Scheme 2.1: Mechanism explaining the regioselectivity for the formation of <i>anti</i> -Markovnikov adducts.....	59
Scheme 2.2: Photocatalyzed <i>anti</i> -Markovnikov addition of carboxylic acids to alkenes in the presence of hydrogen atom-donors.	60
Scheme 2.3: Proposed photocatalyzed mechanism for <i>anti</i> -Markovnikov addition of carboxylic acids to alkenes.....	61
Scheme 2.4: Visible light mediated intramolecular hydroamination of aryl olefins with Iridium-based photocatalyst.....	62
Scheme 2.5: Proposed catalytic cycle for the intramolecular hydroamination of aryl olefins.....	63
Scheme 2.6: Visible-light photocatalytic hydrothiolation of alkenes with ruthenium-based photocatalyst.....	64
Scheme 2.7: Proposed mechanism for the catalytic visible light mediated hydrothiolation of alkenes.....	64
Scheme 2.8: Tautomeric equilibrium of phosphinic acid derivatives between P(V) and P(III) forms.....	67
Scheme 2.9: Palladium catalyzed hydrophosphinylation of unsaturated alkenes and alkynes with hypophosphorus derivatives.....	68
Scheme 2.10: Proposed mechanistic pathway for the palladium-catalyzed hydrophosphinylation reaction.....	69
Scheme 2.11: Triethylborane-initiated hydrophosphinylation of terminal alkenes with hypophosphorus salts.....	69
Scheme 2.12: Triethylborane-initiated hydrophosphinylation of terminal alkenes with hypophosphorus salts.	70
Scheme 2.13: The formation of phosphinoyl radical by means of the use of an organic oxidant.	73
Scheme 2.14: Synthesis of ethyl and butyl phosphinates.....	82
Scheme 2.15: Visible light mediated oxidation of benzylic sp ³ C–H to methyl esters and plausible mechanism.	85
Scheme 2.16: Proposed mechanism for the visible light mediated hydrophosphinylation of phosphinates 66a,b with terminal unactivated alkenes 67 in the presence of 9-mesityl-10-methylacridinium perchlorate (Mes-Acr) as a photocatalyst and diphenyliodonium triflate 85 as external oxidant.....	106
Scheme 3.1: Visible-light mediated formation of phosphinoyl radical in the	

presence of eosin Y as photocatalyst.	107
Scheme 3.2: Photoredox-mediated phosphines arylation reaction <i>via</i> EDA complexes formation.	107
Scheme 3.3: Mechanism of photoredox-mediated phosphine arylation <i>via</i> EDA complexes formation.	108
Scheme 3.4: Plausible phosphine arylation mechanism <i>via</i> electron donor-acceptor complex formation.	109
Scheme 3.5: Two alternatives to form phosphinoyl radical.	109
Scheme 3.6: General mechanism of SET reaction induced by a photocatalyst.	110
Scheme 3.7: General mechanism of SET reaction EDA-induced.	110
Scheme 3.8: Possible pathways for irradiated donor-acceptor complexes.	112
Scheme 3.9: Two pathways to explain electron transfer mechanism.	113
Scheme 3.10: Catalytic asymmetric photochemical α -alkylation of aldehydes with alkyl bromides.	114
Scheme 3.11: Proposed mechanism for asymmetric catalytic photochemical α -alkylation of aldehydes.	115
Scheme 3.12: Tautomeric equilibrium between P(V) and P(III) form of secondary phosphine oxides.	116
Scheme 3.13: Air-induced addition of secondary phosphine oxides to alkenes.	117
Scheme 3.14: Proposed mechanism for air-induced radical addition of secondary phosphine oxides to alkenes.	117
Scheme 3.15: Different examples of C–P bond forming reaction <i>via</i> EDA complexes activation.	118
Scheme 3.16: DFT calculated energies for three possible EDA complexes between $\text{Ph}_2\text{I}^+/\text{Ph}_2\text{P}(\text{O})\text{H}$	121
Scheme 3.17: Generation of the aryl radical through illumination of the EDA complex 93 with blue light.	123
Scheme 3.18: EPR spin-adduct II observation upon irradiation ($\lambda = 450 \text{ nm}$) of a solution of diphenylphosphine oxide 46a and diphenyliodonium triflate 73 in the presence of PBN I in <i>tert</i> -butylbenzene at room temperature.	124
Scheme 3.19: Proposed mechanism for our hydrophosphinylation of unactivated alkenes <i>via</i> EDA-complexes.	129
Scheme 3.20: Regioselective hydrophosphination reaction of unactivated alkenes with aryl secondary phosphine oxides.	130
Scheme 4.1: Reactivity of isatin and its derivatives and different synthetic pathways.	146
Scheme 4.2: One-pot procedure for the formation of 3-alkyl and 3-(ω -hydroxyalkyl)oxindoles from isatins and aldehydes/ketones.	150
Scheme 4.3: Plausible mechanism for the alkylation of isatin with aldehydes/ketones.	151
Scheme 4.4: Nitro-aldol reaction of isatin with nitromethane in the presence of diethylamine as catalyst.	152
Scheme 4.5: Metal-catalyzed domino Heck-cyanation reaction of iodo-substituted arylacrylamides.	153
Scheme 4.6: Plausible mechanism for the domino Heck-cyanation of iodo-substituted arylacrylamides.	154
Scheme 4.7: Copper-catalyzed annulation reaction of <i>N</i> -arylacrylamides with	154

chloroform.....	
Scheme 4.8: Proposed mechanism for the copper-catalyzed annulation reaction of <i>N</i> -arylacrylamides with chloroform.....	155
Scheme 4.9: Visible light-mediated radical trifluoromethylation reaction of <i>N</i> -arylacrylamides.....	156
Scheme 4.10: Proposed mechanism for tandem radical cyclization reaction of <i>N</i> -arylacrylamides with fluorinated agents.....	157
Scheme 4.11: Visible light photocatalytic functionalization of <i>N</i> -arylacrylamides with arylsulfonic acids under mild conditions.....	157
Scheme 4.12: The proposed reaction mechanism for the visible-light photoinduced functionalization of <i>N</i> -arylacrylamides with arylsulfonic acids.	158
Scheme 4.13: Visible-light induced radical addition of diphenylphosphine oxide to <i>N</i> -arylacrylamides <i>via</i> C–P bond formation.....	159
Scheme 4.14: Silver catalyzed phosphorylation of arylacrylamides with secondary phosphine oxides and phosphites.....	159
Scheme 4.15: Proposed mechanism for silver-catalyzed phosphorylation of <i>N</i> -arylacrylamides with phosphine oxides and phosphites.....	160
Scheme 4.16: Visible light photocatalyzed synthesis of benzo[<i>b</i>]phosphole oxides.....	161
Scheme 4.17: The charge transfer complex [EY-Pyr] can be reduced under light irradiation.....	161
Scheme 4.18: Proposed mechanism for the photocatalyzed annulation reaction of <i>N</i> -arylacrylamides with secondary phosphine oxides.....	165

LIST OF ABBREVIATIONS

AHP	Anilinium hypophosphite
AIBN	Azobisisobutyronitrile
ATP	Adenosine Tri-Phosphate
BDE	Bond Dissociation Energy
Bn	Benzyl substituent
CFL	Compact Fluorescent bulb Light
CT	Charge Transfer
δ	Chemical Shift
DFT	Density Functional Theory
DMF	<i>N,N</i> -Dimethylformamide
DMSO	Dimethylsulfoxide
<i>ee</i>	Enantiomeric excess
EDA	Electron Donor-Acceptor
EPR	Electron Paramagnetic Resonance
Et₂O	Diethyl ether
<i>F</i>	Faraday constant
FC	Flash Chromatography
HOMO	Highest occupied molecular orbital
HRMS	High Resolution Mass Spectroscopy
iPrOH	Isopropyl alcohol
LEDs	Light Emitting Diodes
LUMO	Lowest unoccupied molecular orbital
MeCN	Acetonitrile

Mes-Acr	9-mesityl-10-methylacridinium
NHE	Normal Hydrogen Electrode
NMR	Nuclear Magnetic Resonance
Nu	Nucleophile
PBN	α -phenyl- <i>N-tert</i> -butylnitron
Ph	Phenyl substituent
pK_a	Decimal logarithm of hydronium ion concentration
RTK	Receptor Tyrosine Kinase
SET	Single Electron Transfer
SCE	Saturated Calomel Electrode
<i>t</i>Bu	<i>tert</i> -Butyl substituent
TLC	Thin Layer Chromatography
Triflate	Trifluoromethylsulfonate
UV	Ultra-Violet
UV-Vis	Ultra-Violet Visible

ABSTRACT

This Thesis reports three complimentary modes of activation for the generation of phosphorus based radicals, which have been employed for the synthesis of organophosphorus compounds.

We have first described a photocatalytic generation phosphinoyl radicals by using the acridinium salt, 9-mesityl-10-methylacridinium perchlorate known as Fukuzumi' catalyst, as a photocatalyst and diphenyliodonium triflate as an external photooxidant. This purely organic system allowed us to achieve the first metal-free hydrophosphinylation of alkenes. Several mechanistic investigations, such as Electron Paramagnetic Resonance (EPR), Laser Flash Photolysis, fluorescence quenching and quantum yields measurements have been employed to understand factors governing this photoreaction.

In the subsequent chapter, the formation of Electron-Donor-Acceptor complexes (EDA) between secondary phosphine oxides and the diphenyliodonium ion has been used to generate phosphinoyl radical under blue irradiation. A combined experimental and theoretical investigations have been used to elucidate the formation of EDA complexes. This strategy has then been employed to describe hydrophosphinylation of alkenes.

The last chapter reports a metal-free visible light mild method for the synthesis of phosphorylated oxindoles, which are potentially active pharmaceutical compounds. Scope and limitations of this approach have been discussed along with preliminary mechanistic investigations.

ACKNOWLEDGEMENTS

This PhD has been carried out in the “Laboratoire de Chimie Moléculaire et Thioorganique” LCMT directed by Prof. Annie–Claude Gaumont. It was under her supervision that I spent 3 months of internship and decided afterwards to join her group as a PhD Student. I would warmly thank her for giving me the opportunity to be part of her group.

Special thanks go to Dr. Sami Lakhdar for his supervision, help and suggestions during the last three years. His guidance was crucial for the completion of my PhD. His demand and drive for the best have pushed me to become a better chemist, and I greatly appreciate everything he has done to help me get to this point. Thanks a lot Sami!

This work would not have been possible without the generous support of the Labex Synorg, which apart from paying my salary allowed me to attend many national and international conferences. I would therefore thank the whole team of Synorg for their great help!

I also warmly thank my thesis reviewers: Dr. Ghenwa Bouhadir (LHFA-Toulouse) and Prof. Philippe Belmont (University of Paris Descartes) for accepting to evaluate this work and to provide critical comments. Furthermore, I would like to thank Prof. Isabelle Gillaizeau (University of Orléans) for her participation in my defense examination.

The collaborations with the groups of Prof. Jacques Lalevée (ISM2–Mulhouse) and Prof. Martin Breugst (University of Köln, Germany) were extremely important for the mechanistic understanding of our photoinduced processes. I wish to thank both of them for their incredible help.

Grand MERCI à Stéphane, Vincent, Jeff, Hashim for many interesting discussions and advices.

Special thanks go to the whole staff of the LCMT, especially the secretary team (Marie-Cecile, Babeth, Catherine and Jeannine), for your assistance during the last three years.

All my thanks to my office mates, I should say to my friends. Thanks Valentin, Jonathan, David, Alex, Ludovik and Alain. I thank you for allowing me to adapt in a new country, new costumes and new language. You all contributed to make my PhD much more agreeable.

Finally, but not at least, I must thank my family.

You never left me alone, THANK YOU.

*A chi ha deciso di seguirmi.
A chi ha deciso di viaggiare nella mia stessa direzione.
A te, Pau.*

General Introduction

Organophosphorus chemistry has become of pre-eminent importance in modern organic chemistry and continues to occupy a central place in numerous fields such as catalysis, material sciences, agrochemistry, and medicinal chemistry. It is therefore unsurprising that development of robust and sustainable approaches toward the synthesis of these compounds presents a central occupation for researchers in both academia and industry. Though this area of research has been dominated by transition metal catalysis and more recently by organocatalysis, little is known about visible light induced C–P bond formation reactions. This thesis attends to contribute to the development of this emerging field by introducing new concepts for mild and metal free synthesis of phosphorus based molecules.

In this chapter, a general introduction about organophosphorus chemistry and some selected contributions in this area as well as in the field of visible light photoredox will be presented and discussed.

1.1. Phosphorus Nomenclature

Before going ahead with phosphorus chemistry, we judge important to present herein a nomenclature based on oxidation states of phosphorus and the number of carbon-phosphorus bonds of phosphorus containing molecules (Chart 1.1 (for P(III) forms and Chart 1.2 (for P(V) forms)).

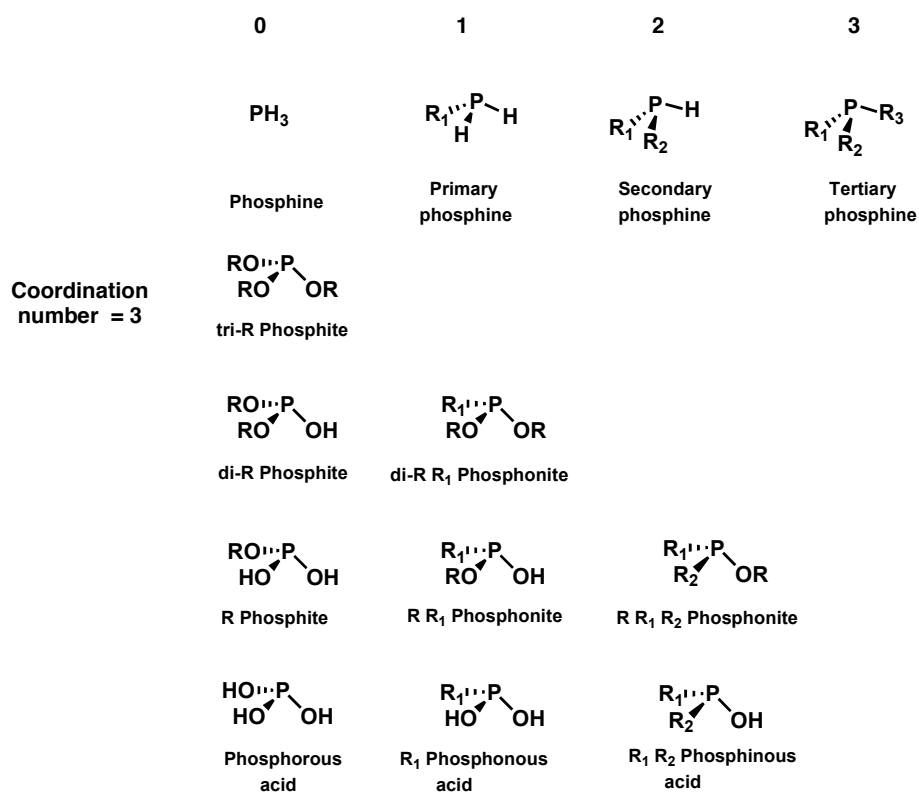


Chart 1.1. Nomenclature of trivalent (P(III)) organophosphorus compounds

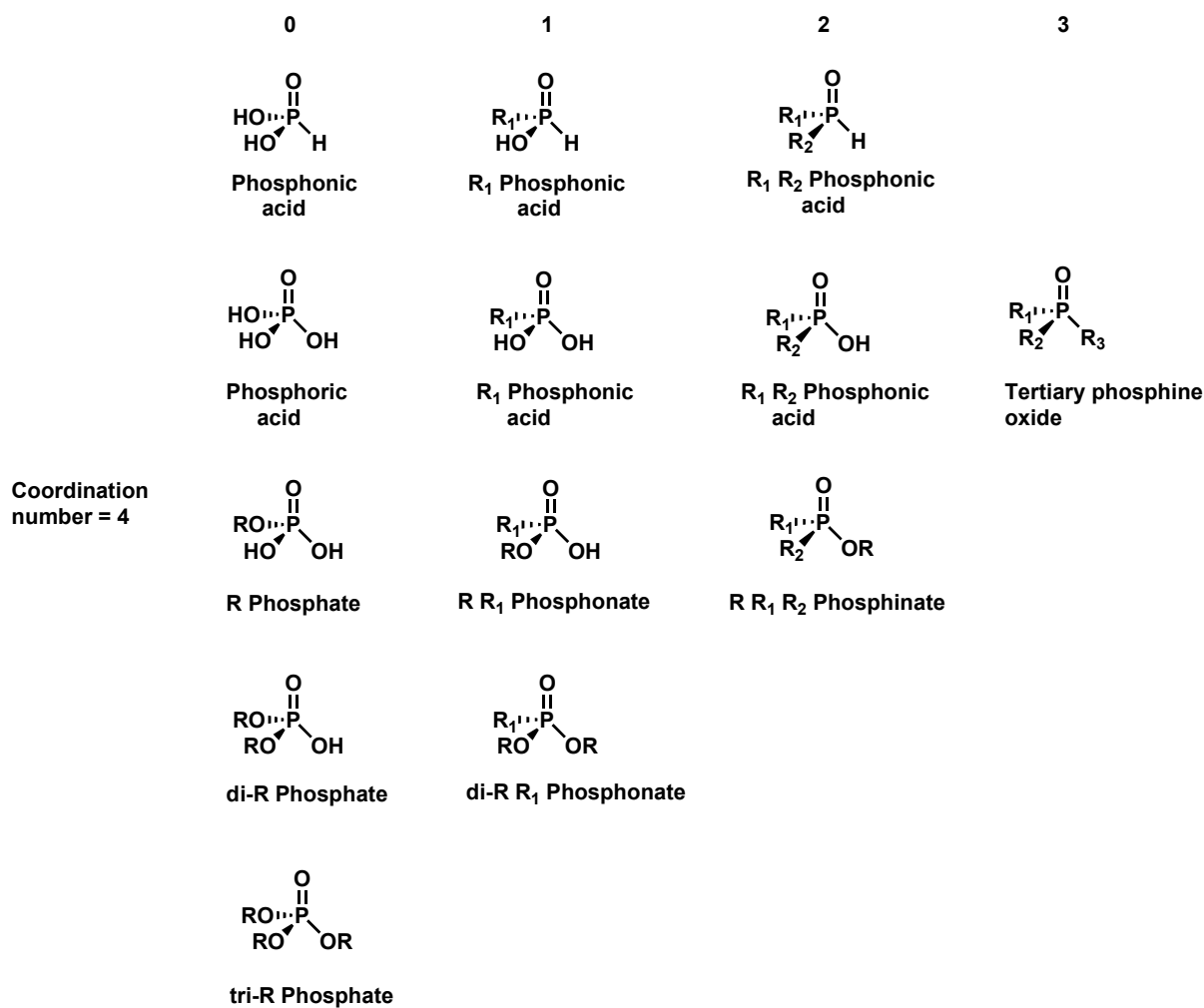
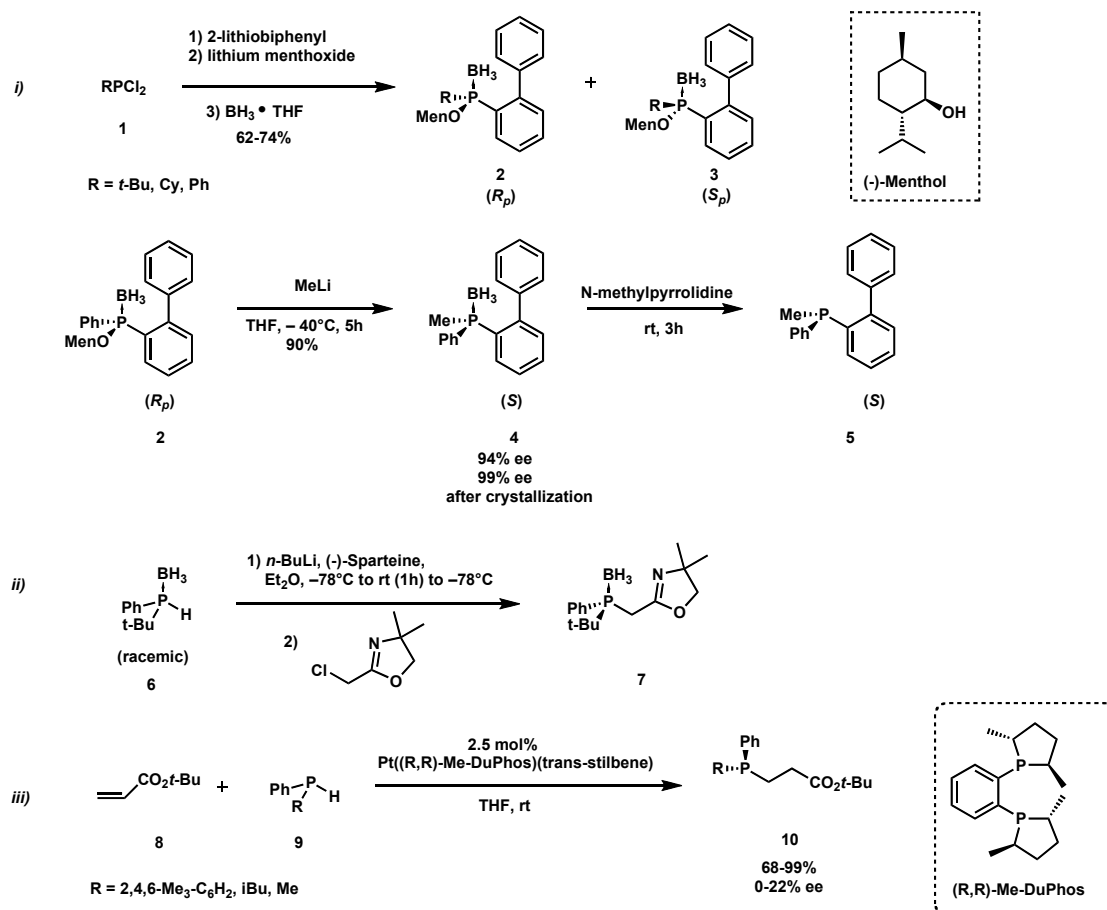


Chart 1.2. Nomenclature of pentavalent (P(V)) organophosphorus compounds

1.2. Synthesis of organophosphorus compounds

The formation of carbon–phosphorus bond can mainly be achieved through three methodologies: *i*) reaction of organometallic compounds with halophosphines, *ii*) reaction of metal phosphides with alkyl halides, and *iii*) hydrophosphination of alkenes and alkynes of secondary phosphines and phosphine oxides (Scheme 1.1).¹

¹ For a comprehensive review on synthesis of organophosphorus, see: Iheany, D.G.; Mitchell, C.M. Preparation of



Scheme 1.1. *i*) Synthesis of *P*-stereogenic phosphines using menthylphosphinite borane diastereoisomers. *ii*) Alkylation reaction of resolved *tert*-butylphenylphosphine borane. *iii*) Pt-catalyzed asymmetric hydrophosphination

While the first two methodologies require the use of strict reaction conditions due to the employment of sensitive organometallic reagents, the last one, which involves the addition of P–H into unsaturated C–C bonds, is known to be atom-economical and in some cases works under mild conditions. As a consequence, interest to this chemistry has grown remarkably and various technologies have been proposed to promote applied efficient and selective hydrophosphinylation reactions.

1.3. Markovnikov's rule

Markovnikov's rule has been developed to explain the outcome of the reactions of HX (X = Cl, Br, I) with unsymmetrical olefins. This hydrohalogenation process *via* the formation of a transient carbocation upon a protonation event. The rule states: “*when a hydro-carbon of unsymmetrical structure combines with a halogen hydroacid, the*

halogen add itself to the less hydrogenated carbon atom, that is, to the carbon atom which is more under the influence of other carbon atoms.”

The observed selectivity has been attributed to the stability of the formed carbocation. As shown in Figure 1.1, the rate-determining step for Markovnikov and *anti*-Markovnikov pathways is that related to the formation of the carbocation. This step is however lower in energy ($\Delta G_1^\ddagger < \Delta G_2^\ddagger$) in the case of the branched carbocation. This is obviously due to the stabilization of this cation through hyperconjugation. In the case of *anti*-Markovnikov pathway, the generated benzylic carbocation (R = Ph) is less stable, which accounts for the observed stability (Figure 1.1).

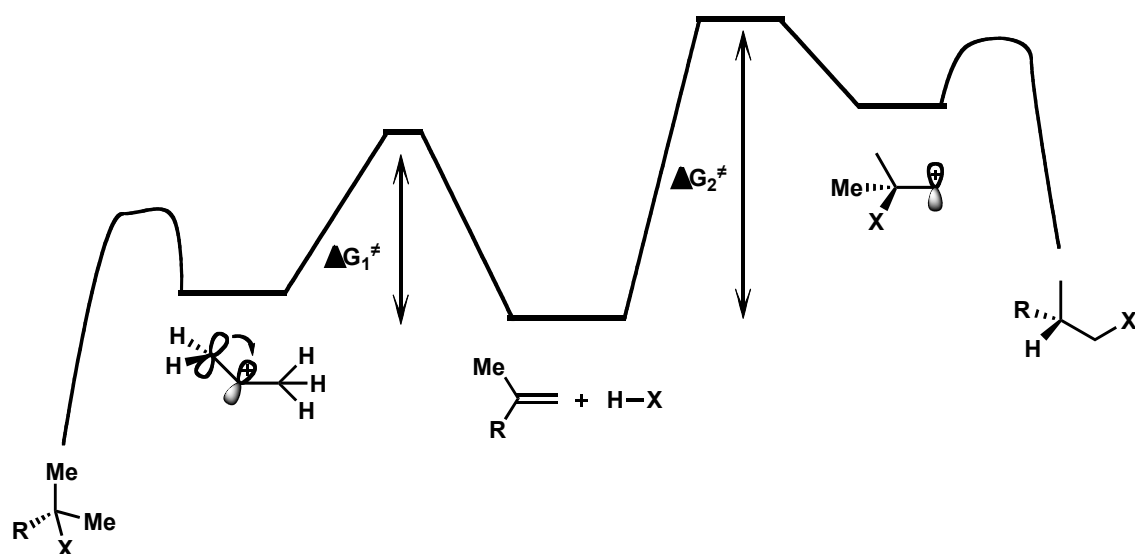
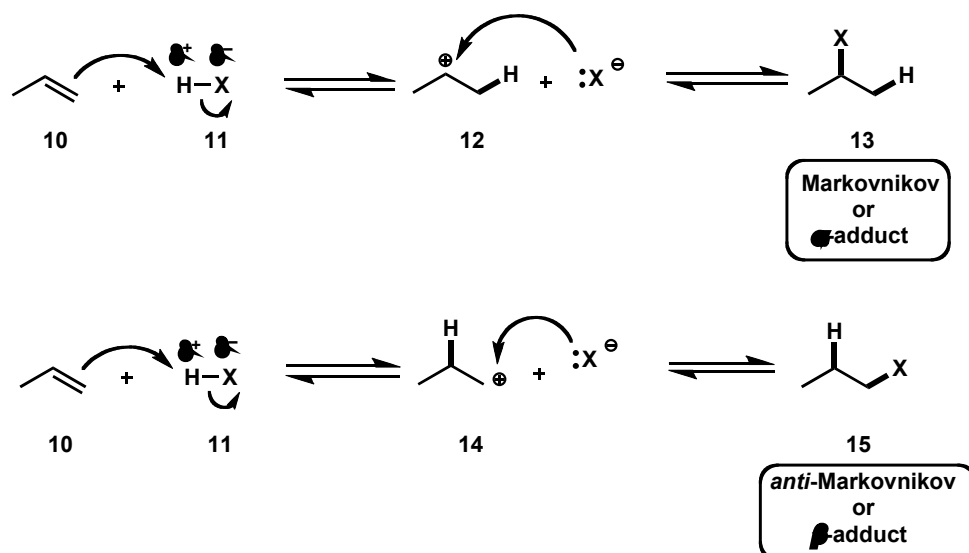


Figure 1.1. Energy diagram related to the addition of H–X to alkenes

As shown in Scheme 1.2, two mechanisms are possible when an alkene reacted with a nucleophile H–X.



Scheme 1.2. Mechanisms for the formation of Markovnikov and *anti*-Markovnikov adducts

The electron pair moves to form a bond between the hydrogen and the right-hand carbon. When the second scenario of the mechanism occurs, and the lone pair on X^- forms a bond with the positive carbon atom, the major product formed is that predicted by the Markovnikov's rule, the major one (Markovnikov adduct, **13**). Alternatively, the β -adduct formed is not the one predicted by the Markovnikov rule. In this way, the minor product is called *anti*-Markovnikov adduct **15**. It is clear from underlying electronic principles that the circumvention of Markovnikov's rule to afford the β -adduct is a major challenge that requires unique and alternative approaches. In this regard many research activities have recently been focused towards this end.

Although numerous efficient heterofunctionalization reactions, using sophisticated activation modes, have recently been reported, this introduction part covers only selected examples in the domain of hydrophosphination reactions.

1.4. Hydrophosphination

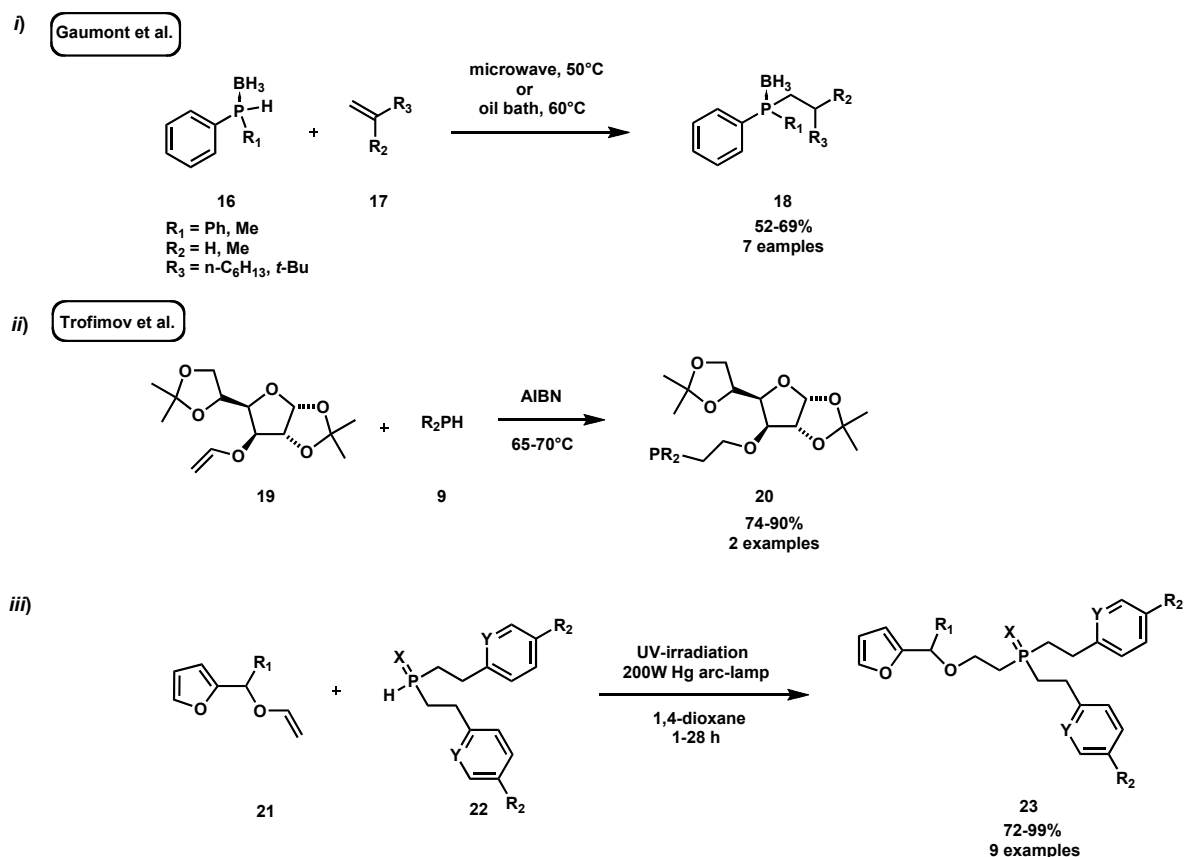
The addition of P-H into unsaturated C-C bonds, known as hydrophosphination reaction, has gained interest as an alternative to the classical phosphine synthesis involving a substitution that is incompatible with some functional groups.

This type of reaction is more efficient than substitution in terms of efficiency and atom economy. The hydrophosphination reaction normally proceeds *via* thermal,² acidic,³

² Mann, F. G.; Millar, I. T. *J. Chem. Soc.* **1952**, 4453–4457.

³ Hoff, M. C.; Hill, P. *J. Org. Chem.* **1959**, *24*, 356–359.

basic⁴ or radical initiation.⁵ Radical addition of phosphines to alkenes can be achieved through the use of radical initiators⁶ or photochemically by irradiation with UV or visible light (Scheme 1.3).⁷



Scheme 1.3. i) Microwave-, ii) radical initiator- and iii) UV-induced hydrophosphination reactions.

1.4.1. Metal-catalyzed hydrophosphination

In the last decades, a remarkable progress has been made in the field of metal-catalyzed hydrophosphination. It has been shown that several metals can act as catalysts for the addition of P-H to unsaturated compounds. The main ones are palladium,⁸ nickel⁹ or

⁴ Bunlaksananusorn, T.; Knochel, P. *Tetrahedron Lett.* **2002**, *43*, 5817–5819.

⁵ Rauhut, M. M.; Currier, H. A.; Semsel, A. M.; Wystrach, V. P. *J. Org. Chem.* **1961**, *26*, 5138–5145.

⁶ (a) Rauhut, M.M.; Currier, H.A.; Semsel, A.M.; Wystrach, V.P. *J. Org. Chem.* **1961**, *26*, 5138-5145. (b) Heesche-Wagner, K.; Mitchell, T.N. *J. Organomet. Chem.* **1994**, *468*, 99-106. (c) Trofimov, B.A.; Sukhov, B.G.; Malysheva, S.F.; Belogorlova, N.A.; Tantsirev, A.P.; Parshina, L.N.; Oparina, L.A.; Tunik, S.P.; Gusarova, N.K. *Tetrahedron Lett.* **2004**, *45*, 9143-9145.

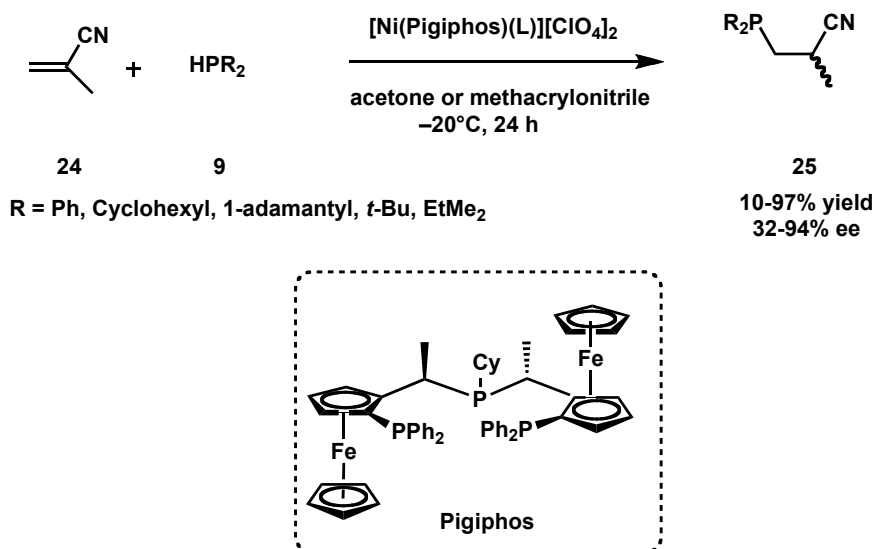
⁷ Oparina, L.A.; Malysheva, S.F.; Gusarova, N.K.; Belogorlova, N.A.; Vysotskaya, O.V.; Stepanov, A.V.; Albanov, A.I.; Trofimov, B.A.; *Synthesis* **2009**, 3427-3432.

⁸ Kazankova, M.A.; Efimova, I.V.; Kotchetkov, A.N.; Afanas'ev, V.V.; Beletskaya, I.P. *Russ. J. Org. Chem.* **2002**, *38*, 1465-1474.

⁹ (a) Shulyupin, M.O.; Kazankova, M.A.; Beletskaya, I.P. *Org. Lett.* **2002**, *4*, 761-763. (b) Kazankova, M.A.; Shulyupin, M.O.; Beletskaya, I.P. *Synlett* **2003**, 2155-2158.

platinum¹⁰ complexes. Less explored catalysts are iron,¹¹ rhodium,¹² copper¹³ and alkaline-earth metals.¹⁴

In this context, the group of Togni has developed the hydrophosphination of vinyl nitriles catalyzed by a dicationic nickel complex, which proceeded through an electrophilic activation of vinyl nitriles (Scheme 1.4).¹⁵



Scheme 1.4. Nickel catalyzed asymmetric hydrophosphination of methacrylonitrile

A plausible mechanism for this process is depicted in Scheme 1.5. The reaction starts with a complexation of the nitrile **24** to the nickel Lewis acid to activate the double bond towards 1,4-addition of the phosphine. Then, a subsequent proton transfer leads to the hydrophosphinated adduct **25** in good yields (up to 97%) and excellent enantioselectivities, up to 94% ee.

¹⁰ (a) Pringle, P.G.; Smith, M.B. *J. Chem. Soc., Chem. Commun.* **1990**, 1701-1702. (b) Wicht, D.K.; Kourkine, I.V.; Lew, B.M.; Nthenge, J.M.; Glueck, D.S. *J. Am. Chem. Soc.* **1997**, *119*, 5039-5040.

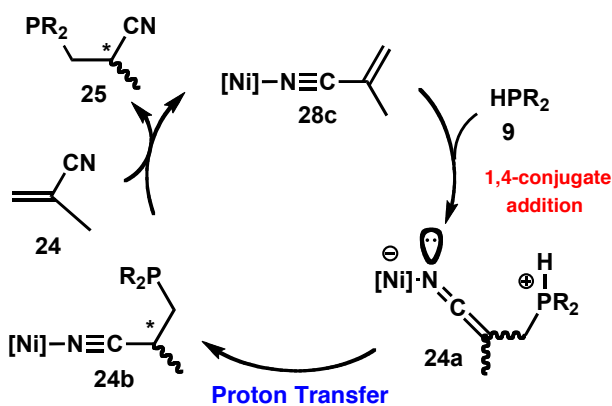
¹¹ (a) Gaumont, A.-C.; Routaboul, L.; Taillefer, M. Method for Synthesizing Phosphine. WO Patent WO2012049424, July 12, **2012**. (b) Routaboul, L.; Toulgat, F.; Gatignol, J.; Lohier, J.-F.; Norah, B.; Delacroix, O.; Alayrac, C.; Taillefer, M.; Gaumont, A.-C. *Chem.-Eur. J.* **2013**, *19*, 8760-8764.

¹² (a) Hayashi, M.; Matsuura, Y.; Watanabe, Y. *J. Org. Chem.* **2006**, *71*, 9248-9251. (b) Trepohl, V.T.; Oestreich, M. *Chem. Commun.* **2007**, 3300-3302.

¹³ Leyva-Pérez, A.; Vidal-Moya, J.A.; Cabrero-Antonino, J.R.; Al-Deyab, S.S.; Al-Resayes, S.I.; Corma, A. *J. Organomet. Chem.* **2011**, *696*, 362-367.

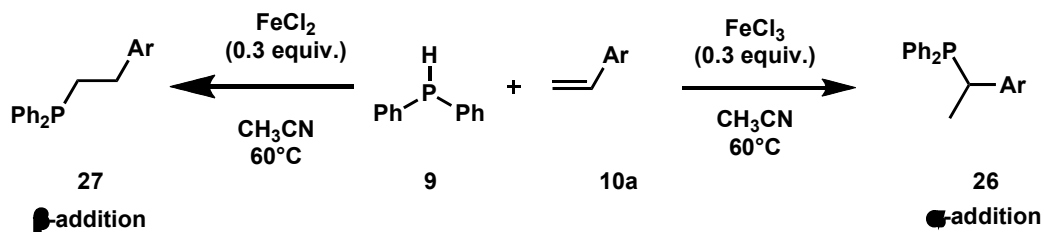
¹⁴ Liu, B.; Roisnel, T.; Carpentier, J.-F.; Sarazin, Y. *Angew. Chem. Int. Ed.* **2012**, *51*, 4943-4946.

¹⁵ (a) Sadow, A.D.; Haller, I.; Fadini, L.; Togni, A. *J. Am. Chem. Soc.* **2004**, *126*, 14704-14705. (b) Sadow, A.D.; Togni, A. *J. Am. Chem. Soc.* **2005**, *127*, 17012-17024.



Scheme 1.5. Proposed catalytic cycle for Nickel-catalyzed hydrophosphination of nitriles

An example of metal-catalyzed hydrophosphination of alkenes with secondary phosphines has recently been reported by our group, by using cheap and environmentally friendly iron salts as catalysts (Scheme 1.6). This approach has the originality of offering a selective access to both regioisomers (α and β -adducts) depending on the oxidation state of the iron catalyst. Compared to other hydrophosphination methodologies,¹⁶ this method offers highly selective access to both α and β -adducts **26** and **27** by selecting the nature of the iron salt (FeCl_3 or FeCl_2 , respectively).

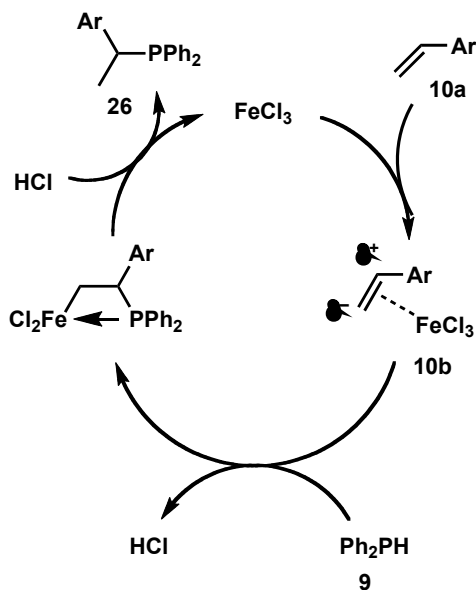


Scheme 1.6. Iron-catalyzed hydrophosphination of alkenes with secondary phosphines

Preliminary investigations revealed that the *anti*-Markovnikov adduct is formed *via* a radical mechanism, where the phosphorus centered radical is formed upon oxidation of the secondary phosphine. The proposed α -adduct mechanism starts with an initial activation of the double bond of the alkenyl arene **10a** by the Lewis acid leading to a polarized π complex **10b**, which is stabilized by electron-donating substituents. Then, the addition of diphenylphosphine **9** followed by protonation of the carbon metal bond

¹⁶ (a) Hoff, M.C.; Hill, P. *J. Org. Chem.* **1959**, *24*, 356-359. (b) Crimmin, M.R.; Barrett, A.G.M.; Hill, M.S.; Hitchcock, P.B.; Procopiou, P.A. *Organometallics* **2008**, *27*, 497-499.

leads to the formation of the final Markovnikov adduct **26** and release of the iron complex for the next catalytic cycle (Scheme 1.7).



Scheme 1.7. Proposed mechanism for the iron-catalyzed Markovnikov hydrophosphination of styrenes

1.4.2. Organocatalyzed hydrophosphination

Because phosphines are known to be good Lewis bases that typically bind to transition metals, those phosphorus nucleophiles or the hydrophosphination adduct can coordinate to the metal, which result in a product inhibition. To overcome part of this limitation, organocatalysis has emerged as a good alternative.

In 2007, Melchiorre and coworkers reported an efficient asymmetric organocatalytic hydrophosphination of nitroalkenes by using diphenyl phosphine and a chiral Cinchona alkaloid/thiourea bifunctional organocatalyst **A** (Scheme 1.8).¹⁷

¹⁷ Bartoli, G.; Bosco, M.; Carlone, A.; Locatelli, M.; Mazzanti, A.; Sambri, L.; Melchiorre, P. *Chem. Commun.* **2007**, 722-724.

As stated earlier, many activation modes have recently emerged as sophisticated and sustainable methods for the formation of C–P bonds. However, many of these approaches suffer either from the use of expensive transition metals or harsh reaction conditions that do not meet green chemistry principles.

During the last few years, visible photoredox catalysis became an appealing method for the synthesis of various organic compounds. While this technology has been applied in different research domains of organic chemistry, it has scarcely been employed in organophosphorus chemistry. The following section aims at providing a general introduction of visible light photoredox chemistry and potential applications in the era of phosphorus chemistry.

1.5. Visible light photoredox catalysis

1.5.1. Theoretical background

Chemists have always been fascinated by the use of visible light to promote organic transformations and the large opportunities that this technology can offer.²¹ In the early 20th century, the observation that sunlight could chemically affect and change organic compounds has conducted photochemists to recognize that the sun could represent an important source of clean energy.²² The most important share of sustainable light source is the visible range ($\lambda = 400\text{--}700\text{ nm}$), in which organic molecules are unable to absorb light (Figure 1.3).

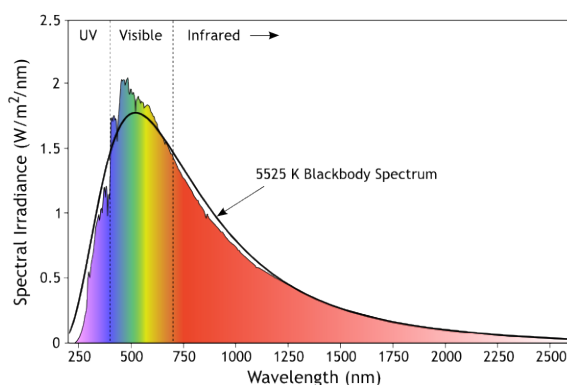


Figure 1.3. The solar spectrum

²¹ a) Prier, C. K.; Rankic, D. A.; MacMillan, D. W. C. *Chem. Rev.* **2013**, *113*, 5322–5363. b) Xuan, J.; Xiao, W.-J. *Angew. Chem., Int. Ed.* **2012**, *51*, 6828–6838. c) Schultz, D. M.; Yoon, T. P. *Science* **2014**, *343*, 985–993. d) Yoon, T. P.; Ischay, M. A.; Du, J. *Nat. Chem.* **2010**, *2*, 527–532.

²² (a) Albinì, A.; Fagnoni, M. *ChemSusChem* **2008**, *1*, 63–66. (b) Roth, H.D. *Angew. Chem. Int. Ed.* **1989**, *28*, 1193–1207.

Over the years, most of chemical transformations were performed by direct excitation of the molecules in the region of near UV-A and UV-B region ($\lambda = 200\text{--}320\text{ nm}$). Regardless, molecules which are unable to absorb light in the region above 320 nm are not excluded by visible light-induced processes. Indeed, there are molecules called *sensitizers* which absorb light in the desired region and transport the photoenergy by light, energy or electron-transfer to the substrate. If the consumed energy for a chemical reaction is covered by the energy of the absorbed light and if the sensitizer is regenerated in its active state, the mechanism is called *photocatalysis* and the sensitizer *photocatalyst*. The photocatalyst is transformed to its *excited state*, which is normally more reactive than its *ground state*, by the absorption of light.

The first important requirement for a molecule to absorb light is that the energy of the photon needs to match the difference between the orbitals ($\Delta E = E_{\text{photon}} = h\nu = hc/\lambda$). Many possible transitions exist to promote an electron from a low-energy occupied to a higher-energy empty orbital, because molecules can have many occupied and empty molecular orbitals.

The transition requiring the lowest-energy photon corresponds to a transition of an electron from the *highest occupied molecular orbital* (HOMO) to the *lowest unoccupied molecular orbital* (LUMO). The HOMO-LUMO energy gap (ΔE) normally determines the color of light we see through a solution.²³

Another important requirement for absorption is that there is no change in electron spin. The highest energy electrons occupy the HOMO, and these electrons are paired with opposite spin ($+\frac{1}{2}$, $-\frac{1}{2}$), so that the total spin of the electrons is $S = 0$ and the multiplicity of the ground state is *singlet*. Excitation with a photon having energy that corresponds to the HOMO-LUMO energy gap would result in a singlet excited state (Figure 1.4).²⁸

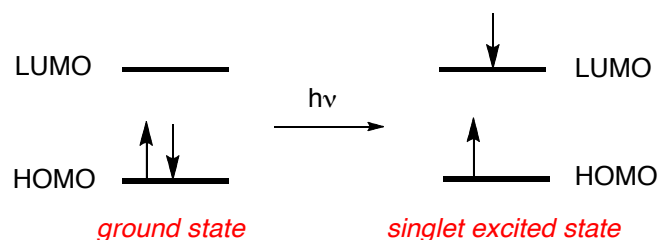


Figure 1.4. Graphic illustration of the electron multiplicity of the excited state after light excitation

²³ P. Klán, J. Wirz, *Photochemistry of Organic Compounds: From Concepts to Practice*, 2009, Wiley-Blackwell, Oxford.

The thermodynamic feasibility of a redox process can be evaluated *via* equation (2), where ΔG is the difference in free energy between an oxidant and a reductant, n is the number of electron exchanged during the process, F is the Faraday constant, E_{red} is the reduction potential of the oxidant and E_{ox} is the oxidation potential of the reductant.

$$\Delta G = -nF(E_{red} - E_{ox}) \quad (2)$$

The reaction is thermodynamically favorable when the equation (2) gives a negative difference in terms of free energy. It means that powerful oxidants possess high reduction potentials and strong reductants possess negative oxidation potentials.

Ground-state one-electron oxidants commonly encountered in organic chemistry are ferrocene,²⁴ iron tris-phenantroline²⁵ and tris-(4-bromophenyl)-aminium hexachloroantimonate (Figure 1.5).²⁶

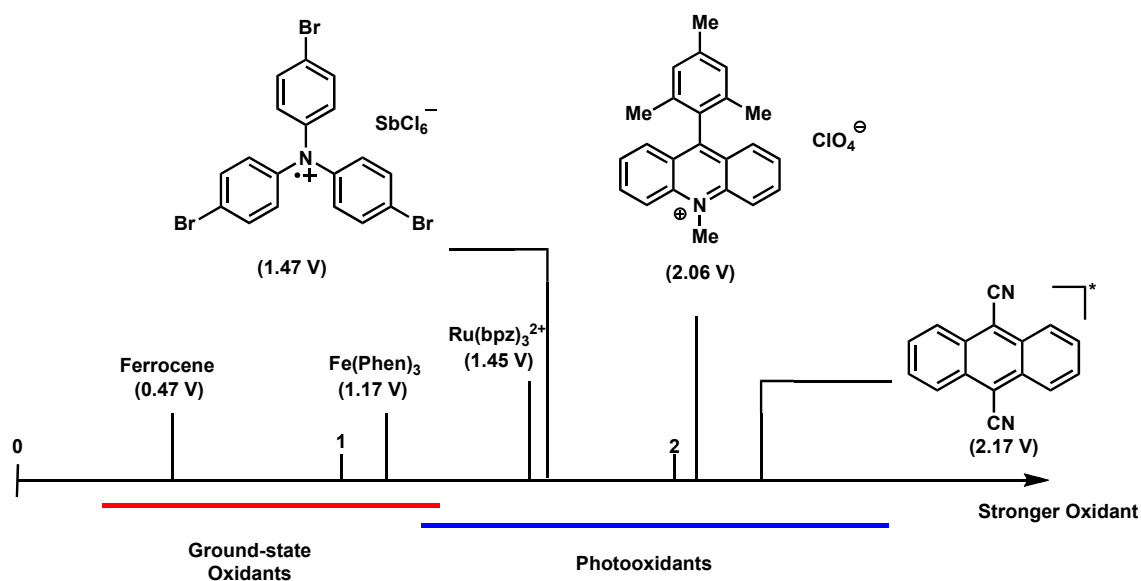


Figure 1.5. Common organic and inorganic oxidants and their oxidizing capabilities (in MeCN vs. SCE)

Figure 1.5 shows that an oxidant on the upper scale is capable to generate radical-cations from substrates to its left. On the other hand, the ground-state oxidants are thermodynamically not capable to perform single electron transfer with common olefins.

²⁴ Batterjee, S.M.; Marzouk, M.I.; Aazab, M.E.; El-Hashash, M.A. *Appl. Organomet. Chem.* **2003**, *17*, 291-334.

²⁵ Schmittel, M.; Ammon, H.; Wöhrle, C. *Chem. Ber.* **1995**, *128*, 845-850.

²⁶ Bauld, N.L.; Stofflebene, G.W.; Lorenz, K.T. *J. Phys. Org. Chem* **1989**, *2*, 585-601.

1.5.2. The Jablonski diagram²⁷

The Jablonski diagram (Figure 1.6) explains the physical principle of photoexcitation, showing electronic states of a molecule and transitions between them.

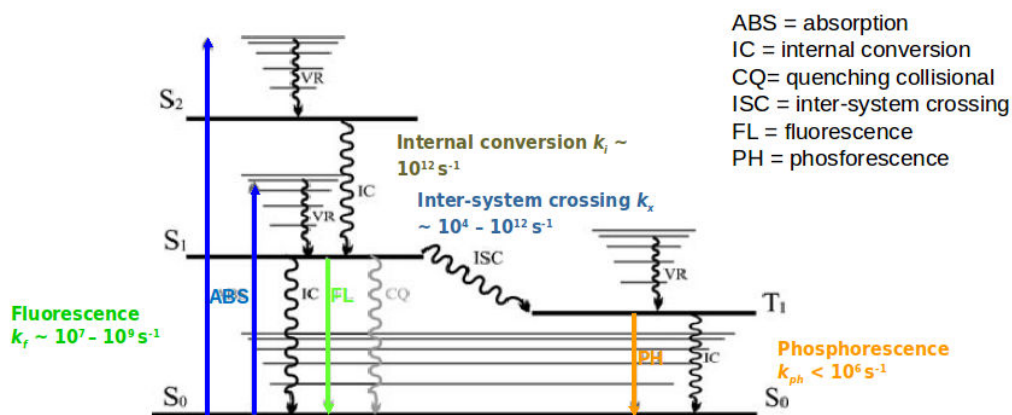


Figure 1.6. The Jablonski diagram and possible scenarios with absorption, fluorescence, internal conversion, intersystem crossing and phosphorescence

What is *absorbance*? It is the process by which an electron is excited from a lower energy level (*ground state*) to a higher energy level (*excited state*). It is a very fast transition, on the order of 10^{-15} seconds. The first transition is the absorbance of a photon of a particular energy, indicated by an arrow pointing up. Once an electron is excited, there are many pathways by which energy can be dissipated. The first one is the *vibrational relaxation*, a non-radiative process indicated in the Jablonski diagram as a curved arrow between the vibrational levels. The energy deposited by the photon into the electron is given away to other vibrational modes as kinetic energy. This kinetic energy can stay in the same molecule, or it can be transferred to other molecules. Also this process is very fast, between 10^{-14} and 10^{-11} seconds. For this reason, it occurs immediately after the absorbance. It can happen that vibrational energy levels strongly overlap electronic energy levels, so that the excited electron can move from a vibrational level in one electronic state to another vibrational level in a lower electronic state. This process is called *internal conversion* and mechanistically is identical to the previous process. It occurs because of the overlap of vibrational and electronic energy states.

²⁷ Taken from:
chem.libretexts.org/Core/Physical_and_Theoretical_Chemistry/Spectroscopy/Electronic_Spectroscopy/Jablonski_diagram

Another pathway for molecules to dissipate energy absorbed by a photon is to emit a photon. This is called *fluorescence*. On the Jablonski diagram it is indicated as a straight arrow pointing down between two electronic states. Fluorescence is a slow process on the order of 10^{-9} and 10^{-7} s. It is most of times observed between the first excited electron state and the ground state because at higher electronic states it is more likely that energy is dissipated through internal conversion or vibrational relaxation.

Another way a molecule can use to spread its energy is called *intersystem crossing*. This is when the electron changes spin multiplicity from an excited singlet state to an excited triplet state. It is the slowest process, several orders of magnitude from fluorescence and it is indicated as a horizontal arrow from a column to another one. Intersystem crossing leads to interesting routes back to the ground electronic state. One plausible direct transition is *phosphorescence*, where a radiative transition from an excited triplet state to a singlet ground state takes place. This process is also very slow.

1.5.3 Selected examples of photoredox catalyzed reactions

The growing research field of UV-A and visible light photocatalysis has become these last years more stimulating than ever as illustrated by the large number of reports, conferences and papers in this field.²⁸ This is due to the technical progress in the development of suitable light sources, mainly high-power LEDs. They represent an easily available, cheap and very efficient source of intense light. Thus, it becomes advantageous to use photo-oxidants because of their elevated excited-state reduction potentials, which cannot be achieved prior to irradiation, making them bench-top stable and chemoselective.

The field of photoredox catalysis is largely dominated by the use of metal-based polypyridyl photoredox catalysts, such as of ruthenium²⁹ and iridium-based photocatalysts (Figure 1.7).³⁰

²⁸ (a) Hoffmann, M.R.; Martin, S.T.; Choi, W.; Bahnemann, D.W. *Chem. Rev.* **1995**, *95*, 69-96. (b) Fujishima, A.; Rao, T.N.; Tryk, D.A. *J. Photochem. Photobiol., C: Photochem. Rev.* **2000**, *1*, 1-21. (c) Hu, J.; Wang, J.; Nguyen, T.H.; Zheng, N. *Beilstein J. Org. Chem.* **2013**, *9*, 1977-2001. (d) Yoon, T.P. *ACS Catalysis* **2013**, *3*, 895-902.

²⁹ (a) Juris, A.; Balzani, V. *Helv. Chim. Acta* **1981**, *64*, 2175-2182. (b) Prier, C.K.; Rankic, D.A.; MacMillan, D.W.C. *Chem. Rev.* **2013**, *113*, 5322-5363.

³⁰ Narayanam, J.M.R.; Stephenson, C.R.J. *Chem. Soc. Rev.* **2011**, *40*, 102-113.

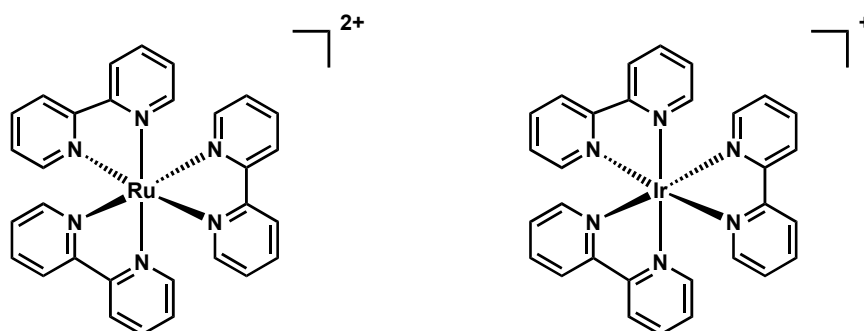


Figure 1.7. Most commonly used metal-based photoredox catalysts

These complexes absorb light in the visible region to give long-lived photoexcited states. The ability of polypyridyl complexes to act as visible light photoredox catalysts has been recognized and deeply investigated for applications in inorganic and materials chemistry.^{26[a]} More specifically, they have been used to afford the splitting of water into hydrogen and oxygen³¹ and the reduction of carbon dioxide to methane.³² They have furthermore been utilized *i*) as components of dye-sensitized solar cells³³ and organic light-emitting diodes,³⁴ *ii*) as photoinitiator for polymerization reactions,³⁵ and *iii*) in photodynamic therapy.³⁶

Irradiation of these transition-metal based chromophores with visible light ($\lambda = 400\text{-}700$ nm) produces photoexcited states which are powerful photoredox catalysts capable to either oxidize or reduce many organic and inorganic substrates. Given the relatively long lifetime of their photoexcited states (~ 600 ns), the high quantum efficiency of their formation, and the excellent stability of their ground state precursors, ruthenium and iridium derivatives have been deeply investigated for the conversion of solar energy, either directly into electrical source or into fuel by photoreduction of water and CO_2 .³⁷

For a while, these complexes were only rarely employed as photocatalysts in organic synthesis. In 2008, independent reports from Yoon and MacMillan groups detailed the use of $\text{Ru}(\text{bpy})_3^{2+}$ as a visible light photocatalyst to afford a [2 + 2] cycloaddition and α -alkylation of aldehydes,^{38, 39} respectively (Scheme 1.11 and 1.12).

³¹ (a) Grätzel, M. *Acc. Chem. Res.* **1981**, *14*, 376-384. (b) Meyer, T.J. *Acc. Chem. Res.* **1989**, *22*, 163-170.

³² Takeda, H.; Ishitani, O. *Coord. Chem. Rev.* **2010**, *254*, 346-354.

³³ Kalyanasundaram, K.; Grätzel, M. *Coord. Chem. Rev.* **1998**, *77*, 347-414.

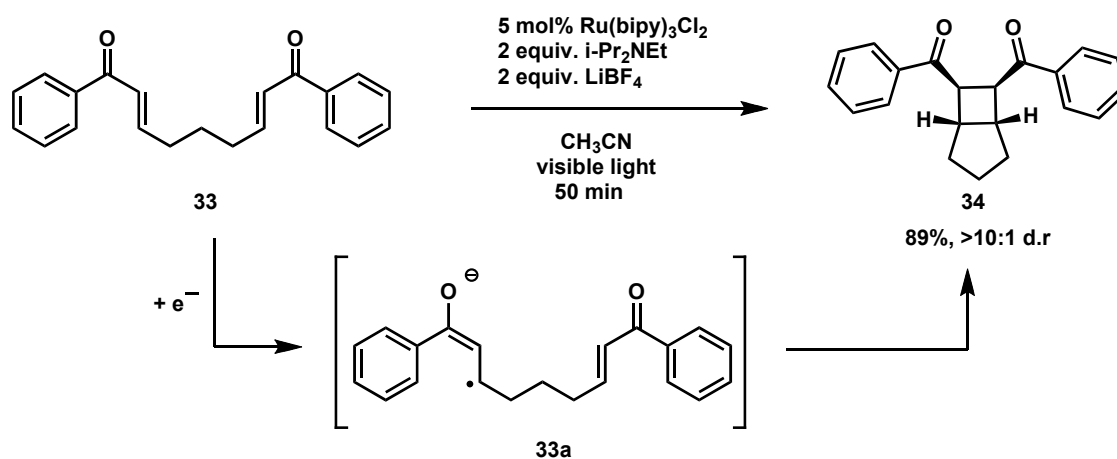
³⁴ Lowry, M.S.; Bernhard, S. *Chem-Eur. J.* **2006**, *12*, 7970-7977.

³⁵ (a) Laleveé, J.; Blanchard, N.; Tehfe, M.-A.; Morlet Savary, F.; Fouassier, J.P. *Macromolecules* **2010**, *43*, 10191-10195. (b) Laleveé, J.; Peter, M.; Dumur, F.; Gigmès, D.; Blanchard, N.; Tehfe, M.-A.; Morlet-Savary, F.; Fouassier, J. P. *Chem.-Eur. J.* **2011**, *17*, 15027-15031. (c) Fors, B. P.; Hawker, C. J. *Angew. Chem., Int. Ed.* **2012**, *51*, 8850-8853.

³⁶ Howerton, B.S.; Heidary, D.K.; Glazer, E.C. *J. Am. Chem. Soc.* **2012**, *134*, 8324-8327.

³⁷ Kalyanasundaram, K.; *Coord. Chem. Rev.* **1982**, *46*, 159-244.

³⁸ Ischay, M.A.; Anzovino, M.E.; Du, J.; Yoon, T.P. *J. Am. Chem. Soc.* **2008**, *130*, 12886-12887.



Scheme 1.11. [2 + 2] photocatalyzed cycloaddition of enones

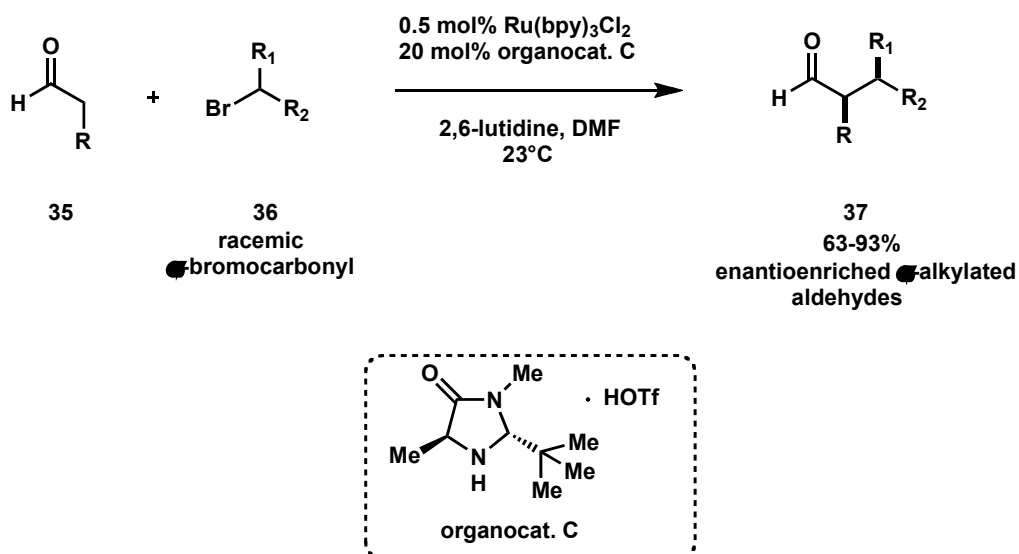
The group of Yoon found that the starting bis(enone) underwent efficient cyclization upon visible light irradiation using of $\text{Ru}(\text{bipy})_3\text{Cl}_2$ as photocatalyst (5 mol%) in the presence of LiBF_4 and $i\text{-Pr}_2\text{NEt}$ as additives. The *meso* diastereoisomer of cyclobutane-containing bicyclic dione **34** is formed with good stereoselectivity. Noteworthy, the light source used in this reaction was a normal 275 W floodlight and no special UV-apparatus is required.

In a seminal work, MacMillan and Nicewicz reported the asymmetric α -alkylation of aldehydes by merging two powerful concepts, namely organocatalysis and photoredox catalysis. It has been shown that the combination of Ru-mediated photoredox catalysis with a SOMO-type aminocatalysis (SOMO: singly occupied molecular orbital) provided a catalytic recycling system for the photocatalyst, where both its oxidation and reduction steps were productive (Scheme 1.12). As a result, α -alkylated aldehydes have been obtained in good yields and outstanding enantioselectivities in a photoredox process where a sacrificial electron donor was not needed. Indeed, the alkyl radicals, which were photocatalytically derived from the corresponding activated halides, were immediately trapped by the electron-rich enamine species (Scheme 1.13). The obtained α -amino radical was in turn oxidized by the photoexcited $^*[\text{Ru}(\text{bpy})_3]^{2+}$, thus providing the reductive Ru^+ species for the dehalogenation.

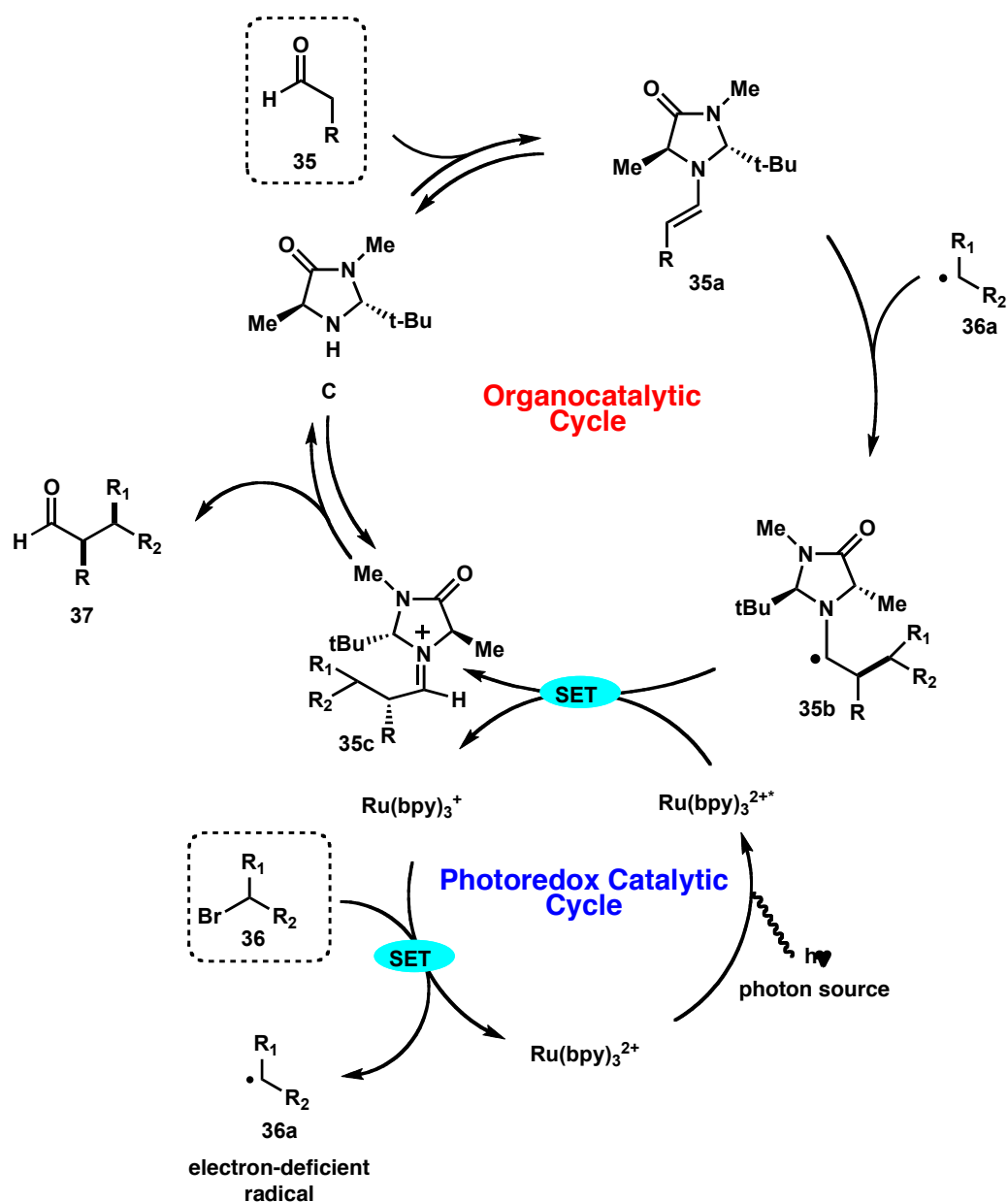
The advantage of this approach is that it proceeded under mild conditions and also required only a standard energy-saving light bulb as a light source. The chiral

³⁹ Nicewicz, D.A.; MacMillan, D.W.C. *Science* **2008**, *322*, 77-80.

imidazolidinone catalyst, also called MacMillan organocatalyst, allows for the effective enantiofacial differentiation for the radical attack of the enamine.⁴³



Scheme 1.12. Direct photocatalyzed α -alkylation of aldehydes



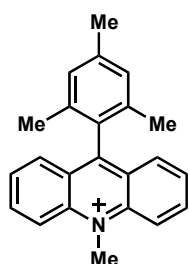
Scheme 1.13. Direct asymmetric alkylation of aldehydes by merging photocatalysis and organocatalysis in the presence of [Ru]-based photocatalyst

It should be noted that a metal-free approach of this reaction has been disclosed by the group of Melchiorre.⁴⁰ It has been shown that a highly enantioselective version of the same process can be achieved through the formation of an electron-donor-acceptor complexes between the enamine **35a** and the bromoalkane **36**. More details about this concept will be given in Chapter 3.

⁴⁰ Arceo, E.; Jurberg, I.D.; Alvarez-Fernandez, A.; Melchiorre, P. *Nature Chemistry* **2013**, *5*, 750-756.

1.5.4. Metal-free photocatalysts

Despite the various examples of efficient catalytic photoredox transformations with transition metal dyes known to date, their high price, toxicity profile and problematic recyclability of many of these dyes limit their use in the context of large scale catalysis. Recently, special attention has focused on environmentally more benign, cheaper and easy-handle photocatalysts (Chart 1.3).



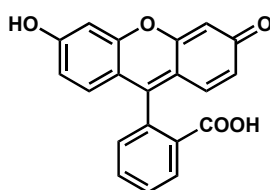
Acridinium salt

$$E_{\text{red}}(\text{PC}^*/\text{PC}^{\bullet-}) = 2.07 \text{ V}$$

$$E_{\text{ox}}(\text{PC}^*/\text{PC}^{\bullet+}) = -0.57 \text{ V}$$

$$\tau = 3 \text{ ns}$$

$$\lambda = 430 \text{ nm}$$



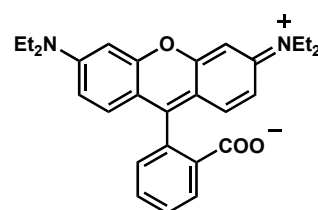
Fluorescein

$$E_{\text{red}}(\text{PC}^*/\text{PC}^{\bullet-}) = 1.21 \text{ V}$$

$$E_{\text{ox}}(\text{PC}^*/\text{PC}^{\bullet+}) = -1.61 \text{ V}$$

$$\tau = 3.1 \text{ ns}$$

$$\lambda = 450 \text{ nm}$$



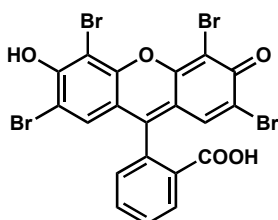
Rhodamine B

$$E_{\text{red}}(\text{PC}^*/\text{PC}^{\bullet-}) = 1.44 \text{ V}$$

$$E_{\text{ox}}(\text{PC}^*/\text{PC}^{\bullet+}) = -0.99 \text{ V}$$

$$\tau = 1.74 \text{ ns}$$

$$\lambda = 524 \text{ nm}$$



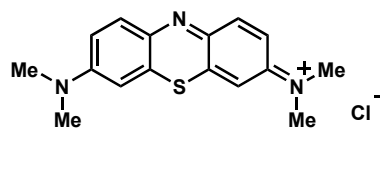
Eosin Y

$$E_{\text{red}}(\text{PC}^*/\text{PC}^{\bullet-}) = 1.18 \text{ V}$$

$$E_{\text{ox}}(\text{PC}^*/\text{PC}^{\bullet+}) = -1.11 \text{ V}$$

$$\tau = 0.09\text{-}2.6 \text{ ps}$$

$$\lambda = 530 \text{ nm}$$



Methylene Blue

$$E_{\text{red}}(\text{PC}^*/\text{PC}^{\bullet-}) = 1.72 \text{ V}$$

$$E_{\text{ox}}(\text{PC}^*/\text{PC}^{\bullet+}) = -0.30 \text{ V}$$

$$\tau = 2\text{-}79.5 \text{ ps}$$

$$\lambda = 665 \text{ nm}$$

Chart 1.3. Electrochemical and photophysical properties of the excited states of some common metal-free photocatalysts

Similar to the redox properties of the organometallic complexes, some organic dyes such as eosin Y, rose bengal, fluorescein, methylene blue and acridinium salts have shown good performances as photocatalysts.⁴¹

Because they are environmentally friendly and inexpensive compared to the corresponding organometallic molecules, organophotocatalysts have become highly important players in visible light-mediated photoredox catalysis.⁴²

For instance, the groups of Fukuzumi, König, Scaiano, Nicewicz, to name a few, have focused large part of their researches to explore the efficiency of organic dyes in photoredox chemistry. As a big part of this PhD thesis deals with the use of the acridinium salt and eosin Y as photocatalysts, the following sections will focus on structure and reactivity of these dyes.

1.5.5. Acridinium salt as photocatalyst

In 2003, Fukuzumi and coworkers⁴³ synthesized and characterized the electron-transfer reagent 9-mesityl-10-methylacridinium (Mes-Acr), which turned out to be a photoredox active organic chromophore bearing an acridinium-core. According to the crystal structure of the dye (Figure 1.8),⁴⁴ the 9-mesityl-substituent was shown to form an angle of nearly 90° with the acridine, so that little π overlap was possible in the charge-separated species.

⁴¹ For a comprehensive review on organic photoredox catalysis, see: Romero, N.A; Nicewicz, D.A. *Chem. Rev.* **2016**, *116*, 10075-10166.

⁴² (a) Vila, C.; Lau, J.; Rueping, M. *Beilstein J. Org. Chem.* **2014**, *10*, 1233-1238. (b) Chen, L.; Chao, C.S.; Pan, Y.; Dong, S.; Teo, Y.C.; Wang, J.; Tan, C.-H. *Org. Biomol. Chem.* **2013**, *11*, 5922-5925. (c) Pitre, S.P.; McTiernan, C.D.; Ismaili, H.; Scaiano, J.C. *I. Am. Chem. Soc.* **2013**, *135*, 13286-13289. (d) Liu, H.; Feng, W.; Kee, C.W.; Zhao, Y.; Leow, D.; Pan, Y.; Tan, C.-H. *Green Chem.* **2010**, *12*, 953-956. (e) Hari, D.P.; König, B. *Org. Lett.* **2011**, *13*, 3852-3855. (f) Condie, A.G.; Gonzalez-Gomez, J.C.; Stephenson, C. R. J. *J. Am. Chem. Soc.* **2010**, *132*, 1464-1465. (g) Neumann, F.; Fuldner, S.; König, B.; Zeitler, K. *Angew. Chem. Int. Ed.* **2011**, *50*, 951-954.

⁴³ Fukuzumi, S.; Kotani, H.; Ohkubo, K.; Ogo, S.; Tkachenko, N. V.; Lemmetyinen, H. *J. Am. Chem. Soc.* **2004**, *126*, 1600-1601.

⁴⁴ Fukuzumi, S.; Ohkubo, K.; Suenobu, T. *Acc. Chem. Res.* **2014**, *47*, 1455-1464.

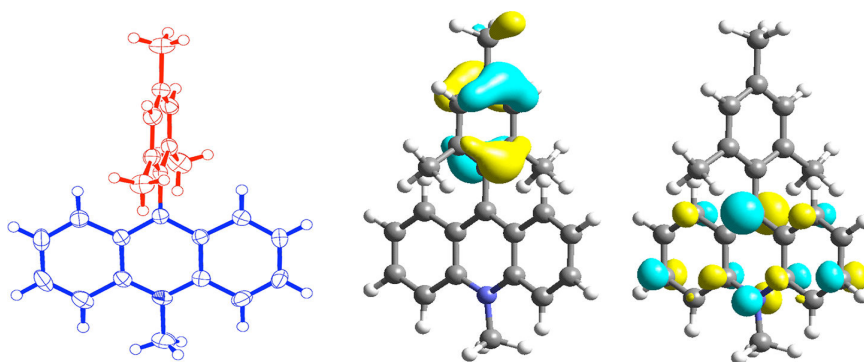


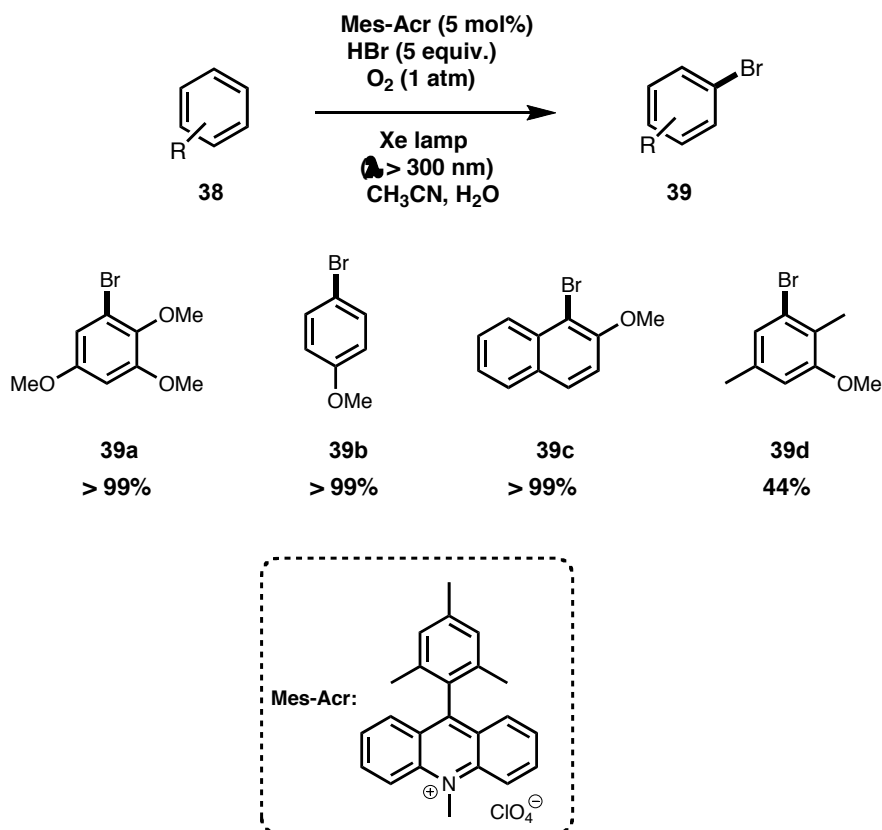
Figure 1.8. The X-ray structure shows the dihedral perpendicular angle between acridinium and mesityl moieties; HOMO and LUMO calculated by DFT method at B3LYP/6-31G

The excited state of Mes-Acr is known to be a strong oxidizing species ($E_{red} = +2.07$ V vs. SCE in MeCN), with broad absorption in the visible range ($\lambda > 430$ nm). These remarkable oxidizing capabilities are deduced, in part, to come from a long-lived charge-separated state where the mesityl group is oxidized by the excited state of the acridinium moiety.

Fukuzumi applied this photoredox catalyst in many organic transformations.⁴⁵ Of particular interest is the bromination of different functionalized arenes using HBr as the bromine source, atmospheric oxygen as the terminal oxidant and the acridinium-salt (Mes-Acr) as photocatalyst was performed under mild conditions (Scheme 1.14).⁴⁶

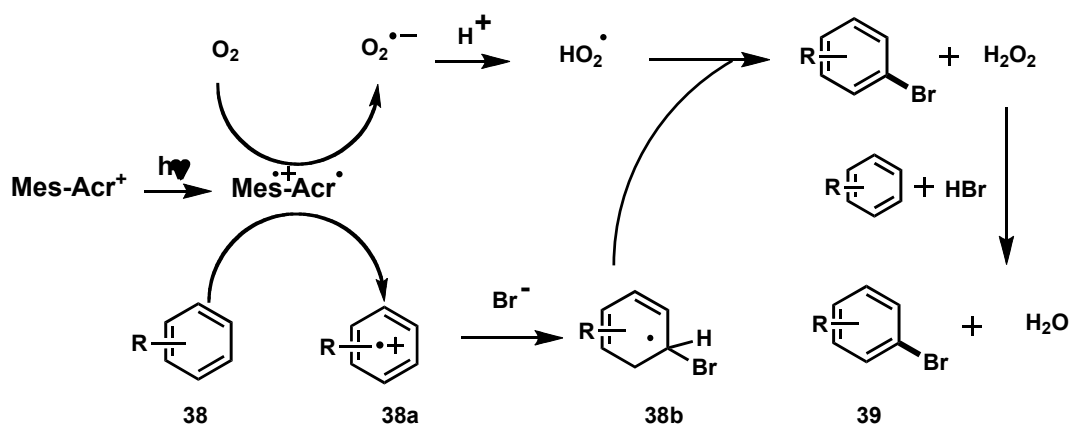
⁴⁵ Fukuzumi, S.; Ohkubo, K. *Org. Biomol. Chem.* **2014**, *12*, 6059-6071.

⁴⁶ Ohkubo, K.; Mizushima, K.; Iwata, R.; Fukuzumi, S. *Chem. Sci.* **2011**, *2*, 715-722.



Scheme 1.14. Photocatalyzed bromination of different functionalized arenes

The photocatalytic cycle is promoted by intramolecular photoinduced electron transfer from the mesityl moiety (Mes) to the singlet excited state of the acridinium moiety (Acr⁺) to form the corresponding reactive excited state, as shown in Scheme 1.15. The excited state of the mesityl moiety can oxidize benzene derivatives, such as 1,2,4-trimethoxybenzene (TMB) or anisole, to afford the corresponding radical cation intermediate, whereas the acridinium part can reduce O₂ to HO₂[•]. The formed radical intermediate reacts with Br⁻ to form the cyclohexadienyl radical, which after a fast hydrogen transfer with HO₂[•] form the corresponding brominated product and hydrogen peroxide. The latter then reacts with the substrate to produce another molecule of brominated adduct **39**.

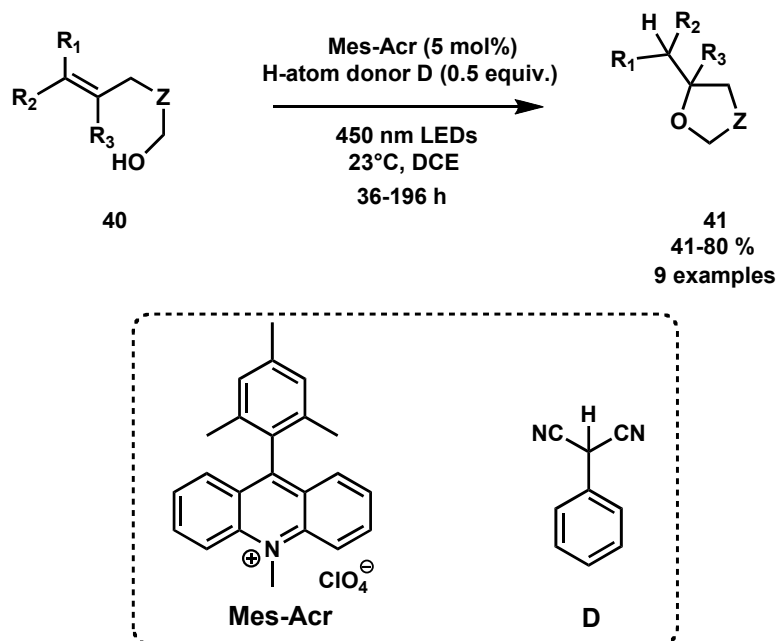


Scheme 1.15. Photocatalytic bromination of functionalized arenes with the acridinium salt as photocatalyst

Based on these seminal contributions from the Fukuzumi group, the group of Nicewicz employed **Mes-Acr** catalyst for a broad range of *anti*-Markovnikov alkene hydrofunctionalization reactions.⁴⁷ Among these, they described the *anti*-Markovnikov intramolecular hydroalkoxylation of alkenols, for which they combined the photocatalytic activity of the acridinium salt (Mes-Acr) with 2-phenylmalononitrile **D**, an essential second component named organic redox-active hydrogen atom donor (Scheme 1.16).^{48[b]}

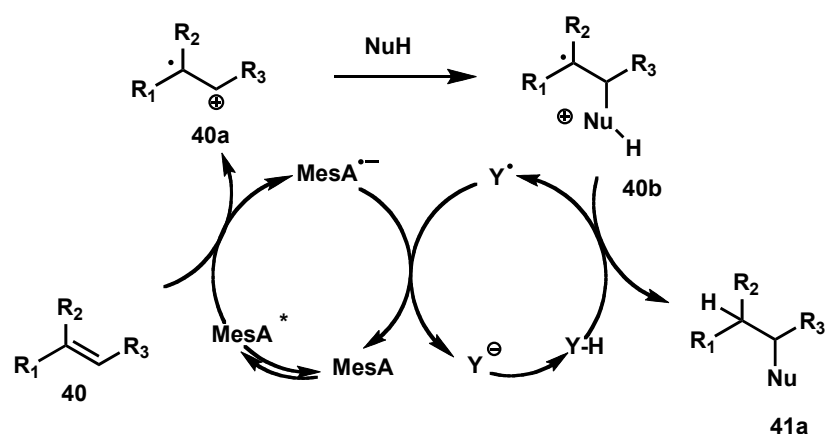
The association of a photocatalyst and the H-atom donor facilitated the transformation that led to *anti*-Markovnikov adducts.

⁴⁷ (a) Wilger, D.J.; Gesmundo, N.J.; Nicewicz, D.A. *Chem. Sci.* **2013**, *4*, 3160-3165. (b) Hamilton, D.H.; Nicewicz, D.A. *J. Am. Chem. Soc.* **2012**, *134*, 18577-18580. (c) Nguyen, T.M.; Nicewicz, D.A. *J. Am. Chem. Soc.* **2013**, *135*, 9588-9591. (d) Perkowski, A.J.; Nicewicz, D.A. *J. Am. Chem. Soc.* **2013**, *135*, 10334. (e) Grandjean, J.M.; Nicewicz, D.A. *Angew. Chem. Int. Ed.* **2013**, *52*, 3967-3971.



Scheme 1.16. Photocatalyzed intramolecular hydroalkoxylation of alkenols

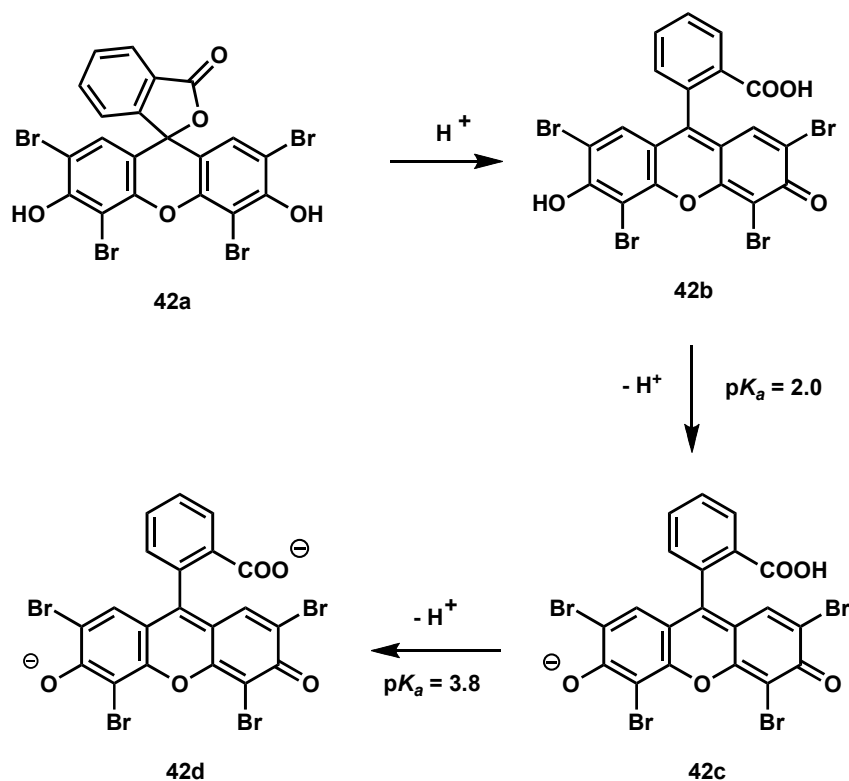
Nicewicz *et al.* proposed an initial photooxidation of the alkene substrates ($E_{ox} < 2.24$ V vs. NHE in CH_3CN) by the excited MesA^+ (MesA^{*+}) affording the corresponding radical cations. Upon addition of a nucleophile, a radical cationic intermediate was obtained. The latter is easily trapped by the hydrogen atom donor **D**, yielding the product **40b**. The photocatalyst is regenerated through an oxidation with the resulting radical Y^\bullet leading to anion Y^- , which is able to accept the proton from the radical cationic intermediate **40a** to close up the two-component catalytic system (Scheme 1.17).



Scheme 1.17. Proposed mechanism for the intramolecular hydroalkoxylation

1.5.6. Eosin Y as a photocatalyst

Eosin Y (EY), the 2',4',5',7'-tetrabromo derivative of fluorescein, is the most widely employed photocatalyst. It can exist, depending on the conditions, in four different structures in solution: the spirocyclic form **42a**, the neutral **42b**, the monoanionic **42c** and the dianionic form **42d** (Scheme 1.18).

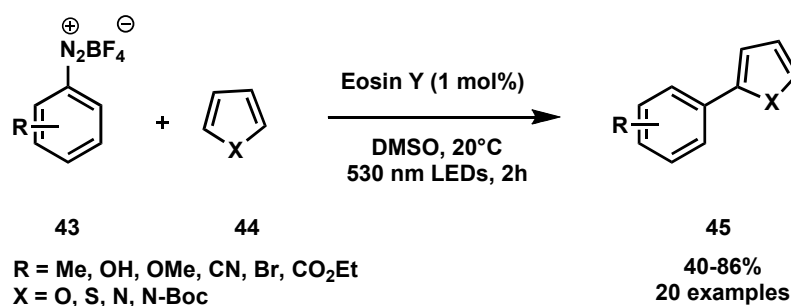


Scheme 1.18. Acid-base behavior of eosin Y

The spirocyclic form **42a** contains an interrupted conjugation of the fluoron ring system and thus is photocatalytically inactive under visible-light irradiation. The neutral form **42b** exhibits only weak fluorescence when irradiated with visible light. The charged forms **42c** and **42d** are photocatalytically active. In such cases, catalytic activity as observed in recent publications⁴⁸ is dependent on the acid-base equilibrium, so that the employed eosin Y is converted in situ to the active species **42c** or **42d**.

Based on its interesting electrochemical and photophysical properties, the group of König employed eosin Y for the direct C–H arylation of heteroarenes with aryl diazonium salts (Scheme 1.19).^{51[a]}

⁴⁸ (a) Hari, D.P.; Schroll, P.; König, B. *J. Am. Chem. Soc.* **2012**, *134*, 2958-2961. (b) Majek, M.; Filace, F.; von Wangelin, A.J. *Beilstein J. Org. Chem.* **2014**, *10*, 981-989.

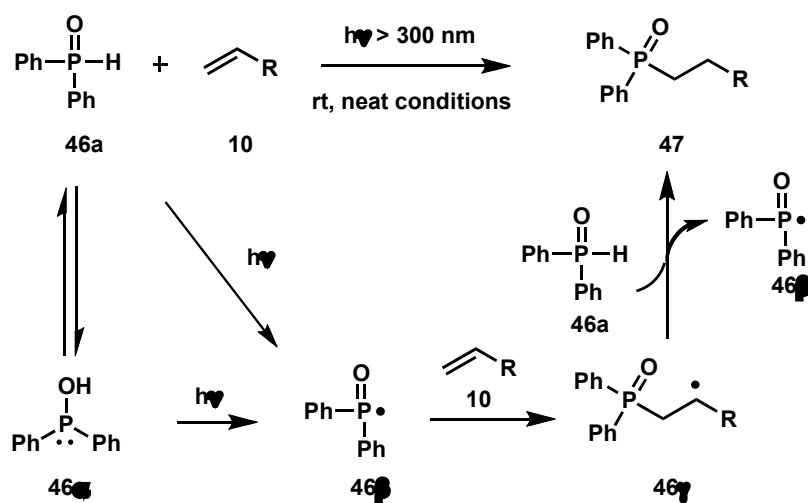


Scheme 1.19. Eosin Y-catalyzed direct C–H arylation of heteroarenes

In contrast to previous report, where these coupling adducts were obtained through the use of a large variety of transition-metal strategies using aryl halides, arylboronic acids, aryltin reagents and high temperatures,⁴⁹ König's approach has been the first metal-free strategy allowing mild access to **45**. It has been postulated that eosin Y absorbs light at $\lambda = 540$ nm to generate the corresponding excited state, which is known to be a good oxidant to reduce the diazonium salt **43** and to form the aryl radical **43a**. The latter adds to heteroarene **44** to form the hexadienyl intermediate **44a**, which undergoes oxidation by EY⁺ to furnish the arenium salt which yields the final coupling adduct **45** after fast deprotonation with BF₄⁻ (Scheme 1.20).

⁴⁹ (a) Join, B.; Yamamoto, T.; Itami, K. *Angew. Chem. Int. Ed.* **2009**, *48*, 3644. (b) Kawai, H.; Kobayashi, I.; Oi, S.; Inoue, Y. *Chem. Commun.* **2008**, 1464. (c) Yanagisawa, S.; Sudo, T.; Noyori, R.; Itami, K. *J. Am. Chem. Soc.* **2006**, *128*, 11748.

46γ. The latter abstracts hydrogen from the secondary phosphine oxide **46a**, affording the hydrophosphinylation product **47** and generates the phosphinoyl radical **46β**.

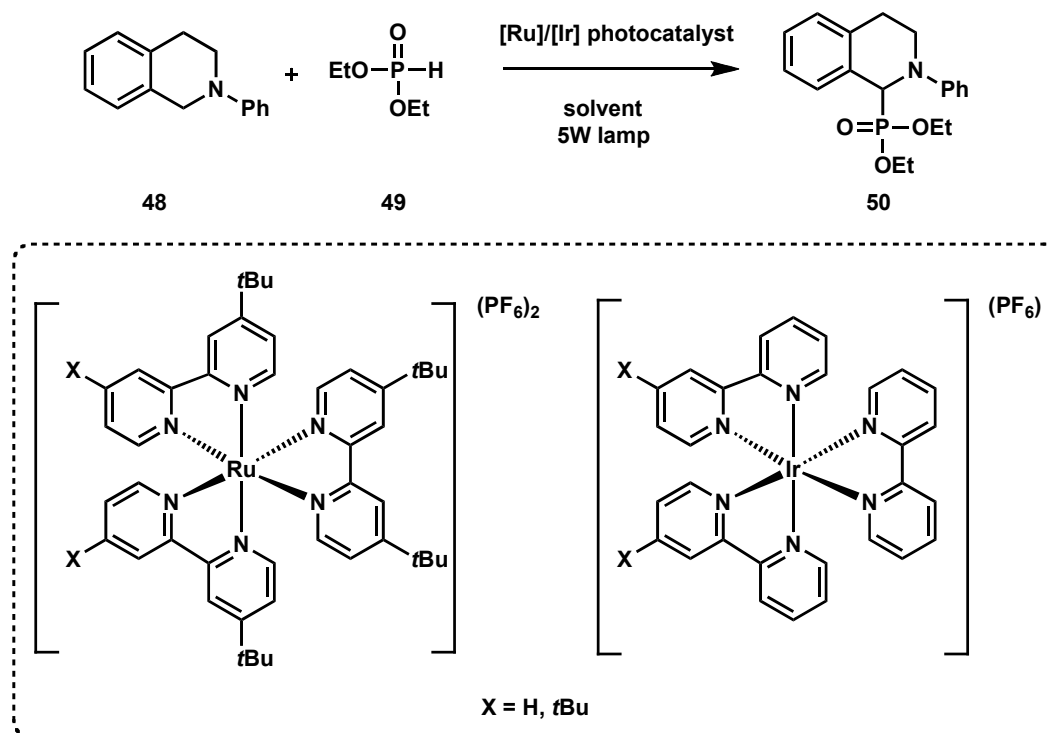


Scheme 1.21. Photoinduced hydrophosphinylation of alkenes in the absence of photocatalyst

On the basis of remarkable reports concerning photoredox catalyzed functionalization of tertiary amines⁵¹, König and co-workers⁵² developed an innovative oxidative phosphorylation reaction by examining the oxidation of *N*-aryl-tetrahydroisoquinolines in the presence of diethyl phosphite and metal-based polypyridyl complexes (Scheme 1.22).

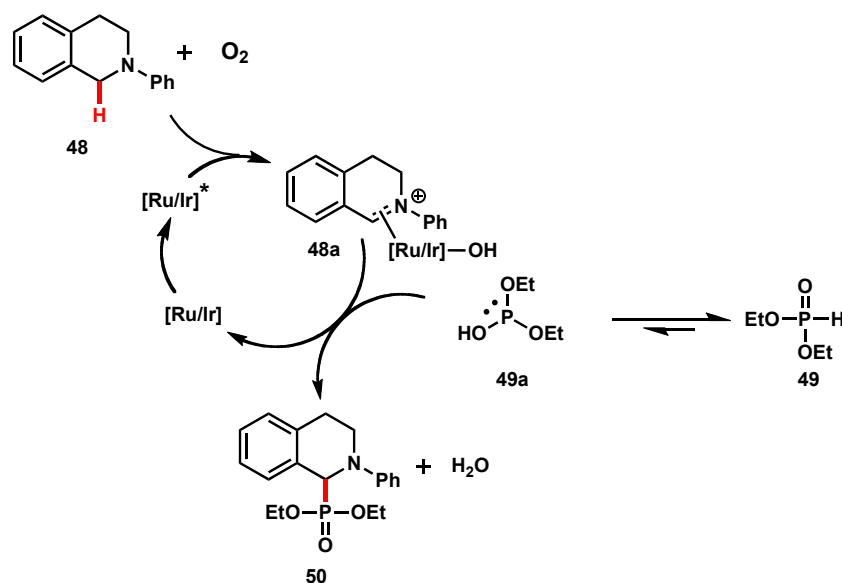
⁵¹ (a) Murahashi, S.I.; Zhang, D. *Chem. Soc. Rev.* **2008**, *37*, 1490-1501. (b) Li, C.J. *Acc. Chem. Res.* **2009**, *42*, 335-344. (c) Klussmann, M.; Sureshkumar, D. *Synthesis* **2011**, 353-369. (d) Murahashi, S.I. *Angew. Chem., Int. Ed. Engl.* **1995**, *34*, 2443-2465. (e) Han, W.; Mayer, P.; Ofial, A.R. *Adv. Synth. Catal.* **2010**, *352*, 1667-1676. (f) Baslé, O.; Li, C.J. *Chem. Commun.* **2009**, 4124-4126.

⁵² Rueping, M.; Zhu, S.; R.M. *Chem. Commun.* **2011**, *47*, 8679-8681.



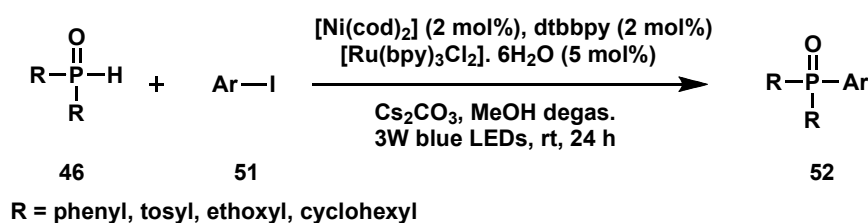
Scheme 1.22. Oxidative phosphorylation of *N*-aryl-tetrahydroisoquinolines in the presence of diethyl phosphite and metal-based polypyridyl complexes

The proposed mechanism of this process is outlined in Scheme 1.23, where the P(III) form of the phosphite **49** is suggested to react as a nucleophile with the iminium ion formed upon oxidation of the nitrogen atom of **48** and subsequent hydrogen transfer reaction, leading to the desired coupling product **50**.



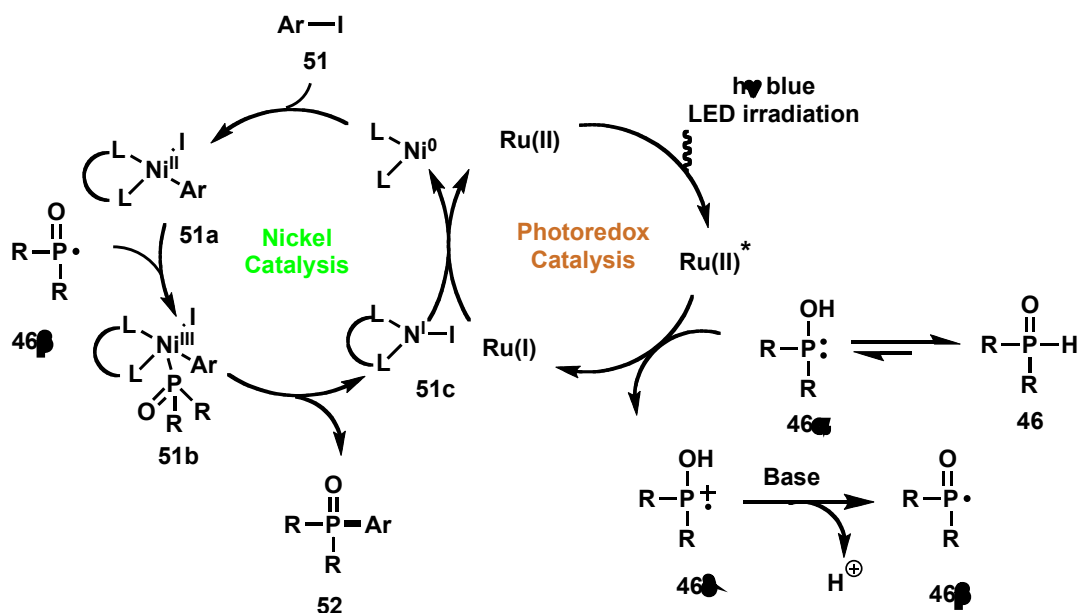
Scheme 1.23. Plausible mechanism for the oxidative phosphorylation of *N*-aryl-tetrahydroisoquinolines with diethyl phosphite and metal-based polypyridyl complexes

Inspired from these studies, Xiao *et al.*⁵³ reported a novel and efficient C–P bond formation reaction of diarylphosphine oxides with aryl iodides by combining visible-light induced photoredox catalysis and nickel catalysis (Scheme 1.24).



Scheme 1.24. Nickel-catalyzed phosphonylation of aryl iodides with secondary phosphine oxides

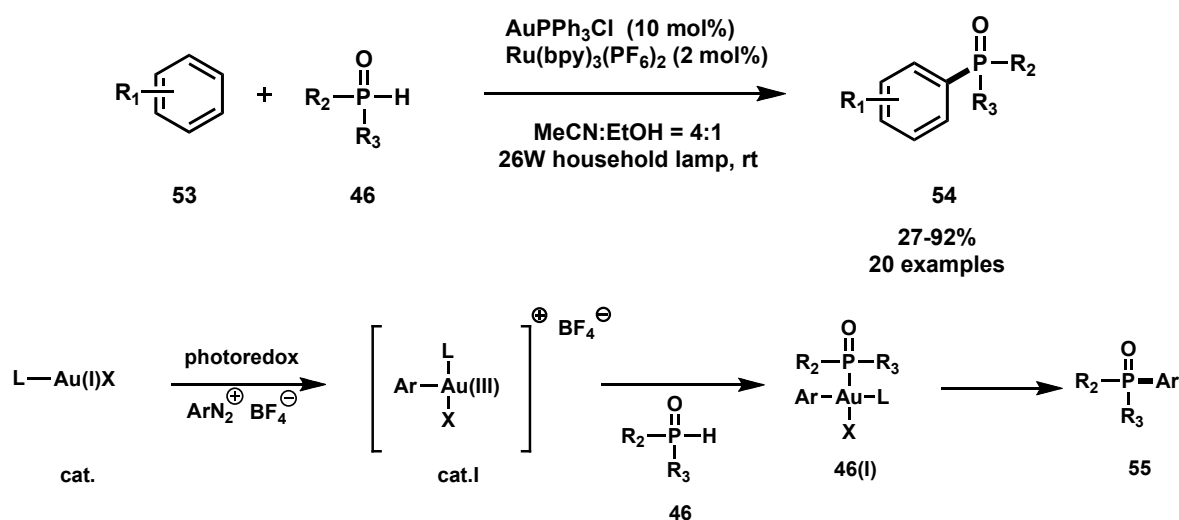
This reaction starts with the reduction of the excited state of Ru(II)* by the trivalent form P(III) **46 α** generating the corresponding radical cationic intermediate **46 δ** and Ru(I) complex. Subsequent deprotonation generates phosphinoyl radical **46 β** . Meanwhile, an oxidative addition of Ni(0) complex to aryl-iodide **51** gives rise to Ni(II) intermediate **51a**. The latter forms the organometallic Ni(III) complex **51b** by reacting with P-centered radical **46 β** . Finally, reductive elimination affords the desired product **52** releasing the reduced species Ni(I) **51c** (Scheme 1.25).



Scheme 1.25. Proposed dual catalytic mechanism for the phosphonylation of aryl iodides with secondary phosphine oxides

⁵³ Xuan, J.; Zeng, T.-T.; Chen, J.-R.; Lu, L.-Q.; Xiao, W.-J. *Chem. Eur. J.* **2015**, *21*, 4962-4965.

More recently, Toste *et al.*⁵⁴ disclosed a new methodology for the *P*-arylation of aryldiazonium salts with *H*-phosphonates via dual gold and photoredox catalysis. Inspired from previous works⁵⁵ on C–P bond formation achieved through the reaction of phosphonate esters or phosphine oxides with highly electrophilic arylcopper(III) intermediates, it has been hypothesized that gold(III) intermediates (**cat.I**) might also be engaged in coupling reactions with nucleophilic phosphorus reagents, such as phosphites and/or phosphine oxides (Scheme 1.26).



Scheme 1.26. Gold-based oxidative *P*-arylation of *H*-phosphonate with aryldiazonium salts under photoredox conditions

Meanwhile, König and co-workers reported an efficient, mild and metal-free alternative to yield aryl phosphonates employing Rhodamine 6G as photocatalyst and the sacrificial electron-donor *N,N*-Diisopropylethylamine (DIPEA) *via* C–Br bond activation (Scheme 1.27).⁵⁶

It was observed that the reaction did not take place in the absence of DIPEA, probably due to the single electron transfer reaction towards the excited form of the photocatalyst. The aryl radical formed in this reaction can easily react with trivalent phosphorus species, affording C–P bonded adducts in moderate to excellent yields.

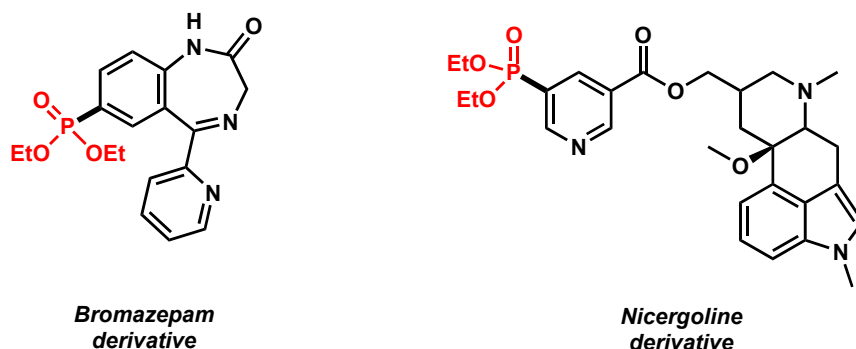
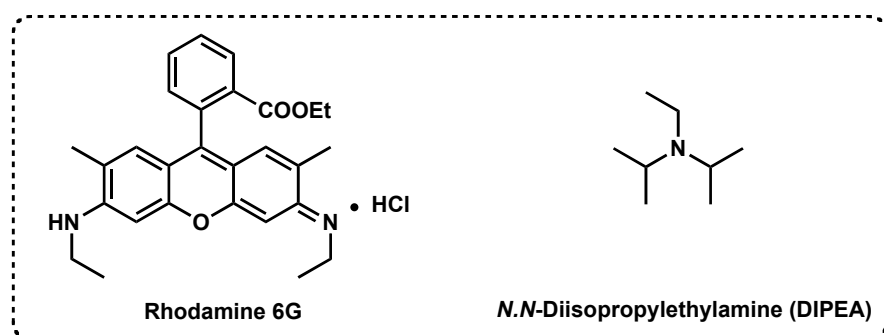
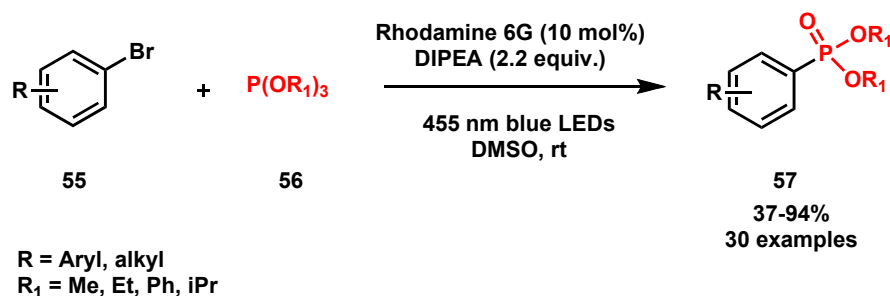
⁵⁴ He, Y.; Wu, H.; Toste, F.D. *Chem. Sci.* **2015**, *6*, 1194-1198.

⁵⁵ (a) Xu, J.; Zhang, P.B.; Gao, Y.Z.; Chen, Y.Y.; Tang, G.; Zhao, Y.F. *J. Org. Chem.* **2013**, *78*, 8176-8183. (b) Walkinshaw, A.J.; Xu, W.; Suero, M.G.; Gaunt, M.J. *J. Am. Chem. Soc.* **2013**, *135*, 12532-12535. (c) Suero, M.G.; Bayle, E.D.; Collins, B.S.L.; Gaunt, M.J. *J. Am. Chem. Soc.* **2013**, *135*, 5332-5335.

⁵⁶ Shaikh, R.S.; Düsel, S.; König, B. *ACS Catal.* **2016**, *6*, 8410-8414.

Different aryl and alkyl phosphites have been tested, even if diethyl phosphite gave the best results.

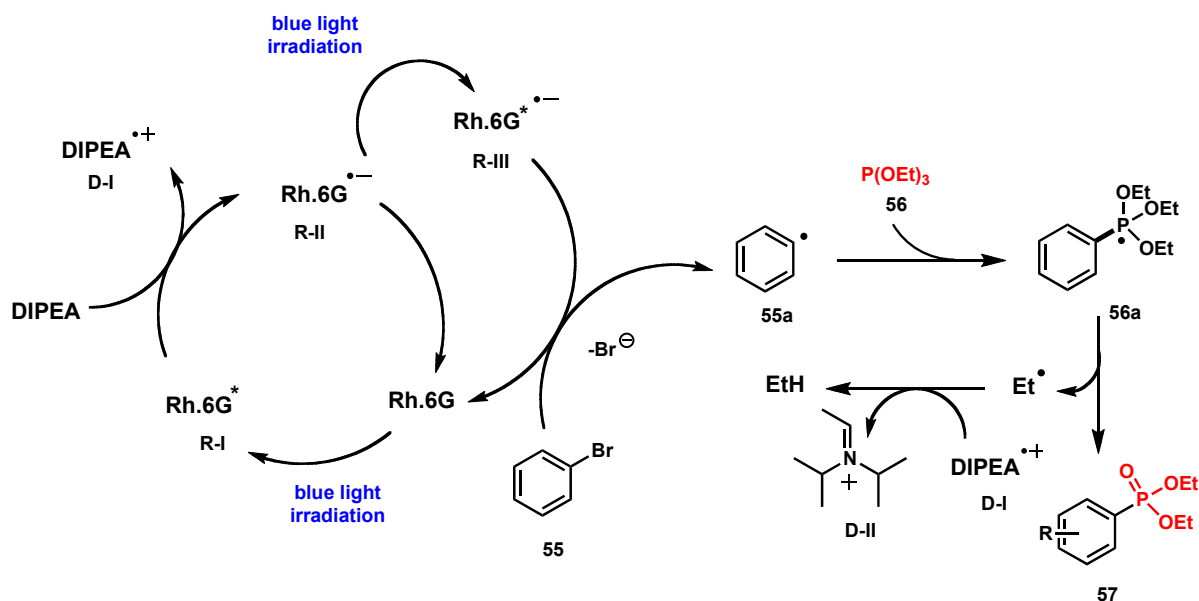
Noteworthy, mild conditions used in this work allowed introducing a phosphonate group into important pharmaceutically active molecules, such as benzodiazepams or nicergoline.



Scheme 1.27. Photocatalytic C–Br activation with Rhodamine 6G as photocatalyst and DIPEA as sacrificial electron donor; phosphonylated active pharmaceutical compounds: bromazepam (*left*) and nicergoline (*right*)

After photoexcitation of Rhodamine 6G to generate the corresponding excited state, DIPEA underwent oxidation to form radical cationic intermediate **D-I** along with the reduced form of the photocatalyst **R-II**. Further irradiation of the latter species gives

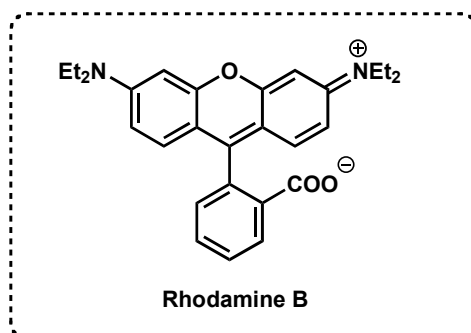
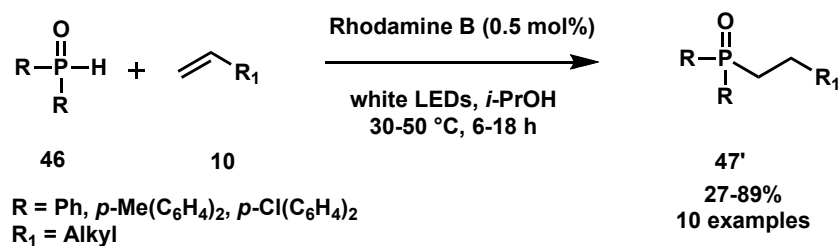
rise to radical anion **R-III** that is responsible of single electron transfer reaction with **55** completing the photocatalytic cycle and generating aryl radical **55a** after fragmentation of aryl bromide. Then, upon addition of alkyl phosphite **56**, an unstable phosphoranyl radical intermediate **56a** is formed, which leads to the desired final adduct **57** after loss of an ethyl radical. The latter can finally abstract hydrogen from the radical cation issued from **DIPEA** or the solvent (Scheme 1.28).



Scheme 1.28. Proposed mechanism for the photocatalytic aryl phosphonates forming reaction *via* C–Br activation

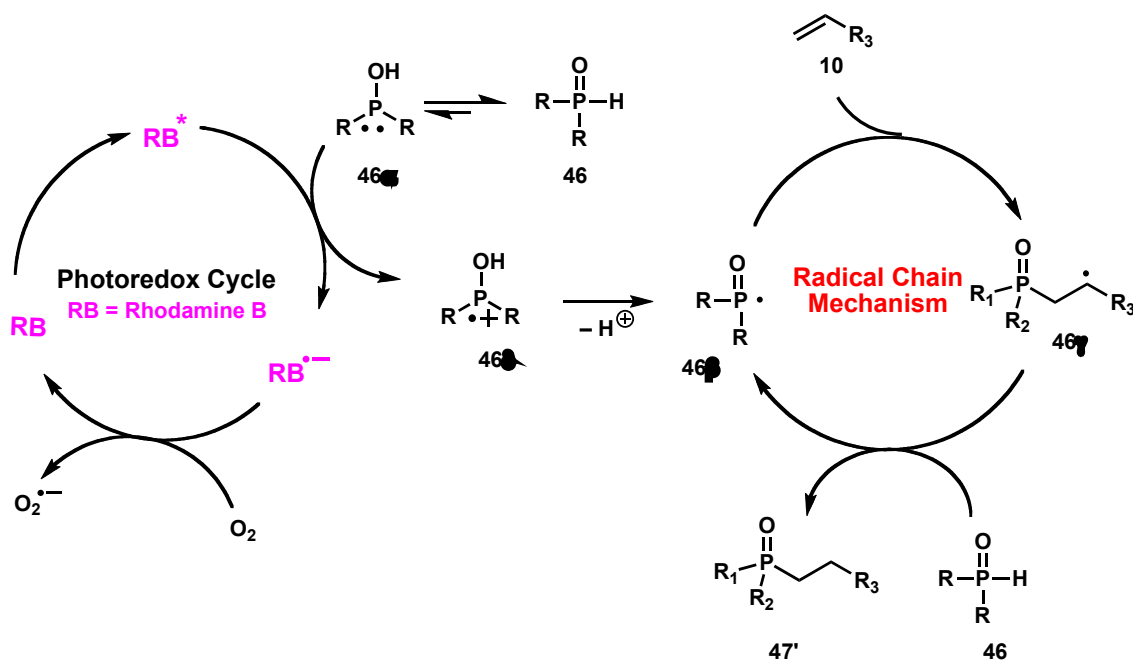
Kobayashi and co-workers⁵⁷ have shown interest in exploring the catalytic abilities of metal-free visible-light photocatalysts (Scheme 1.29).

⁵⁷ Yoo, W.-J.; Kobayashi, S. *Green Chem.* **2013**, *15*, 1844-1848.



Scheme 1.29. Metal-free visible light mediated photocatalyzed hydrophosphinylation of unactivated alkenes

They reported the use of Rhodamine B to promote the initiation step of a radical chain process. As shown in Scheme 1.30, the excited state of the photocatalyst RB^* oxidizes the P(III) form of the secondary phosphine oxide **46** to generate the corresponding radical cation. The latter undergoes fast deprotonation to give rise to the phosphinoyl radical **46 β** that adds to the alkene to form the carbon centered radical **46 γ** . This radical can then abstract hydrogen from **46** to generate a new phosphinoyl radical. To close the photoredox cycle, the reduced form of Rhodamine B may be quenched by the oxygen present in the solvent.



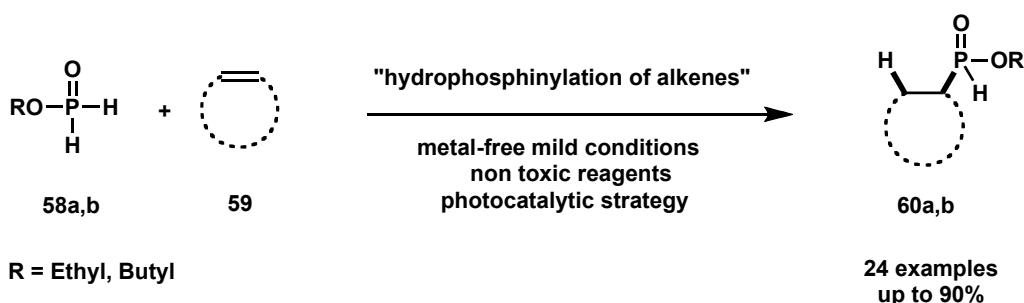
Scheme 1.30. Plausible mechanism for the hydrophosphinylation of unactivated alkenes with secondary phosphine oxides

The selected examples presented in this section demonstrate the great potential to use visible light photoredox catalysis for the synthesis of organophosphorus compounds, but it shows also that this field is in its infancy. In this regard, Belmont and Brachet stated “Indeed, many phosphorus derivatives are still difficult to synthesize, and their access through photoinduced radical reactivity should be investigated”.⁵⁸

⁵⁸ Menigaux, D.; Belmont, P.; Brachet, E. *Eur. J. Org. Chem.* **2017**, *15*, 2008-2055.

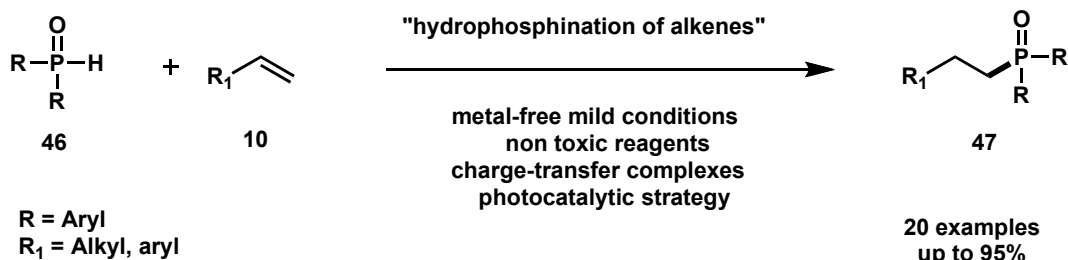
1.6. Goal of the Thesis

This work describes three modes of activation to afford C–P bonds from alkene derivatives under visible-light conditions. In the following chapter (**Chapter 2**) visible light mediated hydrophosphinylation reaction of unactivated olefins with ethyl and butyl phosphinates will be discussed from a synthetic and mechanistic points of view (Scheme 1.31). This mild and atom-economical process provides an attractive alternative to the previously reported methodologies.^{59,60}



Scheme 1.31. Visible light mediated hydrophosphinylation of alkenes employing ethyl and butyl phosphinates

In the third chapter (**Chapter 3**) hydrophosphinylation reaction using secondary phosphine oxides (SPO), as shown in Scheme 1.32, will be reported. Electron donor-acceptor complexes formed between diphenyl phosphine oxides and diphenyliodonium triflate have been shown to be the driving force of this reaction. Mechanistic and synthetic aspects of this metal-free process will be discussed.



Scheme 1.32. Charge-transfer complex based photoinduced hydrophosphinylation of alkenes with secondary phosphine oxides

⁵⁹ a) Ortial, S.; Fisher, H.C.; Montchamp, J-L. *J. Org. Chem.* **2013**, *78*, 6599-6608; b) Deprele, S., Montchamp J.-L., *J. Am. Chem. Soc.*, **2002**, *124*, 9386.

⁶⁰ Fourgeaud, P.; Dayde, B.; Volle, J-N.; Vors, J-P.; Van Der Lee, A.; Pirat, J-L.; Virieux, D.; Campagne, J-M. *Org.Lett.* **2011**, *13*, 5076-5079.

Visible Light Mediated Hydrophosphinylation Reaction

2.1. General context

Because this chapter deals with light mediated hydrophosphinylation of unactivated alkenes with H-phosphinates, we will first introduce the concept of hydrofunctionalization and discuss the main contributions in the field of visible light-mediated hydrofunctionalizations. Then, we will focus on different modes of activation applied in the context of hydrophosphinylation reactions.

2.2. Anti-Markovnikov alkene hydrofunctionalization

2.2.1. Alkenes as challenging substrates

Alkenes are important functional groups that are known to be naturally abundant, cheap and commercially available. In the context of photoinduced chemical transformations, alkene oxidation plays an important role. It refers to the removal of electrons, which typically originates from a π -orbital. The simplest way to predict alkenes oxidation is to consider their oxidation potentials (Chart 2.1).

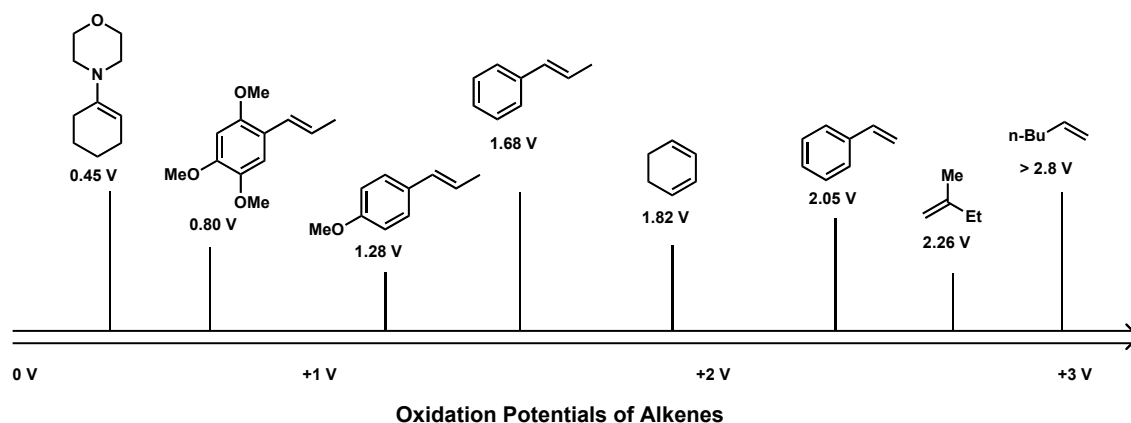


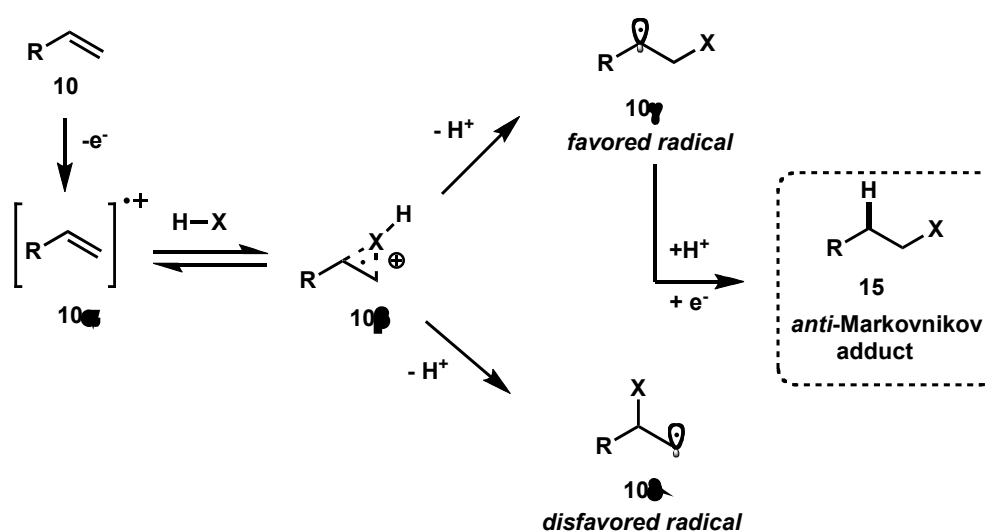
Chart 2.1. Oxidation potentials measured in MeCN vs. SCE of various functionalized alkenes

Terminal aliphatic alkenes such as 1-hexene have oxidation potentials above +2.80 V and are difficult to oxidize. 1,2-disubstituted alkenes and those with electron-donating groups have drastically lower oxidation potentials, due to the increased stability of the subsequent radical cation. This is observed by comparing β -methylstyrene ($E_{ox} = +1.68$ V vs. SCE) and 4-methoxy- β -methylstyrene ($E_{ox} = +1.28$ V vs. SCE). The +0.4 V

difference in stability suggests that substitution on the aromatic ring has a greater impact at decreasing the oxidation potential than substitution of the alkene.⁶³ In agreement with this trend, 2,4,5-trimethoxy- β -methylstyrene possesses an oxidation potential below +1.0 V. Enamines or enol ethers are less positive than alkenes, making them substrates highly susceptible to oxidation, which commonly lead to uncontrolled additions and polymerization.

On the other hand, a challenging prospect for the field of catalysis is occupied by the ready access to the complementary *anti*-Markovnikov addition adducts. All efforts made towards the identification of an applicable direct method for the reversal of Markovnikov selectivity focused on employing transition metal-based catalytic strategies.⁶⁴

Arnold,⁶⁵ Gassman,⁶⁶ Inoue⁶⁷ and Mizuno⁶⁸ demonstrated that heteroatom nucleophiles add with predictable *anti*-Markovnikov regioselectivity to cation radicals derived from single electron oxidation of alkenes (Scheme 2.1).⁶⁹



Scheme 2.1. Mechanism explaining the regioselectivity for the formation of *anti*-Markovnikov adducts

⁶³ PhD Thesis of Michelle Riener: “*Synthesis of C₂ Symmetric Cyclobutanes and γ -Butyrolactones via Photoinduced Electron Transfer*”, University of North Carolina, Chapel Hill, **2014**.

⁶⁴ (a) Utsonomiya, M.; Kuwano, R.; Kawatsura, M.; Hartwig, J.F. *J. Am. Chem. Soc.* **2003**, *125*, 5608-5609. (b) Zhu, S.; Niljianskul, N.; Buchwald, S.L. *J. Am. Chem. Soc.* **2013**, *135*, 15746-15749.

⁶⁵ Neunteufel, R.A.; Arnold, D.R. *J. Am. Chem. Soc.* **1973**, *95*, 4080-4081.

⁶⁶ Gassman, P.G.; Bottorff, K.J. *Tetrahedron Lett.* **1987**, *28*, 5449-5568.

⁶⁷ (a) Asaoka, S.; Wada, T.; Inoue, Y. *J. Am. Chem. Soc.* **2003**, *125*, 3008-3027. (b) Takehara, Y.; Ohta, N.; Shiraishi, S.; Asaoka, S.; Wada, T.; Inoue, Y. *J. Photochem. Photobiol., A* **2001**, *145*, 53-60.

⁶⁸ (a) Mizuno, K.; Nakanishi, I.; Ichinose, N.; Otsuji, Y. *Chem. Lett.* **1989**, *41*, 1095-1098. (b) Mizuno, K.; Tamai, T.; Nishiyama, T.; Tani, K.; Sawasaki, M.; Otsuji, Y. *Angew. Chem. Int. Ed.* **1994**, *33*, 2113-2115.

⁶⁹ For a general review on the reactivity patterns of alkene cation-radicals, see: Schmittel, M.; Burghart, A. *Angew. Chem. Int. Ed. Engl.* **1997**, *36*, 2550-2589.

Alkene oxidation often implies processes that incorporate oxygen atoms in the final oxidized molecule. Thus, identifying chemical oxidants that do not deliver oxygen atoms to the alkene is a significant challenge. In Chart 2.2 reduction potentials of some prevalent classes of alkenes are compared with common ground and excited states oxidants in order to understand when and how alkenes oxidation is possible.

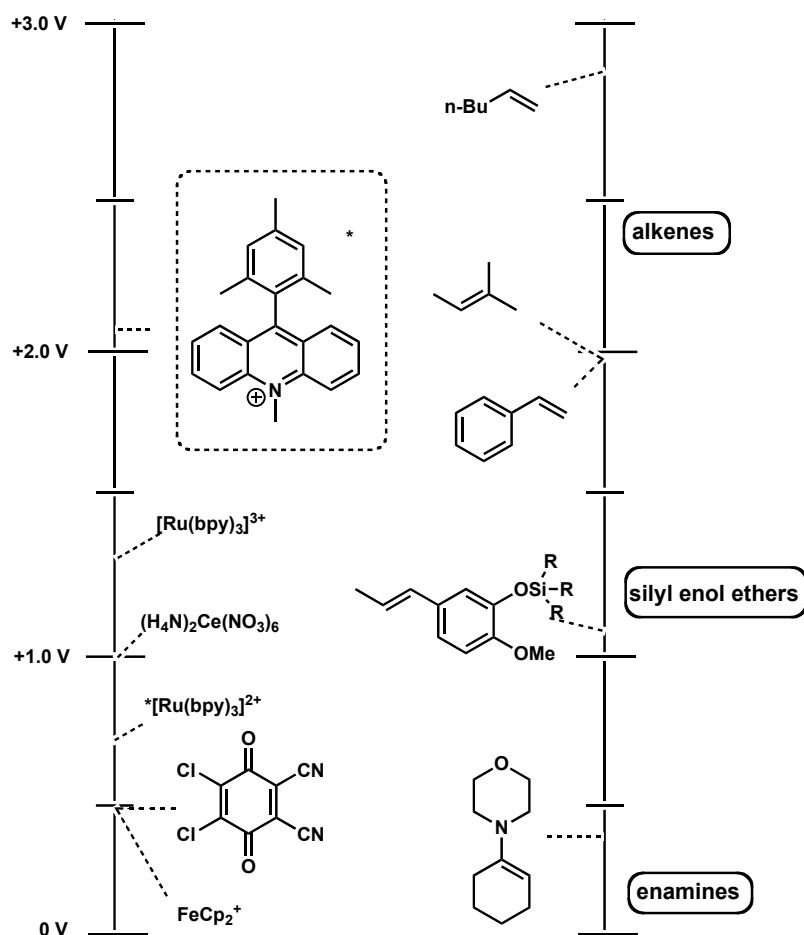


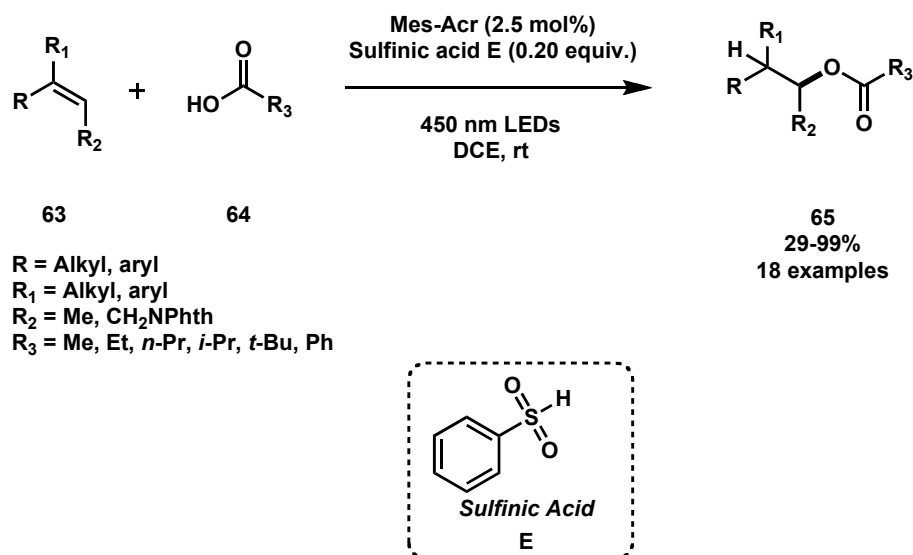
Chart 2.2 Comparison of some reduction potentials to some common alkene oxidation potentials⁷⁰

Electron-rich alkenes such as enamines and silyl enol ethers, which have low oxidation potentials, can be easily oxidized by common ground state oxidants such as ferrocenium ion ($\text{FeCp}_2^+ = +0.4 \text{ V vs. SCE}$), 2,3-dichloro-5,6-dicyano-1,4-benzoquinone (DDQ = $+0.5 \text{ V vs. SCE}$) or cerium(IV) ammonium nitrate (CAN = $+1.0 \text{ V vs. SCE}$). On the other hand, simple alkenes like terminal styrenes and mono-, di- and tri-substituted aliphatic alkenes have oxidation potentials upper than $+1.7 \text{ V}$. At this stage, there are no ground state oxidants that can oxidize those substrates.⁷¹ Providentially, some organic

⁷⁰ Nicewicz, D.A.; Hamilton, D.S. *Synlett* **2014**, 25, 1191-1196.

⁷¹ Connelly, N.G.; Geiger, W.E. *Chem. Rev.* **1996**, 96, 877-910.

photooxidants, such as 9-mesityl-10-methylacridinium perchlorate ($\lambda = 430$ nm), have high reduction potentials in the excited state (excited state reduction potential in excess of +2.06 V) and have been proposed to have a long-lived charge transfer excited state.⁷² In this context, by using supportable light sources for an innovative visible-light assisted methodology, the employment of visible-light for the formation of open-shell species has been considered as a more sustainable and efficient approach.⁷³ Several examples of visible-light mediated alkene hydrofunctionalizations have been reported by Nicewicz *et al.*⁷⁴ For example, in 2013, this author described a regioselective visible-light induced *anti*-Markovnikov addition of carboxylic acids to alkenes catalyzed by acridinium salt (**Mes-Acr**). They took advantage from the high reduction potential of the Fukuzumi photocatalyst ($E_{red}^0 = +2.07$ V vs. SCE in CH₃CN) to oxidize a great variety of alkenes and combine them with numerous nucleophiles (Scheme 2.2).^{74[e]} Since the proposed reaction mechanism proposed implies a hydrogen atom donor, the authors developed a metal-free strategy by combining the photocatalyst with various additives, as shown in Scheme 2.2 (see chapter 1, page 43) and get coupling products in moderate to excellent yields.



Scheme 2.2. Photocatalyzed *anti*-Markovnikov addition of carboxylic acids to alkenes

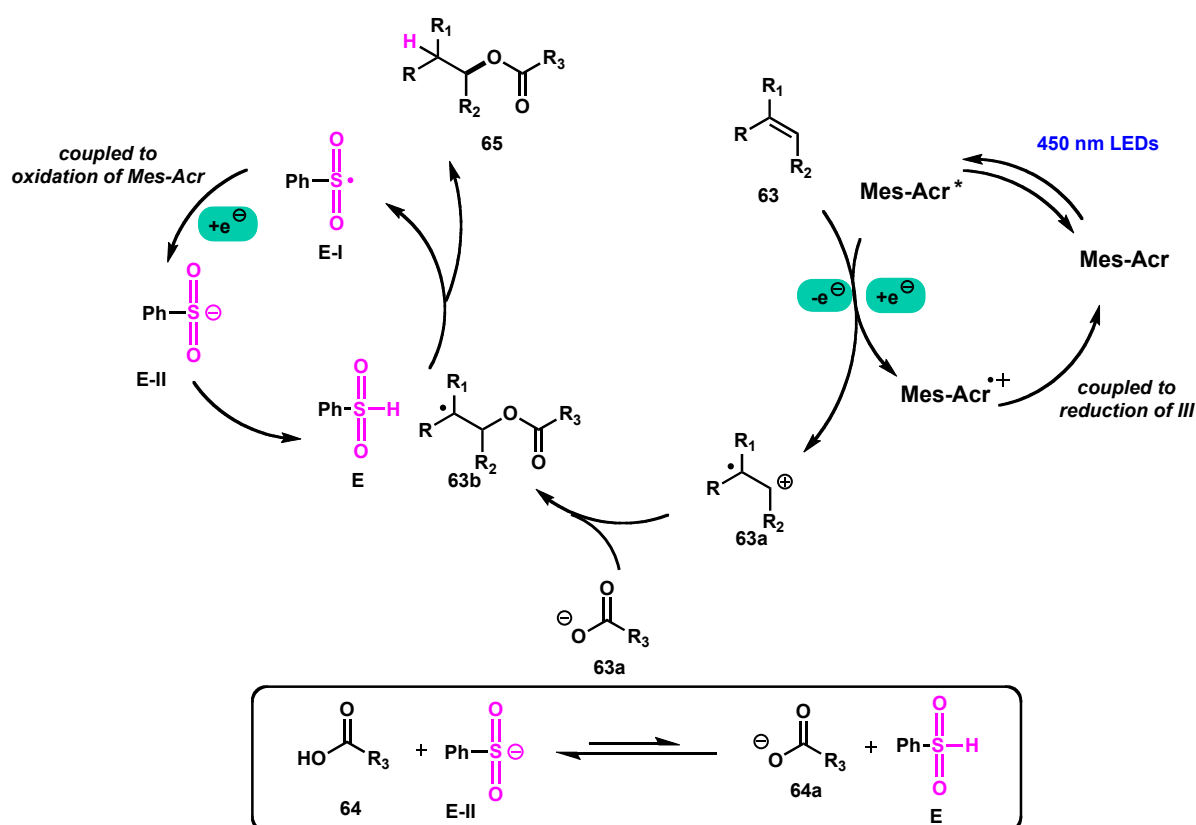
⁷² Ohkubo, K.; Mizushima, K.; Iwata, R.; Souma, K.; Suzuki, N.; Fukuzumi, S. *Chem. Commun.* **2009**, *46*, 601-603.

⁷³ (a) Beatty, J.W.; Stephenson, C.R.J. *Acc. Chem. Res.* **2015**, *48*, 1474-1478. (b) Prier, C.K.; Rankic, D.A.; MacMillan, D.W.C. *Chem. Rev.* **2013**, *113*, 5322-5363.

⁷⁴ (a) Romero, N.A.; Nicewicz, D.A. *Chem. Rev.* **2016**, *116*, 10075-10166. (b) margrey, K.A.; Nicewicz, D.A. *Acc. Chem. Res.* **2016**, *49*, 1997-2006. (c) Nguyen, T.M.; Nicewicz, D.A. *J. Am. Chem. Soc.* **2013**, *135*, 9588-9591. (d) Hamilton, D.S.; Nicewicz, D.A. *J. Am. Chem. Soc.* **2012**, *134*, 18577-18580. (e) Perkowski, A.J.; Nicewicz, D.A. *J. Am. Chem. Soc.* **2013**, *135*, 10334-10337. (f) Zeller, M.A.; Riener, M.; Nicewicz, D.A. *Org. Lett.* **2014**, *16*, 4810-4813.

The use of sulfinic acid derivatives and related H-atom donor is crucial for the reproducibility of the reaction. A photocatalytic mechanism involving a reductive cycle of **Mes-Acr** in combination with H-abstraction process has been proposed. In the first step, initial oxidation of the unsaturated substrate by the excited state of the photocatalyst afforded the alkene radical cation **63a**. The latter can react with formed carboxylate leading to the carbon centered radical **63b**.

Meanwhile, acid-base equilibrium generates the active form of H-atom donor **E** in the presence of carboxylic acid, which can undergo H-abstraction to give rise to the desired product **65**. As the resulting benzenesulfinyl radical **E-I** has an oxidation potential higher enough to oxidize **Mes-Acr**, the photocatalytic process was regenerated (Scheme 2.3).

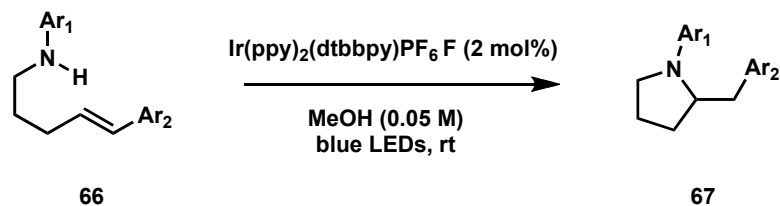


Scheme 2.3. Proposed photocatalyzed mechanism for *anti*-Markovnikov addition of carboxylic acids to alkenes

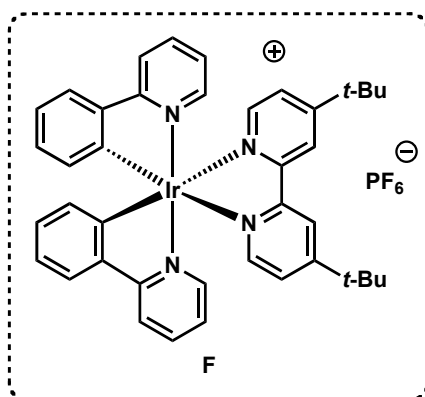
A complementary approach for an intramolecular hydrofunctionalization has been proposed by Knowles *et al.*⁷⁵ who described a visible light-induced hydroamination by

⁷⁵ Musacchio, A.J.; Nguyen, L.Q.; Beard, G.H.; Knowles, R.R. *J. Am. Chem. Soc.* **2014**, *136*, 12217-12220.

using simple secondary amines in the presence of iridium-based photocatalyst (Scheme 2.4).

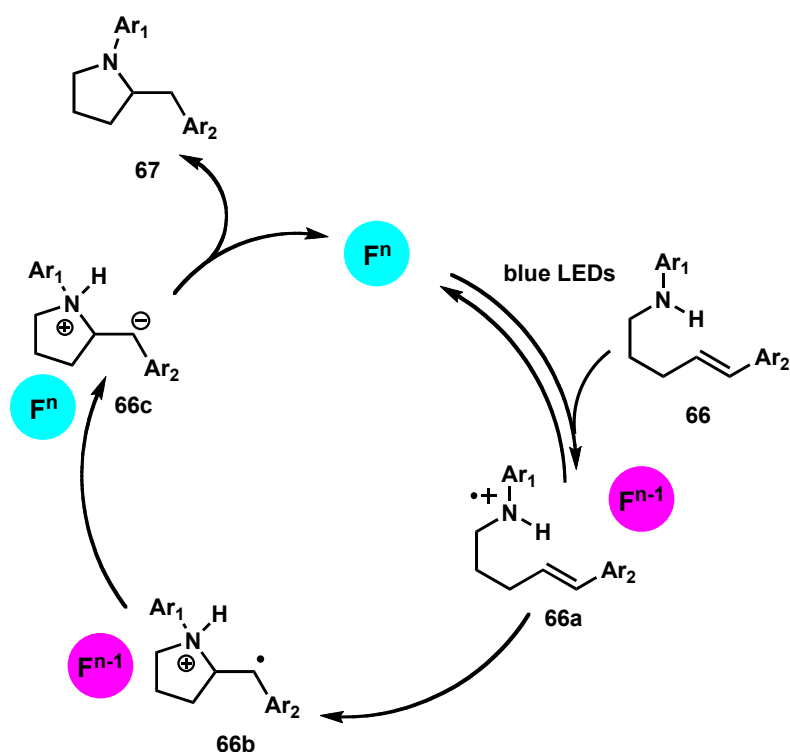


$\text{Ar}_1 = \text{C}_6\text{H}_5, 2\text{-(Me)C}_6\text{H}_4, 3\text{-(Me)C}_6\text{H}_4, 4\text{-(F)C}_6\text{H}_4, 2\text{-(Cl)C}_6\text{H}_4$
 $\text{Ar}_2 = \text{C}_6\text{H}_5, 4\text{-(MeO)C}_6\text{H}_4, 4\text{-(F)C}_6\text{H}_4, 4\text{-(CF}_3\text{)C}_6\text{H}_4, 4\text{-(CN)C}_6\text{H}_4, 2\text{-(Cl)C}_6\text{H}_4$



Scheme 2.4. Visible light mediated intramolecular hydroamination of aryl olefins with Iridium-based photocatalyst

In the proposed catalytic cycle, the excited state of the photocatalyst **F** oxidizes the secondary amine precursor to afford ammonium radical cation **66a**, after single electron transfer reaction. The latter intermediate undergoes olefin addition to achieve C–N carbon centered adduct **66b**, which can react with the reduced form of the photocatalyst **F**, leading to the corresponding carbanion **66c**. At this stage, a favorable proton transfer reaction should yield the desired heterocyclic compound **67** closing the catalytic cycle (Scheme 2.5). This technology, which is mechanistically distinct from the one reported by Nicewicz, has then been applied for the synthesis of natural products.



Scheme 2.5. Proposed catalytic cycle for the intramolecular hydroamination of aryl olefins

In classical radical reactions, most common radical initiators used in organic synthesis and catalysis, such as azo-compounds or peroxides, act as weak bond cleaver by forming new radical species under harsh conditions.

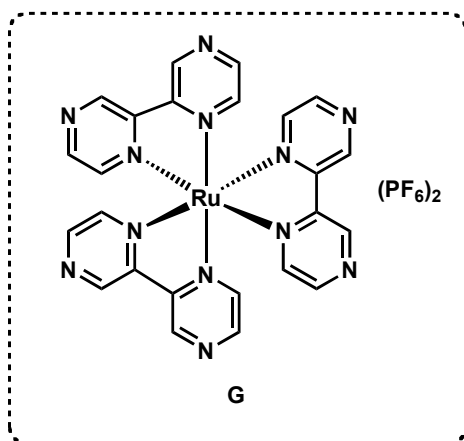
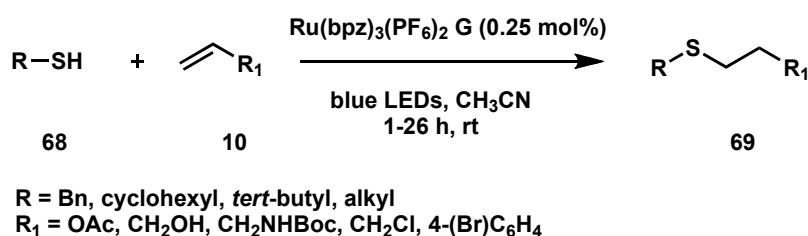
Similarly, oxidants and reductants compounds can serve as radical initiators through single electron transfer reactions and used in stoichiometric amounts in catalyzed reactions. For instance, the catalyst must be able to regenerate the initiator and this is highly depending on the energy required or the co-catalyst employed. Generally, light sources are used as co-catalysts and photons are necessary to close catalytic cycles. When short chains are involved, this type of catalytic initiation can be named “smart initiation”, as recently introduced by Studer and Curran.⁷⁶

In this regard, an interesting example of visible light-mediated hydrofunctionalization of alkenes with thiols has been described by Yoon and coworkers.⁷⁷ Using visible light as initiator, a catalytic radical methodology employing transition metal complexes as photocatalysts, has been found to be efficient to afford thiol-ene coupled products in excellent yields (73-99%).

⁷⁶ Studer, A.; Curran, D.P. *Angew. Chem. Int. Ed.* **2015**, *54*, 2-47.

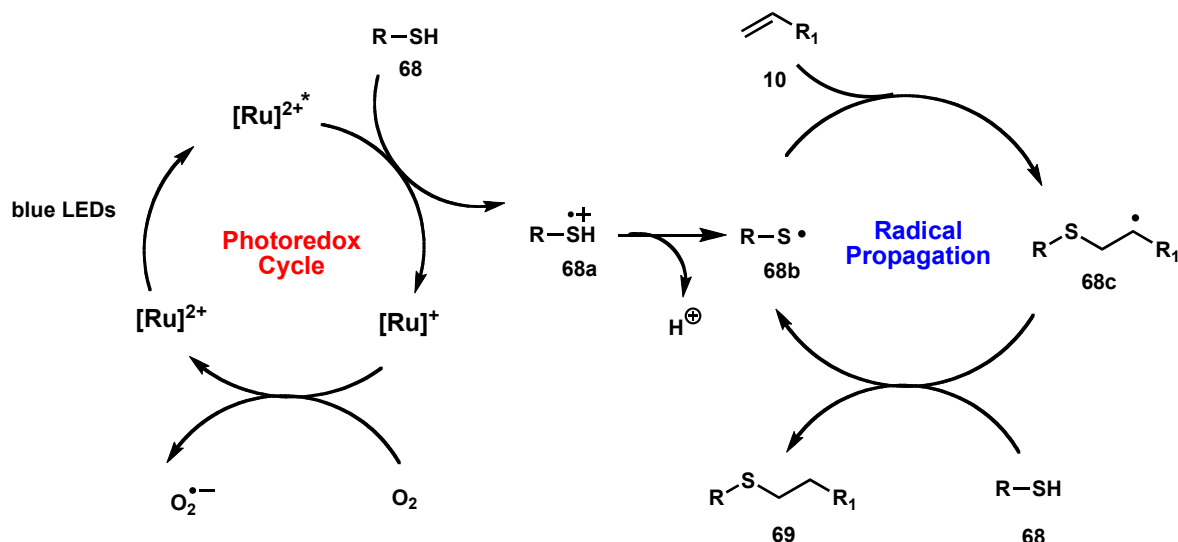
⁷⁷ Tyson, E.L.; Ament, M.S.; Yoon, T.P. *J. Org. Chem.* **2013**, *78*, 2046-2050.

On the basis of catalytic intramolecular hydroamination studied by Knowles *et al.* and on the fact that secondary amines could be easily oxidized by a transition metal complex, the group of Yoon has demonstrated that one-electron photooxidation of thiols *via* excited state of a ruthenium-based photocatalyst could be conducted under mild conditions, at room temperature ranging from 1 to 26 h (Scheme 2.6).



Scheme 2.6. Visible-light photocatalytic hydrothiolation of alkenes with ruthenium-based photocatalyst

A photoredox catalytic initiation and reaction propagation work simultaneously in a synergic way. First, irradiating Ru(bpz)₃(PF₆)₂ a metal-to-ligand charge transfer (MLCT) was formed, generating a metal-center excited state able to promote one-electron oxidation of thiol **68**. The radical cationic intermediate **68a** generates thyl radical **68b**, upon fast deprotonation, leading to the radical propagation process. The olefin addition of **10** to thyl radical **68b** can form regioselectively the carbon centered radical **68c** yielding the *anti*-Markovnikov adduct **69** after H-atom abstraction from another molecule of unreacted thiol and regenerates the radical chain process (Scheme 2.7).



Scheme 2.7. Proposed mechanism for the catalytic visible light mediated hydrothiolation of alkenes

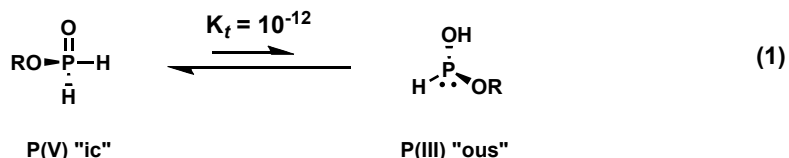
Although the synthetic relevance of the photoredox and smart initiation approaches to promote hydrofunctionalization of alkenes is proven, they both require the presence of a lone pair at the nucleophilic center to be oxidized (Knowles' approach + smart initiation) or to be added to the double bond (Nicewicz). This implies that none of these approaches could be applied to hydrophosphinylation of alkenes with H-phosphinates as the latter exist predominantly in their P(V) form.

Before introducing our approach to circumvent this issue, let us first introduce type of reaction and present previous reports in this field of organic chemistry.

2.3. Hydrophosphinylation reaction with phosphinic acid derivatives

2.3.1. Hypophosphorus derivatives

A particular class of organophosphorus compounds is constituted by phosphorus containing acids, [P(O)(OH)]. Specific members of this group of compounds are characterized by the presence of the phosphinylidene group, P(O)-H, that exist in the P(V) and P(III) forms through a tautomeric equilibrium (Scheme 2.8).⁷⁸



Scheme 2.8. Tautomeric equilibrium of phosphinic acid derivatives between P(V) and P(III) forms

⁷⁸ Janesko, B.G.; Fisher, H.C.; Bridler, M.J.; Montchamp, J.-L. *J. Org. Chem.* **2015**, *80*, 10025-10032.

Phosphinic acid derivatives are potentially versatile substrates for the synthesis of a variety of organophosphorus derivatives, including phosphonates and phosphinates, as well as primary phosphines, secondary phosphine oxides or dichlorophosphines, to name a few examples (Figure 2.1).

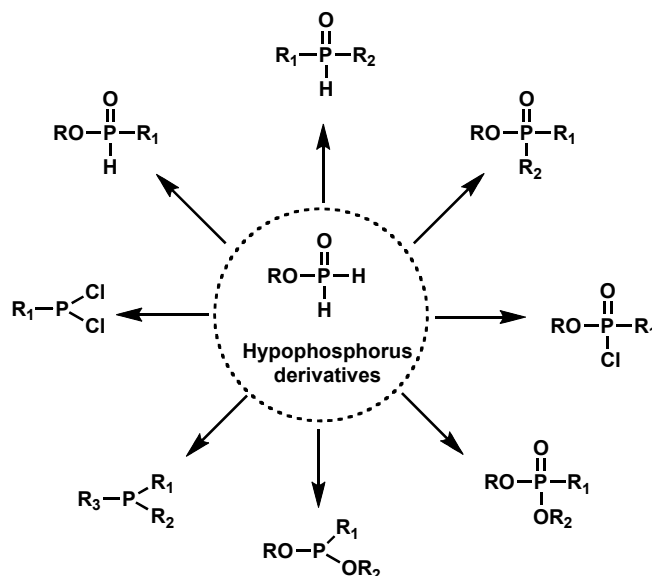


Figure 2.1. Hypophosphorus derivatives as versatile substrates for the synthesis of a variety of organophosphorus derivatives

Phosphinic acids have deeply been used to achieve pharmaceutical activity through the inhibition of important classes of enzymes, such as proteases and esterases.⁷⁹ Figure 2.2 summarizes some important biologically active hypophosphorus active compounds.

⁷⁹ For some representative examples of biologically-active phosphinic acids, see: (a) Gill, S.H.; Eisenber, D. *Biochemistry* **2001**, *40*, 1903-1912. (b) Feng, Y.; Coward, J.K. *J. Med. Chem.* **2006**, *49*, 770-788. (c) Tian, F.; Montchamp, J.-L.; Frost, J.W. *J. Org. Chem.* **1996**, *61*, 7373-7381. (d) Leung, D.; Abbenante, G.; Fairlie, D.P. *J. Med. Chem.* **2000**, *43*, 305-341.

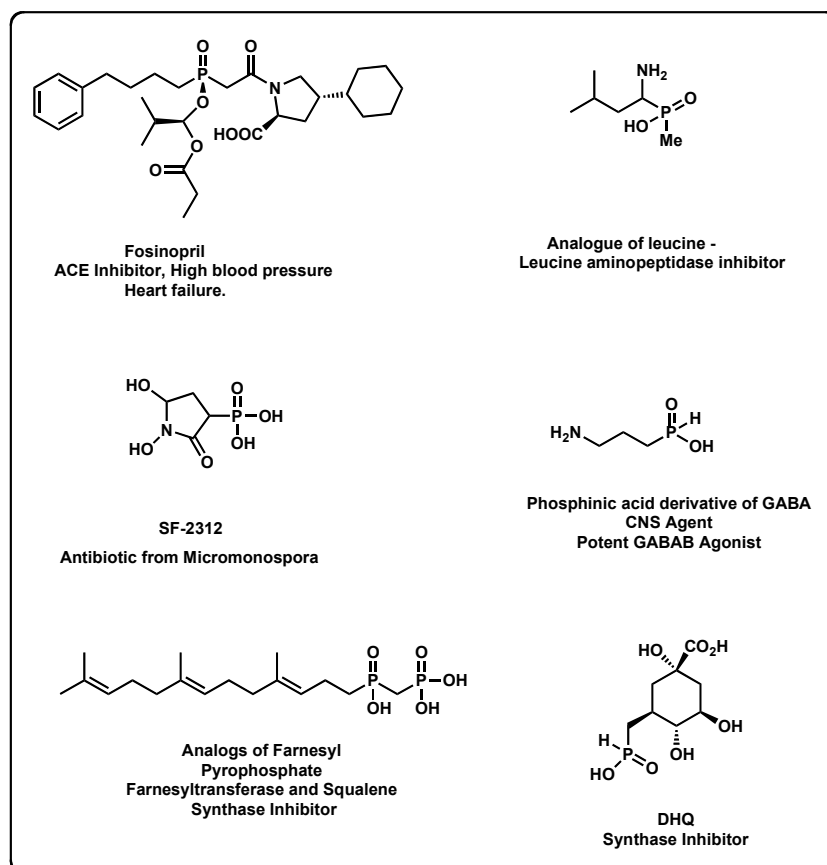


Figure 2.2. Different examples of phosphorylated drugs containing hypophosphorus acid derivatives

2.3.2. Hydrophosphinylation reaction

The term hydrophosphinylation concerns the addition of hypophosphorus acid or its derivatives to C-C double bond. It is one of the most convenient and useful processes to provide phosphorylated drugs, such as antibacterial, antiviral or antitumor agents.⁸⁰

There are several methodologies to afford organophosphorus compounds focusing on the implementation of Grignard reactions⁸¹, Michaelis-Arbuzov reaction⁸² and radical additions.⁸³ During the last decade, a huge progress has been made in transition metal-⁸⁴ catalyzed C-P bond formation as well as in free-radical reactions or microwave activations.⁸⁵ The addition of phosphinates to unsaturated hydrocarbon bonds is perhaps the most important and atom-efficient reaction for the preparation of organophosphorus intermediates.

⁸⁰ Mastalerz, P.; Kafarski, P. *Aminophosphoric and Aminophosphinic Acids*, J Wiley & Sons Ed **2000**, 1.

⁸¹ Pirat, J.-L.; Virieux, D.; Drag, M.; Sobecki, M.; Midrier, C.; Filippini, D.; Volle, J.-N. *Synthesis* **2011**, 15, 2490-2494.

⁸² (a) Falbe, J.; Paatz, R.; Korte, F. *Chem. Ber.* **1965**, 98, 2312-2316. (b) Gali, H.; Karra, S.R.; reddy, V.S.; Katti, K.V. *Angew. Chem. Int. Ed.* **1999**, 38, 2020-2023.

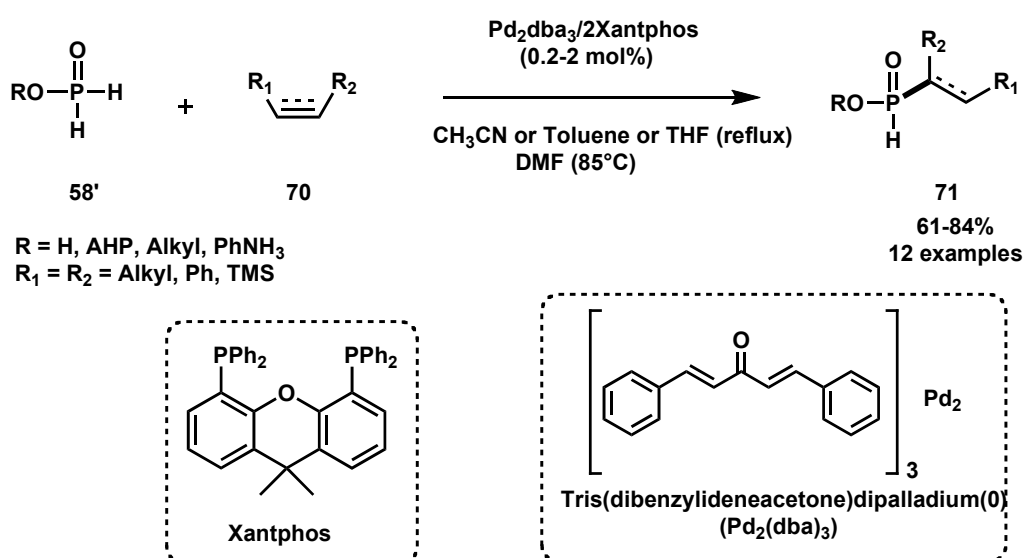
⁸³ Deprèle, S.; Montchamp, J.-L. *J. Org. Chem.* **2001**, 66, 6745-6755.

⁸⁴ Deprèle, S.; Montchamp, J.-L. *J. Am. Chem. Soc.* **2002**, 124, 9386-9387.

⁸⁵ Stockland, R. A. Jr.; Taylor, R. I.; Thompson, L. E.; Patel, P. B. *Org. Lett.* **2005**, 7, 851-853.

2.3.3. Metal-catalyzed hydrophosphinylation

In 2005, Montchamp and co-workers⁸⁶ described the first metal-catalyzed hydrophosphinylation of unactivated unsaturated substrates with hypophosphorus derivatives. They developed a general palladium catalyzed addition of phosphinic acid (H_3PO_2), anilinium hypophosphite (AHP) and alkyl phosphinates to alkenes and alkynes under catalytic conditions. Noteworthy, this reaction did not require strictly anhydrous conditions and the competing transfer hydrogenation could be minimized depending on the choice of the ligand complexed to the palladium (Scheme 2.9).

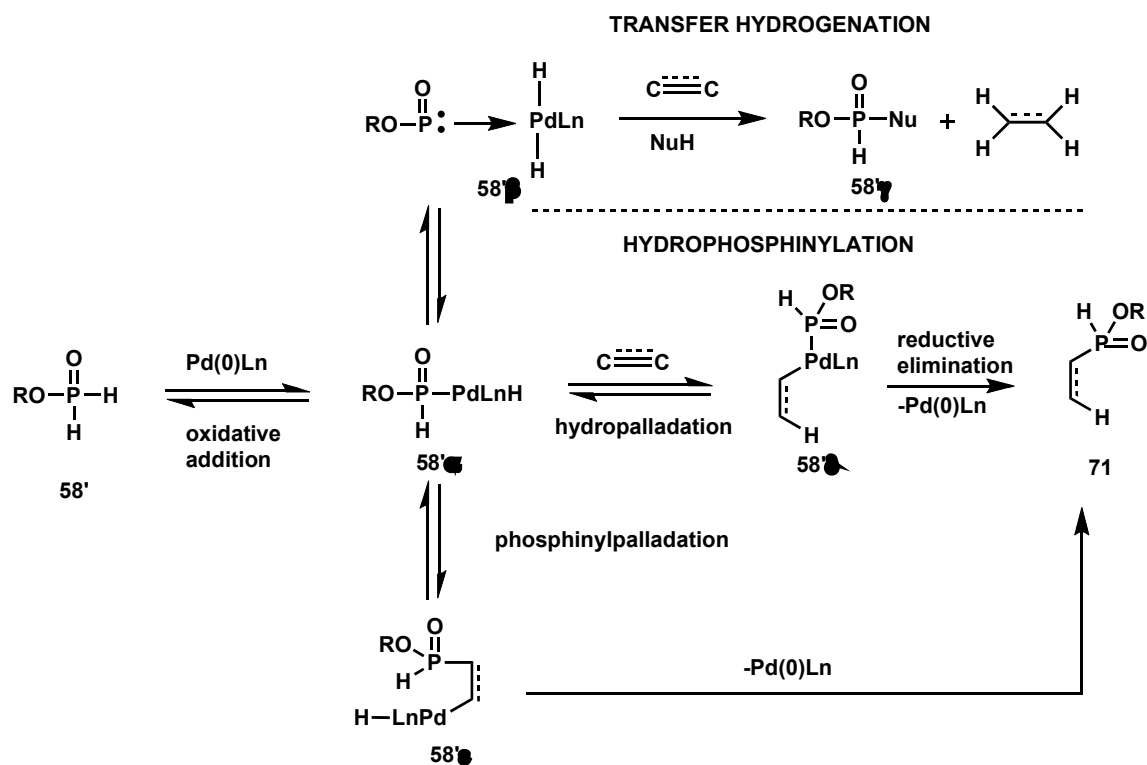


Scheme 2.9. Palladium catalyzed hydrophosphinylation of unsaturated alkenes and alkynes with hypophosphorus derivatives

During this work, they realized that the competing transfer hydrogenation pathway⁸⁷ could represent the unique opportunity for catalytic C–P bond formation, if the reactivity of the phosphinyl palladium hydride intermediate, shown in Scheme 2.10, could be trapped before its transformation into a palladium dihydride species. Based on this concept, the authors have developed a catalytic C–P bond formation reaction, which has been applied to numerous alkenes and alkynes.

⁸⁶ Montchamp, J.-L. *Organomet. Chem.* **2005**, 690, 2388-2406.

⁸⁷ For references on the catalytic transfer hydrogenation with hypophosphorus derivatives, see: (a) Brieger, G.; Nestrück, T.J. *Chem. Rev.* **1974**, 74, 567-580. (b) Johnstone, R.A.W.; Wilby, A.H.; Entwistle, A.I. *Chem. Rev.* **1985**, 85, 129-170. (c) Sala, R.; Doria, G.; Passarotti, C. *Tetrahedron Lett.* **1984**, 25, 4565-4568.



2.3.4. Triethylborane and radical initiators-assisted hydrophosphinylation

Hydrophosphinylation reaction was performed by employing radical initiators such as *tert*-butylperoxyde, benzoyl peroxide and azobisisobutyronitrile (AIBN).⁸⁸ Obviously, these methodologies have shown some drawbacks, such as the requirement of a toxic radical initiator, and the use of large excess among the reagents employed.⁸⁹

In this regard, Montchamp *et al.*⁹⁰ have published an innovative protocol describing the triethylborane-initiated addition of hypophosphites derivatives to olefins. This method proceeds under neutral conditions in the presence of oxygen and tolerates a wide range of functional groups. Usually, free-radical reactions initiated by Et₃B are conducted with a stoichiometric amount and even a 2- to 5-fold excess of the borane.⁹¹

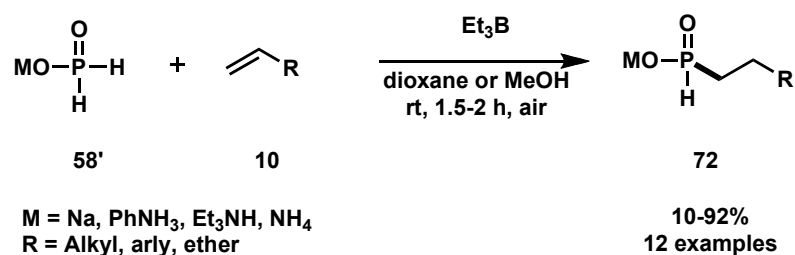
Alternatively, with an equimolar amount of Et₃B relative to the alkene better results have been obtained (Scheme 2.11), even if the introduction of air still appeared to be a delicate parameter.

⁸⁸ Williams, R.-H.; Hamilton, L.A. *J. Am. Chem. Soc.* **1955**, *77*, 3411-3412.

⁸⁹ (a) Piettre, S.R. *Tetrahedron Lett.* **1996**, *37*, 2233-2234. (b) Zeiss, H.-J. *Tetrahedron Lett.* **1992**, *38*, 8263-8266. (c) Farnham, W.B.; Murray, R.K.; Mislow, K. *J. Chem. Soc., Chem. Commun.* **1971**, 146-147.

⁹⁰ Deprèle, S.; Montchamp, J.-L. *J. Org. Chem.* **2001**, *66*, 6745-6755.

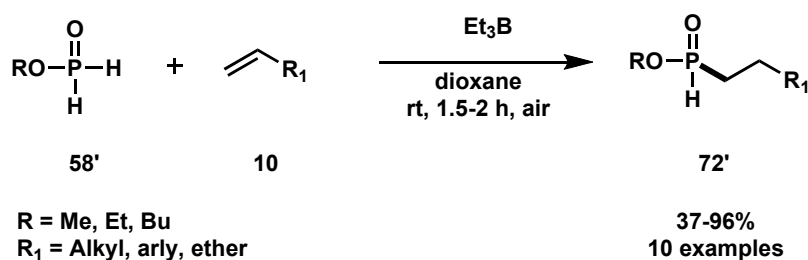
⁹¹ (a) Mase, N.; Watanabe, Y.; Toru, T. *J. Org. Chem.* **1997**, *62*, 7794-7800. (b) Barton, D.H.R.; Jang, D.O.; Jaszberenyi, J.C. *Tetrahedron Lett.* **1990**, *31*, 4681-4760.



Scheme 2.11. Triethylborane-initiated hydrophosphinylation of terminal alkenes with hypophosphorus salts

The reaction proceeded well by employing hypophosphite salts (M = Na, PhNH₃, Et₃NH, NH₄), since they were less Et₃B/air sensitive than alkyl hypophosphites containing O-Me and O-Et groups. Dealing with alkyl phosphinates, before the investigation of Montchamp, only one report describing the hydrophosphinylation reaction of butyl phosphinates and alkenes could be found in the literature.⁹² Alkyl phosphinate was reacted with allyl acetate in the presence of *tert*-butylperoxyde at 130-140°C for 10 h leading to the desired C–P coupling adduct in 25% yield. It should be mentioned that the decomposition of alkyl phosphinate was not deeply investigated.

Montchamp and co-workers applied successfully Et₃B/air mediated hydrophosphinylation to methyl, ethyl and butyl phosphinates with various alkenes (Scheme 2.12).²³



Scheme 2.12. Triethylborane-initiated hydrophosphinylation of terminal alkenes with hypophosphorus salts

They demonstrated that alkyl phosphinates were much more reactive than hypophosphite salts under these conditions, even when a lower amount of initiator (0.1-0.2 equiv.) was used.

⁹² Aleksandrova, I.A.; Ufimtseva, M.I. *Bull. Acad. Sci. USSR, Div. Chem. Sci.* **1971**, *6*, 1218.

Worthy of note is that due to the fast decomposition of alkyl phosphinates, as already mentioned in literature,⁹³ ³¹P-NMR conversions are higher compared to the isolated yields, due to the hydrolysis of hypophosphite esters on silica gel.

Although particularly efficient these approaches require transition metals, ligands and relatively high temperatures. There is thus still a room for milder and less toxic processes.

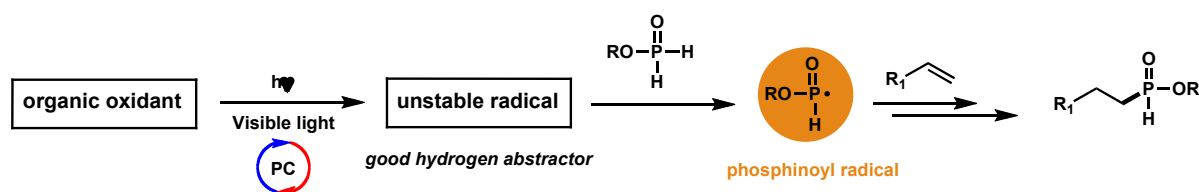
2.4. Results and Discussion

2.4.1. The photocatalytic approach

The main objective of this research project was to develop a mild approach to afford C–P bond forming reactions in the context of H-phosphinates *via* visible light mediated photocatalysis.

H-phosphinates chemistry has extensively been studied by the group of Montchamp^{23, 94}, who developed, over the last decade, elegant methodologies for selective P–H functionalizations of phosphinates and related compounds.

As mentioned above, phosphinates are known to exist mainly in their P(V) tautomeric form ($K_t = 10^{-12}$),¹³ and thus any strategy described in literature⁹⁵ has proved to be inefficient in promoting the hydrophosphinylation of unactivated alkenes. In order to circumvent this issue, we hypothesized that the use of diaryliodonium salts as external photooxidants that form a highly reactive radical species under photoredox conditions, could perform the abstraction of hydrogen from secondary P(V) derivatives, leading to phosphinoyl radical (Scheme 2.13).⁹⁶



⁹³ (a) Fitch, S.J. *J. Am. Chem. Soc.* **1964**, *86*, 61. (b) Gallagher, M.J.; Honegger, H. *Tetrahedron Lett.* **1977**, *34*, 2987.

⁹⁴ Ortial, S.; Fisher, H.C.; Montchamp, J.-L. *J. Org. Chem.* **2013**, *78*, 6599-6608.

⁹⁵ (a) Margrey, K.A.; Nicewicz, D.A. *Acc. Chem. Res.* **2016**, DOI: 10.1021/acs.accounts.6b00304. (b) Hamilton, D.S.; Nicewicz, D.A. *J. Am. Chem. Soc.* **2012**, *134*, 18577-18580. (c) Perkowski, A.J.; Nicewicz, D.A. *J. Am. Chem. Soc.* **2013**, *135*, 10334-10337. (d) Nguyen, T.M.; Nicewicz, D.A. *J. Am. Chem. Soc.* **2013**, *135*, 9588-9591. (e) Musacchio, A.J.; Nguyen, L.Q.; Beard, G.H.; Knowles, R.R. *J. Am. Chem. Soc.* **2014**, *136*, 12217-12220. (f) Studer, A.; Curran, D.P. *Angew. Chem. Int. Ed.* **2016**, *55*, 58-102. (g) Keylor, M.H.; Park, J.E.; Wallentin, C.-J.; Stephenson, C.R.J. *Tetrahedron* **2014**, *70*, 4264-4269. (h) Keshari, T.; Yadav, V.K.; Srivastava, V.P.; Yadav, L.D.S. *Green Chem.* **2014**, *16*, 3986-3992. (i) Fadeyi, O.O.; Mousseau, J.J.; Feng, Y.; Allais, C.; Nuhant, P.; Chen, M.Z.; Pierce, B.; Robinson, R. *Org. Lett.* **2015**, *17*, 5756-5759.

⁹⁶ (a) Xuan, J.; Zeng, T.-T.; Chen, J.-R.; Lu, L.-Q.; Xiao, W.-J. *Chem. –Eur. J.* **2015**, *21*, 4962-4965. (b) Quint, V.; Morlet-Savary, F.; Lohier, J.-F.; Lalevée, J.; Gaumont, A.-C.; Lakhdar, S. *J. Am. Chem. Soc.* **2016**, *138*, 7436-7441. (c) Peng, P.; Peng, L.; Wang, G.Y.; Wang, F.Y.; Luo, Y.; Lei, A.W. *Org. Chem. Front.* **2016**, *3*, 749-752.

Scheme 2.13. the formation of phosphinoyl radical by means of the use of an organic oxidant.

We selected diphenyliodonium triflate **73** as external oxidant to abstract hydrogen from H-phosphate derivatives (Figure 2.3). This compound is capable to abstract hydrogen from alkyl phosphinates thanks to the low bond dissociation energy (BDE) of these molecules (81 kcal/mol).

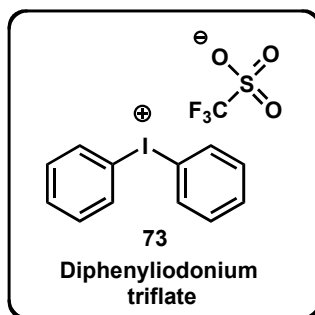


Figure 2.3. Selected photooxidant for our hydrophosphinylation reaction

Iodonium salts have mainly been employed as photoinitiators in photopolymerisation processes, where they are used along with visible photocatalysts. Aryl radical could be generated and abstracts a variety of X–H bonds (X = B, Si). Inspired from this concept, we hypothesized that we could use the same technology in organic chemistry and for C–P bond formations in particular.

2.4.2. Optimization studies

The above described reaction is expected to be thermodynamically achievable as redox potentials of excited states of some common organic photocatalysts⁹⁷ can efficiently reduce diphenyliodonium triflate **73**, whose $E_{red}^0 = -0.2$ V vs. SCE.⁹⁸ To confirm this hypothesis, we investigated the reactivity of ethyl phosphinate **58a** with cyclohexene **59a** in the presence and absence of **73** and different photocatalysts under visible light irradiation (Table 2.1).

Table 2.1. Identification of the optimal reaction conditions

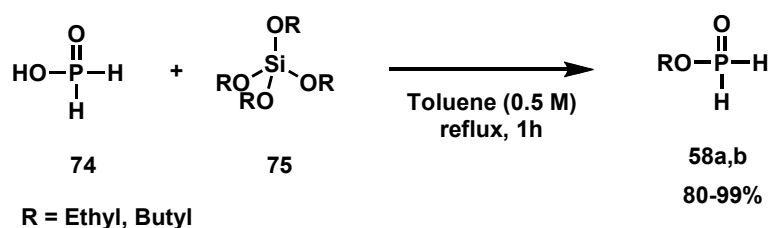
⁹⁷ Nicewicz, D.A.; Nguyen, T.M. *ACS Catal.* **2014**, *4*, 355-360.

⁹⁸ Fouassier, J.-P.; Lalevée, J. *Photoinitiators for Polymer Synthesis: Scope, Reactivity and Efficiency*, Wiley-VCH; Weinheim, **2012**.

reaction proceeded well in toluene (entry 8) or in a (1:1) mixture DMF/Toluene (entry 6), while it did not work when acetonitrile (entry 7), methanol (entry 9), dichloromethane (entry 10) or ethyl acetate (entry 11) were tested as solvents.

Control experiments revealed the essential role of light (entry 12) and the oxidant (entry 13) as only traces of **60a** have been detected in their absence. The photocatalyst was found to be fundamental for this reaction (entry 14) as only 18% conversion was observed even after long reaction time (72h). In order to exclude the involvement of UV light, as dihenyliodonium triflate **73** is well-known to be reduced under UV light,¹⁰⁰ we irradiated the sample through a UV-filter (75% w/v NaNO₂ solution, cut-off: $\lambda = 400$ nm). A reasonable conversion was observed (entry 15), thus attesting that the reaction is visible light mediated. Importantly, the reaction did not require inert conditions or degassed solvents.

Alkyl phosphinates were prepared *via* an already mentioned method,¹⁰¹ as shown in Scheme 2.14, and used as a 0.5 M stock solution in toluene.



Scheme 2.14. Synthesis of ethyl and butyl phosphinates

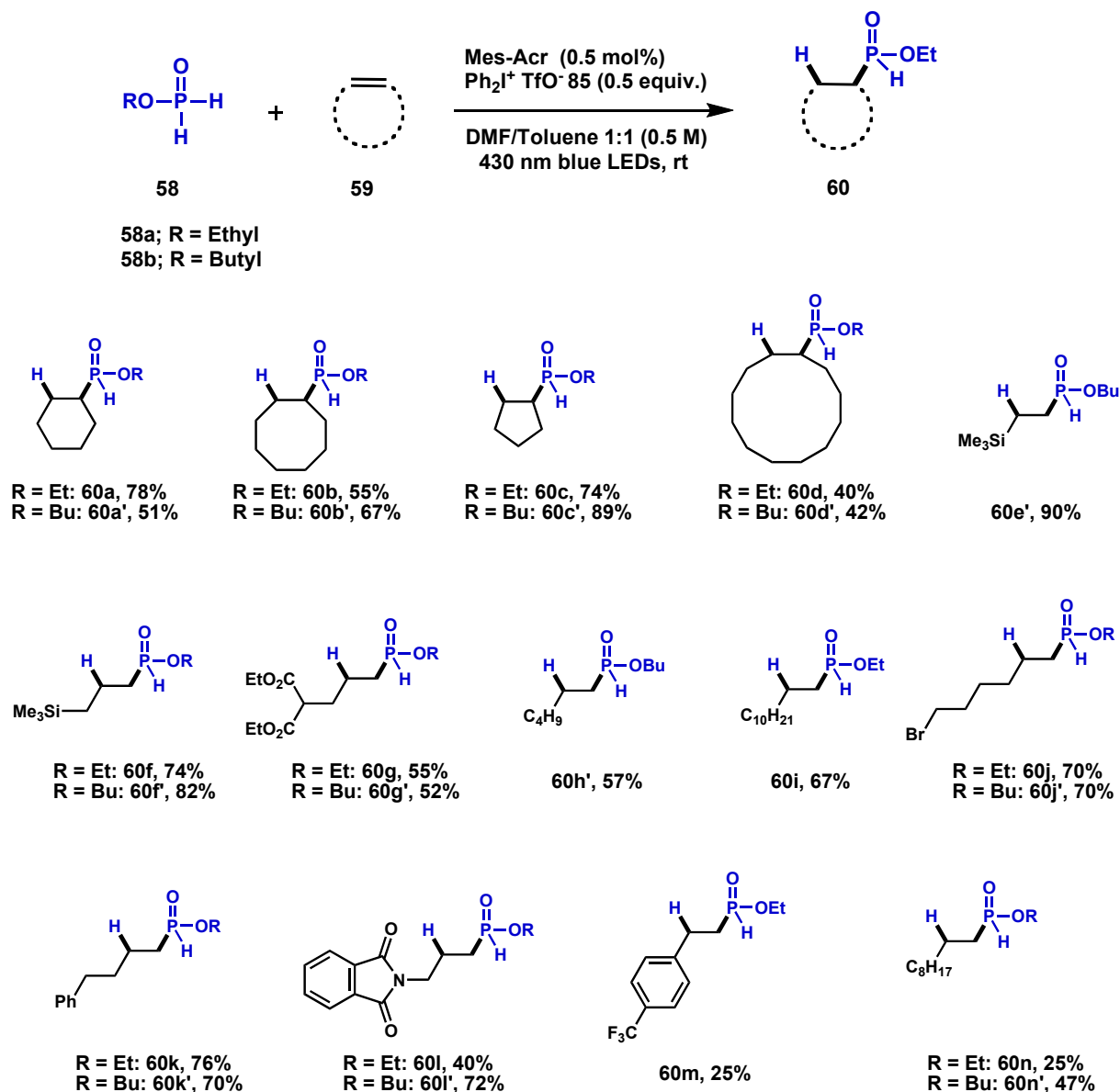
2.4.3. Scope and limitations of the hydrophosphinylation reaction

After identifying the optimized parameters, we turned our attention to studying the scope of the reaction with respect to the alkenes **59a-n** (Table 2.2).

Table 2.2. Scope and limitations of visible light mediated hydrophosphinylation^a

¹⁰⁰ Ortyl, J.; Popielarz, R. *Polimery* **2012**, *57*, 7-8.

¹⁰¹ J.-L. Montchamp, *J. Organomet. Chem.* **2005**, *690*, 2388-2406.



^aReactions were conducted with 2.0 equiv. of **66a,b**, 1.0 equiv. of **67**, and 0.5 equiv. of **85** in the presence of 0.5 mol% of **Mes-Acr** in a 1:1 mixture of DMF/Toluene for 24h under blue light irradiation (5W).

Fair to good yields, ranging from 25 to 74%, were isolated for the reaction of ethyl phosphinate **58a** with alkenes **59a-d**, **59f-g** and **59i-n**. As shown in Table 2.2, the reaction worked well with the both cyclic **59a-d** and non-cyclic **59f-g**, **59i-j**, **59n** alkenes. The reaction tolerates functionalized groups, such as trimethylsilyl, ester and bromide moieties (**60f**, **60g** and **60i** respectively). Although the ³¹P-NMR conversion for the alkenes **59i-n** was higher than 50%, the adduct isolated yields dropped significantly to 40% and 25%, respectively, probably due to the high sensitivity or hydrolysis of *H*-phosphinates esters during purification process on silica gel.¹⁰²

¹⁰² Antczak, M.I.; Montchamp, J.-L. *Synthesis* **2006**, 3080-3084.

When butyl phosphinate **58b** was combined with unactivated alkenes (Table 2.2), under the optimized conditions, the desired adducts **60a'-h'**, **60j'-l'** and **60n'** were isolated in moderate to good yields ranging from 42 to 90%. This is in agreement with the studies reported by Montchamp, who showed that butyl phosphinates **60'** are more stable than ethyl phosphinate **60**.

Noteworthy, the reaction is highly regioselective, as only *anti*-Markovnikov adduct was observed in all the tested cases. The ¹H-NMR showed clearly the formation of β-adduct when ethyl phosphinate **58a** reacted with the alkene **59m** (Figure 2.4).

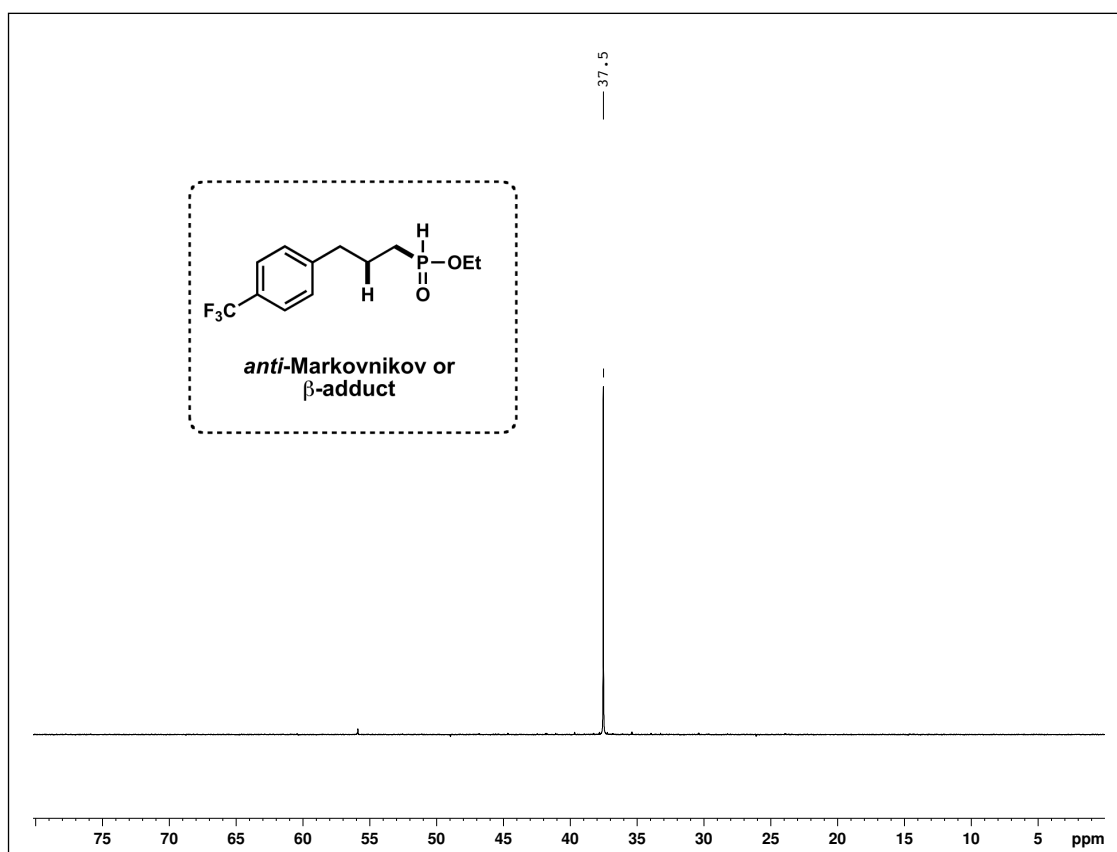


Figure 2.4. ¹H-NMR spectrum showed the formation of only *anti*-Markovnikov or β-adduct

Furthermore, the reaction was found to be chemoselective, in agreement with previous works.¹⁰³

¹⁰³ Ribière, P.; Bravo-Altamirano, K.; Antczak, M.I.; Hawkins, J.D.; Montchamp, J.-L. *J. Org. Chem.* **2005**, *70*, 4064-4072.

Figure 2.5 shows the formation of the mono-addition product by reacting ethyl phosphinate **58a** with alkene **59j** while only traces of the bis-adduct could be detected by ^{31}P -NMR.

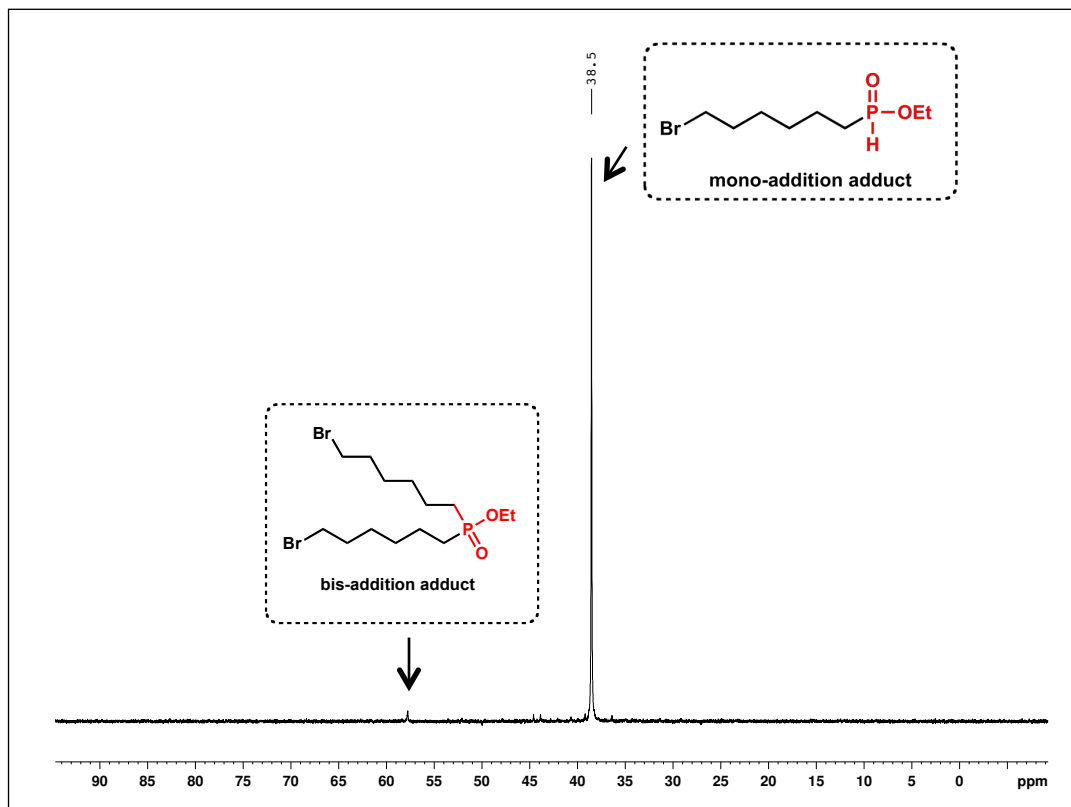


Figure 2.5. ^1H -NMR spectrum showed that traces of bis-adduct were formed by hydrophosphonylation reaction

2.4.4. Mechanistic studies

In order to get insights into the mechanism of visible light mediated hydrophosphonylation of unactivated alkenes, we used different analytical experiments:

- Fluorescence quenching
- Steady state photolysis
- Electron Paramagnetic Resonance (EPR)
- Nuclear Magnetic Resonance (NMR) studies
- Quantum Yields Measurements

First of all, a molecule in its excited state can react with a quencher molecule **Q** by different mechanisms, showed in Figure 2.6.

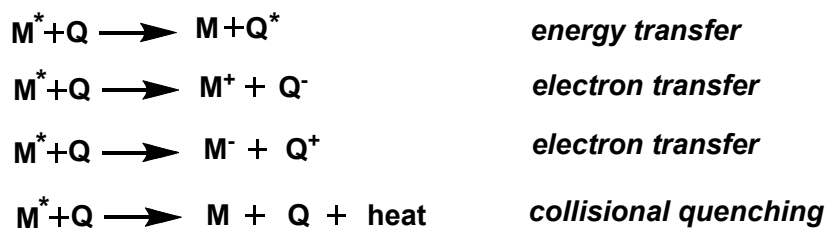


Figure 2.6. Different pathways of reactivity between excited state (M^*) of a molecule and a quencher (Q)

Kinetically, each of these mechanisms is bimolecular so their rate depends on the concentration of excited state molecule M^* and also on the concentration of the quencher Q.

The presence of the quencher in a mixture with a luminescent molecule introduces another rate for deactivating the excited state, which results in a decrease of the intensity of the luminescence, as shown in Figure 2.7, for the reaction of **Mes-Acr** (conc. = 5×10^{-6} M) with increasing concentrations of **73** at room temperature in acetonitrile.

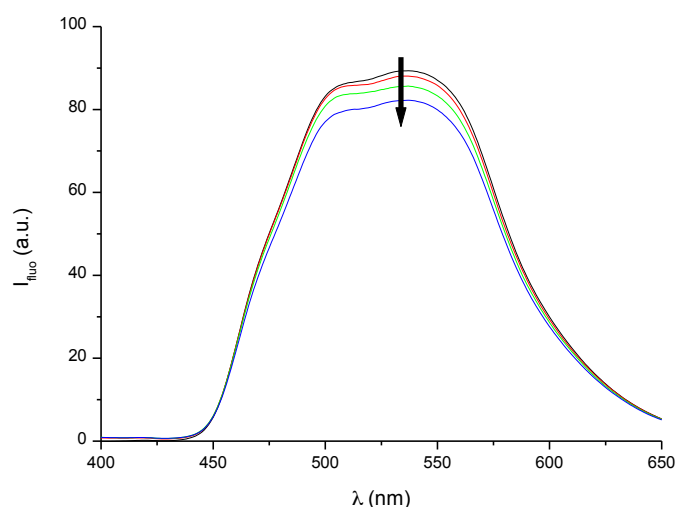


Figure 2.7. Fluorescence spectra ($\lambda_{\text{Ex}} = 430$ nm) of acetonitrile solutions of *N*-methyl-9-mesityl acridinium photocatalyst ($[\text{Mes-Acr}] = 5 \times 10^{-6}$ M) containing increasing concentrations of iodonium triflate at 20°C

The described process is called *quenching*. In our case, fluorescence quenching confirmed the right interaction between the photooxidant (diphenyliodonium salt, **Q**) and the photocatalyst (Mes-Acr, M^*). The experiment, showed in Figure 2.7, demonstrated that by increasing the concentration of the quencher **73** and keeping stable the concentration of the photocatalyst, the result is a decrease of the fluorescence.

Remarkably, the rate law for bimolecular quenching follows a second order kinetics (eq 2).

$$\text{Rate of quenching} = k_q [M^*][Q] \quad (2)$$

The Stern-Volmer method¹⁰⁴ can be used to calculate k_q for this fast excited state quenching reaction. Our resulting Stern-Volmer plot (Figure 2.8) yielded a quenching rate of $k_q = 3.2 \times 10^8 \text{ M}^{-1} \text{ s}^{-1}$, consistent with our initial hypothesis that diphenyliodonium salt **73** is reduced by the excited state of photocatalyst **Mes-Acr***.¹⁰⁵

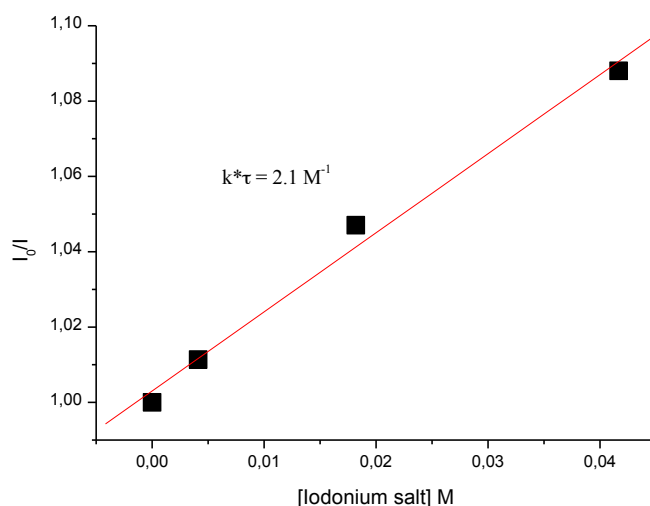


Figure 2.8. Stern-Volmer quenching constant for the reaction of the excited state of **Mes-Acr** with diphenyliodonium triflate in MeCN.

Additional evidences for the reaction of excited state of **Mes-Acr** with **73** came from *steady state photolysis*.¹⁰⁶ Figure 2.9 shows an increase of the UV-Vis absorbance of **Mes-Acr** when **73** is added under blue light irradiation ($\lambda = 430 \text{ nm}$).

¹⁰⁴ Lacowicz, J.R. *Principles of Fluorescence Spectroscopy* (2nd Ed.), Chapter 8.

¹⁰⁵ The reduction potential (E_{red}) of **1*** has been determined by Fukuzumi et al. to be -0.57 V , see: Kotani, H.; Okhubo, K.; Fukuzumi, S. *J. Am. Chem. Soc.* **2004**, *126*, 15999-16006.

¹⁰⁶ The term photolysis concerns a chemical transformation in which a compound is decomposed by photons.

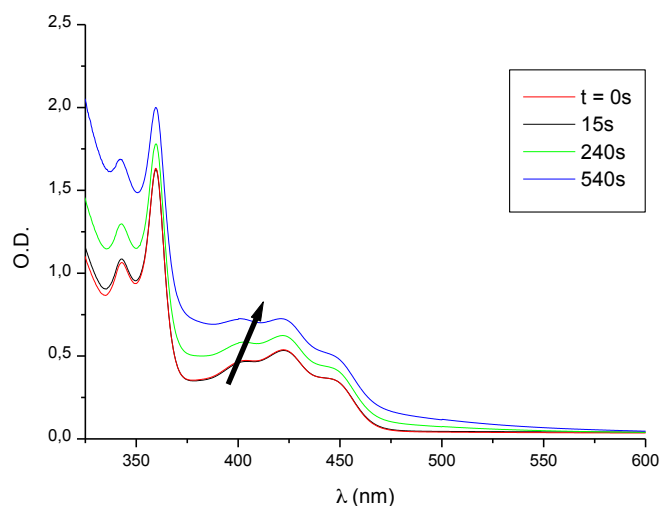
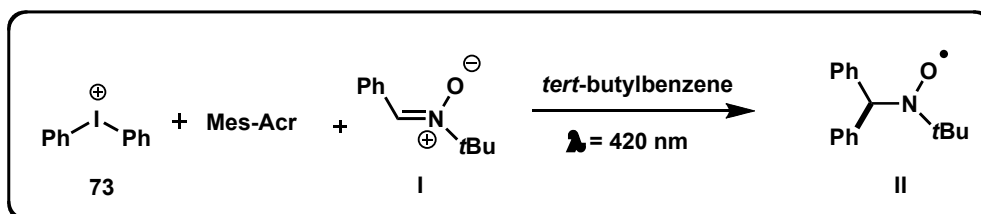


Figure 2.9. Photolysis of acetonitrile solutions of the photocatalyst with diphenyliodonium **73** upon irradiation (LED @ $I_{\text{max}} = 420 \text{ nm}$; from $t = 0$ to 540 s)

We next focused on the analysis of the intermediates involved in our photoreaction. To this end, the group of Prof. Jacques Lalevée investigated, by means of *electron paramagnetic resonance* (EPR), the radical species formed in our photoreaction. This study was first carried out by employing diphenyliodonium triflate **73** with photocatalyst **Mes-Acr** in the presence of the α -phenyl-*N*-*tert*-butylnitrone (PBN) **I** as a radical trap in *tert*-butylbenzene at room temperature.

When this mixture was irradiated with blue light ($\lambda = 420 \text{ nm}$), a clean formation of the spin adduct **II** has been observed. The hyperfine coupling constants of **II** ($a_{\text{N}} = 14.4 \text{ G}$ and $a_{\text{H}} = 2.2 \text{ G}$) are in perfect accordance with those reported in the literature (Figure 2.10).⁵⁵



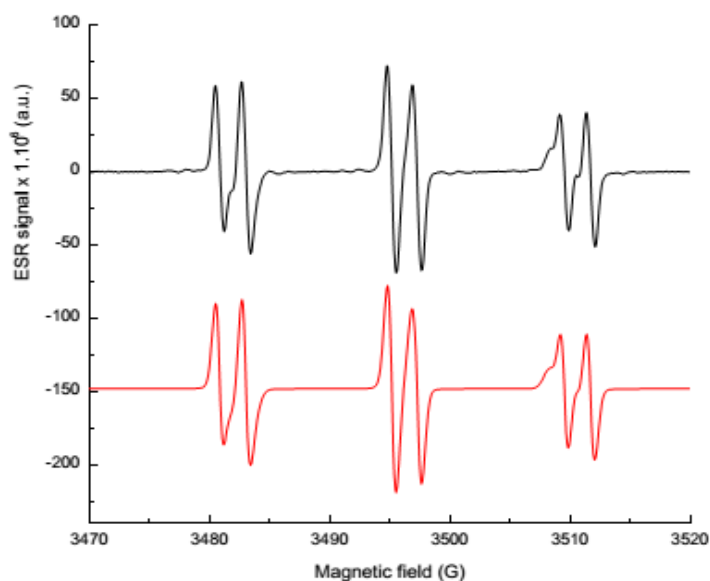
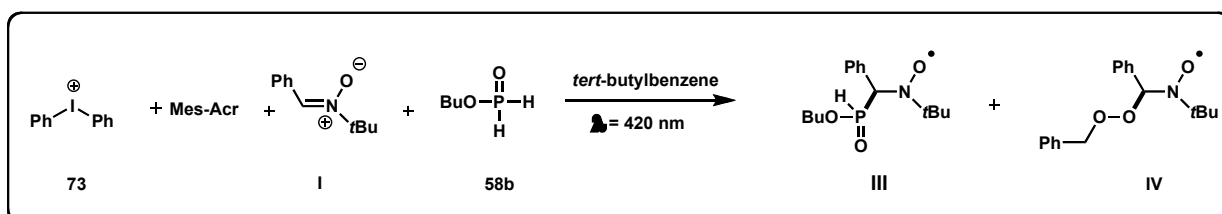


Figure 2.10. EPR spin-trapping spectra resulting upon irradiation ($\lambda = 420$ nm) of a solution of acridinium salt (**Mes-Acr**) and diphenyliodonium **73** in the presence of PBN **I** in *tert*-butylbenzene at room temperature

This observation strongly supports the formation of the phenyl radical *via* reduction of **73** by the excited state of the photocatalyst. The addition of a toluene solution of butyl phosphinate **58b** to this mixture gave a more complex EPR spectrum, as shown in Figure 2.11.



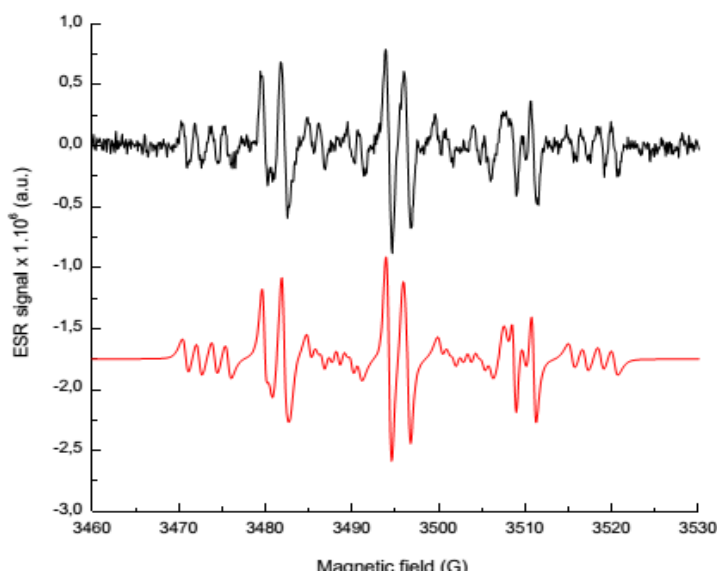


Figure 2.11. EPR spin-trapping spectra resulting upon irradiation ($\lambda = 420$ nm) of acridinium **Mes-Acr** /diphenyliodonium **73** solution in the presence of butyl phosphinate **58b** and PBN **I** in toluene at room temperature.

The simulation of this data indicated the presence of the remaining phenyl radical along with phosphorus and oxygen centered radical species. While the hyperfine coupling constants of the phosphorus species ($a_N = 15.2$ G, $a_{H1} = 3.3$ G, $a_{H2} = 1.6$ G and $a_P = 14.3$ G) are consistent with PBN-phosphinoyl adduct **III**, it was more difficult to assign the structure of the oxygen radical species.

However, as the formation of the latter can be due to the presence of residual air in the solvent, we carried out the reaction of diphenyliodonium triflate **73** with photocatalyst **Mes-Acr** in toluene under blue light irradiation in the presence of O_2 . Interestingly, as shown in Figure 2.12, 1H NMR showed the formation of benzaldehyde **76** along with a small amount of benzoic acid **77**. When the mixture was allowed to stay for a long reaction time (96h), we detected 25% of **77**.

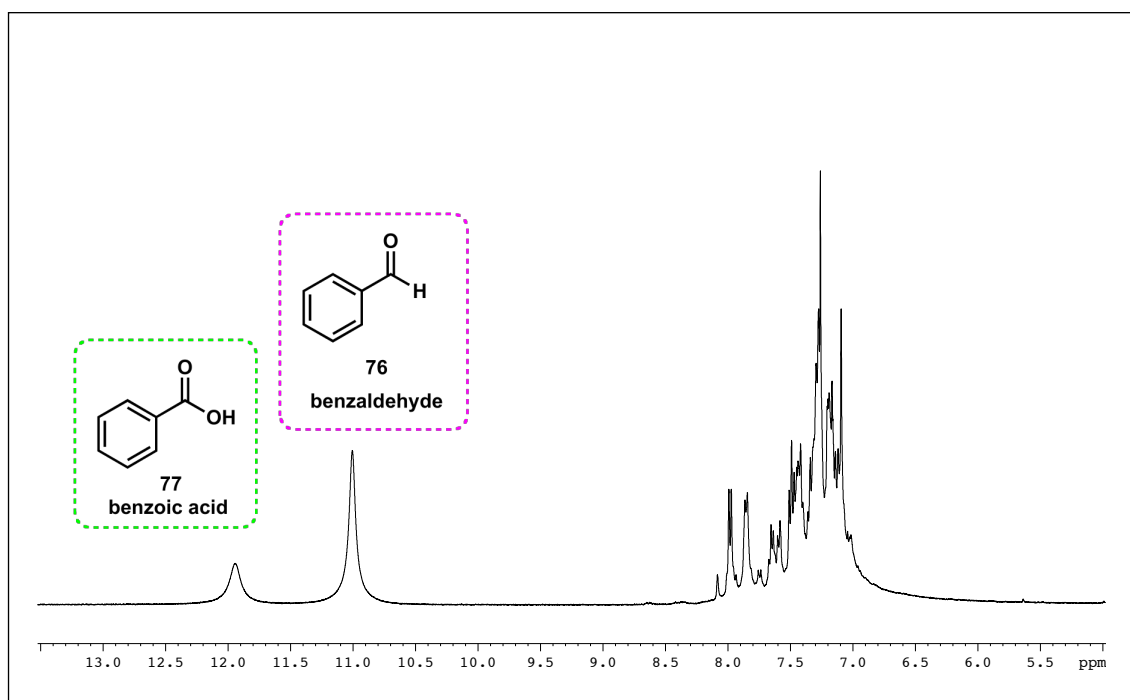
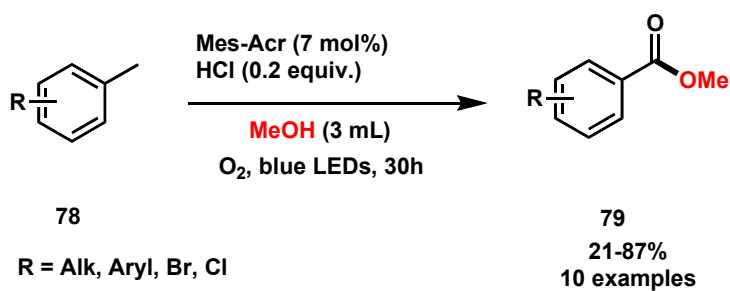
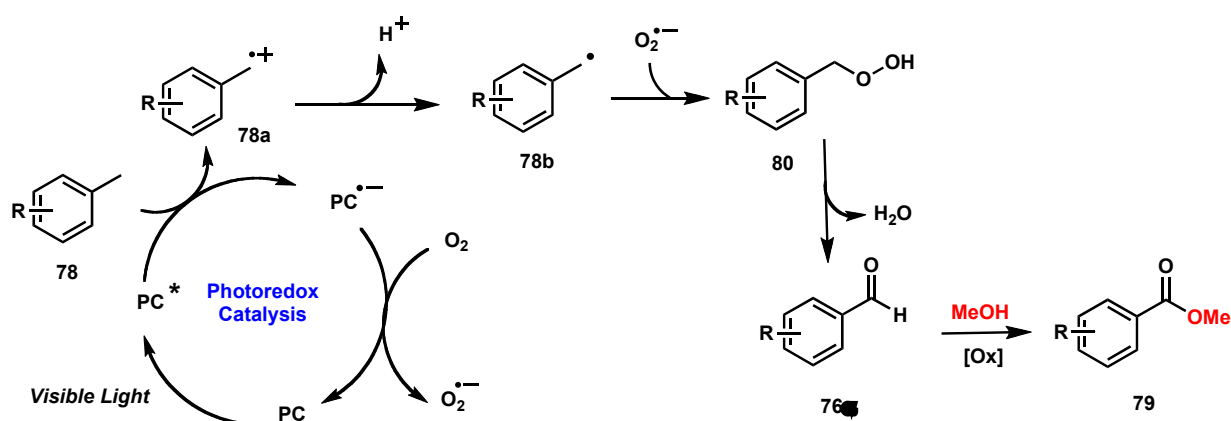


Figure 2.12. ¹H-NMR spectrum showed the formation of benzaldehyde **76** and traces of benzoic acid **77**

This hypothesis has already been supported by a recent contribution of Lei, who showed that the acridinium salt (**Mes-Acr**) could catalyze the oxidation of toluene leading to benzaldehyde in the presence of O₂ (Scheme 2.15).¹⁰⁷



¹⁰⁷ Zhang, L.; Yi, H.; Jue, W.; Lei, A. *Green Chem.* **2016**, *18*, 5122-5126.



PC: Mes-Acr

Scheme 2.15. Visible light mediated oxidation of benzylic sp^3 C–H to methyl esters and plausible mechanism

Lei *et al.* proposed the mechanism depicted in Scheme 2.15. Photocatalyst (PC) is excited by visible light irradiation to generate the excited state PC^* , which reacts *via* single electron transfer reaction with benzylic compound **78**, leading to radical cation intermediate **78a** and PC radical anion. The latter can be easily oxidized by O_2 , thus closing the photocatalytic cycle. The radical cation **78a** can lose a proton to form the radical **78b**, which reacts with O_2 radical anion to generate the hydroperoxide intermediate **80**, followed by loss of water to yield aldehyde **76α**. The final oxidative coupling with methanol leads to methyl ester derivative **79**.

On the basis of this investigation, we can fairly postulated that the observed oxygen centered radical by EPR spectroscopy was the benzoperoxy radical **IV** ($a_{\text{N}} = 13.7$ G and $a_{\text{H}} = 2.0$ G).

Quantum yield measurements have given a further demonstration that our photocatalyzed process is consistent with a radical chain mechanism.¹⁰⁸

When a molecule absorbs a photon of light, an energetically excited state is formed, followed by its deactivation (loss of energy) and return to the ground state. The main deactivation processes are fluorescence (loss of energy by emission of a photon), internal conversion and vibrational relaxation (non-radiative loss of energy as heat to the surrounding), and intersystem crossing.

¹⁰⁸ (a) Pitre, S.P.; McTiernan, Ch. D.; Scaiano, J.C. *Acc. Chem. Res.* **2016**, *49*, 1320-1330. (b) Cismesia, M.A.; Yoon, T.P. *Chem. Sci.* **2015**, *6*, 5426-5434.

The fluorescence quantum yield (Φ_F) is the ratio of photons absorbed to photons emitted through fluorescence. Moreover, the quantum yield of a photochemical reaction is defined as the ratio of the moles of product formed to the einsteins of photons absorbed (eq 3).¹⁰⁹

$$\Phi = \frac{\text{moles of product formed}}{\text{einsteins of light absorbed}} \quad (3)$$

Quantum yields measurements contribute to give useful informations concerning photochemical reactions which involve a radical chain (Figure 2.13).^{67b}

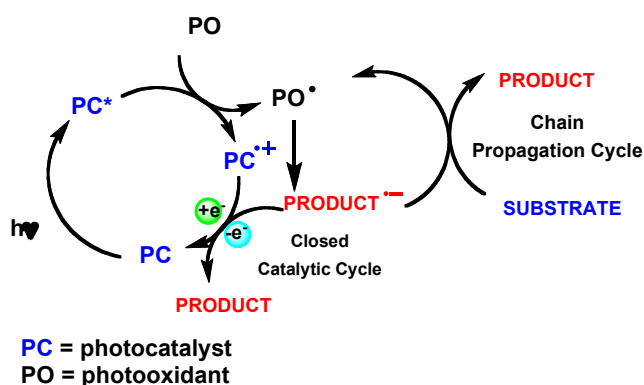


Figure 2.13. General mechanism for oxidative photoredox reactions

Normally, the closed catalytic cycle showed in Figure 2.13 should present a maximum theoretical quantum yield (Φ) value of 1, which means that every photons absorbed by the molecule could afford one product molecule. This condition reflects any non-productive process, such as phosphorescence, intersystem-crossing or internal conversion.

On the other hand, chain processes can afford multiple equivalents of products for each photon absorbed by the photocatalyst. That is the reason why each photoreaction with $\Phi \gg 1$ can be expected to be radical chain transformation.

More in details, following a procedure proposed by Melchiorre *et al.*¹¹⁰, we were able to measure for our photocatalyzed hydrophosphinylation reaction a value of quantum yield

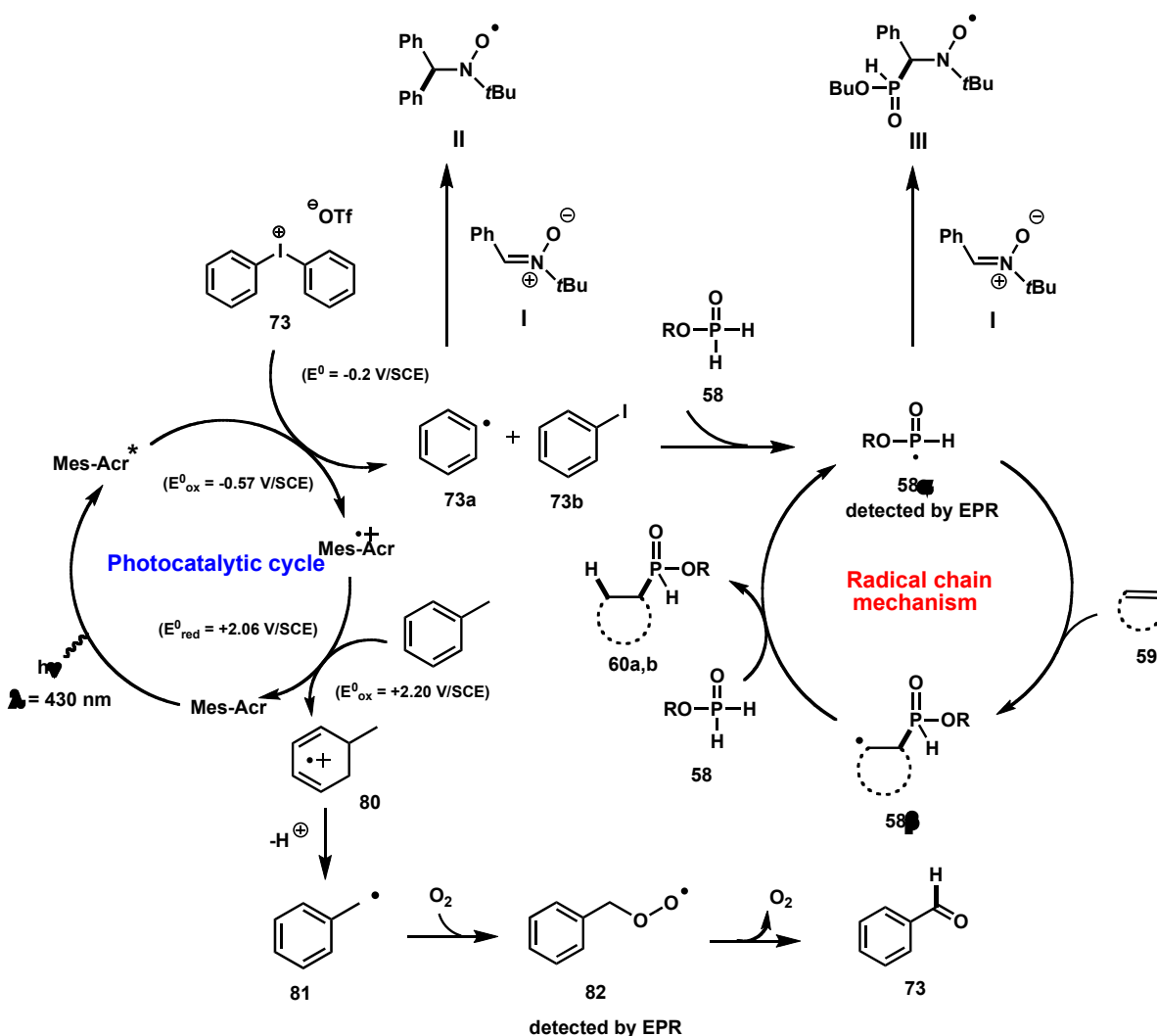
¹⁰⁹ Julliard, M.; Chanon, M. *Chem. Rev.* **1983**, *83*, 425-506.

¹¹⁰ Kandukuri, S.R.; Bahamonde, A.; Chatterjee, I.; Jurberg, I.D.; Escudero-Adan, E.C.; Melchiorre, P. *Angew. Chem. Int. Ed.* **2015**, *54*, 1485-1489.

$\Phi = 22$ (eq 4), which was the confirmation that our process worked as radical chain mechanism.

$$\Phi = \frac{3.41 \times 10^{-4} \text{ mol}}{8.52 \times 10^{-10} \text{ mol s}^{-1} \times 18.000 \text{ s}} = 22 \quad (4)$$

On the basis of our mechanistic investigations, we propose the following reaction mechanism that summarizes all our experimental observations (Scheme 2.16).



Scheme 2.16. Proposed mechanism for the visible light mediated hydrophosphinylation of phosphinates **66a,b** with terminal unactivated alkenes **67** in the presence of 9-mesityl-10-methylacridinium perchlorate (**Mes-Acr**) as a photocatalyst and diphenyliodonium triflate **85** as external oxidant

The reaction starts with excitation of **Mes-Acr** by blue light irradiation to generate **Mes-Acr***, which reduces the diphenyliodonium salt **73** to give rise to the phenyl radical **73a**. The latter abstracts hydrogen from alkyl phosphinate **58** to form the phosphinoyl radical **58 α** , detected by EPR spectroscopy and identically trapped by PBN. This radical adds to alkene **59** to form the carbon centered radical **58 β** , which abstracts hydrogen of **58** to yield the desired adduct **60a,b** and regenerates the phosphinoyl radical **58 α** . To close the photocatalytic cycle, we have assumed that toluene can donate an electron to the oxidized form of the photocatalyst **Mes-Acr⁺** to generate the benzyl radical **81** upon fast deprotonation. The radical intermediate reacts immediately with traces of oxygen present in the solvent to afford the hydroperoxide radical intermediate **82**, which releases O₂, leading to benzaldehyde **73**, depicted by ¹H-NMR.

2.5. Conclusions

In Chapter II, we have described the first metal-free visible light mediated hydrophosphinylation reaction of unactivated alkenes with ethyl and butyl phosphinates **58a,b**.

The reaction has a broad scope and proceeds with perfect regio- and chemoselectivities. The proposed mechanism has been supported by fluorescence quenching, steady state photolysis, quantum yield measurements and EPR spectroscopy.

Our detailed mechanistic investigations feature an original reactivity of **Mes-Acr**, which has been shown to be operative in oxidative catalytic cycle.

Given the importance of phosphinates in various area of chemistry, this mild approach for the generation of phosphinoyl radical should open the way to the development of synthetically useful transformations.

2.6 Materials and methods

2.6.1 General

¹H NMR spectra were recorded on a BRUKER AVANCE III 400 MHz spectrometer, the chemical shifts are reported in parts per million (ppm) referenced to residual chloroform (7.26 ppm). Coupling constants are reported in Hertz (Hz). The following abbreviations were used to express the multiplicities: s (singlet), d (doublet), t (triplet), q (quartet), m (multiplet), bs (broad singlet). ¹³C NMR spectra were recorded on the same instrument at 100 MHz, the chemical shifts are expressed in parts per million (ppm), reported from the central chloroform peak (77.2 ppm). ³¹P NMR spectra were recorded on the same instrument at 162 MHz (decoupled ³¹P NMR). High Resolution Mass Spectrometry (HRMS) was performed on a Varian MAT 311 spectrometer or a QTOF Micro WATERS spectrometer.

All reactions were air or water sensitive and set up under an argon atmosphere in dried glassware using Schlenk techniques with dry solvents. Chromatographic purification of products was accomplished using flash chromatography (FC) on silica gel (35-70 mesh). For Thin Layer Chromatography (TLC) analysis throughout this work, Merck precoated TLC plates (silica gel 60 F₂₅₄) were employed. Visualization was performed with UV light and by immersion in anisaldehyde stain (by volume: 93% ethanol, 3.5% sulfuric acid, 1% acetic acid, 2.5% *p*-anisaldehyde) or basic aqueous potassium permanganate solution (KMnO₄) stain followed by heating as developing tool. Organic solutions of products were dried over anhydrous MgSO₄ and concentrated under reduced pressure on a Büchi rotatory evaporator. Aqueous hypophosphorus acid (50 wt. %) was obtained from Aldrich and used by concentrating it in vacuo on a rotary evaporator, at 30°C for 20-30 min before reaction. Alkenes were purchased at the highest commercial quality by chemical companies (Sigma-Aldrich, TCI Chemicals, Fisher Scientific) and used without further purification. Toluene and dichloromethane were dispensed by PURESOLV™ developed by Innovative Technology Inc. The phosphinates **58a,b** were prepared following a procedure described by Montchamp *et al.*¹¹¹ The iodonium salt **73** was synthesized according to a protocol by Olofsson.¹¹²

¹¹¹ J.-L. Montchamp, *J. Organomet. Chem.* **2005**, 690, 2388-2406.

¹¹² M. Bielawski, B. Olofsson, *Org. Synth.* **2009**, 86, 308-314.

The blue light irradiation was performed using high-power Vision-EL (5W, $\lambda = 460 \pm 10$ nm, 410 lm).

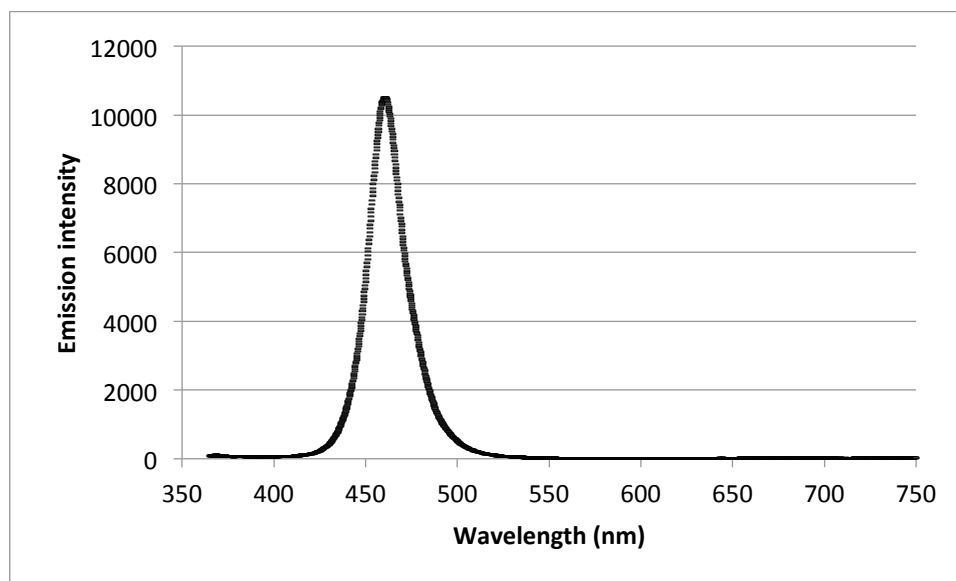


Figure S1. Emission spectrum of the blue LED lamp used in the hydrophoshinylation reactions

2.6.2 EPR-ST, Fluorescence and Laser Flash Photolysis experiments

EPR-ST experiments were performed on X-Band spectrometer (MS 400 Magnettech).

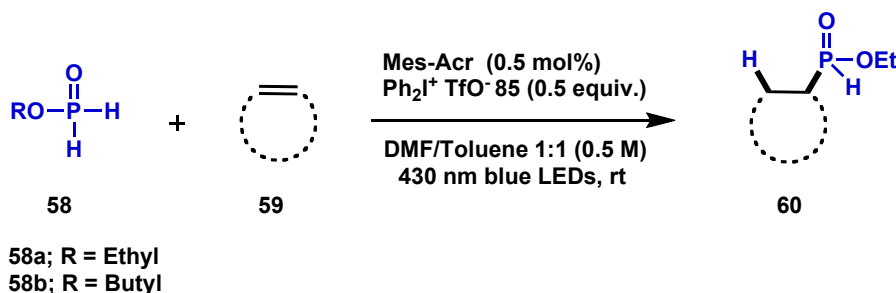
The EPR spectra simulations were carried out using the WINSIM software.

Fluorescence measurements were performed on a JASCO FP-6200 Spectro Fluorimeter.

Photolysis experiments have been done on a JASCO V-730 UV/vis spectrophotometer.

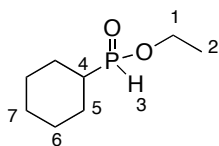
2.7 Anti-Markovnikov Hydrophosphinylation reaction

2.7.1 General procedure



In an oven-dried Schlenk tube, 9-mesityl-10-methylacridinium perchlorate (**Mes-Acr**) (0.5 mol%, 0.005 eq.) and diphenyliodonium triflate **73** (0.25 mmol, 0.5 eq.) were added. To these solids was added 2 ml of a toluene solution of alkyldiphosphinate **58a,b** (0.5 M, 2 eq.), followed by 2 ml of dry DMF and the mixture was stirred until full dissolution of solids. Then, alkene **59** (0.5 mmol, 1 eq.) was added and the solution was irradiated with blue LEDs (5W) for the indicated time. The solvent was removed by using azeotrope method (DMF/heptane) to give oil as crude product. The latter was purified by column chromatography on silica gel ((ratio) ethyl acetate: *n*-pentane, ethyl acetate: acetone or ethyl acetate: dichloromethane) to yield the desired adduct as a colorless oil.

Ethyl cyclohexylphosphinate (60a)

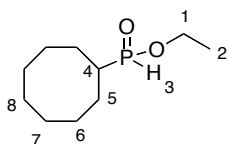


Conditions: (**59a** : 51 μ L, 0.5 mmol, 1 equiv.); ($\text{Ph}_2\text{I}^+ \text{OTf}^-$ (**73**) = 108 mg, 0.25 mmol, 0.5 equiv.); (Mes-Acr = 1 mg, 0.5 mol%, 0.005 equiv). The reaction was carried out following the general procedure.

The crude product was purified by flash column chromatography (ethyl acetate/acetone 90:10). **Yield** : 69 mg, 78%. **$^1\text{H-NMR}$** (400 MHz, CDCl_3) δ (ppm) 6.81 (d, $^1J = 517.0$ Hz, 1H, 3-H), 4.21-3.99 (m, 2H, 1-H), 1.90-1.65 (m, 6H), 1.33 (t, $^3J = 7.4$ Hz, 3H, 2-H), 1.29-1.21 (m, 5H). **$^{13}\text{C}\{\text{H}\}$ -NMR** (100 MHz, CDCl_3) δ (ppm) 62.5 (d, $^2J = 7.4$ Hz, C-1), 37.2 (d, $^1J = 96.0$ Hz, C-4), 25.9 (s), 25.8 (s), 24.3 (s), 16.4 (d, $^3J = 6.0$ Hz, C-2). **$^{31}\text{P-NMR}$** (162 MHz, CDCl_3) δ (ppm) 43.0 (d, $^1J = 517.0$ Hz).

In agreement with previous work of Montchamp et al., due to the sensitivity of the title compound, the determination of its exact mass by mass spectrometry was not possible.

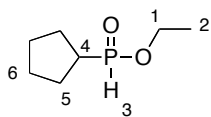
Ethyl cyclooctylphosphinate (60b)



Conditions: (**59b** : 65 μ L, 0.5 mmol, 1 equiv.); ($\text{Ph}_2\text{I}^+ \text{OTf}^-$ (**73**) = 108 mg, 0.25 mmol, 0.5 equiv.); (Mes-Acr = 1 mg, 0.5 mol%, 0.005 equiv). The reaction was carried out following the general

procedure. The crude product was purified by flash column chromatography (ethyl acetate/acetone 90:10). **Yield** : 56 mg, 55%. **$^1\text{H-NMR}$** (400 MHz, CDCl_3) δ (ppm) 6.90 (d, $^1J = 519.0$ Hz, 1H, 3-H), 4.21-4.00 (m, 2H, 1-H), 1.99-1.76 (m, 5H), 1.53-1.51 (m, 10H), 1.33 (t, $^3J = 7.0$ Hz, 3H, 2-H). **$^{13}\text{C}\{\text{H}\}$ -NMR** (100 MHz, CDCl_3) δ (ppm) 62.4 (d, $^2J = 7.3$ Hz, C-1), 36.6 (d, $^1J = 92.0$ Hz, C-4), 26.6 (s), 26.3 (d, $^4J = 1.6$ Hz), 26.1 (d, $^3J = 2.2$ Hz), 24.6 (s), 16.4 (d, $^3J = 6.0$ Hz, C-2). **$^{31}\text{P-NMR}$** (162 MHz, CDCl_3) δ (ppm) 45.8 (d, $^1J = 519.0$ Hz). **HRMS:** calcd for $\text{C}_{10}\text{H}_{22}\text{O}_2\text{P}$ $[\text{M}+\text{H}]^+$ 205.1361, found 205.1357.

Ethyl cyclopentylphosphinate (60c)

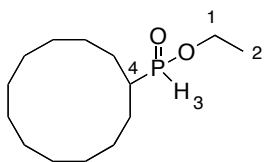


Conditions: (**59c** : 44 μ L, 0.5 mmol, 1 equiv.); ($\text{Ph}_2\text{I}^+ \text{OTf}^-$ (**73**) = 108 mg, 0.25 mmol, 0.5 equiv.); (Mes-Acr = 1 mg, 0.5 mol%, 0.005 equiv). The reaction was carried out following the general procedure.

The crude product was purified by flash column chromatography (ethyl acetate/acetone 90:10). **Yield** : 60 mg, 74%. **$^1\text{H-NMR}$** (400 MHz, CDCl_3) δ (ppm) 6.91 (d, $^1J = 520.0$ Hz, 1H, 3-H), 4.20-4.00 (m, 2H, 1-H), 2.16-2.04 (m, 1H, 4-H), 1.94-1.85 (m, 2H), 1.74-1.57 (m, 6H), 1.33 (t, $^3J = 7$ Hz, 3H, 2-H). **$^{13}\text{C}\{\text{H}\}$ -NMR** (100 MHz, CDCl_3) δ (ppm) 62.4 (d, $^2J = 7.2$ Hz, C-1), 37.0 (d, $^1J = 97.0$ Hz, C-4), 26.5 (d, $^2J = 2.9$ Hz, C-5), 25.6 (s), 16.4 (d, $^3J = 6.0$ Hz, C-2). **$^{31}\text{P-NMR}$** (162 MHz, CDCl_3) δ (ppm) 44.2 (d, $^1J = 520.0$ Hz).

In agreement with previous work of Montchamp et al., due to the sensitivity of the title compound, the determination of its exact mass by mass spectrometry was not possible.

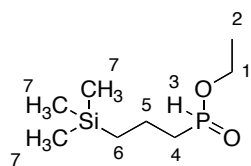
Ethyl cyclododecylphosphinate (60d)



Conditions: (**59d** : 96 μ L, 0.5 mmol, 1 equiv.); ($\text{Ph}_2\text{I}^+ \text{OTf}^-$ (**73**) = 108 mg, 0.25 mmol, 0.5 equiv.); (Mes-Acr = 1 mg, 0.5 mol%, 0.005 equiv). The reaction was carried out following the general procedure. The crude product was purified by flash column

chromatography (ethyl acetate/acetone 90:10). **Yield** : 51 mg, 40%. **H-NMR** (400 MHz, CDCl_3) δ (ppm) 6.92 (d, $^1J = 515.0$ Hz, 1H, 3-H), 4.20-4.01 (m, 2H, 1-H), 1.84-1.77 (m, 1H, 4-H), 1.68-1.29 (m, 25H). **$^{13}\text{C}\{\text{H}\}$ -NMR** (100 MHz, CDCl_3) δ (ppm) 62.5 (s, C-1), 33.5 (d, $^1J = 97$ Hz, C-4), 23.8 (s), 23.3 (s), 22.8 (s), 16.4 (s, C-2). **$^{31}\text{P-NMR}$** (162 MHz, CDCl_3) δ (ppm) 45.3 (d, $^1J = 515.0$ Hz). **HRMS:** calcd for $\text{C}_{14}\text{H}_{29}\text{O}_2\text{NaP}$ $[\text{M}+\text{Na}]^+$ 283.1801, found 283.1803.

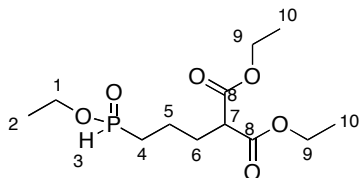
Ethyl 2-(trimethylsilyl)ethylphosphinate (68f)



Conditions: (**67f** : 79 μL , 0.5 mmol, 1 equiv.); ($\text{Ph}_2\text{I}^+ \text{OTf}^-$ (**85**) = 108 mg, 0.25 mmol, 0.5 equiv.); (Mes-Acr = 1 mg, 0.5 mol%, 0.005 equiv). The reaction was carried out following the general procedure. The crude product was purified by flash column chromatography (ethyl acetate/*n*-pentane 90:10). **Yield** : 77 mg, 74%. **$^1\text{H-NMR}$** (400 MHz, CDCl_3) δ (ppm) 7.10 (d, $^1J = 525.0$ Hz, 1H, 3-H), 4.19-3.98 (m, 2H, 1-H), 1.81-1.73 (m, 2H, 4-H), 1.63-1.52 (m, 2H, 5-H), 1.32 (t, $^3J = 7.0$ Hz, 3H, 2-H), 0.60-0.56 (m, 2H, 6-H), -0.05 (s, 9H, 7-H). **$^{13}\text{C}\{\text{H}\}$ -NMR** (100 MHz, CDCl_3) δ (ppm) 62.4 (d, $^2J = 7.0$ Hz, C-1), 32.6 (d, $^1J = 94.0$ Hz, C-4), 18.3 (d, $^2J = 13.5$ Hz, C-5), 16.4 (d, $^3J = 6.1$ Hz, C-2), 15.8 (d, $^3J = 3.1$ Hz, C-6), -1.7 (s, C-7). **$^{31}\text{P-NMR}$** (162 MHz, CDCl_3) δ (ppm) 38.4 (d, $^1J = 525.0$ Hz).

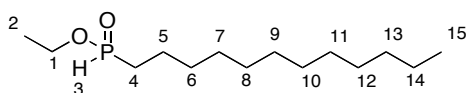
In agreement with previous work of Montchamp et al., due to the sensitivity of the title compound, the determination of its exact mass by mass spectrometry was not possible.

Ethyl 4-(diethylmaleonate)propylphosphinate (60g)



Conditions: (**59g** : 99 μL , 0.5 mmol, 1 equiv.); ($\text{Ph}_2\text{I}^+ \text{OTf}^-$ (**73**) = 108 mg, 0.25 mmol, 0.5 equiv.); (Mes-Acr = 1 mg, 0.5 mol%, 0.005 equiv). The reaction was carried out following the general procedure. The crude product was purified by flash column chromatography (ethyl acetate/*n*-pentane 90:10). **Yield** : 81 mg, 55%. **$^1\text{H-NMR}$** (400 MHz, CDCl_3) δ (ppm) 7.10 (d, $^1J = 531.3$ Hz, 1H, 3-H), 4.20-4.14 (m, 4H, 9-H), 4.12-3.99 (m, 2H, 1-H), 3.31 (t, $^3J = 7.5$ Hz, 1H, 7-H), 2.01-1.94 (m, 2H, 6-H), 1.81-1.73 (m, 2H, 4-H), 1.67-1.57 (m, 2H, 5-H), 1.32 (t, $^3J = 7.0$ Hz, 3H, 2-H), 1.24 (t, $^3J = 7.0$ Hz, 6H, 10-H). **$^{13}\text{C}\{\text{H}\}$ -NMR** (100 MHz, CDCl_3) δ (ppm) 169.1 (s, C-8), 62.5 (d, $^2J = 6.8$ Hz, C-1), 61.6 (s, C-9), 51.6 (s, C-10), 29.4 (d, $^3J = 16.0$ Hz, C-6), 28.6 (d, $^1J = 94.0$ Hz, C-4), 18.9 (d, $^2J = 3$ Hz, C-7), 16.4 (d, $^2J = 6.0$ Hz, C-5), 14.1 (s, C-2). **$^{31}\text{P-NMR}$** (162 MHz, CDCl_3) δ (ppm) 37.3 (d, $^1J = 531.3$ Hz). **HRMS:** calcd for $\text{C}_{12}\text{H}_{23}\text{O}_6\text{NaP}$ $[\text{M}+\text{Na}]^+$ 317.1128, found 317.1130.

Ethyl dodecylphosphinate (60i)

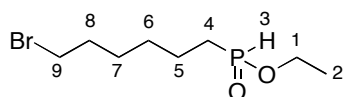


Conditions: (**59i** : 111 μ L, 0.5 mmol, 1 equiv.); ($\text{Ph}_2\text{I}^+ \text{OTf}^-$ (**73**) = 108 mg, 0.25 mmol, 0.5 equiv.); (Mes-Acr = 1 mg, 0.5 mol%, 0.005

equiv). The reaction was carried out following the general procedure. The crude product was purified by flash column chromatography (ethyl acetate/*n*-pentane 90:10). **Yield** : 88 mg, 67%. **$^1\text{H-NMR}$** (400 MHz, CDCl_3) δ (ppm) 7.05 (d, $^1J = 526.1$ Hz, 1H, 3-H), 4.20-3.99 (m, 2H, 1-H), 1.77-1.69 (m, 2H, 4-H), 1.61-1.50 (m, 2H, 5-H), 1.33-1.23 (bs, 21H), 0.85 (t, $^3J = 7.0$ Hz, 3H, 15-H). **$^{13}\text{C}\{\text{H}\}$ -NMR** (100 MHz, CDCl_3) δ (ppm) 62.4 (d, $^2J = 7$ Hz, C-1), 32.0 (s), 30.6 (d, $^2J = 15.2$ Hz, C-5), 29.7 (s), 29.6 (s), 29.4 (s), 29.3 (s), 29.2 (s), 28.3 (s), 22.8 (s), 20.8 (d, $^3J = 3.0$ Hz, C-6), 16.4 (d, $^3J = 6.0$ Hz, C-2), 14.2 (s, C-15). **$^{31}\text{P-NMR}$** (162 MHz, CDCl_3) δ (ppm) 39.1 (d, $^1J = 526.1$ Hz).

In agreement with previous work of Montchamp et al., due to the sensitivity of the title compound, the determination of its exact mass by mass spectrometry was not possible.

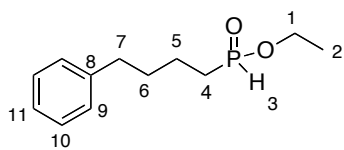
Ethyl 6-bromohexylphosphinate (60j)



Conditions: (**59j** : 67 μ L, 0.5 mmol, 1 equiv.); ($\text{Ph}_2\text{I}^+ \text{OTf}^-$ (**73**) = 108 mg, 0.25 mmol, 0.5 equiv.); (Mes-Acr = 1 mg, 0.5 mol%, 0.005 equiv). The reaction was carried out following the general procedure. The crude product was purified by flash column chromatography (ethyl acetate/dichloromethane 90:10). **Yield** : 90 mg, 70%. **$^1\text{H-NMR}$** (400 MHz, CDCl_3) δ (ppm) 7.1 (d, $^1J = 526.2$ Hz, 1H, 3-H), 4.22-4.01 (m, 2H, 1-H), 3.39 (t, $^3J = 6.7$ Hz, 2H, 9-H), 1.88-1.81 (m, 2H, 8-H), 1.80-1.72 (m, 2H, 4-H), 1.67-1.55 (m, 2H), 1.45-1.43 (m, 4H), 1.35 (t, $^3J = 7.1$ Hz, 3H, 2-H). **$^{13}\text{C}\{\text{H}\}$ -NMR** (100 MHz, CDCl_3) δ (ppm) 62.5 (d, $^2J = 7.1$ Hz, C-1), 33.8 (s, C-9), 32.5 (s, C-8), 29.7 (d, $^2J = 15.0$ Hz, C-5), 28.8 (d, $^1J = 94.0$ Hz, C-4), 27.7 (s, C-7), 20.7 (d, $^3J = 3.0$ Hz, C-6), 16.4 (d, $^3J = 6.0$ Hz, C-2). **$^{31}\text{P-NMR}$** (162 MHz, CDCl_3) δ (ppm) 38.5 (d, $^1J = 526.2$ Hz).

In agreement with previous work of Montchamp et al., due to the sensitivity of the title compound, the determination of its exact mass by mass spectrometry was not possible.

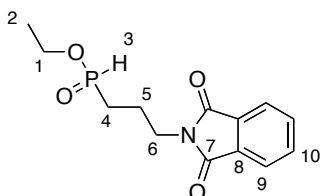
Ethyl 4-phenylbutylphosphinate (60k)



Conditions: (**59k** : 75 μ L, 0.5 mmol, 1 equiv.); ($\text{Ph}_2\text{I}^+ \text{OTf}^-$ (**73**) = 108 mg, 0.25 mmol, 0.5 equiv.); (Mes-Acr = 1 mg, 0.5 mol%, 0.005 equiv). The reaction was carried out following the general procedure. The crude product was purified by flash column chromatography (ethyl acetate/*n*-pentane 90:10). **Yield** : 86 mg, 76%. **$^1\text{H-NMR}$** (400 MHz, CDCl_3) δ (ppm) 7.39-7.35 (m, 2H, Ar-H), 7.29-7.24 (m, 3H, Ar-H), 7.16 (d, $^1J = 528.0$ Hz, 1H, 3-H), 4.31-4.07 (m, 2H, 1-H), 2.73 (t, $^3J = 7.1$ Hz, 2H, 7-H), 1.92-1.67 (m, 6H), 1.44 (t, $^3J = 7.0$ Hz, 3H, 2-H). **$^{13}\text{C}\{\text{H}\}\text{-NMR}$** (100 MHz, CDCl_3) δ (ppm) 141.8 (s, C-8), 128.5 (s, C-Ar), 128.5 (s, C-Ar), 126.0 (s, C-Ar), 62.5 (d, $^2J = 7.0$ Hz, C-1), 35.5 (s, C-7), 32.3 (d, $^3J = 16.0$ Hz, C-6), 28.7 (d, $^1J = 94.0$ Hz, C-4), 20.5 (d, $^2J = 3.2$ Hz, C-5), 16.4 (d, $^3J = 6.0$ Hz, C-2). **$^{31}\text{P-NMR}$** (162 MHz, CDCl_3) δ (ppm) 38.6 (d, $^1J = 528.0$ Hz).

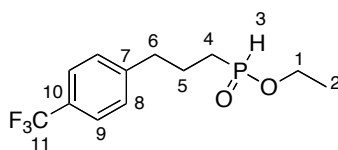
In agreement with previous work of Montchamp et al., due to the sensitivity of the title compound, the determination of its exact mass by mass spectrometry was not possible.

Ethyl 2-(1,3-dioxoisindolin-2-yl)ethylphosphinate (60l)



Conditions: (**59l** : 94 mg, 0.5 mmol, 1 equiv.); ($\text{Ph}_2\text{I}^+ \text{OTf}^-$ (**73**) = 108 mg, 0.25 mmol, 0.5 equiv.); (Mes-Acr = 1 mg, 0.5 mol%, 0.005 equiv). The reaction was carried out following the general procedure. The crude product was purified by flash column chromatography (ethyl acetate/acetone 90:10). **Yield** : 55 mg, 40%. **H-NMR** (400 MHz, CDCl_3) δ (ppm) 7.83-7.81 (m, 2H, Ar-H), 7.71-7.70 (m, 2H, Ar-H), 7.10 (d, $^1J = 535.0$ Hz, 1H, 3-H), 4.18-4.00 (m, 2H, 1-H), 3.75 (t, $^3J = 7.2$ Hz, 2H, 6-H), 2.00-1.92 (m, 2H, 5-H), 1.84-1.77 (m, 2H, 4-H), 1.32 (t, $^3J = 7.4$ Hz, 3H, 2-H). **$^{13}\text{C}\{\text{H}\}\text{-NMR}$** (100 MHz, CDCl_3) δ (ppm) 168.3 (s, C-7), 134.2 (s, C-Ar), 132.0 (s, C-Ar), 123.4 (s, C-Ar), 62.7 (d, $^2J = 7.1$ Hz, C-1), 38.1 (d, $^3J = 24.0$ Hz, C-6), 26.4 (d, $^1J = 95.0$ Hz, C-4), 20.4 (d, $^2J = 12.1$ Hz, C-5), 16.3 (d, $^3J = 6.0$ Hz, C-2). **$^{31}\text{P-NMR}$** (162 MHz, CDCl_3) δ (ppm) 36.8 (d, $^1J = 535.0$ Hz). **HRMS:** calcd for $\text{C}_{13}\text{H}_{16}\text{NO}_4\text{PNa}$ $[\text{M}+\text{Na}]^+$ 304.0719, found 304.0715.

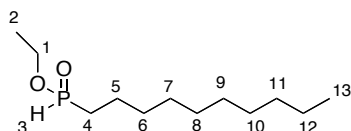
Ethyl 3-(4-(trifluoromethyl)phenyl)propylphosphinate (60m)



Conditions: (**59m** : 84 μ L, 0.5 mmol, 1 equiv.); ($\text{Ph}_2\text{I}^+ - \text{OTf}^-$ (**73**) = 108 mg, 0.25 mmol, 0.5 equiv.); (Mes-Acr = 1 mg, 0.5 mol%, 0.005 equiv). The reaction was carried out following the general procedure. The crude product was purified by flash column chromatography (ethyl acetate/dichloromethane 80:20). **Yield** : 35 mg, 25%. **$^1\text{H-NMR}$** (400 MHz, CDCl_3) δ (ppm) 7.51-7.49 (d, $^3J = 8.0$ Hz, 2H, 9-H), 7.25-7.22 (d, $^3J = 8.0$ Hz, 2H, 8-H), 7.06 (d, $^1J = 529.2$ Hz, 1H, 3-H), 4.19-3.98 (m, 2H, 1-H), 2.75 (t, $^3J = 7.4$ Hz, 2H, 6-H), 1.97-1.86 (m, 2H, 4-H), 1.77-1.69 (m, 2H, 5-H), 1.32 (t, $^3J = 7.1$ Hz, 3H, 2-H). **$^{13}\text{C}\{\text{H}\}$ -NMR** (100 MHz, CDCl_3) δ (ppm) 144.9 (s, C-7), 128.9 (s, C-Ar), 125.6 (s, C-Ar), 125.5 (s, C-Ar), 62.7 (d, $^2J = 7.2$ Hz, C-1), 36.2 (d, $^3J = 16.0$ Hz, C-6), 28.2 (d, $^1J = 94.3$ Hz, C-4), 22.3 (s, C-5), 16.4 (d, $^3J = 6.1$ Hz, C-2). **$^{31}\text{P-NMR}$** (162 MHz, CDCl_3) δ (ppm) 37.5 (d, $^1J = 529.2$ Hz).

In agreement with previous work of Montchamp et al., due to the sensitivity of the title compound, the determination of its exact mass by mass spectrometry was not possible.

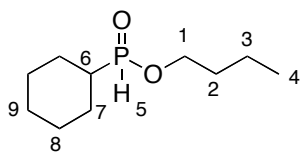
Ethyl decylphosphinate (60n)



Conditions: (**59n** : 101 μ L, 0.5 mmol, 1 equiv.); ($\text{Ph}_2\text{I}^+ - \text{OTf}^-$ (**73**) = 108 mg, 0.25 mmol, 0.5 equiv.); (Mes-Acr = 1 mg, 0.5 mol%, 0.005 equiv). The reaction was carried out following the general procedure. The crude product was purified by flash column chromatography (ethyl acetate/*n*-pentane 90:10). **Yield** : 29 mg, 25%. **$^1\text{H-NMR}$** (400 MHz, CDCl_3) δ (ppm) 7.10 (d, $^1J = 526.1$ Hz, 1H, 3-H), 4.22-4.01 (m, 2H, 1-H), 1.79-1.71 (m, 2H, 4-H), 1.63-1.52 (m, 2H, 5-H), 1.35 (t, $^3J = 7.1$ Hz, 3H, 2-H), 1.25 (bs, 14H), 0.87 (t, $^3J = 6.3$ Hz, 3H, 13-H). **$^{13}\text{C}\{\text{H}\}$ -NMR** (100 MHz, CDCl_3) δ (ppm) 62.5 (d, $^2J = 7.0$ Hz, C-1), 32.0 (s), 30.6 (d, $^3J = 16.0$ Hz, C-6), 29.6 (s), 29.5 (s), 29.4 (s), 29.3 (s), 29.2 (s), 28.4 (s), 22.8 (s), 16.5 (d, $^3J = 6.2$ Hz, C-2), 14.2 (s, C-13). **$^{31}\text{P-NMR}$** (162 MHz, CDCl_3) δ (ppm) 39.1 (d, $^1J = 526.1$ Hz).

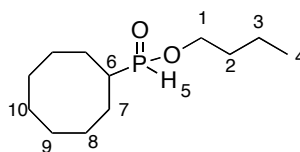
In agreement with previous work of Montchamp et al., due to the sensitivity of the title compound, the determination of its exact mass by mass spectrometry was not possible.

Butyl cyclohexylphosphinate (60a)



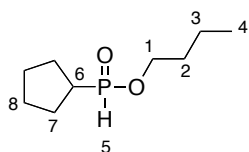
Conditions: (**59a** : 51 μ L, 0.5 mmol, 1 equiv.); ($\text{Ph}_2\text{I}^+ \text{OTf}^-$ (**73**) = 108 mg, 0.25 mmol, 0.5 equiv.); (Mes-Acr = 1 mg, 0.5 mol%, 0.005 equiv). The reaction was carried out following the general procedure. The crude product was purified by flash column chromatography (ethyl acetate/dichloromethane 90:10). **Yield** : 52 mg, 51%. **$^1\text{H-NMR}$** (400 MHz, CDCl_3) δ (ppm) 6.80 (d, $^1J = 518.4$ Hz, 1H, 5-H), 4.13-3.91 (m, 2H, 1-H), 1.89-1.81 (m, 4H), 1.70-1.62 (m, 4H), 1.43-1.21 (m, 7H), 0.92 (t, $^3J = 7.3$ Hz, 3H, 4-H). **$^{13}\text{C}\{\text{H}\}$ -NMR** (100 MHz, CDCl_3) δ (ppm) 66.2 (d, $^2J = 10.1$ Hz, C-1), 37.3 (d, $^1J = 100.2$ Hz, C-6), 32.6 (d, $^3J = 5.7$ Hz, C-2), 25.9 (s, C-8), 25.8 (d, $^4J = 1.2$ Hz, C-9), 24.3 (d, $^2J = 12.8$ Hz C-7), 18.9 (s, C-3), 13.7 (s, C-4). **$^{31}\text{P-NMR}$** (162 MHz, CDCl_3) δ (ppm) 43.4 (d, $^1J = 518.4$ Hz). **HRMS:** calcd for $\text{C}_{10}\text{H}_{21}\text{O}_2\text{NaP}$ $[\text{M}+\text{Na}]^+$ 227.1178, found 227.1177.

Butyl cyclooctylphosphinate (60b)



Conditions: (**59b** : 65 μ L, 0.5 mmol, 1 equiv.); ($\text{Ph}_2\text{I}^+ \text{OTf}^-$ (**73**) = 108 mg, 0.25 mmol, 0.5 equiv.); (Mes-Acr (**1**) = 1 mg, 0.5 mol%, 0.005 equiv). The reaction was carried out following the general procedure. The crude product was purified by flash column chromatography (ethyl acetate/*n*-pentane 90:10). **Yield** : 78 mg, 67%. **$^1\text{H-NMR}$** (400 MHz, CDCl_3) δ (ppm) 6.84 (d, $^1J = 519.0$ Hz, 1H), 4.13-3.92 (m, 2H, 1-H), 1.99-1.76 (m, 5H), 1.69-1.62 (m, 2H, 2-H), 1.54 (bs, 10H), 1.44-1.35 (m, 2H, 3-H), 0.93 (t, $^3J = 7.2$ Hz, 3H, 4-H). **$^{13}\text{C}\{\text{H}\}$ -NMR** (100 MHz, CDCl_3) δ (ppm) 66.3 (d, $^2J = 10.0$ Hz, C-1), 36.6 (d, $^1J = 90.1$ Hz, C-6), 32.6 (d, $^3J = 6.0$ Hz, C-2), 26.6 (s, C-10), 26.3 (s, C-9), 26.1 (d, $^3J = 15.1$ Hz, C-8), 24.5 (d, $^2J = 40.2$ Hz, C-7), 18.9 (s, C-3), 13.7 (s, C-4). **$^{31}\text{P-NMR}$** (162 MHz, CDCl_3) δ (ppm) 46.2 (d, $^1J = 519.0$ Hz). **HRMS:** calcd for $\text{C}_{12}\text{H}_{25}\text{O}_2\text{PNa}$ $[\text{M}+\text{Na}]^+$ 255.1488, found 255.1490.

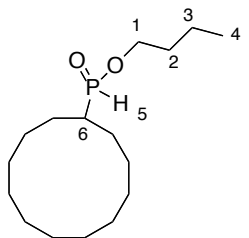
Butyl cyclopentylphosphinate (60c)



Conditions: (**59c** : 44 μ L, 0.5 mmol, 1 equiv.); ($\text{Ph}_2\text{I}^+ \text{OTf}^-$ (**73**) = 108 mg, 0.25 mmol, 0.5 equiv.); (Mes-Acr = 1 mg, 0.5 mol%, 0.005 equiv). The reaction was carried out following the general procedure. The crude product was purified by flash column chromatography (ethyl acetate/dichloromethane 80:20). **Yield** : 85 mg, 89%. **$^1\text{H-NMR}$** (400 MHz, CDCl_3) δ (ppm) 6.90 (d, $^1J = 521.1$ Hz, 1H, 5-H), 4.14-3.93 (m, 2H, 1-H), 2.17-2.08 (m, 1H, 6-H), 1.92-1.85 (m, 2H, 2-H), 1.82-1.75 (m, 2H), 1.72-1.58 (m, 6H), 1.44-1.34 (m, 2H, 3-H), 0.92 (t, $^3J = 7.5$ Hz, 3H, 4-H). **$^{13}\text{C}\{\text{H}\}$ -NMR** (100 MHz, CDCl_3) δ (ppm) 66.2 (d, $^2J = 7.5$ Hz, C-1), 37.0 (d, $^1J = 100.2$ Hz, C-6), 32.6 (d, $^3J = 10.3$ Hz, C-2), 26.5 (d, $^2J = 1.4$ Hz, C-7), 26.4 (d, $^3J = 12.1$ Hz, C-8), 18.9 (s, C-3), 13.7 (s, C-4). **$^{31}\text{P-NMR}$** (162 MHz, CDCl_3) δ (ppm) 44.7 (d, $^1J = 521.1$ Hz).

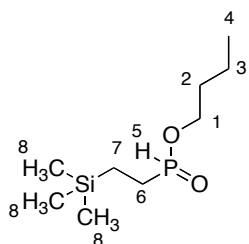
In agreement with previous work of Montchamp et al., due to the sensitivity of the title compound, the determination of its exact mass by mass spectrometry was not possible.

Butyl cyclododecylphosphinate (60d)



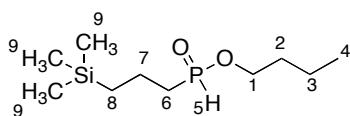
Conditions: (**59d** : 96 μ L, 0.5 mmol, 1 equiv.); ($\text{Ph}_2\text{I}^+ \text{OTf}^-$ (**73**) = 108 mg, 0.25 mmol, 0.5 equiv.); (Mes-Acr = 1 mg, 0.5 mol%, 0.005 equiv). The reaction was carried out following the general procedure. The crude product was purified by flash column chromatography (ethyl acetate/acetone 90:10). **Yield** : 60 mg, 42%. **$^1\text{H-NMR}$** (400 MHz, CDCl_3) δ (ppm) 6.91 (d, $^1J = 520.2$ Hz, 1H, 5-H), 4.14-3.94 (m, 2H, 1-H), 1.85-1.78 (m, 1H, 6-H), 1.69-1.61 (m, 4H), 1.58-1.28 (m, 22H), 0.92 (t, $^3J = 7.4$ Hz, 3H, 4-H). **$^{13}\text{C}\{\text{H}\}$ -NMR** (100 MHz, CDCl_3) δ (ppm) 66.4 (d, $^2J = 7.8$ Hz, C-1), 33.5 (d, $^1J = 96.0$ Hz, C-6), 32.6 (d, $^3J = 6.1$ Hz, C-2), 23.8 (s), 23.8 (s), 23.8 (s), 23.7 (s), 23.7 (s), 23.3 (s), 22.8 (s), 18.9 (s, C-3), 13.7 (s, C-4). **$^{31}\text{P-NMR}$** (162 MHz, CDCl_3) δ (ppm) 45.8 (d, $^1J = 520.2$ Hz). **HRMS:** calcd for $\text{C}_{16}\text{H}_{33}\text{O}_2\text{NaP}$ $[\text{M}+\text{Na}]^+$ 311.2119, found 311.2116.

Butyl 2-(trimethylsilyl)ethylphosphinate (60e)



Conditions: (**59e** : 73 μ L, 0.5 mmol, 1 equiv.); ($\text{Ph}_2\text{I}^+ \text{OTf}^-$ (**73**) = 108 mg, 0.25 mmol, 0.5 equiv.); (Mes-Acr = 1 mg, 0.5 mol%, 0.005 equiv). The reaction was carried out following the general procedure. The crude product was purified by flash column chromatography (ethyl acetate/acetone 90:10). **Yield** : 100 mg, 90%. **$^1\text{H-NMR}$** (400 MHz, CDCl_3) δ (ppm) 7.00 (d, $^1J = 524.0$ Hz, 1H, 5-H), 4.10-3.94 (m, 2H, 1-H), 1.71-1.64 (m, 4H), 1.45-1.36 (m, 2H, 7-H), 0.93 (t, $^3J = 7.3$ Hz, 3H, 4-H), 0.70-0.65 (m, 2H, 6-H), 0.02 (s, 9H, 8-H). **$^{13}\text{C}\{\text{H}\}\text{-NMR}$** (100 MHz, CDCl_3) δ (ppm) 66.3 (d, $^2J = 7.3$ Hz, C-1), 32.5 (d, $^2J = 5.9$ Hz, C-2), 22.8 (d, $^2J = 92$ Hz, C-6), 18.8 (s, C-3), 13.7 (s, C-4), 6.2 (d, $^2J = 7.1$ Hz, C-7), -2.1 (s, C-8). **$^{31}\text{P-NMR}$** (162 MHz, CDCl_3) δ (ppm) 43.0 (d, $^1J = 524.0$ Hz). **HRMS:** calcd for $\text{C}_9\text{H}_{23}\text{O}_2\text{NaSiP}$ $[\text{M}+\text{Na}]^+$ 245.1103, found 245.1103.

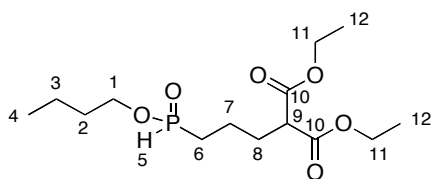
Butyl 3-(trimethylsilyl)propylphosphinate (60f)



Conditions: (**59f** : 79 μ L, 0.5 mmol, 1 equiv.); ($\text{Ph}_2\text{I}^+ \text{OTf}^-$ (**73**) = 108 mg, 0.25 mmol, 0.5 equiv.); (Mes-Acr (**1**) = 1 mg, 0.5 mol%, 0.005 equiv). The reaction was carried out following the general procedure. The crude product was purified by flash column chromatography (ethyl acetate/dichloromethane 90:10). **Yield** : 97 mg, 82%. **$^1\text{H-NMR}$** (400 MHz, CDCl_3) δ (ppm) 7.06 (d, $^1J = 526.0$ Hz, 1H, 5-H), 4.11-3.90 (m, 2H, 1-H), 1.80-1.73 (m, 2H, 6-H), 1.67-1.51 (m, 4H), 1.41-1.32 (m, 2H, 7-H), 0.89 (t, $^3J = 7.3$ Hz, 3H, 4-H), 0.59-0.55 (m, 2H, 8-H), -0.06 (s, 9H, 9-H). **$^{13}\text{C}\{\text{H}\}\text{-NMR}$** (100 MHz, CDCl_3) δ (ppm) 66.2 (d, $^2J = 10.1$ Hz, C-1), 32.5 (d, $^1J = 10$ Hz, C-6), 18.8 (s, C-2), 18.3 (s, C-8), 18.2 (s, C-3), 15.8 (s, C-4), 13.6 (s, C-7), -1.8 (s, C-9). **$^{31}\text{P-NMR}$** (162 MHz, CDCl_3) δ (ppm) 39.0 (d, $^1J = 526.0$ Hz).

In agreement with previous work of Montchamp et al., due to the sensitivity of the title compound, the determination of its exact mass by mass spectrometry was not possible.

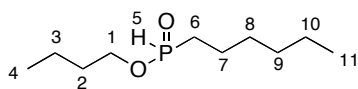
Butyl 4-(diethylmaleonate)propylphosphinate (60g)



Conditions: (**59g** : 99 μ L, 0.5 mmol, 1 equiv.); ($\text{Ph}_2\text{I}^+ \text{OTf}^-$ (**73**) = 108 mg, 0.25 mmol, 0.5 equiv.); (Mes-Acr = 1 mg, 0.5 mol%, 0.005 equiv). The reaction was carried out following the general

procedure. The crude product was purified by flash column chromatography (ethyl acetate/dichloromethane 90:10). **Yield** : 84 mg, 52%. **$^1\text{H-NMR}$** (400 MHz, CDCl_3) δ (ppm) 7.07 (d, $^1J = 530.1$ Hz, 1H, 5-H), 4.20-4.15 (m, 4H, 10-H), 4.12–3.93 (m, 2H, 1-H), 3.31 (t, $^3J = 7.3$ Hz, 1H, 9-H), 2.01-1.95 (m, 2H, 8-H), 1.83–1.75 (m, 2H, 7-H), 1.69-1.60 (m, 4H), 1.43-1.35 (m, 2H, 3-H), 1.25 (t, $^3J = 7.0$ Hz, 6H, 11-H), 0.92 (t, $^3J = 7.3$ Hz, 3H, 4-H). **$^{13}\text{C}\{\text{H}\}$ -NMR** (100 MHz, CDCl_3) δ (ppm) 169.2 (s, C-10), 65.5 (d, $^2J = 7.0$ Hz, C-1), 61.7 (s, C-11), 51.6 (s, C-9), 30.6 (s, C-8), 29.4 (d, $^3J = 6.0$ Hz, C-2), 19.1 (s, C-3), 18.5 (d, $^1J = 90.0$ Hz, C-6), 14.1 (s, C-7), 13.7 (s, C-4, C-12). **$^{31}\text{P-NMR}$** (162 MHz, CDCl_3) δ (ppm) 37.8 (d, $^1J = 530.1$ Hz). **HRMS:** calcd for $\text{C}_{14}\text{H}_{28}\text{O}_6\text{P}$ $[\text{M}+\text{H}]^+$ 323.1627, found 323.1624.

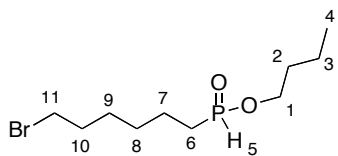
Butyl hexylphosphate (**60h**)



Conditions: (**59h** : 62 μ L, 0.5 mmol, 1 equiv.); ($\text{Ph}_2\text{I}^+ \text{OTf}^-$ (**73**) = 108 mg, 0.25 mmol, 0.5 equiv.); (Mes-Acr = 1 mg, 0.5 mol%, 0.005 equiv).

The reaction was carried out following the general procedure. The crude product was purified by flash column chromatography (ethyl acetate/acetone 90:10 \rightarrow 50:50). **Yield** : 59 mg, 57%. **$^1\text{H-NMR}$** (400 MHz, CDCl_3) δ (ppm) 7.03 (d, $^1J = 532.0$ Hz, 1H, 5-H), 4.13-3.92 (m, 2H, 1-H), 1.79-1.71 (m, 2H, 2-H), 1.67-1.60 (m, 2H, 6-H), 1.48-1.42 (m, 3H), 1.35-1.26 (m, 4H), 1.26 (m, 3H), 0.91 (t, $^3J = 7.6$ Hz, 3H, 4-H), 0.85 (t, $^3J = 6.6$ Hz, 3H, 11-H). **$^{13}\text{C}\{\text{H}\}$ -NMR** (100 MHz, CDCl_3) δ (ppm) 66.4 (d, $^2J = 7.0$ Hz, C-1), 32.5 (d, $^2J = 6.0$ Hz, C-2), 31.4 (s), 30.1 (d, $^2J = 16.0$ Hz, C-3), 28.6 (d, $^1J = 94.0$ Hz, C-6), 22.4 (s), 20.7 (s), 18.9 (s), 14.0 (s, C-4), 13.7 (s, C-11). **$^{31}\text{P-NMR}$** (162 MHz, CDCl_3) δ (ppm) 40.2 (d, $^1J = 532.0$ Hz). **HRMS:** calcd for $\text{C}_{10}\text{H}_{23}\text{NO}_2\text{PNa}$ $[\text{M}+\text{Na}]^+$ 229.1337, found 229.1333.

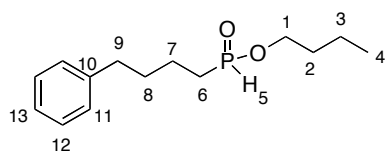
Butyl 6-bromohexylphosphinate (60j)



Conditions: (**59j** : 67 μ L, 0.5 mmol, 1 equiv.); ($\text{Ph}_2\text{I}^+ \text{OTf}^-$ (**73**) = 108 mg, 0.25 mmol, 0.5 equiv.); (Mes-Acr = 1 mg, 0.5 mol%, 0.005 equiv). The reaction was carried out following the general procedure. The crude product was purified by flash column chromatography (ethyl acetate/dichloromethane 90:10). **Yield** : 100 mg, 70%. **$^1\text{H-NMR}$** (400 MHz, CDCl_3) δ (ppm) 7.05 (d, $^1J = 528.5$ Hz, 1H, 5-H), 4.12-3.91 (m, 2H, 1-H), 3.37 (t, $^3J = 7.0$ Hz, 2H, 11-H), 1.86-1.81 (m, 2H, 10-H), 1.78-1.71 (m, 2H, 6-H), 1.69-1.58 (m, 4H), 1.43-1.33 (m, 6H), 0.91 (t, $^3J = 7.0$ Hz, 3H, 4-H). **$^{13}\text{C}\{\text{H}\}$ -NMR** (100 MHz, CDCl_3) δ (ppm) 66.3 (d, $^2J = 10$ Hz, C-1), 33.7 (s, C-11), 32.5 (s, C-10), 32.4 (s, C-2), 29.6 (d, $^2J = 15.1$ Hz, C-7), 28.7 (d, $^1J = 93.0$ Hz, C-6), 27.7 (s, C-9), 20.7 (d, $^3J = 3.1$ Hz, C-8), 18.9 (s, C-3), 13.7 (s, C-4). **$^{31}\text{P-NMR}$** (162 MHz, CDCl_3) δ (ppm) 39.0 (d, $^1J = 528.5$ Hz).

In agreement with previous work of Montchamp et al., due to the sensitivity of the title compound, the determination of its exact mass by mass spectrometry was not possible.

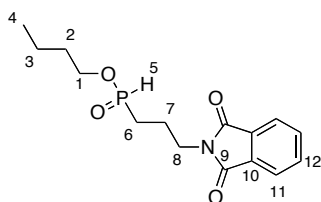
Butyl-4-phenylphosphinate (60k)



Conditions: (**59k** : 75 μ L, 0.5 mmol, 1 equiv.); ($\text{Ph}_2\text{I}^+ \text{OTf}^-$ (**73**) = 108 mg, 0.25 mmol, 0.5 equiv.); (Mes-Acr = 1 mg, 0.5 mol%, 0.005 equiv). The reaction was carried out following the general procedure. The crude product was purified by flash column chromatography (ethyl acetate/dichloromethane 90:10). **Yield** : 89 mg, 70%. **$^1\text{H-NMR}$** (400 MHz, CDCl_3) δ (ppm) 7.15 (d, $^1J = 528.0$ Hz, 1H, 5-H), 7.39-7.35 (m, 2H, Ar-H), 7.29-7.24 (m, 3H, Ar-H), 4.24-4.01 (m, 2H, 1-H), 2.73 (t, $^3J = 7.5$ Hz, 2H, 9-H), 1.92-1.65 (m, 8H), 1.54-1.44 (m, 2H, 3-H), 1.03 (t, $^3J = 7.4$ Hz, 3H, 4-H). **$^{13}\text{C}\{\text{H}\}$ -NMR** (100 MHz, CDCl_3) δ (ppm) 141.7 (s, C-10), 128.5 (s, C-Ar), 128.4 (s, C-Ar), 126.0 (s, C-Ar), 66.3 (d, $^2J = 10.0$ Hz, C-1), 35.5 (s, C-9), 32.5 (d, $^3J = 6.2$ Hz, C-2), 32.3 (d, $^2J = 10.1$ Hz, C-7), 28.7 (d, $^1J = 94.0$ Hz, C-6), 20.5 (d, $^4J = 3.0$ Hz, C-3), 18.9 (s, C-8), 13.7 (s, C-4). **$^{31}\text{P-NMR}$** (162 MHz, CDCl_3) δ (ppm) 39.1 (d, $^1J = 528.0$ Hz).

In agreement with previous work of Montchamp et al., due to the sensitivity of the title compound, the determination of its exact mass by mass spectrometry was not possible.

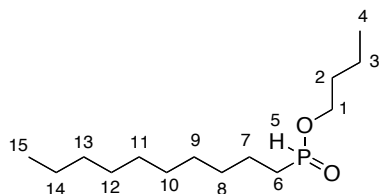
Butyl-3-(1,3-dioxoisindolin-2-yl)propylphosphinate (60l')



Conditions: (**59l** : 94 mg, 0.5 mmol, 1 equiv.); ($\text{Ph}_2\text{I}^+ \text{OTf}^-$ (**73**) = 108 mg, 0.25 mmol, 0.5 equiv.); (Mes-Acr = 1 mg, 0.5 mol%, 0.005 equiv). The reaction was carried out following the general procedure. The crude product was purified by flash column chromatography (ethyl acetate/dichloromethane 90:10). **Yield** : 111 mg, 72%. **H-NMR** (400 MHz, CDCl_3) δ (ppm) 7.83-7.81 (m, 2H, Ar-H), 7.72-7.70 (m, 2H, Ar-H), 7.10 (d, $^1J = 536.0$ Hz, 1H, 5-H), 4.12-3.93 (m, 2H, 1-H), 3.75 (t, $^3J = 7.0$ Hz, 2H, 8-H), 2.02-1.92 (m, 2H, 2-H), 1.86-1.78 (m, 2H, 7-H), 1.67-1.60 (m, 2H, 6-H), 1.41-1.32 (m, 2H, 3-H), 0.90 (t, $^3J = 7.3$ Hz, 3H, 4-H). **$^{13}\text{C}\{\text{H}\}$ -NMR** (100 MHz, CDCl_3) δ (ppm) 168.3 (s, C-9), 134.2 (s, C-Ar), 132.0 (s, C-Ar), 123.4 (s, C-Ar), 66.6 (d, $^2J = 7.0$ Hz, C-1), 38.1 (d, $^1J = 20.0$ Hz, C-8), 32.5 (d, $^3J = 6.0$ Hz, C-2), 26.4 (d, $^1J = 90.0$ Hz, C-6), 20.4 (d, $^2J = 2.0$ Hz, C-7), 18.8 (s, C-3), 13.7 (s, C-4). **^{31}P -NMR** (162 MHz, CDCl_3) δ (ppm) 37.5 (d, $^1J = 536$ Hz). **HRMS:** calcd for $\text{C}_{15}\text{H}_{20}\text{NO}_4\text{PNa}$ $[\text{M}+\text{Na}]^+$ 332.1030, found 332.1028.

In agreement with previous work of Montchamp et al., due to the sensitivity of the title compound, the determination of its exact mass by mass spectrometry was not possible.

Butyl decylphosphinate (60m')



Conditions: (**59m** : 101 μL , 0.5 mmol, 1 equiv.); ($\text{Ph}_2\text{I}^+ \text{OTf}^-$ (**73**) = 108 mg, 0.25 mmol, 0.5 equiv.); (Mes-Acr = 1 mg, 0.5 mol%, 0.005 equiv). The reaction was carried out following the general procedure. The crude product was purified by flash column chromatography (ethyl acetate/*n*-pentane 90:10). **Yield** : 62 mg, 47%. **^1H -NMR** (400 MHz, CDCl_3) δ (ppm) 7.03 (d, $^1J = 525.1$ Hz, 1H, 5-H), 4.12-3.90 (m, 2H, 1-H), 1.76-1.68 (m, 2H, 6-H), 1.66-1.61 (m, 2H, 2-H), 1.60-1.49 (m, 2H, 3-H), 1.42-1.32 (m, 4H), 1.22 (bs, 12H), 0.92 (t, $^3J = 7.4$ Hz, 3H, 4-H), 0.85 (t, $^3J = 6.7$ Hz, 3H, 15-H). **$^{13}\text{C}\{\text{H}\}$ -NMR** (100 MHz, CDCl_3) δ (ppm) 66.2 (d, $^2J = 10.0$ Hz, C-1), 32.5 (d, $^3J = 6.0$ Hz, C-2), 31.9 (s, C-6), 30.5 (d, $^2J = 15.0$ Hz, C-8), 29.6 (s, C-10), 29.4 (d, $^4J = 5.2$ Hz, C-9), 29.3 (s, C-11),

29.2 (s, C-12), 28.3 (s, C-13), 22.7 (s, C-14), 20.8 (d, $^4J = 3.0$ Hz, C-3), 18.9 (s, C-7), 14.2 (s, C-4), 13.7 (s, C-15). $^{31}\text{P-NMR}$ (162 MHz, CDCl_3) δ (ppm) 39.6 (d, $^1J = 525.1$ Hz).

In agreement with previous work of Montchamp et al., due to the sensitivity of the title compound, the determination of its exact mass by mass spectrometry was not possible.

Generation of Phosphinoyl Radicals through EDA complexes and their Reactivity towards Unactivated Alkenes

3.1. Background

In the previous chapter, we have shown that the generation of phosphinoyl radicals from H-phosphinates required the use of an external oxidant, for instance diphenyliodonium ion, which is reduced by the excited state of the photocatalyst to generate the phenyl radical.

As largely discussed in previous chapter, due to the existence of H-phosphinates predominantly in their P(V) forms, the employment of Ph_2I^+ was highly important for the feasibility of the hydrophosphinylation reaction of unactivated alkenes.

As part of our continued effort to establish efficient and sustainable approaches for the generation of different phosphorus based radicals, we become interested in secondary phosphine oxides. The corresponding radicals have traditionally been generated through classical radical methods and have been employed for the synthesis of organophosphorus molecules (*vide infra*), where some of them have potential medical applications.

As depicted in Figure 3.1, bond dissociation energies of secondary phosphine oxides and related derivatives are ranging from 72 to 87 Kcal/mol and can therefore be cleaved to form the desired phosphorus based radical. Figure 3.1 also shows that P=S compounds could be remarkably more reactive towards C=C bonds than P=O species, because of their lower BDE values. The P-H bond dissociation energy for secondary phosphine oxides is low enough (79 kcal/mol) to allow transformations such as radical addition towards unactivated substrates, under mild conditions avoiding the use of expensive additives or high temperatures.

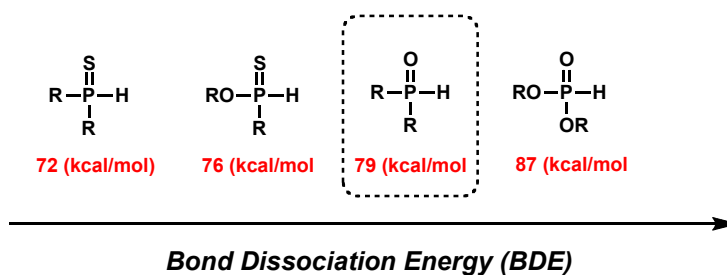


Figure 3.1. Bond Dissociation Energy (BDE) of most common organophosphorus compounds

The different reactivity of phosphorus-centered radical species has been attributed to the different *bond dissociation energies* (BDE) of the P–H bond, which have been largely studied and calculated by *density functional theory* (DFT).

The substituents at the phosphorus atom clearly influence the BDE of P–H bonds, and it has already been demonstrated that those possessing the lowest value of BDE add easier to unsaturated C–C bonds. This order of reactivity also depends on the pyramidalization at the phosphorus atom of the radical. Figure 3.2 shows that diethoxyphosphonyl radicals add easily onto olefins, even those exhibiting steric hindrance.

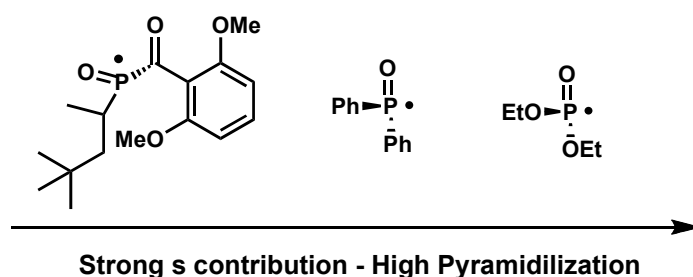


Figure 3.2. Graphic illustration of phosphorus based radicals with high pyramidalization.

Useful and common methodologies for the generation of phosphorus centered radicals starting from secondary phosphine oxides or sulfides are shown in Figure 3.3 and include: *a*) photolysis and thermolysis, *b*) reaction with azo and peroxide radical initiators,¹¹³ *c*) reaction with single electron oxidants such as $\text{Mn}(\text{OAc})_2/\text{O}_2$ or $\text{Mn}(\text{OAc})_3$.¹¹⁴

¹¹³ (a) Myers, T.N. *Initiators, Free-Radical*, in *Kirk-Othmer Encyclopedia of Chemical Technology*. (b) Kita, Y.; Matsugi, M. in *Radicals in Organic Synthesis*, Vol. 1, Renaud, P.; Sibi, M.; Eds, M.P. Wiley-VCH, Weinheim, **2001**, 1-10.

¹¹⁴ (a) Mondal, M.; Bora, U. *RSC Adv.* **2013**, *3*, 18716-18754. (b) Pan, X.-Q.; Zou, J.-P.; Zhang, W. *Mol. Diver.* **2009**, *13*, 421-438. (c) Snider, B.B. *Tetrahedron* **2009**, *65*, 10738-10744.

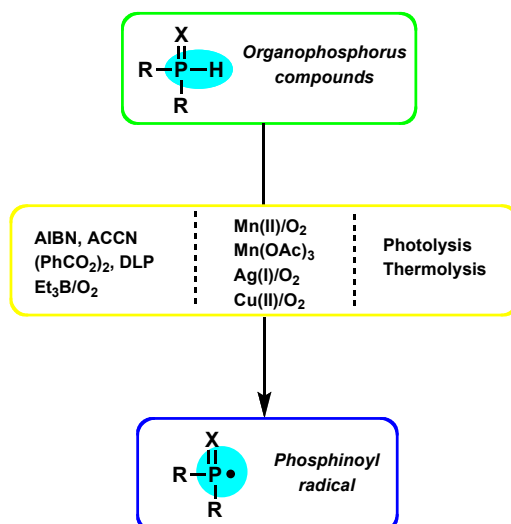
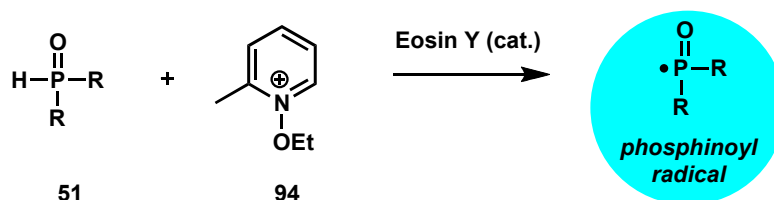


Figure 3.3. Formation of phosphinoyl radical *via* different activation modes

On the basis of previous investigation by Turro *et al.*,¹¹⁵ on the kinetics of reactions of phosphinoyl radicals with alkenes, aromatics, alkyl halogenates, it appears clearly that those radicals add smoothly to all these compounds. This implies that the high temperature required in most of radical processes involving phosphinoyl radicals is actually needed for the generation of radicals themselves. With the aim to define new approaches for the generation of P-based radicals, we have recently showed that visible light photoredox catalysis can be effective towards this end (Scheme 3.1).¹¹⁶



Scheme 3.1. Visible-light mediated formation of phosphinoyl radical in the presence of eosin Y as photocatalyst

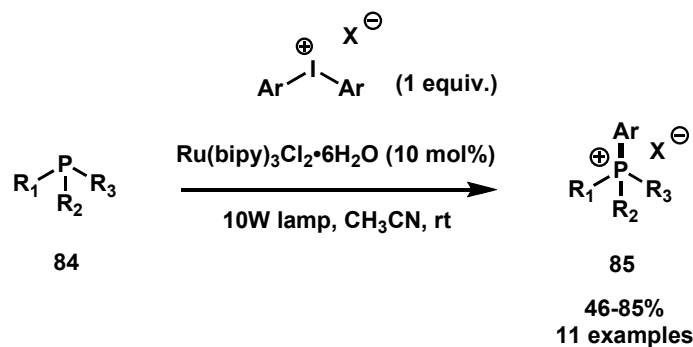
On the other hand, Denton *et al.*¹¹⁷ have recently reported an elegant approach for the arylation of tertiary phosphines. As depicted in Scheme 3.2, the method takes advantage on the high reducing abilities of diaryliodonium salts and the high oxidizing abilities of tertiary phosphines to generate aryl radicals and phosphorus radical cations that

¹¹⁵ Jockusch, S.; Turro, N.J. *J. Am. Chem. Soc.* **1998**, *120*, 11773-11777.

¹¹⁶ Quint, V.; Morlet-Savary, F.; Lohier, J.-F.; Lalevée, J.; Gaumont, A.-C.; Lakhdar, S. *J. Am. Chem. Soc.* **2016**, *138*, 7436-7441.

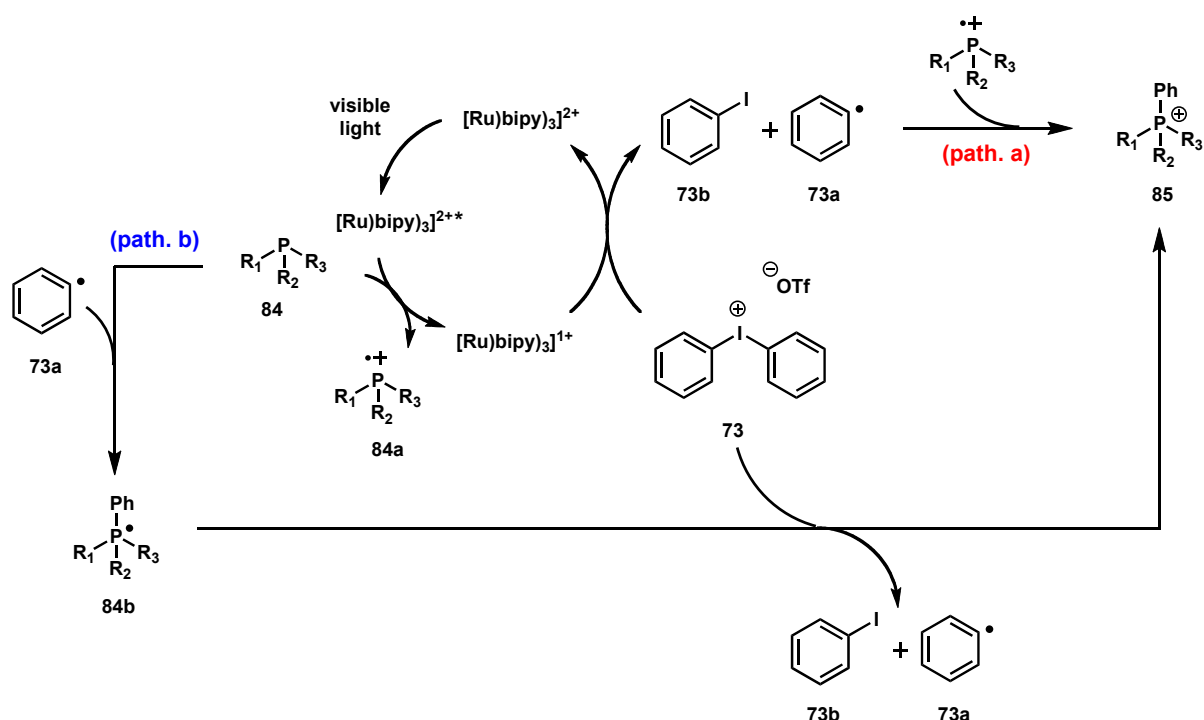
¹¹⁷ Fearnley, A.F.; An, J.; Jackson, M.; Lindovska, P.; Denton, R.M. *Chem. Commun.* **2016**, *52*, 4987-4990.

combine together to form the desired quaternary phosphonium salts. In this regard, $\text{Ru}(\text{bipy})_3^{2+}$, whose redox potentials are +0.77 V and -0.81 V (vs. SCE), has been found to be an ideal photocatalyst to accomplish this transformation.



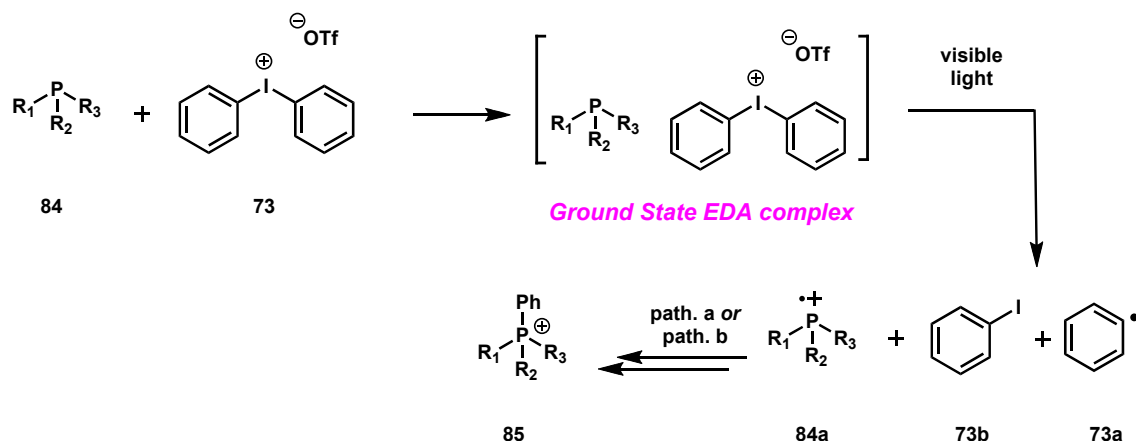
Scheme 3.2. Photoredox-mediated phosphines arylation reaction *via* EDA complexes formation

From a mechanistic point of view, the excited state of the ruthenium-based photocatalyst is capable to reduce triaryl phosphine **84** to generate the radical cationic species **84a**. The resulting ruthenium(I) species can reduce diaryliodonium ion **73** to generate aryl iodide **73b** as a by-product along with phenyl radical **73a**. Two pathways are now possible to form the desired arylated phosphine **85**. Either, the phosphonium radical intermediate **84b** can react with phenyl radical **73a** (path. a), or **73a** reacts with starting triarylphosphine **84** leading to the desired product **85** *via* radical chain process (path. b). The latter consists in the formation of a phosphoranyl intermediate **84a**, followed by oxidation by iodonium salt **73** to afford the phosphonium salt **85** and propagating the radical process (Scheme 3.3).



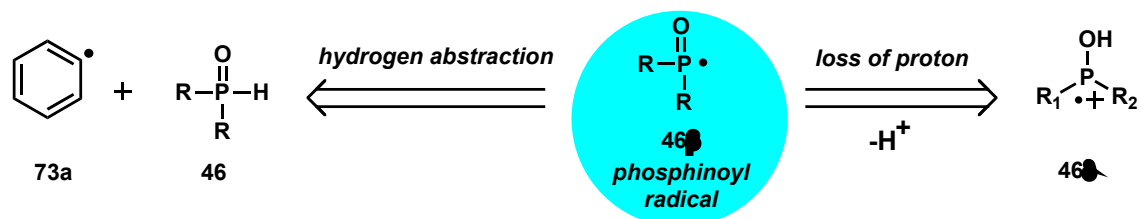
Scheme 3.3. Mechanism of photoredox-mediated phosphine arylation *via* EDA complexes formation

Importantly, when testing the effect of light, photocatalyst and additives on their photoreaction, Denton *et al.* noticed that the reaction could take place in the absence of the photocatalysts as 12% of the final product was detected by ³¹P-NMR after a reaction time of 12 min. This observation has been attributed to the formation of an electron donor acceptor complex (EDA) between the tertiary phosphine, for instance triphenylphosphine, and diphenyliodonium ion. This complex is then excited by blue light and a single electron transfer event takes place from the donor (PPh₃) to the acceptor (Ph₂I⁺), thereby generating the phenyl radical and the oxidized form of the phosphine. Both species combines at the diffusion limit to give rise to the phosphonium salt **85** (Scheme 3.4).



Scheme 3.4. Plausible phosphine arylation mechanism *via* electron donor-acceptor complex formation

Inspired by this important observation, we reasoned that one could explore the capability of phosphines/diphenyliodonium salt in forming EDA complexes for the generation of phosphorus-based radicals under photocatalytic free conditions. In this regard, we have assumed that secondary phosphine oxides, which exist in solution as mixture of P(III) and P(V), could form a EDA complex with Ph_2I^+ . This complex can presumably generate a phenyl radical along with the phosphine radical cation. The latter lost a proton to give rise to the phosphinoyl radical. This radical can also be generated by a hydrogen abstraction of P–H bond by the phenyl radical (Scheme 3.5).



Scheme 3.5. Two alternatives to form phosphinoyl radical

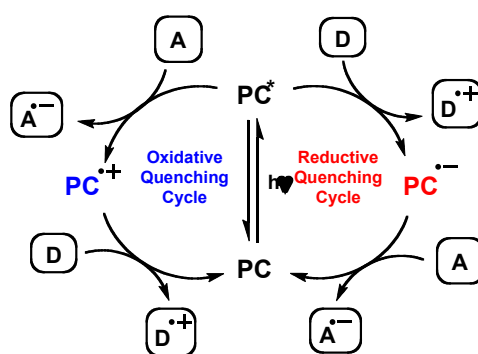
As a proof of concept, we decided to apply this methodology to the hydrophosphination reaction of unactivated alkenes.

Before presenting our results in this topic, we will first introduce the concept of EDA complexes and cover most important contributions in the area of hydrophosphinylation of alkenes.

3.2. Theoretical background for electron-donor-acceptor (EDA) complexes

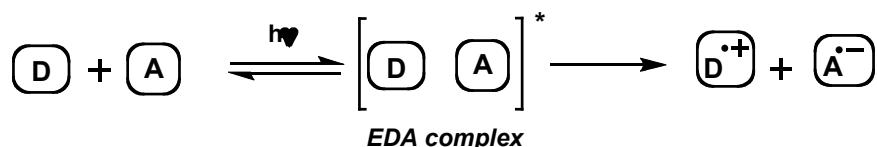
3.2.1. General scenario

As already demonstrated in the previous Chapter, the use of an external photocatalyst (PC) is often required in order to accomplish useful chemical transformations for C–P bond forming reactions (Scheme 3.6).¹¹⁸



Scheme 3.6. General mechanism of SET reaction induced by a photocatalyst

Because many organic molecules do not absorb in the visible light region, it is absolutely necessary to employ a photocatalyst. On the other hand, in contrast to this conventional approach, the association between an electron-rich (D, donor) and an electron-poor (A, acceptor) molecule, is known to lead to the formation of an electron donor-acceptor (EDA) complex. The latter can easily absorb light in the visible region and thus be useful for a great variety of organic transformations. Contrarily to the previous strategy, this one does not require the use of a photocatalyst (Scheme 3.7).¹¹⁹



Scheme 3.7. General mechanism of SET reaction EDA-induced

Let's focus now on the (EDA) complex. There are many interpretations on its appropriate meaning. In 1965, Longuet-Higgins¹²⁰ proposed his concept about a *molecule*. He suggested that it can be defined as “a group of atom, or a single atom,

¹¹⁸ (a) Narayanam, J.M.R.; Stephenson, C.R.J. *Chem. Soc. Rev.* **2011**, *40*, 102-113. (b) Prier, C.K.; Rankic, D.A. MacMillan, D.W.C. *Chem. Rev.* **2013**, *113*, 5322-5363. (c) Nicewicz, D.A.; Nguyen, T.M. *ACS Catal.* **2014**, *4*, 355-360.

¹¹⁹ (a) Lima, C.G.S.; Lima, T.de M.; Duarte, M.; Jurberg, I.D.; Paixão, M.W. *ACS Catal.* **2016**, *6*, 1389-1407. (b) Tucker, J.W.; Stephenson, C. *J. Org. Chem.* **2012**, *77*, 1617-1622.

¹²⁰ Longuet-Higgins, H.C. *Faraday Soc. Discuss.* **1965**, *40*, 7-18.

with a binding energy large in comparison with the thermal energy, and which can interact with the environment without losing its identity”.

Consequently, in the 80's, Foster gave a new definition of the term complex, described as follows “a group of atoms or molecules with a binding energy which is **not** large in comparison with the thermal energy, and whose identity can be shaken, or even lost, by interactions with the environment”.³

Electron donor and acceptors are reagents that are traditionally considered with different connotations: *a*) reductants and oxidants in electron transfer reactions, *b*) nucleophiles and electrophiles in bond formation, *c*) bases and acids in coupling reactions and *d*) anions and cations in ion-pair annihilation (Table 3.1).¹²¹

Table 3.1. Different meanings of electron-donor (D) and electron-acceptor (A)

Electron-Donor (D)	Electron-Acceptor (A)
Reductant	Oxidant
Nucleophile	Electrophile
Base (Lewis)	Acid (Lewis)
Anion	Cation

Generally, the occurrence of a process that works *via* EDA-forming reaction follows these circumstances: a donor D, which is an electron-rich compound (see Table 3.1), and an acceptor A, electron-poor molecule (see Table 3.1) in solution combine each other to form a complex (Scheme 3.7): $[D,A]_{EDA}$. Molecules associate between them to give rise to a weak and reversible bond, more sensitive to variations of solvent, temperature and concentration¹²² than any weak bond such as hydrogen bonding.¹²³ We can assume that the bond strength in such complexes is an average between a strong covalent bond and a weak Van der Waals bond.

During recent years, this new methodology has started to grow up either both in the field of photochemistry or in simple metal-free mild processes thanks to a large number

¹²¹ Kochi, J.K. *Pure Appl. Chem.* **1991**, *63*, 255-264.

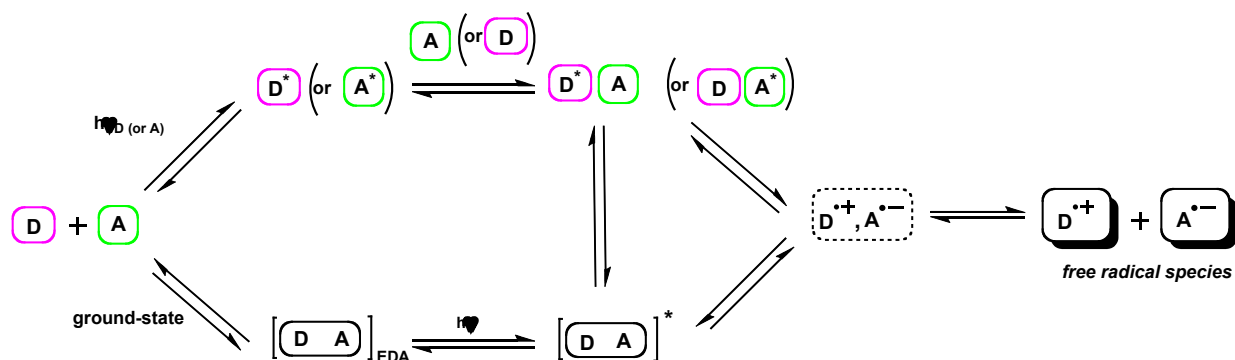
¹²² (a) Foster, R. *J. Phys. Chem.* **1980**, *84*, 2135-2141. (b) Rosokha, S.V.; Kochi, J.K. *Acc. Chem. Res.* **2008**, *41*, 641-653.

¹²³ Zhao, G.J.; Han, K.L. *Acc. Chem. Res.* **2012**, *45*, 404-413.

of contributions reported,¹²⁴ and then to be extensively studied, although its application is still limited.

3.2.2. Photogeneration of radical donor-acceptor (EDA) species and related contributions

There are two main pathways to afford radical species by starting from a donor-acceptor complex. Under light irradiation, $[D,A]_{EDA}$ changes from ground state to excited state complex $[D,A]^*$. Afterwards, such excited complex can give rise to an electron-transfer event generating a radical ion pair trapped in the solvent cage $[D^{\bullet+}, A^{\bullet-}]_{SOLV.}$. The latter can finally undergo various reaction pathways, such as eliminations, additions or rearrangements (Scheme 3.8).¹²⁵



Scheme 3.8. Possible pathways for irradiated donor-acceptor complexes

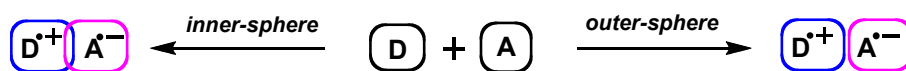
The other pathway is that excitation of individual components D (or A), can lead to excited forms D^* (or A^*) which can react with non-excited components A (or D) to afford D^* (or A) or D (or A^*) complexes, respectively. Such complexes can lead to electron-transfer events or be converted to the same ion-radical pair already mentioned $[D^{\bullet+}, A^{\bullet-}]_{SOLV.}$

In this context, to describe the electron transfer process between donor (D) and acceptor (A) in a complex, two definitions can be used: *outer-* and *inner-sphere electron transfer*

¹²⁴ (a) Biermann, U.; Butte, W.; Koch, R.; Fokou, P.A.; Türünç, O.; Meier, M.A.R.; Metzger, J.O. *Chem. –Eur. J.* **2012**, *18*, 8201-8207. (b) Cheng, Y.; Yuan, X.; Ma, J.; Yu, S. *Chem. – Eur. J.* **2015**, *21*, 8355-8359. (c) Dohi, T.; Ito, M.; Yamaoka, N.; Morimoto, K.; Fujioka, H.; Kita, Y. *Angew. Chem. Int. Ed.* **2010**, *49*, 3334-3337.

¹²⁵ (a) Gould, I.R.; Moody, R.; Farid, S. *J. Am. Chem. Soc.* **1988**, *110*, 7242-7244. (b) Mori, T.; Inoue, Y. *Chem. Soc. Rev.* **2013**, *42*, 8122-8133.

(Scheme 3.9).¹²⁶ The terms bonded and no bonded electron-transfer, corresponding to inner- and outer-sphere, respectively, could be more appropriate for organic molecules.



Scheme 3.9. Two pathways to explain electron transfer mechanism

The non-bonded (outer-sphere) electron-transfer is a non-adiabatic process,¹²⁷ while the bonded (inner-sphere) electron-transfer is typically an adiabatic mechanism. In the first case, the electron-transfer is the rate-determining step,¹²⁸ in the other one it cannot be the rate-determining step.¹²⁹

Although the high importance of this concept in organic chemistry, it has surprisingly been restricted to the field of physical organic chemistry and only Kochi *et al.*¹³⁰ have turned their attention on using this paradigm in organic synthesis.

More recently, the group of Prof. Paolo Melchiorre from ICIQ-Tarragona has nicely explored the EDA chemistry in the field of enantioselective photocatalysis. As depicted in Scheme 3.10, by combining aldehydes with bromobenzyle derivatives in the presence of chiral secondary amines as catalysts under 23W compact fluorescent (CFL) bulb light, enantioselective α -alkylation of aldehydes has been accomplished with high yields (up to 96%) and outstanding enantioselectivities (83-94% *ee*).¹³¹

¹²⁶ (a) Taube, H. *Angew. Chem., Int. Ed. Engl.* **1984**, *23*, 329-394. (b) Rosokha, S.V.; Kochi, J.K. *Acc. Chem. Res.* **2012**, *45*, 404-413.

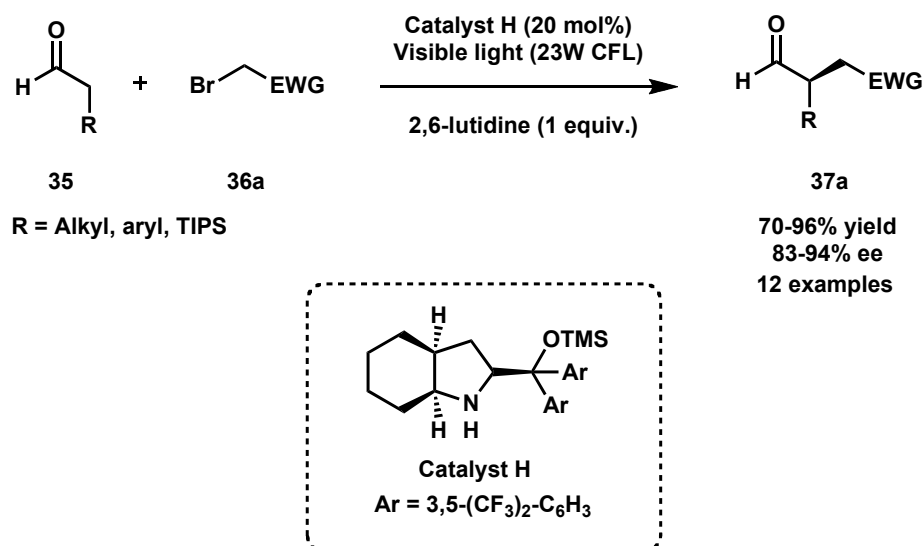
¹²⁷ (a) Marcus, R.A. *Angew. Chem., Int. Ed. Engl.* **1993**, *32*, 1111-1222. (b) Marcus, R.A. *Rev. Mod. Phys.* **1993**, *65*, 599-610. (c) Zusman, L.D. *Chem. Phys.* **1980**, *49*, 295-304.

¹²⁸ Patz, M.; Fukuzumi, S. *J. Phys. Org. Chem.* **1997**, *10*, 129-137.

¹²⁹ Zwickel, A.; Taube, H. *J. Am. Chem. Soc.* **1961**, *83*, 793-796.

¹³⁰ Hubig, S.M.; Bockman, T.M.; Kochi, J.K. *J. Am. Chem. Soc.* **1996**, *118*, 3842-3851.

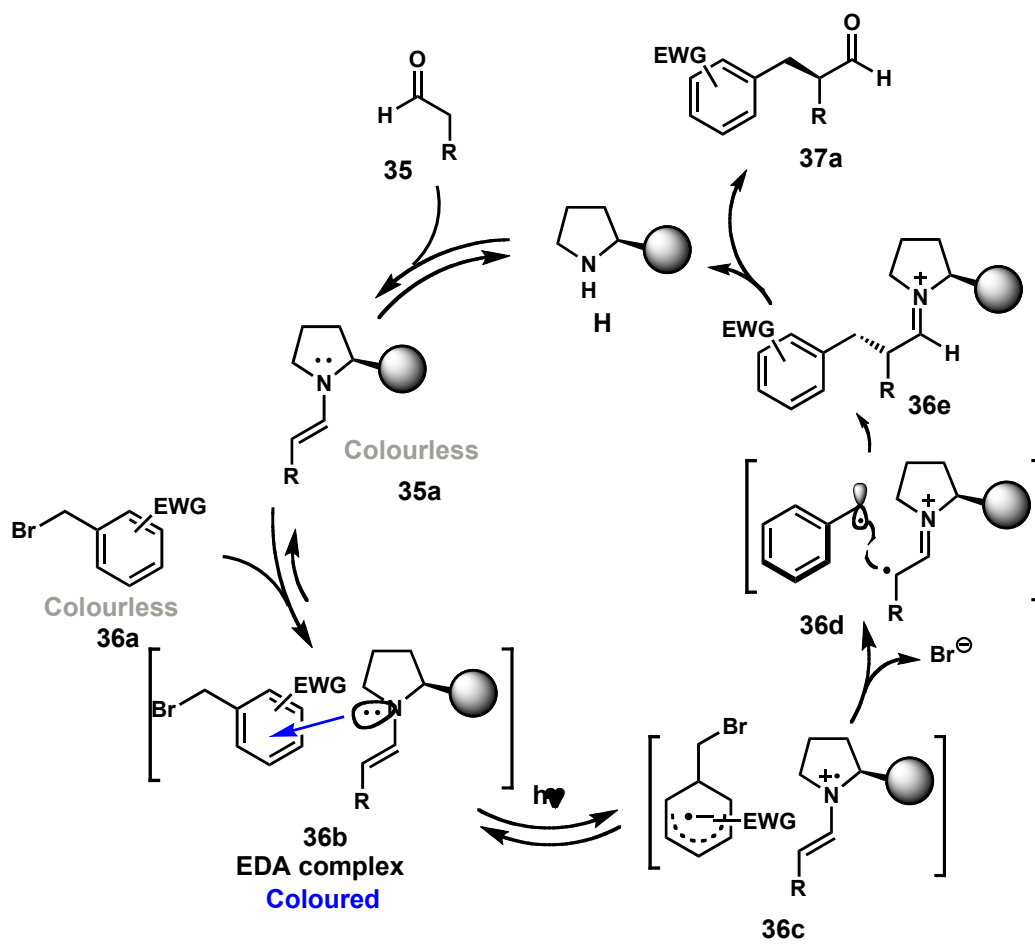
¹³¹ Arceo, E.; Jurberg, I.D.; Alvarez-Fernandez, A.; Melchiorre, P. *Nature Chemistry* **2013**, *5*, 750-756.



Scheme 3.10. Catalytic asymmetric photochemical α -alkylation of aldehydes with alkyl bromides

Detailed mechanistic investigations revealed that the enamine intermediate **35a** formed upon addition of secondary amine **H** with aldehyde **35** formed a EDA complex **36b** with the alkyl bromide **36a**. This EDA complex has been characterized in solution as well as in the solid state.

When this complex absorbs a blue photon it undergoes SET, leading to the formation of benzyl and iminium radicals (complex **36c**). At this stage, experiments with intervals of light and dark were performed and have shown that the chemical process underwent total interruption in the absence of light and regeneration of reactivity when light was switched on again. Then, two radical species reacted to give rise to the iminium cationic intermediate **36d**, which afforded the desired adduct **37a** after hydrolysis of **36e** (Scheme 3.11).



Scheme 3.11. Proposed mechanism for asymmetric catalytic photochemical α -alkylation of aldehydes

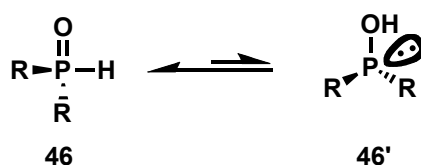
Melchiorre *et al.* have been capable to connect two important fields of organic chemistry, organocatalysis and photocatalysis, thanks to the vast capability of chiral enamines to behave as key intermediates in organocatalytic processes. They demonstrated that an elegant alternative to achieve α -alkylation of aldehydes could be performed in absence of an external photocatalyst. For instance, enamines can easily participate in photoinduced processes. Detailed mechanistic investigations have been carried out to firmly confirm the formation of the EDA complex. This new approach enabled access to chiral molecules under organocatalytic conditions with high yields and excellent enantioselectivities (ee <99%). Although this approach can differ from standard photoredox methodologies, it can open new avenues in the field of photocatalysis.

3.3. The phosphinoyl radical and hydrophosphination reaction

3.3.1. General overview

It has been shown that such reaction can occur under thermal conditions, *via* radical initiators or photo-chemically by irradiating with UV or visible light, in the presence of transition metals or in the presence of organocatalysts. In the literature, there is plethora of examples which concerns either phosphorus radical addition to C=C bonds or C–P bond forming reactions.¹³² To our knowledge, hydrophosphination reaction *via* EDA complexes activated by light irradiation has not been investigated so far.

Secondary phosphine oxides (SPO) are air- and moisture-stable compounds¹³³ that are used as weak acids¹³⁴ or preligands.¹³⁵ In solution, they exist in equilibrium between pentavalent (secondary phosphine oxides **46**) and trivalent (phosphinous acid **46'**) tautomeric structures (Scheme 3.12).¹³⁶



Scheme 3.12. Tautomeric equilibrium between P(V) and P(III) form of secondary phosphine oxides

In radical addition reactions, phosphorus centered radical adds to the carbon-carbon double bond to generate a carbon centered radical species that is able to abstract hydrogen atom from the starting phosphorus compound.

In this context, Han and co-workers¹³⁷ have reported the *anti*-Markovnikov hydrophosphination of alkenes with secondary phosphine oxides under aerobic conditions (Scheme 3.13).

¹³² (a) Semenzin, D.; Etemad-Moghadam, G.; Albouy, D.; Diallo, O.; Koenig, M. *J. Org. Chem.* **1997**, *62*, 2414-2422. (b) Lopin, C.; Gouhier, G.; Gautier, A.; Piettre, S.R. *J. Org. Chem.* **2003**, *68*, 9916-9923. (c) Rey, P.; Taillades, J.; Rossi, J.C.; Gros, G. *Tetrahedron Lett.* **2003**, *48*, 6169-6171. (d) Caddick, S.; Hamza, D.; Judd, D.B.; Reich, M.T.; Wadman, S.N.; Wilden, J.D. *Tetrahedron Lett.* **2004**, *45*, 2363-2366. (e) Dubert, O.; Gautier, A.; Condamine, E.; Piettre, S.R. *Org. Lett.* **2002**, *4*, 359-362. (f) Piettre, S.R. *Tetrahedron Lett.* **1996**, *37*, 2233-2236. (g) Piettre, S.R. *Tetrahedron Lett.* **1996**, *37*, 4707-4710. (h) Gautier, A.; Garipova, G.; Dubert, O.; Oulyadi, H.; Piettre, S.R. *Tetrahedron Lett.* **2001**, *42*, 5673-5676. (i) Herpin, T.F.; Motherwell, W.B.; Roberts, B.P.; Roland, S.; Weibel, J.-M. *Tetrahedron* **1997**, *53*, 15085-15100. (j) Jessop, C.M.; Parsons, A.F.; Routledge, A.; Irvine, D. *Tetrahedron Lett.* **2003**, *44*, 6169-6171. (k) Jessop, C.M.; Parsons, A.F.; Routledge, A.; Irvine, D. *Tetrahedron Lett.* **2004**, *45*, 5095-5098. (l) Parsons, A.F.; Sharpe, D.J.; Taylor, P. *Synlett* **2005**, 2981-2983.

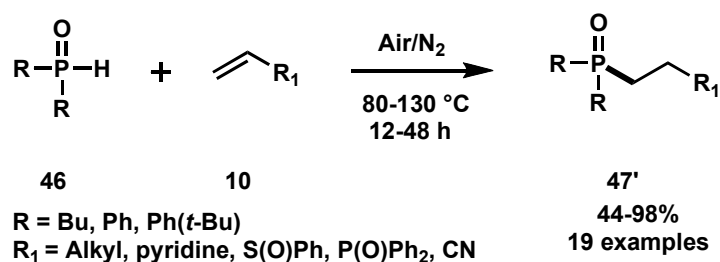
¹³³ (a) Griffiths, J.E.; Burg, A.B. *J. Am. Chem. Soc.* **1960**, *82*, 1507-1507. (b) Hoge, B.; Neufeind, S.; Hettel, S.; Wiebe, W.; Thoesen, C. *J. Organomet. Chem.* **2005**, *690*, 2382-2387.

¹³⁴ Quin, L.D. *A Guide to Organophosphorus Chemistry*; Wiley-Interscience: New York, **2000**.

¹³⁵ Dubrovina, N.V.; Börner, A. *Angew. Chem. Int. Ed.* **2004**, *43*, 5883-5886.

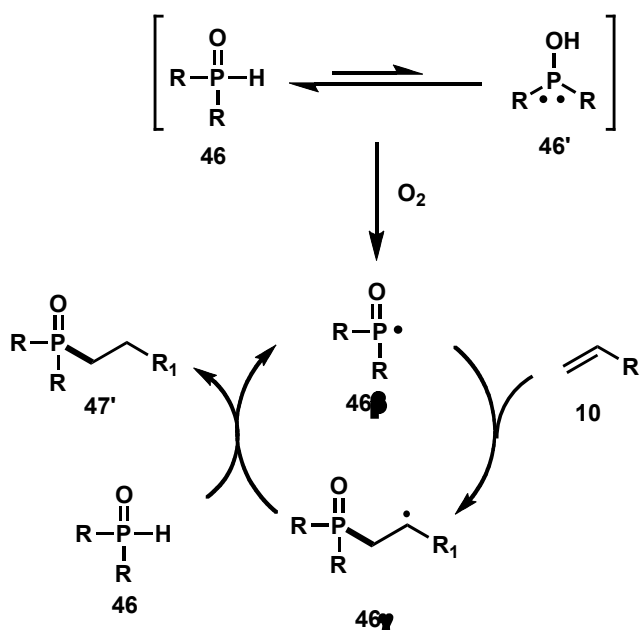
¹³⁶ Ackermann, L. *Synthesis* **2006**, *10*, 1557-1571.

¹³⁷ Hirai, T.; Han, L.-B. *Org. Lett.* **2007**, *9*, 53-55.



Scheme 3.13. Air-induced addition of secondary phosphine oxides to alkenes

The proposed mechanism of this transformation is depicted in Scheme 3.14.



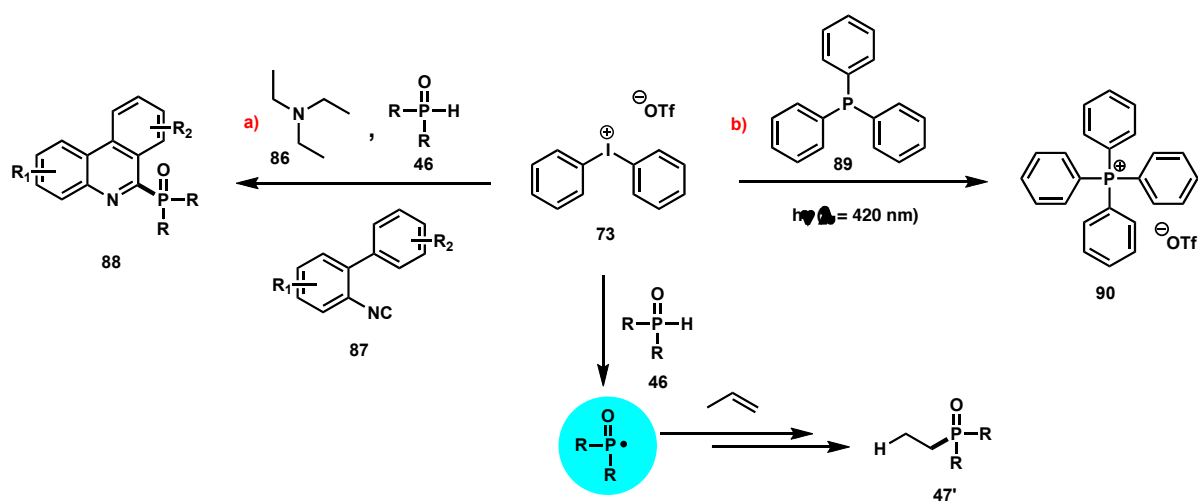
Scheme 3.14. Proposed mechanism for air-induced radical addition of secondary phosphine oxides to alkenes

P(III) form of the secondary phosphine oxide, in the presence of trace amounts of oxygen, generates the P-centered radical **46β**, which can react with alkene **10** to form the carbon centered radical **46γ**. The latter undergoes hydrogen abstraction reaction by secondary phosphine oxide **46** leading to the final product **47'** and regenerating the starting P-radical. In this way, the authors revealed that traces of air can easily induce P–H addition to alkenes *via* a radical chain mechanism.

As stated in the general introduction as well as in the previous chapter, recently, much attention has been turned to visible light photoredox catalysis as an elegant approach to generate phosphorus-centered radicals under mild and metal-free conditions.

A seminal work in this area has been published by the group of S. Kobayashi, who reported a visible light mediated hydrophosphinylation of unactivated olefins catalyzed by Rhodamine B as photocatalyst (see chapter 1, ref. [61]). It was described as a metal-free approach to generate phosphinoyl radical under white LED irradiation at 30 °C for a reaction time of 6-18 hours. This radical reacted with different olefins leading to regioselective *anti*-Markovnikov products. In the proposed photoredox cycle, the excited state of Rhodamine B acted as a single-electron oxidizing agent to form the phosphinous radical cation intermediate, which afforded the desired phosphinoyl radical upon deprotonation.

Based on Denton's observations that Ar_2I^+ forms EDA complexes when combined with tertiary phosphines and on recent work from our group that phosphinoyl radicals can be formed upon mixture of diphenyliodonium triflate with triethylamine (electron-donor) in the presence of secondary phosphine oxide at 40 °C (Scheme 3.15, a),¹³⁸ we hypothesized, as stated in the introduction part, that such radical can be achieved by simply mixing bisaryl secondary phosphine oxides with Ph_2I^+ . This hypothesis is based on the fact that many secondary phosphine oxides exist in solution as a mixture of P(V) and P(III) forms. Because the latter can be considered as electron-donor, it may form EDA complex with Ph_2I^+ , thus generating the corresponding phosphorus radical (Scheme 3.15).



Scheme 3.15. Different examples of C-P bond forming reaction *via* EDA complexes activation.

¹³⁸ Noël-Duchesneau, L.; Lagadic, E.; Morlet-Savary, F.; Lohier, J.-F.; Chataigner, I.; Breugst, M.; Lalevée, J.; Gaumont, A.-C.; Lakhdar, S. *Org. Lett.* **2016**, *18*, 5900-5903.

3.4. Results and Discussion

3.4.1. Mechanistic investigations

To test this hypothesis, we started investigating the formation of EDA complex between diphenyliodonium triflate (**73**) and diphenylphosphine oxide (**46**) by UV-Visible spectrophotometry in different solvents. Unfortunately, the combination of both components in either acetonitrile, *N,N*-dimethylformamide, dichloromethane or dimethyl sulfoxide did not show the appearance of a new peak in the visible region, which is characteristic of EDA complex. Addition of excess of diphenylphosphine oxide with respect to Ph_2I^+ (approximately 50 eq. : 1 eq.) did not change the previous result.

It should be mentioned that Lalevée *et al.* have thoroughly investigated the formation of EDA complexes from reactions of Ph_2I^+ (electron-acceptors) with TEA or 4-*N,N*-TMA (triethylamine or 4-*N,N*-trimethylaniline) and triphenylphosphine (electron-donors).¹³⁹ As shown in Figure 3.4, when Ph_2I^+ is mixed with a Lewis bases, such as *N,N*-trimethylaniline, a yellow color appeared, attesting the formation of the charge transfer complex Ph_2I^+ /electron-donor.



Figure 3.4. a) 4-*N,N*-trimethylaniline in solution exhibits any colour, it means any absorption below 380 nm. b) *N,N*-trimethylaniline and diaryliodonium salt mixed in DCM. c) Diaryliodonium salt in DCM

The formation of these complexes can also be deduced from the UV-Vis spectrum depicted in Figure 3.5, which shows the appearance of a new broad peak in the visible region.

¹³⁹ Garra, P.; Morlet-Savary, F.; Dietlin, C.; Fouassier, J.P.; Lalevée, J. *Macromolecules* **2016**, *49*, 9371-9381.

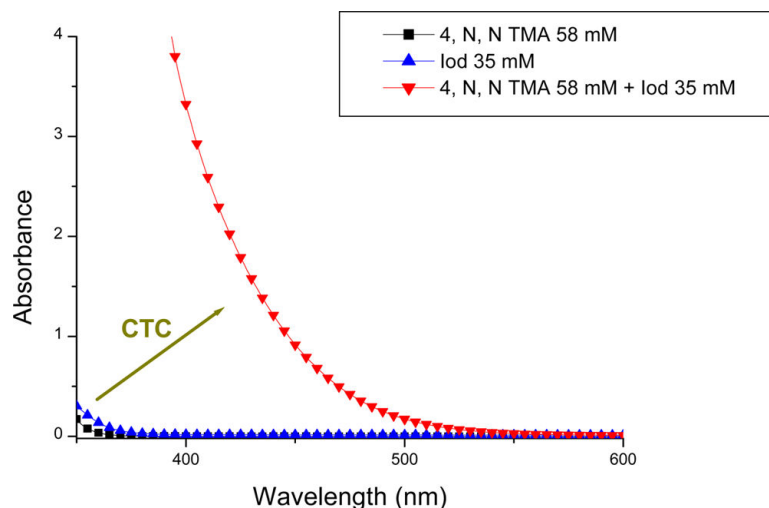


Figure 3.5. UV-Vis absorption spectrum of 4-*N,N*-trimethylaniline (4-*N,N*-TMA, black), 4-*N,N*-trimethylaniline and diphenyliodonium (red) and diphenyliodonium (Iod, blue) (spectrum taken from ref. [30])

To gain more insights in thermodynamics of the association of these reactants DFT calculations have been performed by our collaborator, Dr. Martin Breugst from the University of Köln, who studied the formation of different EDA complexes between Ph_2I^+ and $\text{Ph}_2\text{P}(\text{O})\text{H}$ (Figure 3.6).

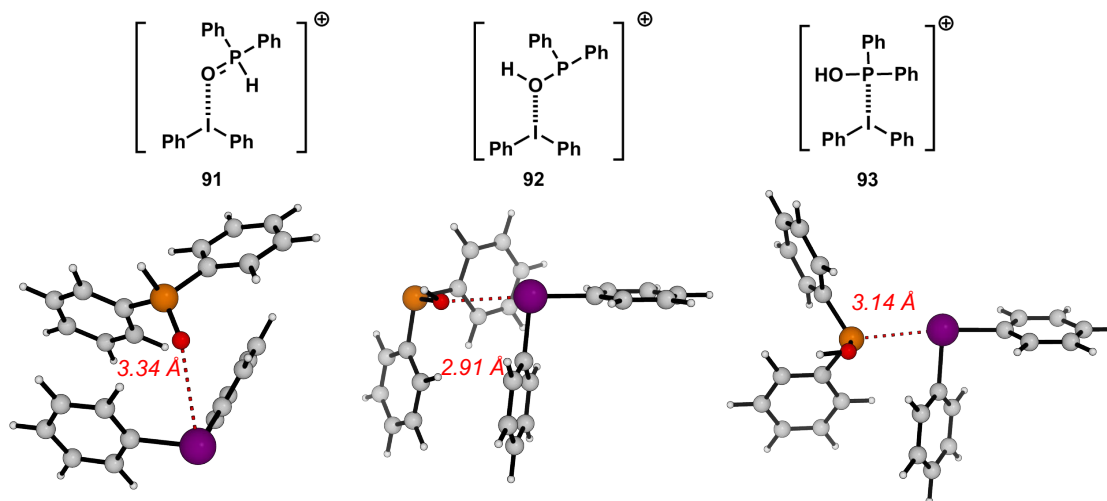
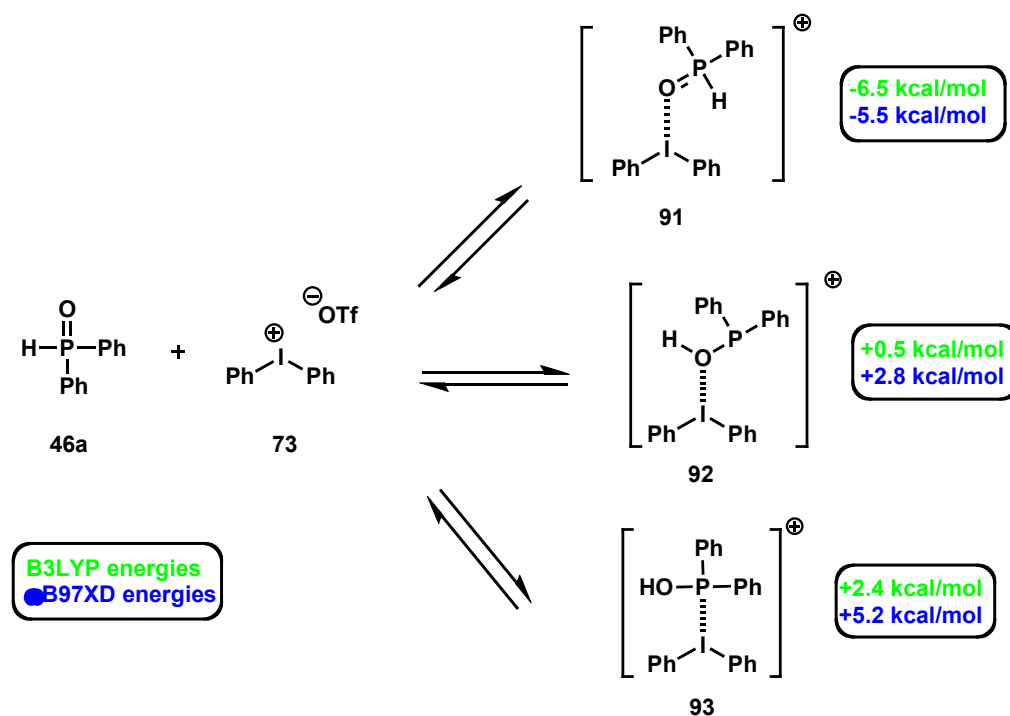


Figure 3.6. EDA-complex structures of three possible interactions between Ph_2I^+ / $\text{Ph}_2\text{P}(\text{O})\text{H}$

As shown in Scheme 3.16, energies of three possible Ph_2I^+ / $\text{Ph}_2\text{P}(\text{O})\text{H}$ complexes have been calculated at B3LYP-D3BJ/aug-cc-pVTZ or at ωB97XD /aug-cc-pVTZ in CH_2Cl_2 solution. In term of stability, the complex **91** resulting from the interaction of the

oxygen atom of P(V) with the iodine center has been found to be about 7 to 8 kcal/mol more stable than that resulting from the interaction of the oxygen atom of the diphenylphosphinous acid tautomer **92**. Interaction of the phosphorus lone pair of this tautomer to Ph_2I^+ gives the thermodynamically less stable complex **93** (Scheme 3.16).



Scheme 3.16. DFT calculated energies for three possible EDA complexes between $\text{Ph}_2\text{I}^+/\text{Ph}_2\text{P}(\text{O})\text{H}$

More importantly, the UV-Vis spectra of the three postulated EDA complexes calculated by TD-DFT calculations at B3LYP-D3BJ/6-31+G(d,p), aug-cc-pVTZ-PP (for iodine) in CH_2Cl_2 showed that the less stable complex (**93**) exhibited an absorption in the visible region, whereas the two other EDA-complexes are visible-inactive (Figure 3.7). These results are important as they enabled to rationalize the difficulty we had to detect the EDA complex, which is due to the thermodynamic instability of that species.

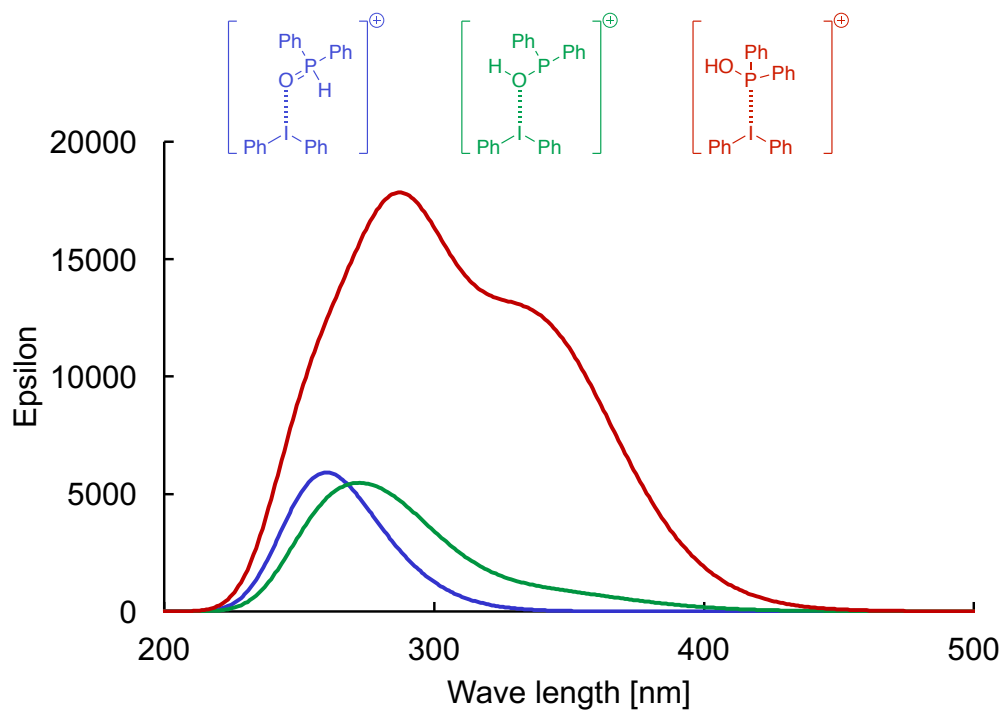


Figure 3.7. UV-Vis spectra of different EDA-complexes calculated by TP-DFT

Because DFT calculations suggested the formation of a stable EDA-complex (**91**), we investigated by NMR spectroscopy the addition of both components in CH_2Cl_2 . Interestingly, ROESY experiment of this mixture recorded at $-15\text{ }^\circ\text{C}$ showed through-space interactions between H_1 of diphenylphosphine oxide and H_a of diphenyliodonium triflate (Figure 3.8), which suggests that the two components are in close proximity one to another. This result fully supports the DFT calculations.

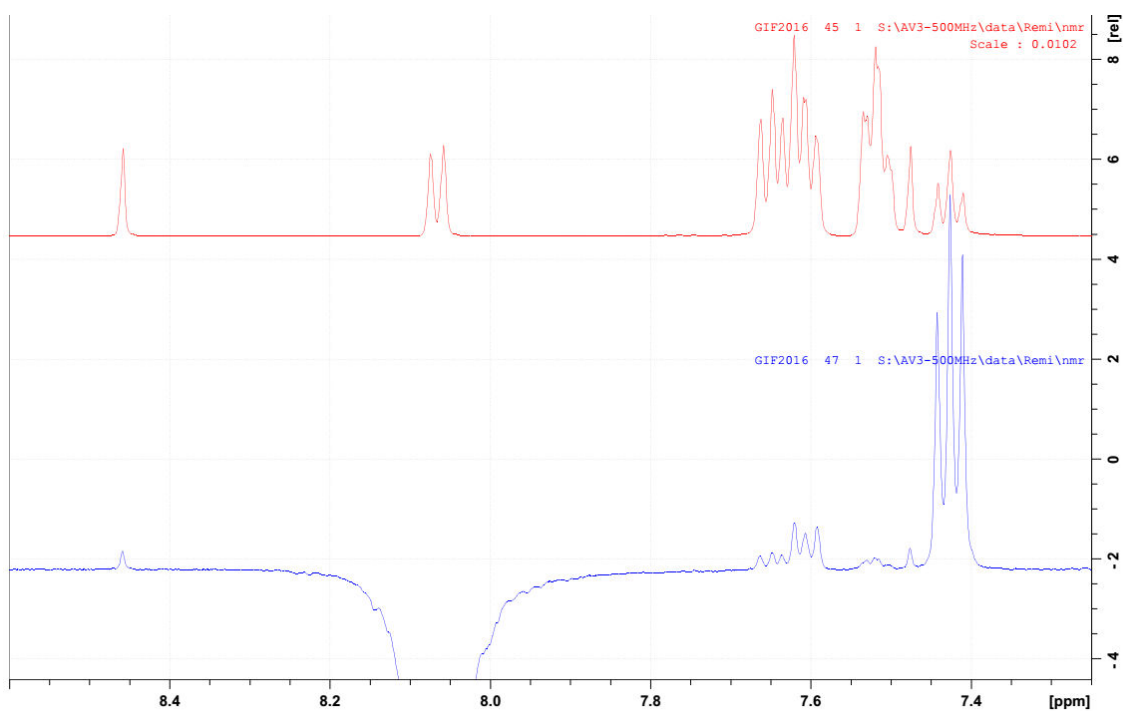
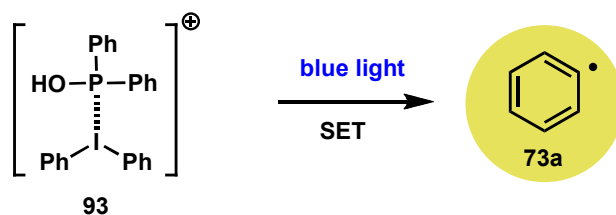


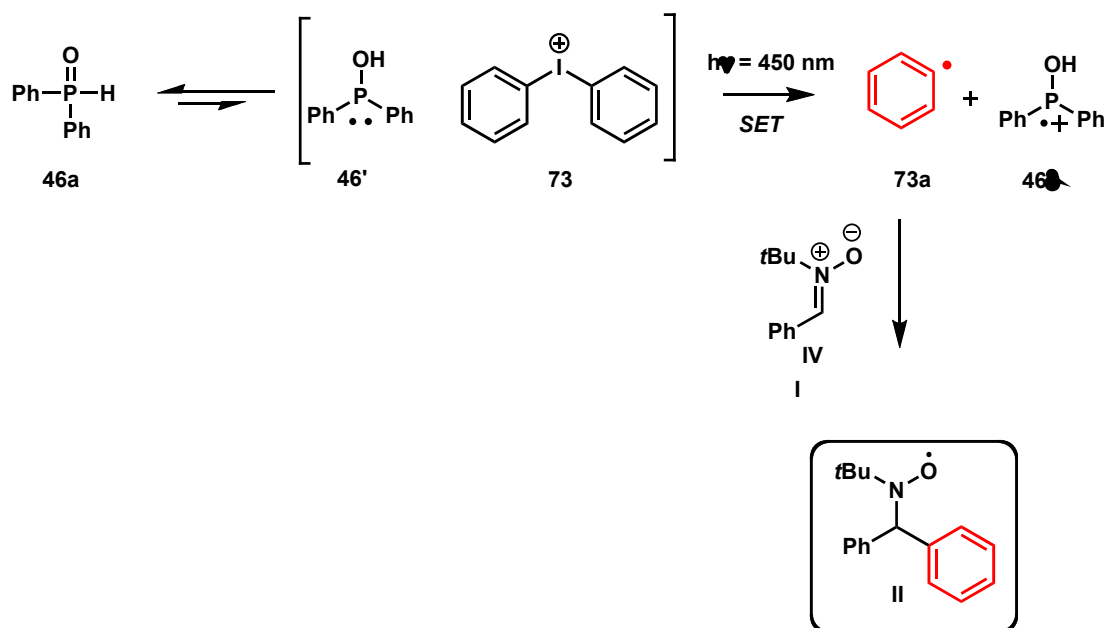
Figure 3.8. ROESY-NMR spectrum of an equimolar mixture of SPO and Ph_2I^+ in dichloromethane at -15°C

Although DFT calculations predict the visible light active EDA-complex to be highly unstable, blue irradiation should promote single electron transfer within the complex thus forming the reactive phenyl radical, as shown in Scheme 3.17.



Scheme 3.17. Generation of the aryl radical through illumination of the EDA complex **93** with blue light.

To confirm this hypothesis, we investigated, by means of EPR spectroscopy, the reaction of SPO with Ph_2I^+ in *tert*-butylbenzene under blue irradiation ($\lambda = 420 \text{ nm}$) in the presence of PBN as spin trap radical. As shown in Scheme 3.18, by mixing diphenylphosphine oxide (**46a**) and diphenyliodonium triflate (**73**) in the presence of PBN as radical trapping agent, the spin adduct **II** has been observed.



Scheme 3.18. EPR spin-adduct **II** observation upon irradiation ($\lambda = 450 \text{ nm}$) of a solution of diphenylphosphine oxide **46a** and diphenyliodonium triflate **73** in the presence of PBN **I** in *tert*-butylbenzene at room temperature

When a mixture of SPO and Ph_2I^+ was irradiated with blue light ($\lambda = 450 \text{ nm}$), a clean formation of the spin adduct **II** was observed (Figure 3.9). The hyperfine coupling constants are in good agreements with those previously reported in the literature ($a_{\text{N}} = 14.18 \text{ G}$, $a_{\text{H}} = 1.9 \text{ G}$).

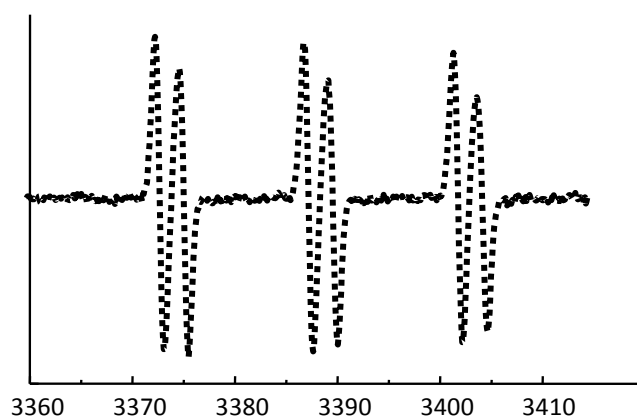


Figure 3.9. EPR-spin trapping spectra for the reaction between diphenyliodonium triflate **73** and diphenylphosphine oxide **46a** in the presence of PBN **I** in *tert*-butylbenzene at room temperature

The addition of an excess of SPO with respect to Ph_2I^+ under the same reaction conditions showed the appearance of new peaks related to the phosphinoyl-PBN adduct ($a_{\text{P}} = 18.7 \text{ G}$, $a_{\text{N}} = 14.18 \text{ G}$, $a_{\text{H}} = 3.03 \text{ G}$) were observed, which indicate the formation of the diphenylphosphinoyl radical (Figure 3.10). These EPR results clearly demonstrated the formation of two key species that can be generated through the formation of an EDA complex ($\text{SPO}/\text{Ph}_2\text{I}^+$).

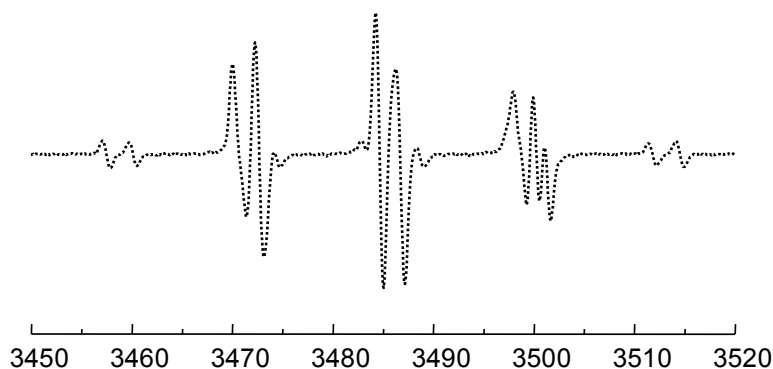


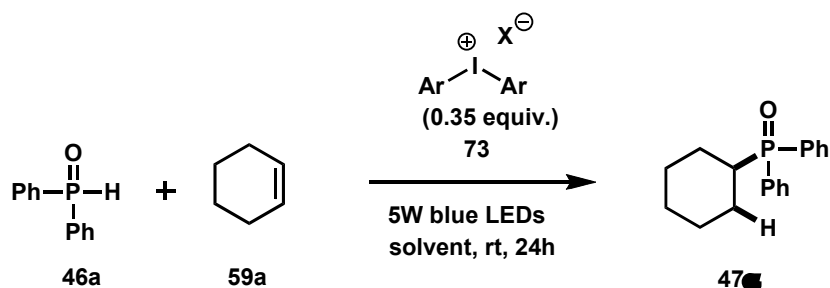
Figure 3.10. EPR-spin trapping spectra for the reaction between diphenyliodonium triflate **73** and excess of diphenylphosphine oxide **46a** in the presence of PBN **I**

Having firmly confirmed the formation of phosphinoyl radical upon reacting diphenylphosphine oxide with diphenyliodonium under blue irradiation, we next envisioned applying this approach in the hydrophosphinylation of alkenes.

3.4.2. Optimization studies

Our investigations started with optimizing the reaction conditions of the addition of diphenylphosphine oxide **46a** to cyclohexene **59a**, starting by focusing on the exact loading of phosphorus species, diphenyliodonium salt and alkene (Table 3.2).

Table 3.2. Optimization studies for the hydrophosphinylation of alkenes *via* EDA-complexes activation



entry	solvent ^a	Ph ₂ I ⁺ TfO ⁻ (73) load. (eq.)	³¹ P-NMR yield (%)
1	MeCN	0.5	25 ^b
2	MeCN	0.5	20 ^c
3	MeCN	0.5	56 ^d
4	MeCN	0.25	53 ^d
5	MeCN	0.15	16 ^d
6	MeCN	0.35	≤5 ^{d,e}
7	MeCN	none	0 ^d
8	DMF	0.35	51 ^d
9	MeCN	0.35	70^d
10	DCM	0.35	56 ^d
11	Toluene	0.35	57 ^b

[^a] The reaction did not require deoxygenated solvents. [^b] Diphenylphosphine oxide **46a** (1 equiv.) and cyclohexene **59a** (1 equiv.). [^c] Diphenylphosphine oxide **46a** (1 equiv.) and cyclohexene **59a** (2 equiv.). [^d] Diphenylphosphine oxide **46a** (2 equiv.) and cyclohexene **59a** (1 equiv.). [^e] Without light, in oil bath at T = 55°C.

While the reaction proceeded well in DMF (51%, entry 8), dichloromethane (56%, entry 10), toluene (57%, entry 11), the best conversion was obtained by using acetonitrile (70%, entry 9), which was selected as the solvent of choice for further studies.

Further investigations revealed that two equivalents of phosphine oxide with respect to cyclohexene are necessary to reach high conversion (entries 3,4 and 5). The stoichiometric combination of both components led to only 25% of NMR conversion after 24h (entry 1). The amount of added diphenyliodonium triflate has been found to be critical and the best conversion has been performed when 0.35 equiv. of **73** was used (entry 9). While increasing the amount of **73** to 0.5 equiv. reduced the conversion to 56% (entry 3). Reducing the loading to 0.15 equiv. almost shut down the reaction (16%, entry 5). Background experiments have also been undertaken and showed the essential role of light (entry 6), diphenyliodonium salt (entry 7) as the reaction did not take place in their absence.

Having identified optimal conditions for this reaction, we next investigated scope and limitations of our approach by testing different alkenes and secondary phosphine oxides.

Table 3.3. Scope and limitations of hydrophosphinylation reaction

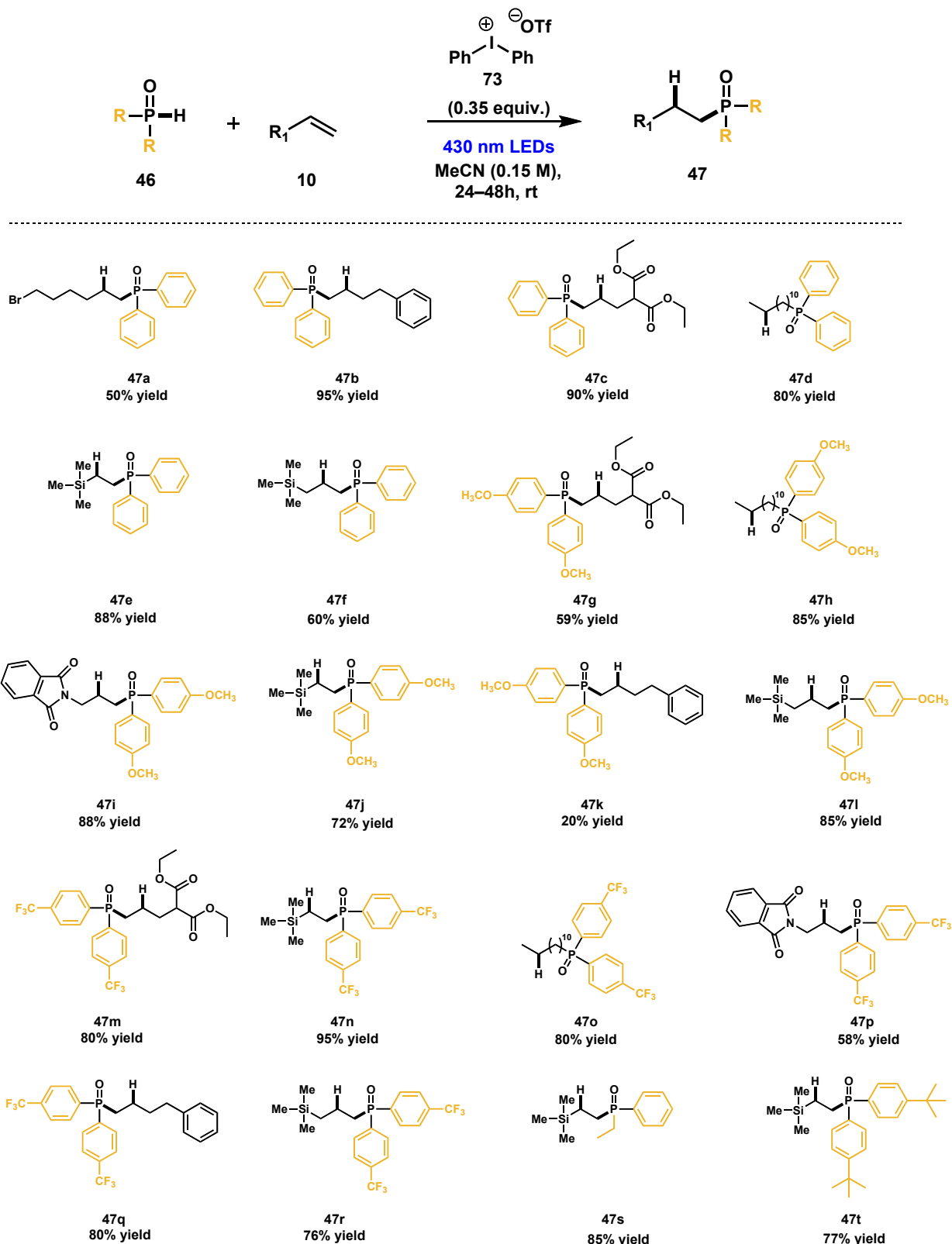


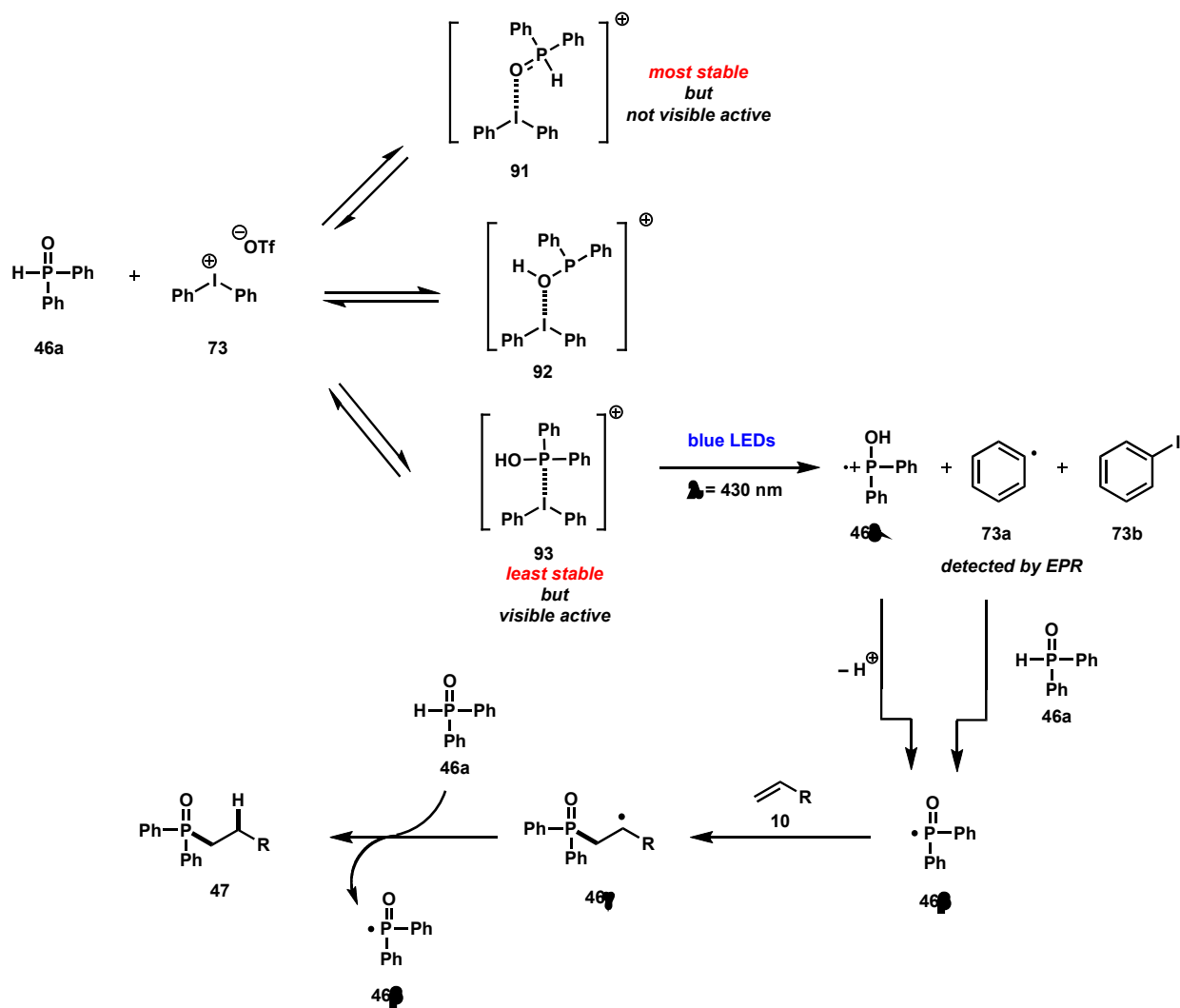
Table 3.3 shows that the reaction proceeds smoothly with different alkenes, leading to moderate to excellent isolated yields (50 to 95%). Here, I referred only to

diphenylphosphine oxide. The process tolerated various functional groups such as bromo, ester and trimethylsilyl groups (**47g**, **47m**, **47e**, **47f**, **47j**, **47l**, **47n**, **47r**, **47t**). The efficiency of the reaction is not restricted to diphenylphosphine oxide as also other arylphosphine oxides (*p*-CF₃-, *p*-OMe-, *p*-tBu-, ethylphenyl-phosphine oxides) have been found to react smoothly with unactivated alkenes, furnishing the desired products on good to excellent yields. Noteworthy, when bis-(4-(trifluoromethyl)phenyl)phosphine oxide was combined with alkenes **10m-r** under optimized conditions, hydrophosphinated adducts (**47m-r**) were isolated in good to excellent yields varying from 58 to 95%. This can be explained by the stability of P(III) tautomeric form of the aryl secondary phosphine oxide when having an electron withdrawing group, as already investigated by Montchamp. Although isolated yield of **47k** was not satisfactory, the reaction worked also when electron-rich secondary phosphine oxides were employed, leading to the desired products (**47g-j** and **47l**) in variable yields ranging from 59 to 88%. A high regioselectivity was obtained as only *anti*-Markonikov adducts were isolated in all the cases (**47a-t**).

3.4.3. Mechanistic proposal for the photocatalytic approach

In light of our mechanistic and synthetic investigations, we propose the reaction mechanism depicted in Scheme 3.19. The reaction starts with the association of Ph₂I⁺ with diphenylphosphine oxide to form EDA complexes **91**, **92**, **93**. Though the latter is the less stable, it is the only one visible active in the visible spectrum and undergoes a single electron transfer event (SET) upon blue light irradiation to form the phenyl radical, along with the radical cation **46δ**.

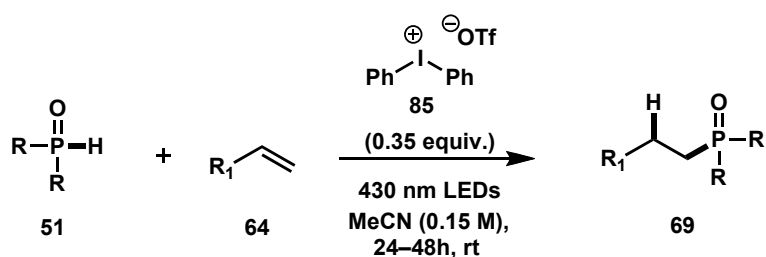
Being highly unstable, the phenyl radical abstracts hydrogen from the secondary phosphine oxide to generate the corresponding phosphinoyl radical, which adds at the double bond to form the carbon centered radical **46γ**. This radical abstracts the hydrogen from Ph₂P(O)H to yield the hydrophosphinated adduct **47** and regenerate the phosphorus radical **I**.



Scheme 3.19. Proposed mechanism for our hydrophosphinylation of unactivated alkenes *via* EDA-complexes

3.5. Conclusions

In this chapter, a mild generation of phosphinoyl radical has been described through the combination of diphenyliodonium triflate with aryl substituted secondary phosphine oxides under blue light irradiation. The strategy has been tested in the hydrophosphination reaction of unactivated alkenes (Scheme 3.20), affording the desired adduct with a high regioselectivity.



Scheme 3.20. Regioselective hydrophosphination reaction of unactivated alkenes with secondary aryl phosphine oxides

The driving force of this reaction relies on the use of EDA complex between secondary aryl phosphine oxides and diphenyliodonium triflate under mild reaction condition. This mode of activation has been applied for the first time for C–P bond formation reaction. Based on the first insights outlined in this chapter, this concept should attract more attention not only in the field of phosphorus chemistry but in other fields as well.

3.6 Materials and methods

3.6.1 General

¹H NMR spectra were recorded on a BRUKER AVANCE III 400 MHz spectrometer, the chemical shifts are reported in parts per million (ppm) referenced to residual chloroform (7.26 ppm). Coupling constants are reported in Hertz (Hz). The following abbreviations were used to express the multiplicities: s (singlet), d (doublet), t (triplet), q (quartet), m (multiplet), bs (broad singlet). ¹³C NMR spectra were recorded on the same instrument at 100 MHz, the chemical shifts are expressed in parts per million (ppm), reported from the central chloroform peak (77.2 ppm). ³¹P NMR spectra were recorded on the same instrument at 162 MHz (decoupled ³¹P NMR). High Resolution Mass Spectrometry (HRMS) was performed on a Varian MAT 311 spectrometer or a QTOF Micro WATERS spectrometer.

All reactions were air or water sensitive and set up under an argon atmosphere in dried glassware using Schlenk techniques with dry solvents. Chromatographic purification of products was accomplished using flash chromatography (FC) on silica gel (35-70 mesh). For Thin Layer Chromatography (TLC) analysis throughout this work, Merck precoated TLC plates (silica gel 60 F₂₅₄) were employed. Visualization was performed with UV light and by immersion in anisaldehyde stain (by volume: 93% ethanol, 3.5% sulfuric acid, 1% acetic acid, 2.5% *p*-anisaldehyde) or basic aqueous potassium permanganate solution (KMnO₄) stain followed by heating as developing tool. Organic solutions of products were dried over anhydrous MgSO₄ and concentrated under reduced pressure on a Büchi rotatory evaporator. Aqueous hypophosphorus acid (50 wt. %) was obtained from Aldrich and used by concentrating it in vacuo on a rotary evaporator, at 30°C for 20-30 min before reaction. Alkenes were purchased at the highest commercial quality by chemical companies (Sigma-Aldrich, TCI Chemicals, Fisher Scientific) and used without further purification. Diphenyliodonium triflate,¹⁴⁰ diphenylphosphine oxide, bis(4-trifluoromethylphenyl)phosphine oxide,¹⁴¹

¹⁴⁰ M. Bielawski and B. Olofsson, *Org. Synth.*, **2009**, *86*, 308.

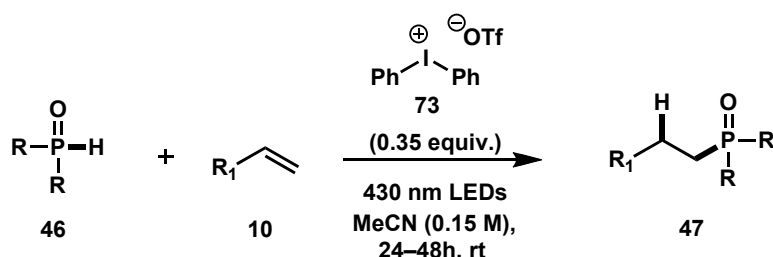
¹⁴¹ N. T. McDougal; J. Streuff; H. Mukherjee; S.C. Virgil; B.M. Stoltz *Tetrahedron Letters* **2010**, *51*, 5550-5554.

bis(4-*tert*-butylphenyl)phosphine oxide, ethylphenylphosphine oxide and bis(4-methoxyphenyl)phosphine oxide¹⁴² were synthesized according to literature procedures. Acetonitrile and tetrahydrofuran were dispensed by PURESOLVTM developed by Innovative Technology Inc.

¹⁴² S. Shao, J. Ding, T. Ye, Z. Xie, L. Wang, X. Jing, and F. Wang, *Adv. Mater.*, **2011**, *23*, 3570.

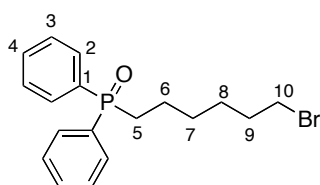
3.7 Hydrophosphinylation reaction products

3.7.1 General procedure



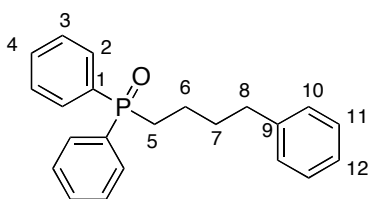
In an oven-dried Schlenk tube, diphenyliodonium triflate **73** (0.35 mmol, 0.35 equiv.) and the secondary phosphine oxide **46a-e** (2 mmol, 2 equiv.) were dissolved in dry acetonitrile (0.15 M). To this solution, alkene **10a-g** (1 mmol, 1 equiv.) was added and the mixture was stirred until complete dissolution. The solution was surrounded by blue LEDs (5 W). The mixture was concentrated under reduced pressure to give an oil as crude product. The latter was purified by flash column chromatography on silica gel (ethyl acetate or ethyl acetate /ethanol) to yield the desired adduct **47** as solid or colorless oil.

Diphenyl-1-(6-bromohexyl)phosphine oxide (**47a**)



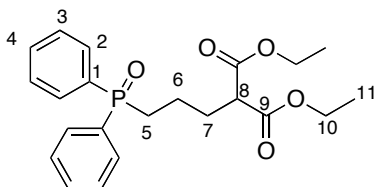
Conditions: ((**46a**) : 100 mg, 0.5 mmol, 2 equiv.); ($\text{Ph}_2\text{I}^+ \text{OTf}^-$ (**73**) = 39 mg, 0.25 mmol, 0.35 equiv.); (**10a**) = 33 μL , 0.25 mmol, 1 equiv). The reaction was carried out following the general procedure. The crude product was purified by flash column chromatography (ethyl acetate) to give a colorless oil. **Yield** : 46 mg, 50%. **¹H-NMR** (400 MHz, CDCl_3) δ (ppm) 7.72-7.68 (m, 4H, Ar-H), 7.48-7.38 (m, 6H, Ar-H), 3.29 (t, $^3J = 6.7$ Hz, 10-H), 2.24-2.17 (m, 2H, 9-H), 1.75-1.69 (m, 2H, 8-H), 1.56-1.54 (m, 2H, 7-H), 1.33 (m, 4H). **¹³C-NMR** (100 MHz, CDCl_3) δ (ppm) 132.7 (d, $^1J = 100.0$ Hz, C-1), 131.8 (d, $^4J = 2.5$ Hz, C-4), 130.9 (d, $^2J = 9.0$ Hz, C-6), 128.7 (d, $^3J = 11.0$ Hz, C-7), 33.8 (s), 32.4 (s), 30.0 (s), 29.9 (s), 29.2 (s), 27.5 (s), 21.3 (d, $^3J = 4.1$ Hz, C-7). **³¹P-NMR** (162 MHz, CDCl_3) δ (ppm) 33.1 (s). **HRMS:** calcd for $\text{C}_{18}\text{H}_{23}\text{OPBr}$ $[\text{M}+1]^+$ 365.0669, found 365.0670.

Diphenyl-1-(4-phenylbutyl)phosphine oxide (47b)



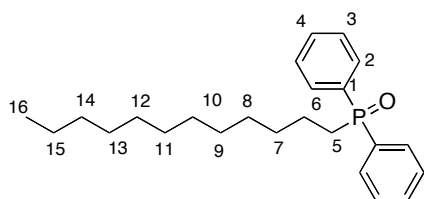
Conditions: ((46a) : 100 mg, 0.5 mmol, 2 equiv.); (Ph₂I⁺ OTf⁻ (73) = 39 mg, 0.25 mmol, 0.35 equiv.); (10b) = 38 μL, 0.25 mmol, 1 equiv). The reaction was carried out following the general procedure. The crude product was purified by flash column chromatography (ethyl acetate) to give a colorless oil. **Yield** : 79 mg, 95%. **¹H-NMR** (400 MHz, CDCl₃) δ (ppm) 7.57-7.52 (m, 4H, Ar-H), 7.34-7.24 (m, 6H, Ar-H), 7.08-7.03 (m, 2H, Ar-H), 6.98-6.90 (m, 3H, Ar-H), 2.38 (t, ³J = 6.7 Hz, 2H, 8-H), 2.13-2.06 (m, 2H), 1.53-1.52 (m, 4H). **¹³C-NMR** (101 MHz, CDCl₃) δ (ppm) 141.9 (s, C-9), 131.7 (d, ⁴J = 2.7 Hz, C-4), 130.9 (d, ³J = 9.3 Hz, C-3), 128.7 (d, ²J = 11.4 Hz, C-2), 128.3 (s), 125.8 (s), 35.4 (s), 32.7 (d, ³J = 14.5 Hz, C-7), 29.7 (d, ¹J = 71.2 Hz, C-5), 21.2 (d, ²J = 3.7 Hz, C-6). **³¹P-NMR** (162 MHz, CDCl₃) δ (ppm) 32.6 (s). **HRMS:** calcd for C₂₂H₂₄OP [M+H]⁺ 335.1568, found 335.1565.

Diphenyl-1-(4-diethylmaleonyl)phosphine oxide (47c)



Conditions: ((46a) : 100 mg, 0.5 mmol, 2 equiv.); (Ph₂I⁺ OTf⁻ (73) = 39 mg, 0.25 mmol, 0.35 equiv.); (10c) = 49 μL, 0.25 mmol, 1 equiv). The reaction was carried out following the general procedure. The crude product was purified by flash column chromatography (ethyl acetate) to give a colorless oil. **Yield** : 90 mg, 90%. **¹H-NMR** (400 MHz, CDCl₃) δ (ppm) 7.69-7.64 (m, 4H, Ar-H), 7.47-7.40 (m, 6H, Ar-H), 4.10-4.05 (qd, ³J = 5.5 Hz, 4H), 3.25 (t, ³J = 7.5 Hz, 1H, 8-H), 2.27-2.20 (m, 2H, 5-H), 1.98-1.92 (m, 2H), 1.66-1.56 (m, 2H), 1.14 (t, ³J = 7.2 Hz, 6H, 11-H). **¹³C-NMR** (100 MHz, CDCl₃) δ (ppm) 169.0 (s, C-Ar), 133.2 (d, ¹J = 99.0 Hz, C-1), 131.7 (d, ⁴J = 2.7 Hz, C-4), 130.7 (d, ³J = 9.3 Hz, C-3), 128.7 (d, ²J = 11.4 Hz, C-2), 61.4 (s), 51.5 (s), 29.8 (d, ¹J = 15.9 Hz, C-5), 29.0 (s), 19.6 (d, ²J = 3.4 Hz, C-6), 13.9 (s). **³¹P-NMR** (162 MHz, CDCl₃) δ (ppm) 31.8 (s). **HRMS:** calcd for C₂₂H₂₇O₅P [M+H]⁺ 403.168, found 403.167.

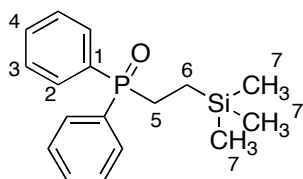
Diphenyl-1-dodecylphosphine oxide (47d)



Conditions: ((**46a**) : 100 mg, 0.5 mmol, 2 equiv.); ($\text{Ph}_2\text{I}^+ \text{OTf}^-$ (**73**) = 39 mg, 0.25 mmol, 0.35 equiv.); (**10d**) = 55 μL , 0.25 mmol, 1 equiv). The reaction was carried out following the general procedure. The

crude product was purified by flash column chromatography (ethyl acetate) to give a white solid. **Yield** : 74 mg, 80%. **M_p** = 60°C. **¹H-NMR** (400 MHz, CDCl_3) δ (ppm) 7.73-7.68 (m, 4H, Ar-H), 7.49-7.41 (m, 6H, Ar-H), 2.26-2.19 (m, 2H, 5-H), 1.64-1.54 (m, 2H), 1.37-1.32 (m, 2H), 1.19 (bs, 16H), 0.84 (t, $^3J = 7.0$ Hz, 3H, 16-H). **¹³C-NMR** (100 MHz, CDCl_3) δ (ppm) 133.7 (d, $^1J = 97.6$ Hz, C-Ar), 131.6 (d, $^4J = 2.7$ Hz, C-Ar), 130.8 (d, $^3J = 9.2$ Hz, C-Ar), 128.6 (d, $^2J = 11.5$ Hz, C-Ar), 31.9 (s), 31.0 (d, $^2J = 14.6$ Hz, C-6), 30.1 (s), 29.6 (s), 29.5 (s), 29.4 (s), 29.3 (d, $^4J = 2.5$ Hz, C-8), 29.1 (s), 22.7 (s), 21.4 (d, $^3J = 3.5$ Hz, C-7), 14.1 (s). **³¹P-NMR** (162 MHz, CDCl_3) δ (ppm) 32.5 (s). **HRMS:** calcd for $\text{C}_{17}\text{H}_{23}\text{OPSiNa}$ [$\text{M}+\text{Na}$] $^+$ 371.2493, found 371.2504.

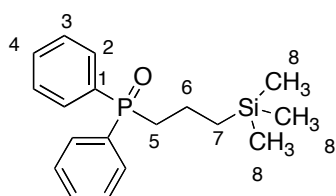
Diphenyl-1-(2-trimethylvinylsilylethyl)phosphine oxide (**69e**)



Conditions: ((**46a**) : 100 mg, 0.5 mmol, 2 equiv.); ($\text{Ph}_2\text{I}^+ \text{OTf}^-$ (**73**) = 39 mg, 0.25 mmol, 0.35 equiv.); (**10e**) = 37 μL , 0.25 mmol, 1 equiv). The reaction was carried out following the general procedure. The crude product was purified by

flash column chromatography (ethyl acetate) to give a white solid. **Yield** : 67 mg, 88%. **M_p** = 107°C. **¹H-NMR** (400 MHz, CDCl_3) δ (ppm) 7.73-7.68 (m, 4H, Ar-H), 7.49-7.42 (m, 6H, Ar-H), 2.16-2.09 (m, 2H, 5-H), 0.73-0.66 (m, 2H, 6-H), -0.03 (s, 9H, 7-H). **¹³C-NMR** (100 MHz, CDCl_3) δ (ppm) 135.4 (d, $^1J = 96.0$ Hz, C-Ar), 133.7 (d, $^4J = 2.7$ Hz, C-Ar), 133.1 (d, $^3J = 9.1$ Hz, C-Ar), 130.8 (d, $^2J = 11.4$ Hz, C-Ar), 26.3 (d, $^1J = 70.0$ Hz, C-5), 9.0 (d, $^2J = 7.0$ Hz, C-6), 0.0 (s, C-7). **³¹P-NMR** (162 MHz, CDCl_3) δ (ppm) 34.6 (s). **HRMS:** calcd for $\text{C}_{17}\text{H}_{23}\text{OPSiNa}$ [$\text{M}+\text{Na}$] $^+$ 325.1160, found 325.1154.

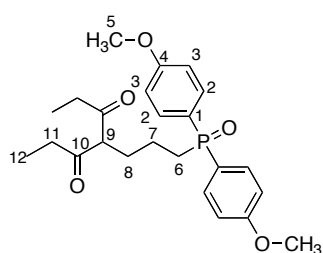
Diphenyl-1-(3-trimethylsilylpropyl)phosphine oxide (**69f**)



Conditions: ((**46a**) : 100 mg, 0.5 mmol, 2 equiv.); ($\text{Ph}_2\text{I}^+ \text{OTf}^-$ (**85**) = 39 mg, 0.25 mmol, 0.35 equiv.); (**64f**) = 40 μL ,

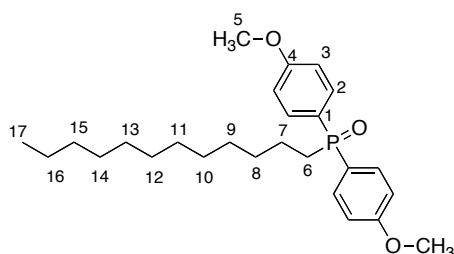
0.25 mmol, 1 equiv). The reaction was carried out following the general procedure. The crude product was purified by flash column chromatography (ethyl acetate) to give a white solid. **Yield** : 47 mg, 60%. **M_p** = 86-88°C. **¹H-NMR** (400 MHz, CDCl₃) δ (ppm) 7.55-7.50 (m, 4H, Ar-H), 7.31-7.26 (m, 6H, Ar-H), 2.13-2.06 (m, 2H), 1.45-1.43 (m, 2H), 0.42 (t, ³J = 8.2 Hz, 2H, 7-H), -0.28 (s, 9H, 8-H). **¹³C-NMR** (100 MHz, CDCl₃) δ (ppm) 133.4 (d, ¹J = 97.4 Hz, C-1), 131.8 (d, ⁴J = 2.8 Hz, C-4), 131.0 (d, ³J = 9.0 Hz, C-3), 128.8 (d, ³J = 11.7 Hz, C-2), 33.9 (d, ¹J = 70.0 Hz, C-5), 19.0 (d, ³J = 12.6 Hz, C-7), 16.6 (d, ²J = 4.0 Hz, C-6), -1.6 (s, C-8). **³¹P-NMR** (162 MHz, CDCl₃) δ (ppm) 32.2 (s). **HRMS**: calcd for C₁₈H₂₆OPSi [M+H]⁺ 317.1497, found 317.1491.

1-(bis(4-methoxy)phenyl)-4-diethylmaleonylphosphine oxide (69g)



Conditions: ((**46c**) : 100 mg, 0.381 mmol, 2 equiv.); (Ph₂I⁺ OTf (**85**) = 29 mg, 0.066 mmol, 0.35 equiv.); (**64c**) = 37 μL, 0.190 mmol, 1 equiv). The reaction was carried out following the general procedure. The crude product was purified by flash column chromatography (ethyl acetate:methanol 95:5) to give a colorless oil. **Yield** : 52 mg, 59%. **¹H-NMR** (400 MHz, CDCl₃) δ (ppm) 7.62-7.57 (m, 4H, Ar-H), 6.95-6.93 (m, 4H, Ar-H), 4.10-4.09 (q, ³J = 6.8 Hz, 4H, 11-H), 3.81 (s, 6H, 5-H), 3.27 (t, ³J = 7.4 Hz, 1H, 9-H), 2.23-2.21 (m, 2H, 8-H), 2.00-1.94 (m, 2H, 7-H), 1.65-1.60 (m, 2H, 6-H), 1.19 (t, ³J = 6.8 Hz, 6H, 12-H). **¹³C-NMR** (100 MHz, CDCl₃) δ (ppm) 169.1 (s), 162.2 (d, ⁴J = 2.7 Hz, C-4), 132.6 (d, ³J = 10.5 Hz, C-3), 124.3 (d, ¹J = 104.2 Hz, C-1), 114.2 (d, ²J = 12.5 Hz, C-2), 61.4 (s), 55.3 (s), 51.6 (s), 30.1 (d, ¹J = 48.7 Hz, C-6), 29.8 (d, ²J = 39.6 Hz, C-7), 19.8 (d, ³J = 3.2 Hz, C-8), 14.0 (s). **³¹P-NMR** (162 MHz, CDCl₃) δ (ppm) 31.8 (s). **HRMS**: calcd for C₂₄H₃₂O₇P [M+H]⁺ 463.1886, found 463.1886.

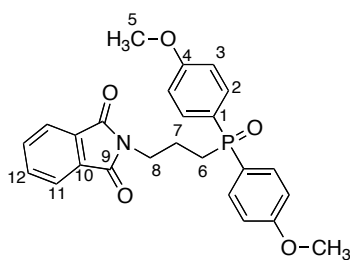
1-(bis(4-methoxy)phenyl)-2-dodecylphosphine oxide (69h)



Conditions: ((**46c**) : 100 mg, 0.381 mmol, 2 equiv.); (Ph₂I⁺ OTf (**85**) = 29 mg, 0.066 mmol, 0.35 equiv.); (**64d**) = 42 μL, 0.190 mmol, 1

equiv). The reaction was carried out following the general procedure. The crude product was purified by flash column chromatography (ethyl acetate) to give a colorless oil. **Yield** : 69 mg, 85%. **¹H-NMR** (400 MHz, CDCl₃) δ (ppm) 7.64-7.59 (m, 4H, Ar-H), 6.94-6.93 (m, 4H, Ar-H), 3.82 (s, 6H, 5-H), 2.19-2.13 (m, 2H), 1.55-1.53 (m, 2H), 1.28-1.19 (m, 18H), 0.86 (t, ³J = 6.7 Hz, 3H, 17-H). **¹³C-NMR** (100 MHz, CDCl₃) δ (ppm) 162.2 (d, ⁴J = 2.7 Hz, C-4), 132.7 (d, ³J = 10.7 Hz, C-3), 124.7 (d, ¹J = 105.4 Hz, C-1), 114.2 (d, ²J = 12.6 Hz, C-2), 55.3 (s), 31.9 (d, ¹J = 61.8 Hz, C-6), 31.0 (d, ²J = 61.7 Hz, C-7), 29.7 (s), 29.6 (s), 29.5 (s), 29.4 (d, ³J = 6.1 Hz, C-8), 22.7 (s), 21.5 (d, ⁴J = 3.7 Hz, C-9), 14.1 (s). **³¹P-NMR** (162 MHz, CDCl₃) δ (ppm) 33.6 (s). **HRMS**: calcd for C₂₆H₄₀O₃P [M+H]⁺ 431.2714, found 431.2715.

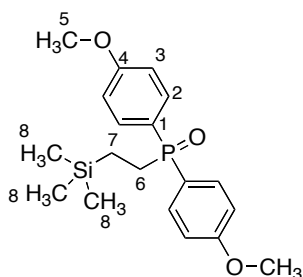
1-(bis(4-methoxy)phenyl)-3-phthalimidylphosphine oxide (69i)



Conditions: ((46c) : 100 mg, 0.381 mmol, 2 equiv.); (Ph₂I⁺ OTf⁻ (85) = 29 mg, 0.066 mmol, 0.35 equiv.); (64g) = 36 mg, 0.190 mmol, 1 equiv). The reaction was carried out following the general procedure. The crude product was purified by flash column chromatography (ethyl

acetate:methanol 95:5) to give a white solid. **Yield** : 75 mg, 88%. **M_p** = 93-95°C. **¹H-NMR** (400 MHz, CDCl₃) δ (ppm) 7.81-7.79 (m, 2H, Ar-H), 7.70-7.68 (m, 2H, Ar-H), 7.62-7.57 (m, 4H, Ar-H), 6.94-6.91 (m, 4H, Ar-H), 3.81 (s, 6H, 5-H), 3.74 (t, ³J = 6.9 Hz, 2H, 8-H), 2.28-2.21 (m, 2H, 7-H), 2.00-1.91 (m, 2H, 6-H). **¹³C-NMR** (100 MHz, CDCl₃) δ (ppm) 168.4 (s, C-9), 162.4 (d, ⁴J = 2.7 Hz, C-4), 134.1 (s, C-Ar), 132.8 (d, ³J = 10.6 Hz, C-3), 132.1 (s, C-Ar), 124.5 (s, C-Ar), 123.4 (s, C-Ar), 114.4 (d, ²J = 13.0 Hz, C-2), 55.4 (s, C-5), 38.7 (d, ³J = 17.2 Hz, C-8), 28.0 (d, ¹J = 73.0 Hz, C-6), 21.5 (d, ²J = 3.1 Hz, C-7). **³¹P-NMR** (162 MHz, CDCl₃) δ (ppm) 32.1 (s). **HRMS**: calcd for C₂₅H₂₅NO₃P [M+H]⁺ 450.1469, found 450.1470.

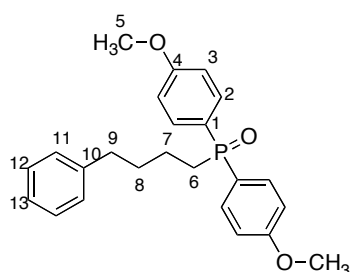
1-(bis(4-methoxy)phenyl)-2-trimethylsilylethylphosphine oxide (69j)



Conditions: ((46c) : 100 mg, 0.381 mmol, 2 equiv.); (Ph₂I⁺ OTf⁻ (85) = 29 mg, 0.066 mmol, 0.35 equiv.); (64e) = 28 μL, 0.190 mmol, 1 equiv). The reaction was carried out following

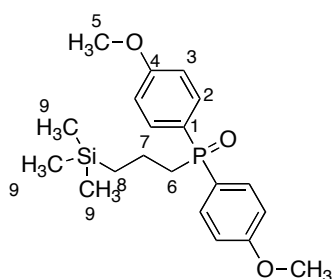
the general procedure. The crude product was purified by flash column chromatography (ethyl acetate:methanol 95:5) to give a colorless oil. **Yield** : 50 mg, 72%. **¹H-NMR** (400 MHz, CDCl₃) δ (ppm) 7.64-7.59 (m, 4H, Ar-H), 6.95-6.93 (m, 4H, Ar-H), 3.81 (s, 6H, 5-H), 2.10-2.03 (m, 2H, 6-H), 0.72-0.65 (m, 2H, 7-H), -0.04 (s, 9H, 8-H). **¹³C-NMR** (100 MHz, CDCl₃) δ (ppm) 162.2 (d, ⁴J = 2.7 Hz, C-4), 132.9 (d, ³J = 10.0 Hz, C-3), 124.4 (d, ¹J = 102.1 Hz, C-1), 114.3 (d, ²J = 12.1 Hz, C-2), 55.4 (s, C-5), 24.1 (d, ¹J = 71.0 Hz, C-6), 7.01 (d, ²J = 6.8 Hz, C-7), -2.05 (s, C-8). **³¹P-NMR** (162 MHz, CDCl₃) δ (ppm) 34.4 (s). **HRMS**: calcd for C₁₉H₂₈O₃PSi [M+H]⁺ 363.1545, found 363.1545.

1-(bis(4-methoxy)phenyl)-4-phenylbutylphosphine oxide (69k)



Conditions: ((46c) : 100 mg, 0.381 mmol, 2 equiv.); (Ph₂I⁺ OTf⁻ (85) = 29 mg, 0.066 mmol, 0.35 equiv.); (64b) = 29 μL, 0.190 mmol, 1 equiv). The reaction was carried out following the general procedure. The crude product was purified by flash column chromatography (ethyl acetate:methanol 95:5) to give a colorless oil. **Yield** : 15 mg, 20%. **¹H-NMR** (400 MHz, CDCl₃) δ (ppm) 7.63-7.59 (m, 4H, Ar-H), 7.26-7.22 (m, 2H, Ar-H), 7.17-7.09 (m, 3H, Ar-H), 6.97-6.95 (m, 4H, Ar-H), 3.84 s, 6H, 5-H), 2.57 (t, ³J = 7.0 Hz, 2H, 9-H), 2.25-2.18 (m, 2H), 1.71-1.65 (m, 4H). **¹³C-NMR** (100 MHz, CDCl₃) δ (ppm) 162.4 (d, ⁴J = 2.7 Hz, C-4), 142.1 (s, C-10), 132.8 (d, ³J = 10.7 Hz, C-3), 128.5 (s, C-Ar), 125.9 (s, C-Ar), 114.4 (d, ²J = 12.7 Hz, C-2), 55.5 (s, C-5), 35.5 (s), 32.8 (d, ³J = 15.0 Hz, C-8), 30.1 (d, ¹J = 73.1 Hz, C-6), 21.5 (d, ⁴J = 3.7 Hz, C-9). **³¹P-NMR** (162 MHz, CDCl₃) δ (ppm) 32.3 (s). **HRMS**: calcd for C₂₄H₂₈O₃P [M+H]⁺ 395.1776, found 395.1776.

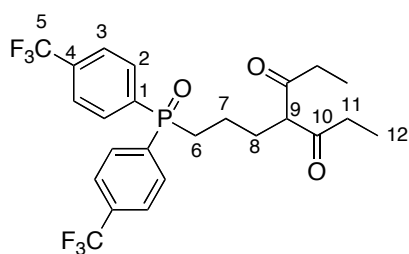
1-(bis(4-methoxy)phenyl)-3-trimethylsilylpropylphosphine oxide (69l)



Conditions: ((46c) : 100 mg, 0.381 mmol, 2 equiv.); (Ph₂I⁺ OTf⁻ (85) = 29 mg, 0.066 mmol, 0.35 equiv.); (64f) = 30 μL, 0.190 mmol, 1 equiv). The reaction was carried out following the general procedure. The crude product was purified by flash column chromatography (ethyl

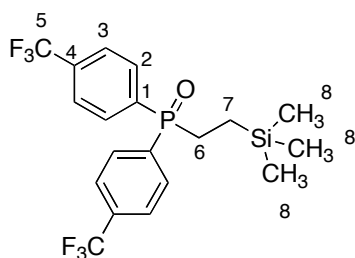
acetate:methanol 95:5) to give a colorless oil. **Yield** : 61 mg, 85%. **¹H-NMR** (400 MHz, CDCl₃) δ (ppm) 7.63-7.58 (m, 4H, Ar-H), 6.95-6.93 (m, 4H, Ar-H), 3.82 (s, 6H, 5-H), 2.25-2.18 (m, 2H, 6-H), 1.65-1.55 (m, 2H, 7-H), 0.59 (t, ³J = 8.5 Hz, 2H, 8-H), -0.09 (s, 9H, 9-H). **¹³C-NMR** (100 MHz, CDCl₃) δ (ppm) 162.3 (d, ⁴J = 2.7 Hz, C-4), 132.7 (d, ³J = 10.6 Hz, C-3), 124.8 (d, ¹J = 103.0 Hz, C-1), 114.3 (d, ²J = 12.5 Hz, C-2), 55.4 (s, C-5), 34.3 (d, ¹J = 70.0 Hz, C-6), 19.0 (t, ³J = 13.2 Hz, C-8), 16.6 (d, ²J = 4.0 Hz, C-7), -1.6 (s, C-9). **³¹P-NMR** (162 MHz, CDCl₃) δ (ppm) 32.2 (s). **HRMS**: calcd for C₂₀H₃₀O₃PSi [M+H]⁺ 377.1710, found 377.1702.

1-(bis(4-trifluoromethyl)phenyl)-4-diethylmaleonylphosphine oxide (69m)



Conditions: ((**46b**) : 100 mg, 0.296 mmol, 2 equiv.); (Ph₂I⁺ OTf (**85**) = 22 mg, 0.052 mmol, 0.35 equiv.); (**64c**) = 29 μL, 0.148 mmol, 1 equiv). The reaction was carried out following the general procedure. The crude product was purified by flash column chromatography (ethyl acetate) to give a colorless oil. **Yield** : 64 mg, 80%. **¹H-NMR** (400 MHz, CDCl₃) δ (ppm) 7.88-7.83 (m, 4H, Ar-H), 7.74-7.73 (m, 4H, Ar-H), 4.15-4.09 (d, ³J = 4.8 Hz, 4H, 3-H), 3.29 (t, ³J = 7.3 Hz, 1H, 9-H), 2.38-2.31 (m, 2H), 2.04-1.98 (m, 2H), 1.71-1.61 (m, 2H), 1.18 (t, ³J = 7.2 Hz, 6H, 12-H). **¹³C-NMR** (100 MHz, CDCl₃) δ (ppm) 168.9 (s, C-10), 136.9 (d, ¹J = 96.0 Hz, C-1), 134.2 (d, ⁴J = 2.7 Hz, C-4), 131.2 (d, ³J = 9.6 Hz, C-3), 125.8 (d, ²J = 8.2 Hz, ⁴J_{CF} = 3.5 Hz, C-2), 124.7 (d, ¹J_{CF} = 273.1 Hz, C-5), 61.5 (s), 51.4 (s), 29.7 (d, ¹J = 99.4 Hz, C-6), 29.5 (d, ³J = 10.8 Hz, C-8), 19.4 (d, ²J = 3.5 Hz, C-7), 13.9 (s). **³¹P-NMR** (162 MHz, CDCl₃) δ (ppm) 30.0 (s). **HRMS**: calcd for C₂₄H₂₅O₅F₆NaP [M+Na]⁺ 561.1219, found 561.1242.

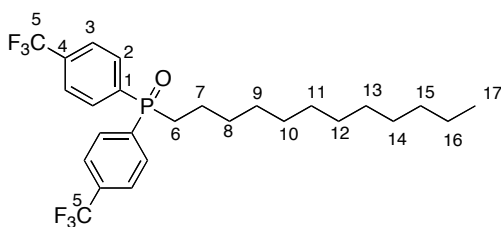
1-(bis(4-trifluoromethyl)phenyl)-2-trimethylsilylethylphosphine oxide (69n)



Conditions: ((**46b**) : 100 mg, 0.296 mmol, 2 equiv.); (Ph₂I⁺ OTf (**85**) = 22 mg, 0.052 mmol, 0.35 equiv.); (**64e**) = 22 μL, 0.148 mmol, 1 equiv). The reaction was carried out following the general procedure. The crude

product was purified by flash column chromatography (ethyl acetate) to give a white solid. **Yield** : 62 mg, 95%. **M_p** = 175°C. **¹H-NMR** (400 MHz, CDCl₃) δ (ppm) 7.89-7.85 (m, 4H, Ar-H), 7.76-7.74 (m, 4H, Ar-H), 2.24-2.18 (m, 2H), 0.75-0.70 (m, 2H), 0.02 (s, 9H, 8-H). **¹³C-NMR** (100 MHz, CDCl₃) δ (ppm) 139.2 (d, ¹J = 93.8 Hz, C-1), 136.2 (d, ⁴J = 2.7 Hz, ²J_{CF} = 30.0 Hz, C-4), 133.6 (d, ³J = 9.3 Hz, C-3), 127.9 (d, ²J = 7.8 Hz, ⁴J_{CF} = 3.7 Hz, C-2), 127.0 (d, ¹J_{CF} = 273.1 Hz, C-5), 26.1 (d, ¹J = 70.2 Hz, C-6), 8.8 (d, ²J = 7.1 Hz, C-7), -0.0 (s, C-8). **³¹P-NMR** (162 MHz, CDCl₃) δ (ppm) 32.5 (s). **HRMS**: calcd for C₁₉H₂₁OF₆NaSiP [M+Na]⁺ 461.0889, found 461.0901.

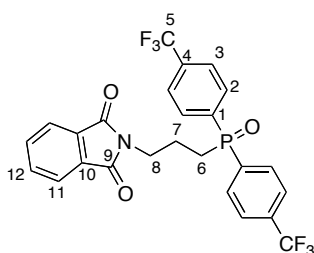
1-(bis(4-trifluoromethyl)phenyl)dodecylphosphine oxide (69o)



Conditions: ((**46b**) : 100 mg, 0.296 mmol, 2 equiv.); (Ph₂I⁺ OTf (**85**) = 22 mg, 0.052 mmol, 0.35 equiv.); (**64d**) = 33 μL, 0.148 mmol, 1 equiv). The reaction was carried out following the general

procedure. The crude product was purified by flash column chromatography (ethyl acetate) to give a white solid. **Yield** : 60 mg, 80%. **M_p** = 71°C. **¹H-NMR** (400 MHz, CDCl₃) δ (ppm) 7.89-7.85 (m, 4H, Ar-H), 7.74-7.73 (m, 4H, Ar-H), 2.34-2.27 (m, 2H), 1.66-1.56 (m, 2H), 1.41-1.36 (m, 2H), 1.21 (m, 16H), 0.85 (t, ³J = 6.7 Hz, 2H, 17-H). **¹³C-NMR** (100 MHz, CDCl₃) δ (ppm) 137.1 (d, ¹J = 96.0 Hz, C-1), 134.0 (dq, ⁴J = 2.9 Hz, ²J_{CF} = 33 Hz, C-4), 131.4 (d, ²J = 9.6 Hz, C-2), 125.8 (dq, ³J = 11.6 Hz, ³J_{CF} = 3.7 Hz, C-3), 123.4 (q, ¹J_{CF} = 271.0 Hz, C-5), 32.0 (s), 31.0 (d, ²J = 15.1 Hz, C-7), 29.8 (s), 29.7 (s), 29.6 (s), 29.4 (s), 29.1 (s), 22.8 (s), 21.4 (d, ³J = 4.0 Hz, C-8), 14.2 (s). **³¹P-NMR** (162 MHz, CDCl₃) δ (ppm) 30.7 (s). **HRMS**: calcd for C₂₆H₃₄OF₆P [M+H]⁺ 507.2245, found 507.2251.

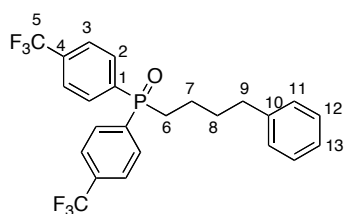
2-(3-(bis(4-(trifluoromethyl)phenyl)phosphoryl)propyl)isoindoline-1,3-dione (69p)



Conditions: ((**46b**) : 100 mg, 0.296 mmol, 2 equiv.); (Ph₂I⁺ OTf (**85**) = 22 mg, 0.052 mmol, 0.35 equiv.); (**64g**) = 28 mg, 0.148 mmol, 1 equiv). The reaction was carried out following

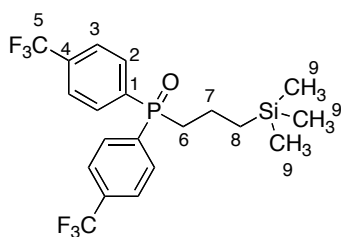
the general procedure. The crude product was purified by flash column chromatography (ethyl acetate) to give a white solid. **Yield** : 45 mg, 58%. **M_p** = 185-187°C. **¹H-NMR** (400 MHz, CDCl₃) δ (ppm) 7.87-7.81 (m, 6H, Ar-H), 7.73-7.72 (m, 6H, Ar-H), 3.79 (t, ³J = 6.9 Hz, 2H, 8-H), 2.42-2.36 (m, 2H, 7-H), 2.05-1.96 (m, 2H, 6-H). **¹³C-NMR** (100 MHz, CDCl₃) δ (ppm) 168.4 (s, C-9), 136.3 (d, ¹J = 96.0 Hz, C-1), 132.0 (s), 131.4 (d, ²J = 10.1 Hz, C-2), 126.0 (dq, ⁴J = 3.7 Hz, ²J_{CF} = 23.0 Hz, C-4), 124.0 (q, ¹J_{CF} = 272.0 Hz, C-5), 123.5 (s), 38.4 (d, ³J = 17.2 Hz, C-8), 27.3 (d, ¹J = 73.1 Hz, C-6), 21.1 (d, ²J = 3.0 Hz, C-7). **³¹P-NMR** (162 MHz, CDCl₃) δ (ppm) 30.0 (s). **HRMS**: calcd for C₂₅H₁₉NO₃PF₆ [M+H]⁺ 526.1014, found 526.1007.

1-(bis(4-trifluoromethyl)phenyl)-4-phenylbutylphosphine oxide (69q)



Conditions: ((46b) : 100 mg, 0.296 mmol, 2 equiv.); (Ph₂I⁺ OTf⁻ (85) = 22 mg, 0.052 mmol, 0.35 equiv.); (64b) = 22 μL, 0.148 mmol, 1 equiv). The reaction was carried out following the general procedure. The crude product was purified by flash column chromatography (ethyl acetate) to give a colorless oil. **Yield** : 56 mg, 80%. **¹H-NMR** (400 MHz, CDCl₃) δ (ppm) 8.02-7.97 (m, 4H, Ar-H), 7.89-7.88 (m, 4H, Ar-H), 7.42-7.38 (m, 2H, Ar-H), 7.34-7.33 (m, 1H, Ar-H), 7.26-7.24 (m, 2H, Ar-H), 2.75 (t, ³J = 7.2 Hz, 2H, 9-H), 2.52-2.45 (m, 2H), 1.91-1.81 (m, 4H). **¹³C-NMR** (100 MHz, CDCl₃) δ (ppm) 141.6 (s, C-10), 136.8 (d, ¹J = 96.0 Hz, C-1), 134.1 (dq, ⁴J = 3 Hz, ²J_{CF} = 33 Hz, C-4), 131.4 (d, ²J = 9.6 Hz, C-2), 128.5 (d, ³J = 10.0 Hz, C-3), 126.1 (s), 126.0 (s), 125.9 (s), 125.8 (s), 123.6 (q, ¹J_{CF} = 273.1 Hz, C-5), 35.3 (s), 32.5 (d, ³J = 15.0 Hz, C-8), 29.4 (d, ¹J = 72.0 Hz, C-6), 21.0 (d, ²J = 4.2 Hz, C-7). **³¹P-NMR** (162 MHz, CDCl₃) δ (ppm) 31.2 (s). **HRMS**: calcd for C₂₄H₂₂OF₆P [M+H]⁺ 471.1314, found 471.1312.

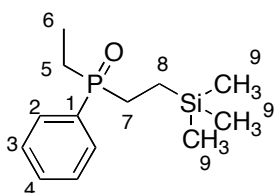
1-(bis(4-trifluoromethyl)phenyl)-3-trimethylsilylpropylphosphine oxide (69r)



Conditions: ((46b) : 100 mg, 0.296 mmol, 2 equiv.); (Ph₂I⁺ OTf⁻ (85) = 22 mg, 0.052 mmol, 0.35 equiv.); (64f) = 24 μL, 0.148 mmol, 1 equiv). The reaction was carried

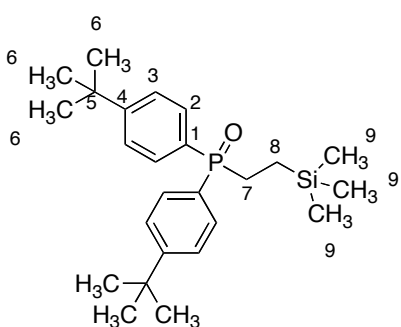
out following the general procedure. The crude product was purified by flash column chromatography (ethyl acetate) to give a white solid. **Yield** : 51 mg, 76%. **M_p** = 107-110°C. **¹H-NMR** (400 MHz, CDCl₃) δ (ppm) 7.88-7.84 (m, 4H, Ar-H), 7.75-7.73 (m, 4H, Ar-H), 2.39-2.32 (m, 2H), 1.70-1.59 (m, 2H), 0.63 (t, ³J = 8.2 Hz, 2H, 8-H), -0.07 (s, 9H, 9-H). **¹³C-NMR** (100 MHz, CDCl₃) δ (ppm) 137.2 (d, ¹J = 97.0 Hz, C-1), 134.1 (dq, ⁴J = 2.8 Hz, ²J_{CF} = 33 Hz, C-4), 131.4 (d, ²J = 9.7 Hz, C-2), 125.9 (d, ³J = 3.8 Hz, C-3), 123.6 (d, ¹J_{CF} = 272 Hz, C-5), 33.4 (d, ¹J = 70 Hz, C-6), 19.0 (d, ³J = 12.7 Hz, C-8), 16.4 (d, ²J = 4.0 Hz, C-7), -1.6 (s, C-9). **³¹P-NMR** (162 MHz, CDCl₃) δ (ppm) 29.9 (s). **HRMS**: calcd for C₂₀H₂₄OPSiF₆ [M+Na]⁺ 453.1246, found 453.1238.

1-Ethylphenyl-2-trimethylsilylethylphosphine oxide (69s)



Conditions: ((**46d**) : 100 mg, 0.648 mmol, 2 equiv.); (Ph₂I⁺ OTf (**85**) = 49 mg, 0.113 mmol, 0.35 equiv.); (**64e**) = 47 μL, 0.324 mmol, 1 equiv). The reaction was carried out following the general procedure. The crude product was purified by flash column chromatography (ethyl acetate:methanol 95:5) to give a white solid. **Yield** : 70 mg, 85%. **M_p** = 47-50°C. **¹H-NMR** (400 MHz, CDCl₃) δ (ppm) 7.67-7.64 (m, 2H, Ar-H), 7.52-7.44 (m, 3H, Ar-H), 2.04-1.70 (m, 4H), 1.11-1.05 (m, 3H), 0.78-0.47 (m, 2H), -0.05 (s, 9H, 9-H). **¹³C-NMR** (100 MHz, CDCl₃) δ (ppm) 132.3 (d, ¹J = 91.0 Hz, C-1), 131.6 (d, ⁴J = 2.7 Hz, C-4), 130.7 (d, ³J = 8.4 Hz, C-3), 128.7 (d, ²J = 11.0 Hz, C-2), 23.5 (d, ¹J = 67.1 Hz, C-7), 22.1 (d, ¹J = 67.0 Hz, C-5), 7.0 (d, ²J = 7.1 Hz, C-8), 5.8 (d, ²J = 7.0 Hz, C-6), -2.12 (s, C-9). **³¹P-NMR** (162 MHz, CDCl₃) δ (ppm) 44.3 (s). **HRMS**: calcd for C₁₃H₂₄OSiP [M+H]⁺ 255.1335, found 255.1334.

1-(bis(4-tertbutyl)phenyl)-2-trimethylsilylethylphosphine oxide, (69t)



Conditions: ((**46e**) : 100 mg, 0.318 mmol, 2 equiv.); (Ph₂I⁺ OTf (**85**) = 24 mg, 0.055 mmol, 0.35 equiv.); (**64e**) = 23 μL, 0.159 mmol, 1 equiv). The reaction was carried out following the general procedure. The crude product was purified by flash column

chromatography (ethyl acetate:methanol 95:5) to give a white solid. **Yield** : 51 mg, 77%. **M_p** = 200 °C. **¹H-NMR** (400 MHz, CDCl₃) δ (ppm) 7.67-7.62 (m, 4H, Ar-H), 7.48-7.45 (m, 4H, Ar-H), 2.15-2.08 (m, 2H), 1.31 (s, 18H, 6-H), 0.78-0.72 (m, 2H, 7-H), -0.00 (s, 9H, 9-H). **¹³C-NMR** (100 MHz, CDCl₃) δ (ppm) 155.0 (d, ⁴J = 2.8 Hz, C-4), 131.0 (d, ²J = 9.0 Hz, C-2), 130.0 (d, ¹J = 99.1 Hz, C-1), 125.7 (d, ³J = 12.0 Hz, C-3), 35.1 (s, C-5), 31.2 (s, C-6), 24.2 (d, ¹J = 71.0 Hz, C-7), 7.1 (d, ²J = 6.7 Hz, C-8), -1.99 (s, C-9). **³¹P-NMR** (162 MHz, CDCl₃) δ (ppm) 34.2 (s). **HRMS**: calcd for C₂₅H₃₉OSiPNa [M+Na]⁺ 437.2396, found 437.2398.

Photocatalyzed Annulation Reaction for the Formation of Phosphorylated Oxindoles

4.1. Background

Isatin or 1H-indole-2,3-dione (Figure 4.1) and its functionalized derivatives occupy an outstanding position in the field of organic¹⁴³ and medicinal chemistry.¹⁴⁴ In nature, isatin has been found in many plants of the genus *Isatis*¹⁴⁵, in *Calanthe Discolor*¹⁴⁶ and in *Couroupita guianensis*.¹⁴⁷ In humans, it is an important component of the metabolism of adrenaline.¹⁴⁸

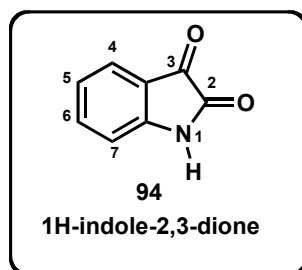


Figure 4.1. Isatin or 1H-indole-2,3-dione

The chemistry of isatin was investigated for the first time by Sumpter¹⁴⁹ and later amended by Popp¹⁵⁰ and by da Silva.¹⁵¹

Outstanding contributions in literature have demonstrated the growing interest in bioactivity of isatin derivatives and the synthesis of those compounds which showed

¹⁴³ da Silva, J.F.; Garden, S.J.; Pinto, A.C. *J. Braz. Chem. Soc.* **2001**, *12*, 273-324.

¹⁴⁴ Chiyanzu, I.; Hansell, E.; Gut, J.; Rosenthal, P.J.; McKerrowb, J.H.; Chibale, K. *Bioorg. Med. Chem. Lett.* **2003**, *13*, 3527-3530.

¹⁴⁵ Guo, Y.; Chen, F. *Zhongcaoyao* **1986**, *17*, 8.

¹⁴⁶ Yoshikawa, M.; Murakami, T.; Kishi, A.; Sakurama, T.; Matsuda, H.; Nomura, M.; Matsuda, H.; Kubo, M. *Chem. Pharm. Bull.* **1998**, *46*, 886-888.

¹⁴⁷ Bergman, J.; Lindström, J.O.; Tilstam, U. *Tetrahedron* **1985**, *41*, 2879-2881.

¹⁴⁸ (a) Ischia, M.; Palumbo, A.; Prota, G. *Tetrahedron* **1988**, *44*, 6441-6446. (b) Halket, J.M.; Watkins, P.J.; Przyborowska, A.; Goodwin, B.L.; Clow, A.; Glover, V.; Sandler, M. *J. Chromatogr.* **1991**, *562*, 279.

¹⁴⁹ Sumpter, W.C. *Chem. Rev.* **1944**, *34*, 393-434.

¹⁵⁰ Popp, F.D. *Adv. Heterocycl. Chem.* **1975**, *18*, 1-58.

excellent biological activities, such as anticonvulsant,¹⁵¹ antitumor,¹⁵² antimicrobial,¹⁵³ antitubercular,¹⁵⁴ antiviral¹⁵⁵ and anti-HIV.¹⁵⁶

Several synthetic methodologies leading to isatin derivatives have been described, generalized in the following strategies and shown in Scheme 4.1:¹⁵¹

- a) Partial or total reduction of heterocyclic ring, leading to indoles or other derivatives (Scheme 4.1a);
- b) Oxidation of the heterocyclic ring to obtain isatoic anhydride (Scheme 4.1b),¹⁵⁷
- c) Nucleophilic addition at position C-3 (Scheme 4.1c);
- d) Nucleophilic attack at position C-2 employing isatin functionalized derivatives (Scheme 4.1d).

¹⁵¹ Verma, M.; Pnadeya, S.N.; Singh, K.N.; Stables, J.P. *Acta Pharm.* **2004**, *54*, 49-56.

¹⁵² Tripathy, R.; Reiboldt, A.; Messina, P.A.; Iqbal, M.; Singh, J.; Bacon, E.R.; Angeles, T.S.; Yang, S.X.; Albom, M.S.; Robinson, C.; Chang, H.; Ruggeri, B.A.; Mallamo, J.P. *Bioorg. Med. Chem. Lett.* **2006**, *16*, 2158-2161.

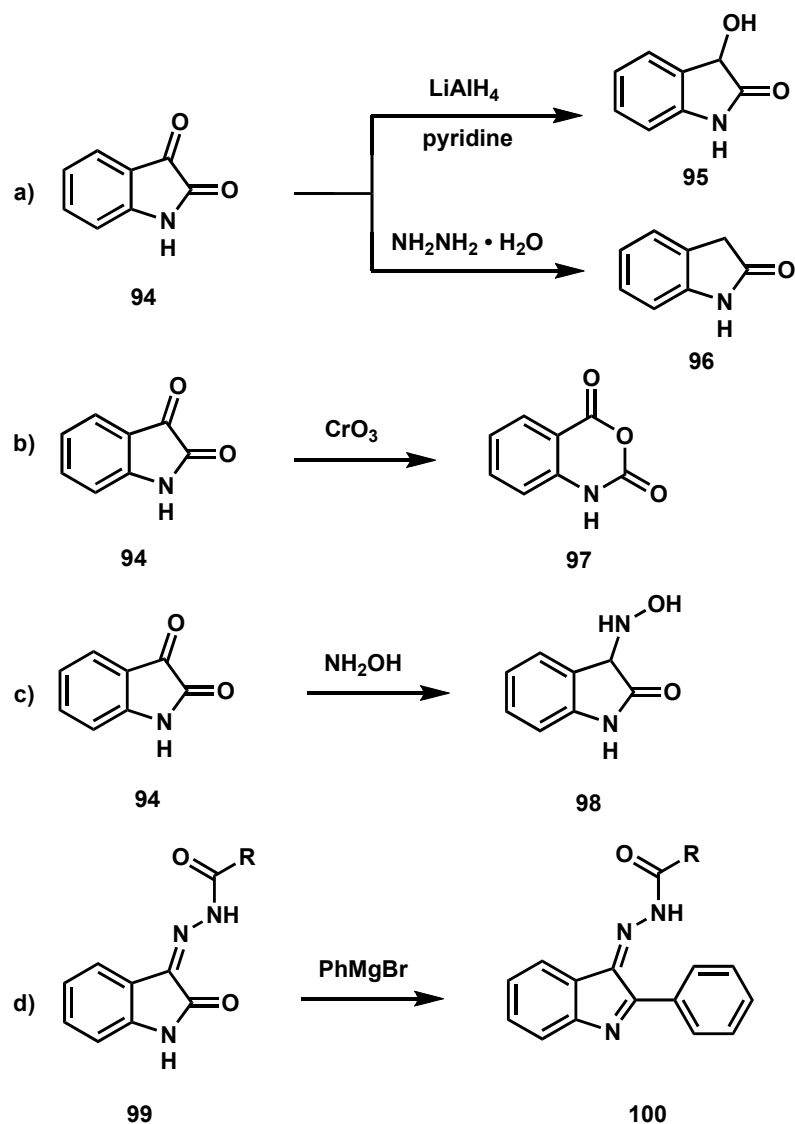
¹⁵³ (a) Raj, A.; Raghutanathan, R.; Sridevikumaria, M.R.; Raman, N. *Bioorg. Med. Chem.* **2003**, *11*, 407-410. (b) Patel, A.; Bari, S.; Talele, G.; Patel, J.; Sarangapani, M. *Iran. J. Pharm. Res.* **2006**, *4*, 249-254.

¹⁵⁴ Aboul-Fadl, T.; Bin-Jubair, F.A.S. *Int. J. Res. Pharm. Sci.* **2010**, *1*, 113-126.

¹⁵⁵ Jiang, T.; Kuhen, K.L.; Wolff, K.; Yin, H.; Bieza, K.; Caldwell, J.; Bursulaya, B.; Tuntlad, T.; Zhang, K.; Karanewsky, D.; He, Y. *Bioorg. Med. Chem. Lett.* **2006**, *16*, 2109-2112.

¹⁵⁶ Rattan, B.T.; Anand, B.; Yogeewari, P.; Sriram, D. *Bioorg. Med. Chem. Lett.* **2005**, *15*, 4451-4454.

¹⁵⁷ Czuba, W.; Sedzik-Hibner, D. *Pol. J. Chem.* **1989**, *63*, 113.



Scheme 4.1. Reactivity of isatin and its derivatives and different synthetic pathways

Although it has not been shown, isatin can undergo electrophilic aromatic substitutions at positions C-5 and C-7 of the phenyl ring, *N*-substitutions, ring-expansions and spiro-annulations.¹⁵¹

Among these, the most attracting transformation of isatin concerns the carbonyl position C-3, due to the presence of a prochiral center. This leads to nucleophilic addition or annulation reactions, transforming isatin into oxindoles derivatives (Figure 4.2).

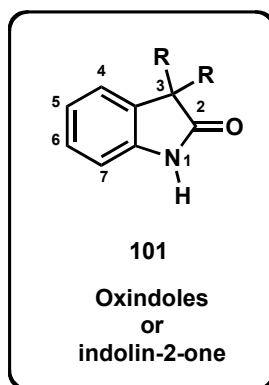


Figure 4.2. General structure of oxindoles (indolin-2-one)

4.2. Oxindoles, cyclic isatin derivative frameworks

4.2.1. Bioactive pharmaceutical compounds

Oxindoles (Figure 4.2) are reduced derivatives of the isatin family and were synthesized, for the first time, by Baeyer in the 19th century by the reduction of isatin.¹⁵⁸ These molecules are endogenous aromatic heterocyclic compounds with a bicyclic structure, which consists in a six-membered ring fused with a five-membered ring containing a nitrogen atom.¹⁵⁹ They are constituents of the indole family; the only difference with the indoline structure is the carbonyl group at the position C-3 of the five-membered ring.

Oxindoles, C-3 functionalized and also those that are spiro-fused to other cyclic moieties, have attracted an extraordinary interest in organic chemistry due to their presence in natural products¹⁶⁰ and because they are reported to exhibit amazing biological activities such as progesterone receptor modulators,¹⁶¹ MDM2¹⁶² inhibitors,¹⁶³ antiproliferative,¹⁶⁴ antihypertensive,¹⁶⁵ anti-inflammatory¹⁶⁶ and many others (Figure 4.3).¹⁶⁷

¹⁵⁸ Baeyer, A. *Berichte Deuten Chemischen G.* **1879**, 582.

¹⁵⁹ Cerchiaro, G.; Ferreira, A.M. *J. Braz. Chem. Soc.* **2006**, *17*, 1473-1485.

¹⁶⁰ (a) James, M.N.G.; Williams, G.J.B. *Can. J. Chem.* **1972**, *50*, 2407-2412. (b) Jossang, A.; Jossang, P.; Hamid, A.H.; Sevenet, T.; Bodo, B. *J. Org. Chem.* **1991**, *56*, 6527-6530. (c) Cui, C.-B.; Kakeya, H.; Osada, H.J. *J. Antibiot.* **1996**, *49*, 832-835. (d) Cui, C.-B.; Kakeya, H.; Osada, H.J. *Tetrahedron* **1996**, *52*, 12651-12666. (e) Anderton, N.; Cockrum, P.A.; Cologate, S.M.; Edgar, J.A.; Flower, K.; Vit, I.; Willing, R.I. *Photochemistry* **1998**, *48*, 437-439.

¹⁶¹ Fensome, A.; Adams, W.R.; Adams, A.L.; Berroddin, T.J.; Cohen, J.; Huselton, C.; Illenberger, A.; Karen, J.C.; Hudak, M.A.; Marella, A.G.; Melenski, E.G.; McComas, C.C.; Mugford, C.A.; Slayeden, O.D.; Yudt, M.; Zhang, J.; Zhang, P.; Zhu, Y.; Winneker, R.C.; Wrobel, J.E. *J. Med. Chem.* **2008**, *51*, 1861-1873.

¹⁶² *Mouse double minute 2 homolog* (MDM2) is also known as E3-ubiquitin-protein ligase MDM2 and it is an important regulator of the p53 tumor suppressor. It works mainly as inhibitor of transcriptional activation.

¹⁶³ Ding, K.; Lu, Y.; Nikolovska-Coleska, Z.; Wang, G.; Qiu, S.; Shangary, S.; Gao, W.; Qin, D.; Stuke, J.; Krajewski, K.; Roller, P.P.; Wang, S. *J. Med. Chem.* **2006**, *49*, 3432-3435.

¹⁶⁴ Natarajan, A.; Guo, Y.; Harbinski, F.; Fan, Y.-H.; Chen, H.; Luus, L.; Diercks, J.; Aktas, H.; Chorev, M.; Halper J.A. *J. Med. Chem.* **2004**, *47*, 4979-4982.

¹⁶⁵ Martin, W.; John, J.K. *Aminomethylene oxindoles* US19794145422, **1979**.

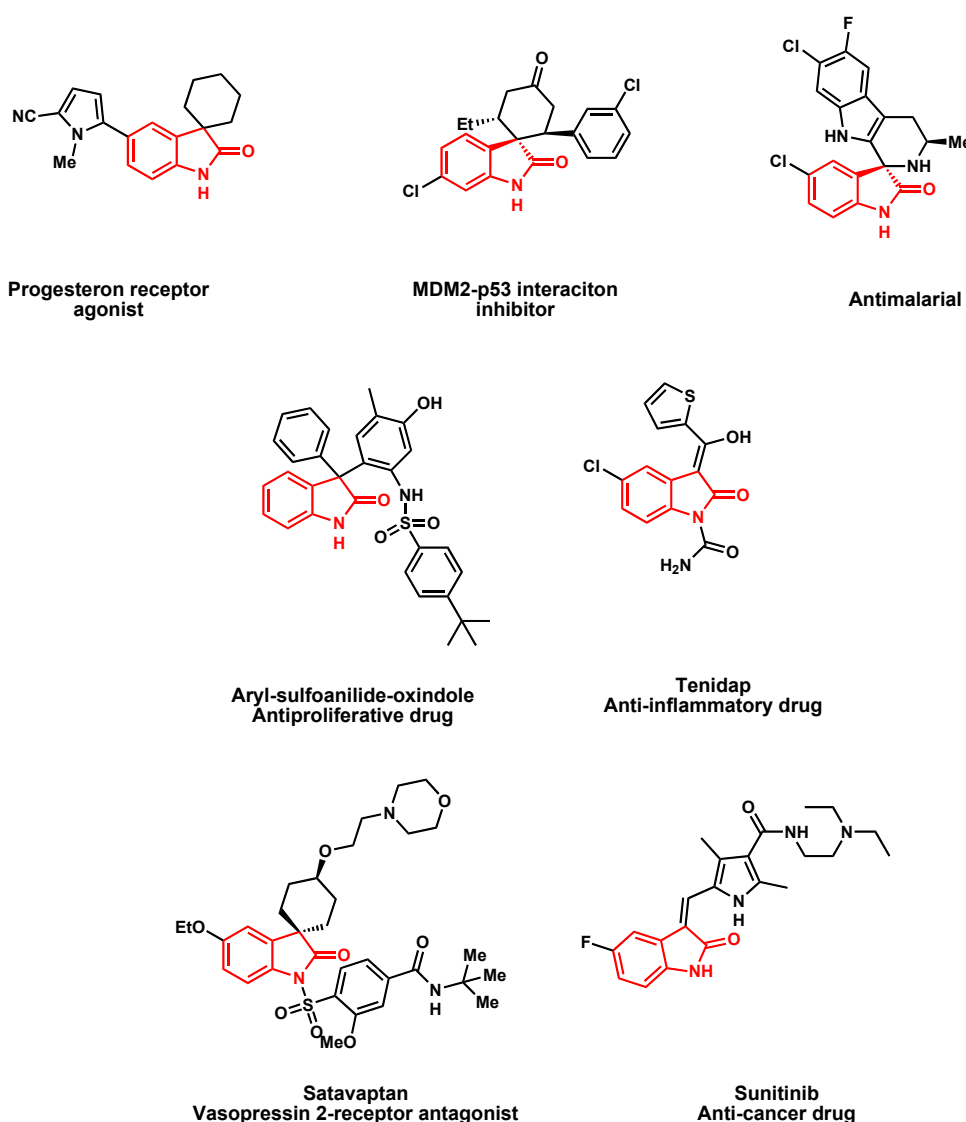


Figure 4.3. Some examples of bioactive molecules possessing 2-oxindole moiety (red)

Oxindoles exhibit excellent antitumor properties; sunitinib (Figure 4.3) has been widely used in the treatment of gastrointestinal stromal tumor, and metastatic renal cell cancer.¹⁶⁸

¹⁶⁶ (a) Melvin, Jr.; Lawrence, S. *Oxindole anti-inflammatory agents* US19874686224, **1987**. (b) Saul, B.K. *3-Substituted 2-oxindole-1-carboxamides as analgesic and anti-inflammatory agents* US19854556672, **1985**.

¹⁶⁷ (a) Kumari, G.; Nutan, ; Modi, M.; Gupta, S.K.; Singh, R.K. *Eur. J. Med. Chem.* **2011**, *46*, 1181-1188. (b) Lo, M.M.-C.; Newmann, C.S.; Nagayama, S.; Perlstein, E.O.; Schreiber, S.L. *J. Am. Chem. Soc.* **2005**, *127*, 10130-10131. (c) Rottmann, M.; McNamara, C.; Yeung, B.K.S.; Lee, M.C.S.; Zhou, B.; Russell, B.; Seitz, P.; Plouffe, D.M.; Dharia, N.V.; Tan, J.; Cohen, S.B.; Spencer, K.R.; Gonzalez-Paez, G.E.; Lakshminarayana, S.B.; Goh, A.; Suwanarusk, R.; Jegla, T.; Schmitt, E.K.; Beck, H.-P.; Brun, R.; Nosten, F.; Renia, L.; Dartois, V.; Keller, T.H.; Fidock, D.A.; Winzeler, E.A.; Diagana, T.T. *Science* **2010**, *329*, 1175-1180. (d) Ding, K.; Lu, Y.; Nikolovska-Coleska, Z.; Qiu, S.; Ding, Y.; Gao, W.; Stucky, J.; Krajewski, K.; Roller, P.P.; Tomita, Y.; Parrish, D.A.; Deschamps, J.R.; Wang, S. *J. Am. Chem. Soc.* **2004**, *126*, 16077-16086.

¹⁶⁸ Silva, B.V.; Ribeiro, N.M.; Pinto, A.C.; Vargas, M.D.; Dias, L.C. *J. Braz. Chem. Soc.* **2008**, *19*, 1244-1247.

Aryl sulfoanilides oxindoles (Figure 4.3) have been largely used as antiproliferatives because it has been shown that the oxindole moiety is responsible of inhibiting the growth of cancer cells by partial depletion of intracellular calcium stores. Meanwhile, sulfoanilide-oxindole hybrid has been found to inhibit the initiation of translation. Various non-steroidal oxindoles have shown interesting anti-inflammatory properties. They are reported to be efficient inhibitors of the enzymes lipoxygenase (LO) and cyclooxygenase (CO). For instance, they are used for the treatment of chronic diseases such as osteo-arthritis and rheumatoid arthritis. Tenidap (Figure 4.3) is the most representative and powerful remedy in this field.

Although the wide range of biological applications of oxindoles, the most significant role is perhaps represented by protein kinase inhibitors.¹⁶⁹ Arylidene oxindoles, as those shown in Figure 4.4, were the first identified structures useful as receptor tyrosine kinase (RTK) inhibitors in 1988.¹⁷⁰ X-ray data demonstrated that either the proton at the N-1 position or oxygen atom at the C-2 position were fundamentals for the coordination with a peptide in the ATP binding pocket of these RTKs.

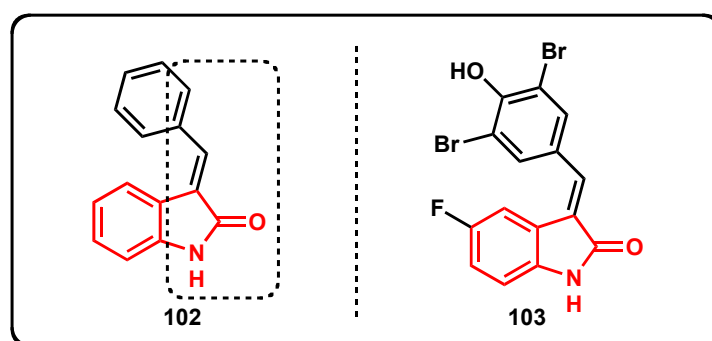


Figure 4.4. Motif of general structure (**102**); GW5074 (**103**), potent inhibitor of neurodegeneration

Noteworthy, after investigations it was found that alkylation of N-1 position drastically decreased the efficacy of inhibition of arylidene oxindoles and that general substitutions around two-fused rings influenced the specificity and potency of the inhibitors.¹⁷¹

¹⁶⁹ (a) Cohen, P. *Nature Rev., Drug Discov.* **2002**, *1*, 309-315. (b) Prakash, C.R.; Theivendren, P.; Raja, S. *Pharmacology & Pharmacy* **2012**, *3*, 62-71. (c) Noble, M.E.M.; Endicott, J.A.; Johnson, L.N. *Science* **2004**, *303*, 1800-1805.

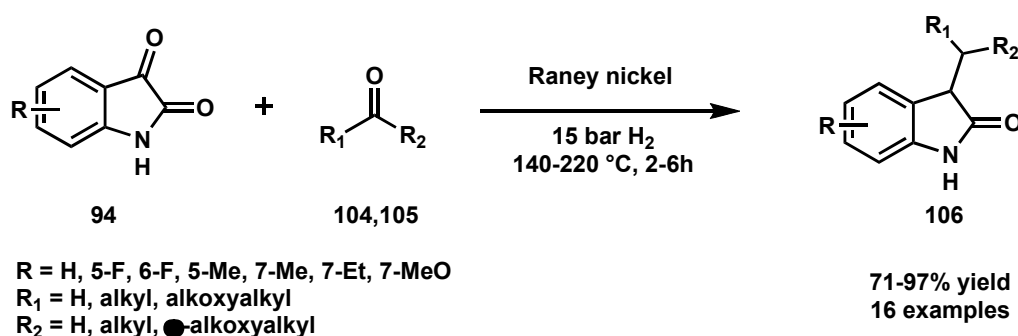
¹⁷⁰ Sun, L.; Tran, N.; Tang, F.; App, H.; Hirth, P.; McMahon, G.; Tang, C. *J. Med. Chem.* **1998**, *41*, 2588-2603.

¹⁷¹ Sun, L.; Tran, N.; Liang, C.; Tang, F.; Rice, A.; Schreck, R.; Waltz, K.; Shawver, L.K.; McMahon, G.; Tang, C. *J. Med. Chem.* **1999**, *42*, 5120-5130.

4.2.2. Synthetic pathways to access to C-3 functionalized oxindoles from isatin derivatives

It is important to consider the reactivity on the carbonyl at C-3 position of isatin to have an easy access to functionalized oxindoles. It was reported that the ketone carbonyl group of isatin reacts with different nitrogen nucleophiles,¹⁷² Wittig reagents,¹⁷³ 1,3-diketones,¹⁷⁴ phosphites,¹⁷⁵ simple ketones and aldehydes,¹⁷⁶ activated alkenes,¹⁷⁷ alkynes¹⁷⁸ and allenes.¹⁷⁹

A representative example of C-3 functionalization is the reaction of easily available isatin **94** with ketones or aldehydes **104,105** catalyzed by Raney nickel to afford 3-alkyl and 3-hydroxyalkyl oxindoles **106**, described by Simig and co-workers (Scheme 4.2).^{177b}



Scheme 4.2. One-pot procedure for the formation of 3-alkyl and 3-(ω -hydroxyalkyl)oxindoles from isatins and aldehydes/ketones

From a mechanistic perspective, it was investigated if a complex reaction sequence could be carried out in one-pot *via* regioselective alkylation of oxindole **101**, obtained

¹⁷² (a) Piccirilli, R.M.; Popp, F.D. *J. Heterocycl. Chem.* **1973**, *10*, 671. (b) Khan, K.M.; Mughal, U.R.; Samreen; Perveen, S.; Choudhary, M.I. *Lett. Drug Des. Discovery* **2008**, *5*, 243. (c) Sridhar, S.K.; Pandeya, S.N.; Stables, J.P.; Ramesh, A. *Eur. J. Pharm. Sci.* **2002**, *16*, 129. (d) Pandeya, S.N.; Raja, A.S. *J. Pharm. Pharm. Sci.* **2002**, *5*, 266.

¹⁷³ (a) Wood, J.L.; Holubec, A.A.; Stoltz, B.M.; Weiss, M.M.; Dixon, J.A.; Doan, B.D.; Shamji, M.F.; Chen, J.F.; Haffron, T.P. *J. Am. Chem. Soc.* **1999**, *121*, 6326. (b) Raunak, Kumar, V.; Mukherjee, S.; Poonam; Prasad, A.K.; Olsen, C.E.; Schaffer, S.J.C.; Sharma, S.K.; Watterson, A.C.; Errington, W.; Parmar, V.S. *Tetrahedron* **2005**, *61*, 2687.

¹⁷⁴ Elinson, M.N.; Merkulova, V.N.; Ilovaisky, A.I.; Chizhov, A.O.; Belyakov, P.A.; Barba, F.; Batanero, B. *Electrochim. Acta* **2010**, *55*, 2129.

¹⁷⁵ Andreani, A.; Rambaldi, M.; Locatelli, A.; Bossa, R.; Galatulas, I.; Ninci, M. *Eur. J. Med. Chem.* **1990**, *25*, 187-190.

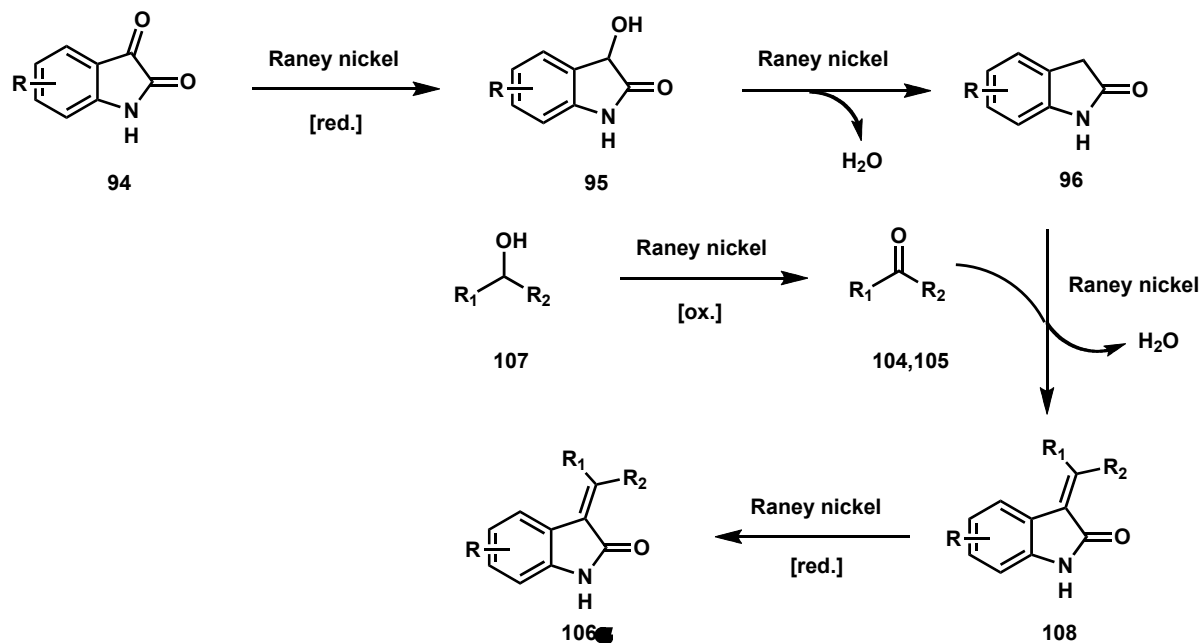
¹⁷⁶ (a) Chen, J.-R.; Liu, X.-P.; Zhu, X.-Y.; Li, L.; Qiao, Y.-F.; Zhang, J.-M.; Xiao, W.-J. *Tetrahedron* **2007**, *63*, 10437. (b) Volk, B.; Simig, G. *Eur. J. Org. Chem.* **2003**, 3991-3996.

¹⁷⁷ (a) Garden, S.J.; Skakle, J.M.S. *Tetrahedron Lett.* **2002**, *43*, 1969. (b) Chung, Y.M.; Im, Y.J.; Kim, J.N. *Bull. Korean Chem. Soc.* **2002**, *23*, 1651.

¹⁷⁸ Alcaide, B.; Almendros, P.; Rodriguez-Acebes, R. *J. Org. Chem.* **2005**, *70*, 3198.

¹⁷⁹ Itoh, J.; Han, S.B.; Krische, M.J. *Angew. Chem. Int. Ed.* **2009**, *48*, 6313.

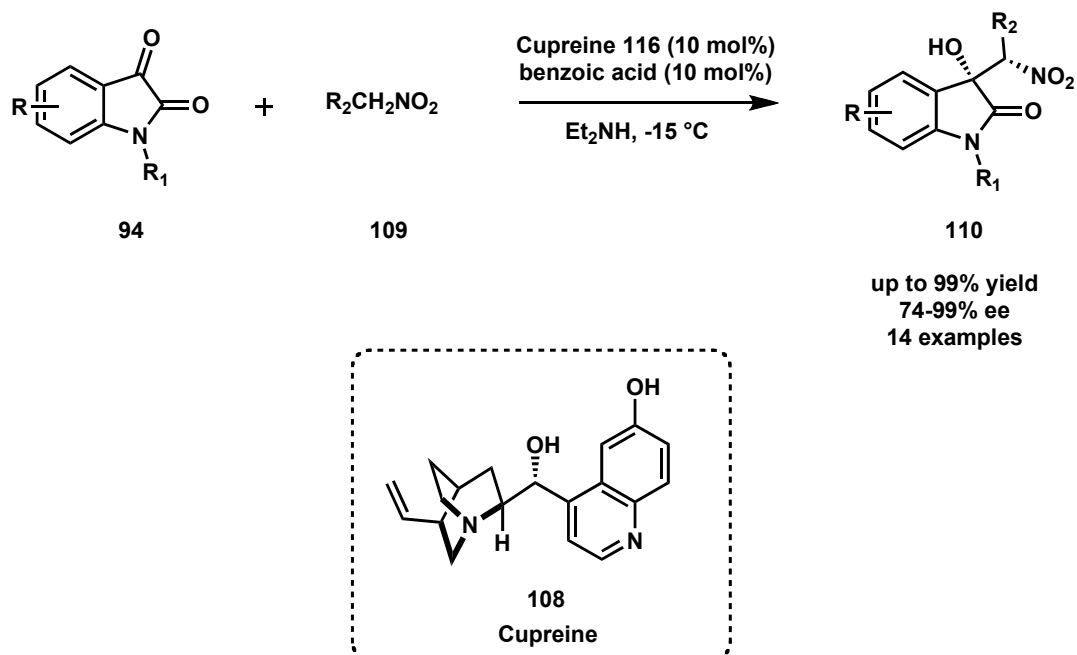
through reduction of isatin **94** with Raney nickel (Scheme 4.3). Oxidation of alcohol **107** to aldehyde/ketone **104,105** leads to regioselective alkylation/alkoxyalkylation affording the desired alkylated oxindole **106 α** .



Scheme 4.3. Plausible mechanism for the alkylation of isatin with aldehydes/ketones

A further example of functionalization at C-3 position starting from isatin derivatives was nitro-aldol reaction, also called Henry reaction. Simig *et al.*¹⁸⁰ have proposed the asymmetric version of such reaction employing cupreine **108** as organocatalyst and benzoic acid to improve and increase enantioselectivity (Scheme 4.4).

¹⁸⁰ Porcks-Maccay, M.; Volk, B.; Kapiller-Dezsofi, R.; Mezei, T.; Simig, G. *Monatsh. Chem.* **2004**, *135*, 697-711.



Scheme 4.4. Nitro-aldol reaction of isatin **94** with nitromethane **109** in the presence of diethylamine as catalyst

4.2.3. Synthetic pathways to access to C-3 functionalized oxindoles from *N*-acrylamides

4.2.3.1. Metal catalyzed annulation reaction

An efficient method for the synthesis of functionalized oxindoles is the annulation reaction using *N*-arylacrylamides as starting substrates. As already known, *annulation* (also called *annelation*¹⁸¹) concerns the chemical transformations in which the formation of a new ring is obtained on a given molecule.¹⁸²

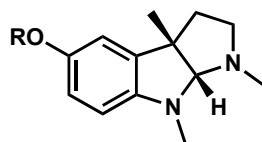
In the literature, there are various examples of metal-catalyzed cyclization reaction of arylacrylamides using copper¹⁸³, palladium¹⁸⁴ and iron complexes⁴². A remarkable example of metal-catalyzed annulation reaction of *N*-arylacrylamides is the palladium-catalyzed Heck-cyanation using iodo-substituted acrylamides **113** with the applications in total synthesis of esermethole **111** and physostygmine **112**, two bioactive compounds (Figure 4.5).

¹⁸¹ *Glossary of terms used in physical organic chemistry*, PAC, **1994**, 66, 1077-1184.

¹⁸² IUPAC, *Compendium of Chemical Terminology*, 2nd. Ed. of the Gold Book, **1997**.

¹⁸³ Chan, C.-W.; Lee, P.-Y.; Yu, W.-Y. *Tetrahedron Lett.* **2015**, 56, 2559-2563.

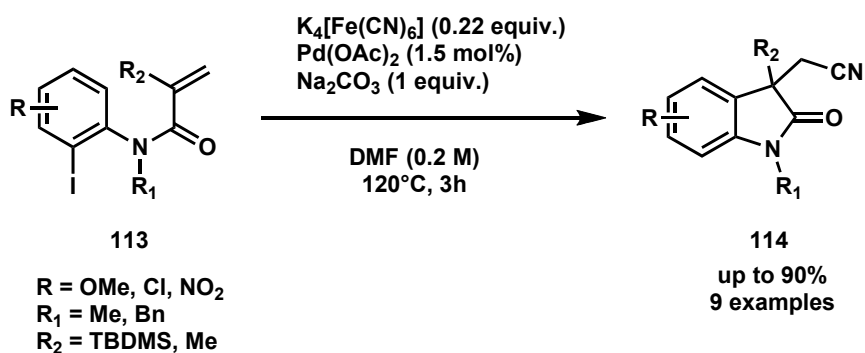
¹⁸⁴ Pinto, A.; Jia, Y.; Neuville, L.; Zhu, J. *Chem. Eur. J.* **2007**, 13, 961-967.



111: R = Me, esermethole
 112: R = CONHMe, physostigmine

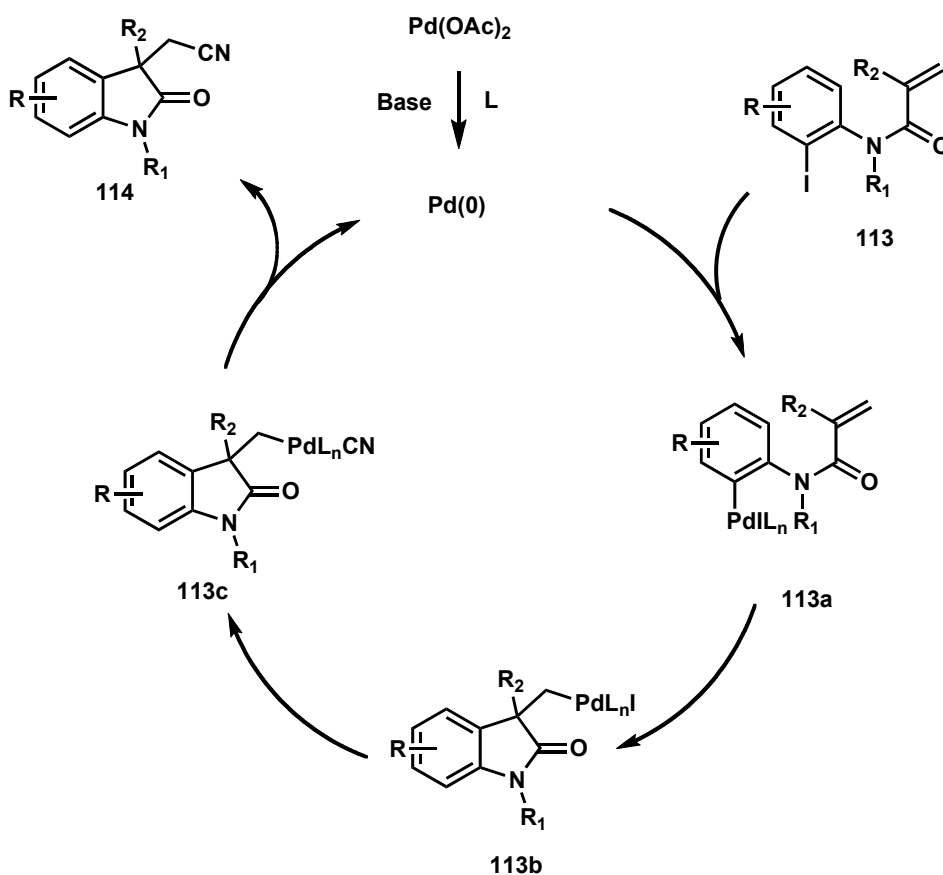
Figure 4.5. Esermethole (R = Me) is an intermediate of the synthesis of Physostigmine (R = CONHMe), reversible natural alkaloid cholinesterase inhibitor

Zhu and co-workers demonstrated that the synthesis of 3,3-disubstituted 2-oxindoles can efficiently be achieved through a domino Heck-cyanation reaction, employing ferro(II)cyanide as cyanide donor in the presence of a catalytic amount of palladium (1.5 mol%) acetate and sodium carbonate (Scheme 4.5).



Scheme 4.5. Metal-catalyzed domino Heck-cyanation reaction of iodo-substituted arylacrylamides

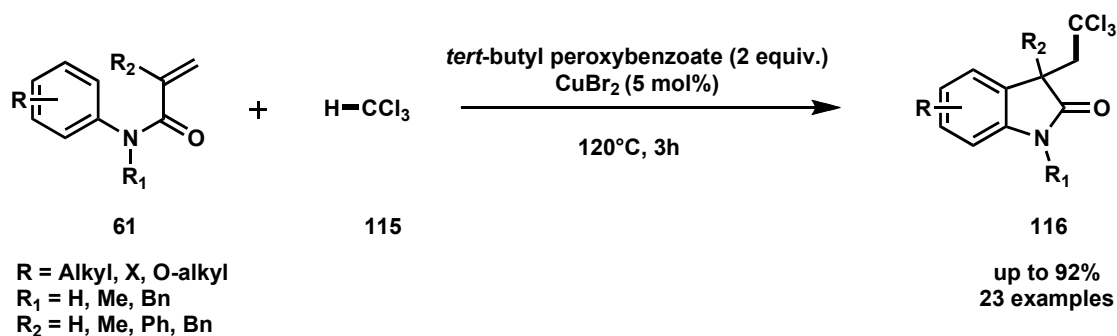
The reaction is described to proceed via oxidative pathway. In a first step, iodo-substituted arylacrylamides **113** add to Pd(0) to generate intermediate **113a**. The latter undergoes intramolecular cyclization to form palladium intermediate **113b**, which affords the desired oxindole **114** after displacement of iodide by cyanide (intermediate **113c**) and reductive elimination leading to the regeneration of the Pd(0) species (Scheme 4.6).



Scheme 4.6. Plausible mechanism for the domino Heck-cyanation of iodo-substituted arylacrylamides⁴²

Recently, an excellent report published by the group of Yu described the copper-catalyzed formation of trichloromethylated oxindoles *via* the reaction between *N*-arylacrylamides and chloroform in the presence of *tert*-butyl peroxybenzoate.

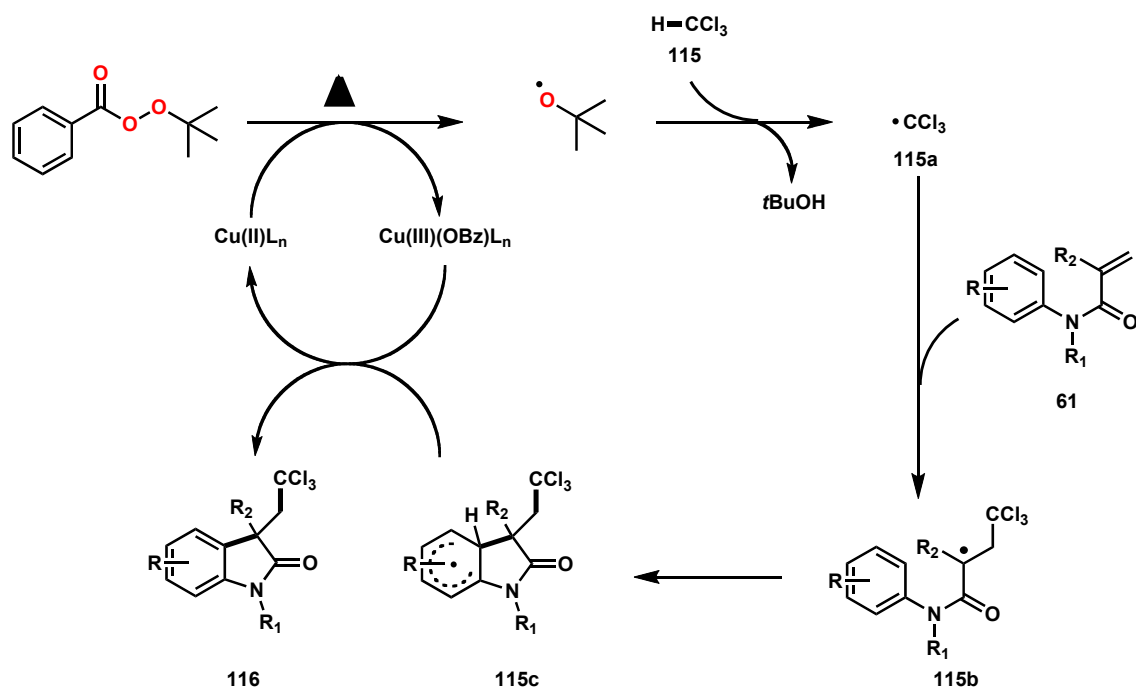
The reaction was expected to proceed *via* the formation of $\cdot\text{CCl}_3$ radical, which then added to C=C bond, followed by aryl cyclization (Scheme 4.7).



Scheme 4.7. Copper-catalyzed annulation reaction of *N*-arylacrylamides with chloroform

Concerning mechanistic hypothesis, it was found that *tert*-butyl peroxybenzoate could lead to the formation of *tert*-butoxy radicals *via* the generation of Cu(III)(OBz) species

as intermediate. *Tert*-butoxy radical would undergo hydrogen abstraction by chloroform **115** to form carbon centered radical $\cdot\text{CCl}_3$ **115a**, which attacks the C=C bond of **61** to form carboradical intermediate **115b**. The latter can cyclize quickly to give the intermediate **115c**, followed by hydrogen abstraction leading the desired product **116** regenerating Cu(II) catalyst (Scheme 4.8).



Scheme 4.8. Proposed mechanism for the copper-catalyzed annulation reaction of *N*-arylacrylamides with chloroform.

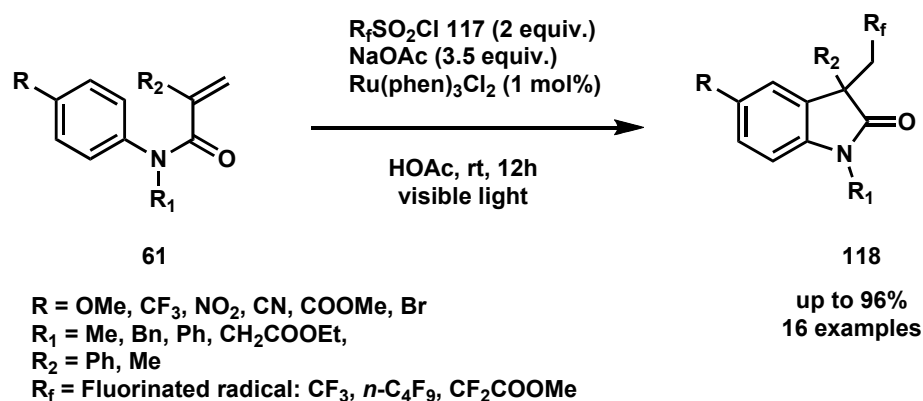
Although the robustness of these methodologies, they suffer from the use of transition metals and high temperatures. It is therefore important to develop a metal-free approach that can circumvent these issues. In this regard, metal-free visible light mediated strategies are appealing.

4.2.3.2. Metal-free photoinduced annulation reaction

The functionalization of *N*-arylacrylamides *via* direct cyclization employing free radicals has attracted more and more organic and pharmaceutical chemists. Over the last years, different metal-free photoinduced pathways have been studied and developed to afford *N*-heterocycle pharmaceutical and bioactive compounds.¹⁸⁵

¹⁸⁵ (a) Marti, C.; Carreira, E.M. *Eur. J. Org. Chem.* **2003**, 2209-2219. (b) Galliford, C.V.; Scheidt, K.A. *Angew. Chem. Int. Ed.* **2007**, *46*, 8748-8758. (c) Zhou, F.; Liu, Y.-L.; Zhou, J. *Adv. Synth. Catal.* **2010**, *352*, 1381-1407.

Because incorporation of a fluorine into a molecule can alter their physical and biological properties,¹⁸⁶ Dolbier *et al.*¹⁸⁷ reported a visible light mediated generation of fluorinated radicals and their addition on arylacrylamides substrates *via* tandem radical cyclization process (Scheme 4.9).

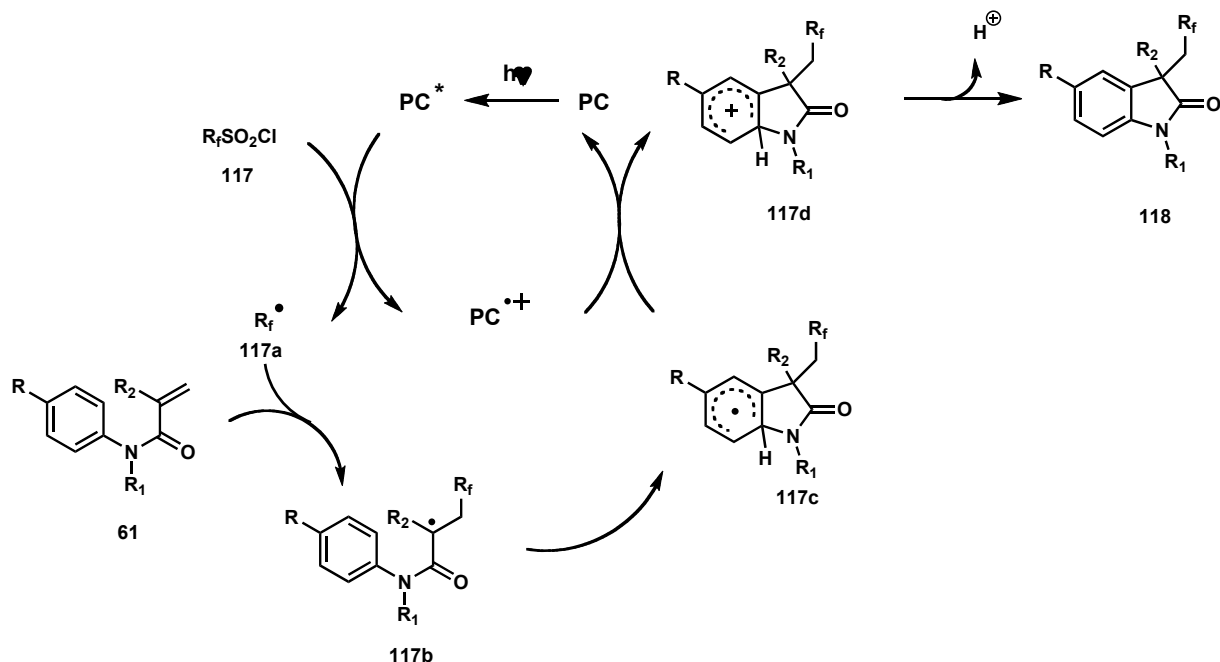


Scheme 4.9. Visible light-mediated radical trifluoromethylation reaction of *N*-arylacrylamides

For this reaction, a radical cyclization mechanism accompanied by the cyclization of the radical intermediate has been proposed. Particularly, free fluorinated radical agent **117** can be generated through the excited state of the photocatalyst. After a fast addition on **61** and formation of the carbon centered radical **117a**, the cyclization step gives rise to the non-aromatic radical intermediate **117b**. Subsequent oxidation and base-induced deprotonation of **117d** afford the desired adduct **118** (Scheme 4.10) in good to excellent yields.

¹⁸⁶ (a) Hagan, D.J. *Chem. Soc. Rev.* **2008**, *37*, 308. (b) Kirk, K.L. *Org. Process Res. Dev.* **2008**, *12*, 305. (c) Krisch, P. *Modern Fluoroorganic Chemistry*; Wiley-VHC: Weinheim, **2004**. (d) Muller, K.; Faeh, C.; Diederich, F. *Science* **2007**, *317*, 1881. (e) Hagmann, W.K. *J. Med. Chem.* **2008**, *51*, 4359.

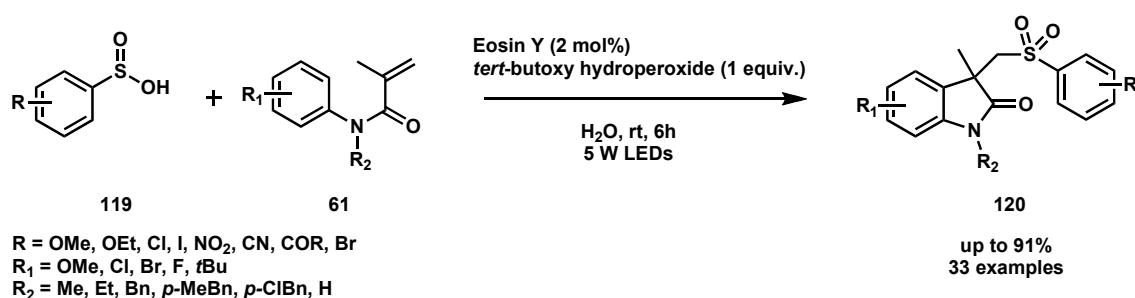
¹⁸⁷ Tang, X.-J.; Thomason, C.S.; Dolbier Jr., W.R. *Org. Lett.* **2014**, *16*, 4594-4597.



Scheme 4.10. Proposed mechanism for tandem radical cyclization reaction of *N*-arylacrylamides with fluorinated agents

Recently, the group of Wang¹⁸⁸ has developed a new pathway for C–S bond formation in addition to those already present in the literature,¹⁸⁹ through the synthesis of sulfonated oxindoles with *N*-arylacrylamides and arylsulfonic acids (Scheme 4.11).

One example was reported for the formation of sulfones starting from corresponding arylsulfonic acids,¹⁹⁰ so that Wang and co-workers have started to investigate on such reaction under mild photoredox conditions.



Scheme 4.11. Visible light photocatalytic functionalization of *N*-arylacrylamides with arylsulfonic acids under mild conditions

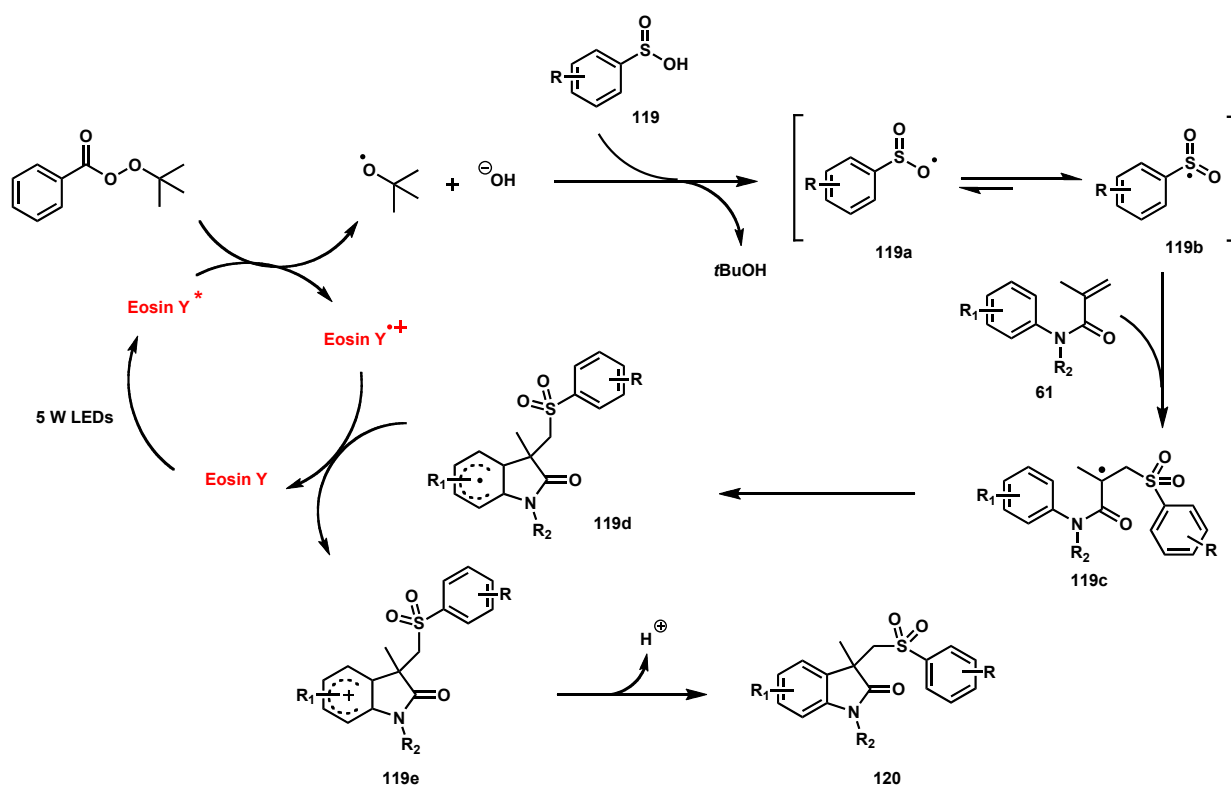
¹⁸⁸ Xia, D.; Miao, T.; Li, P.; Wang, L. *Chem. Asian J.* **2015**, *10*, 1919-1925.

¹⁸⁹ (a) Modha, S.G.; Mehta, V.P.; Van Eycken, P. *Chem. Soc. Rev.* **2013**, *42*, 5042-5055. (b) Miao, T.; Wang, G.-W. *Chem. Commun.* **2011**, *47*, 9501-9503. (c) Miao, T.; Wang, L. *Adv. Synth. Catal.* **2014**, *356*, 967-971. (d) Xi, Y.; Dong, B.; McClain, E.J.; Wang, Q.; Gregg, T.L.; Akhmedov, N.G.; Petersen, J.L.; Shi, X. *Angew. Chem. Int. Ed.* **2014**, *53*, 4657-4661. (e) Wu, X.-S.; Chen, Y.; Li, M.-B.; Zhou, M.-G.; Tian, S.-K. *J. Am. Chem. Soc.* **2012**, *134*, 14694-14697. (f) Miao, T.; Wang, L. *Adv. Synth. Catal.* **2014**, *356*, 429-436.

¹⁹⁰ Yang, W.; Yang, S.; Li, P.; Wang, L. *Chem. Commun.* **2015**, *51*, 7520-7523.

Based on previous observations, a multi-step radical process has been proposed for the functionalization of *N*-arylacrylamides with arylsulfonic acids. Importantly, the radical process has been confirmed by adding in the mixture 2,2,6,6-tetramethyl-1-piperidinyloxy (TEMPO), obtaining total inhibition.

Irradiation of Eosin Y by 5 W LEDs and formation of its excited state generates *tert*-butoxy radical, that reacts with **119** to form two radical intermediates, oxygen- and sulfonyl-radical species **119a** and **119b**. Within them, the most stable radical **119b** may afford radical addition leading to C–S bond formation to give rise to carbon-centered radical intermediate **119c** after addition of **61**. The latter intermediate undergoes fast cyclization to form **119d**, followed by oxidation by radical cation of eosin Y and deprotonation to afford the final sulfonated oxindole **120** (Scheme 4.12).

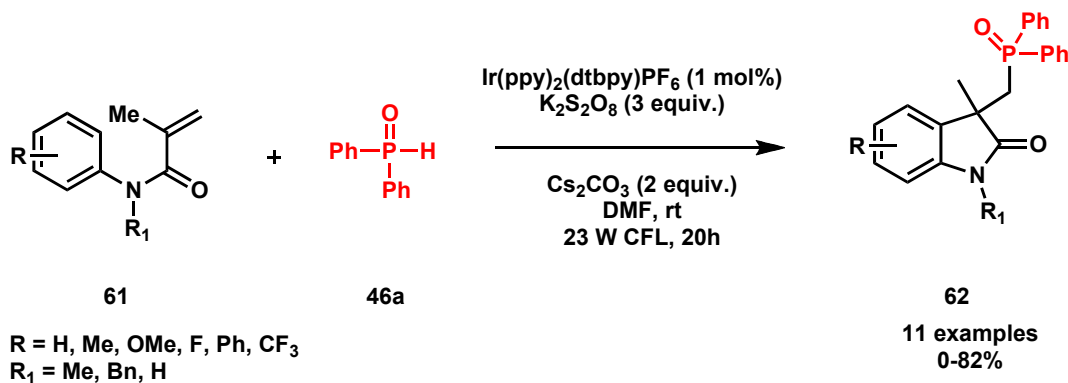


Scheme 4.12. The proposed reaction mechanism for the visible-light photoinduced functionalization of *N*-arylacrylamides with arylsulfonic acids

To the best of our knowledge, only a single example dealing with this chemistry has been reported so far by the group of Lu.¹⁹¹ In this work, Ir-based photocatalyst has been used along with K₂S₂O₈ as an oxidant. The key step of this reaction consists in

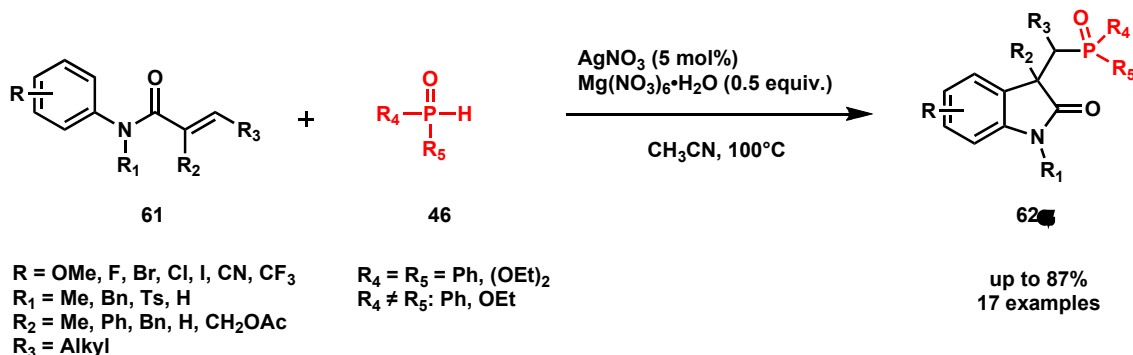
¹⁹¹ Li, C.-X.; Tu, D.-S.; Yao, R.; Yan, H.; Lu, C.-S. *Org. Lett.* **2016**, *18*, 4928-4931.

generating the phosphinoyl radical upon reduction of the persulfate by the excited state of the photocatalyst (Scheme 4.13).



Scheme 4.13. Visible-light induced radical addition of diphenylphosphine oxide to *N*-arylacrylamides via C-P bond formation

Besides this example, a transition metal catalyzed version of this reaction has previously been reported by the group of Yang,¹⁹² which developed an efficient and innovative strategy that employed silver salts to catalyze photo-induced addition of phosphorus radical species to *N*-arylacrylamides. After several optimization studies, silver nitrate (AgNO₃) was identified as the best choice in the presence of a nitrogen containing catalyst as additive, Mg(NO₃)₆•H₂O. The reaction gave satisfactory results, even if it was absolutely necessary to carry out the reaction at 100°C in CH₃CN (Scheme 4.14).

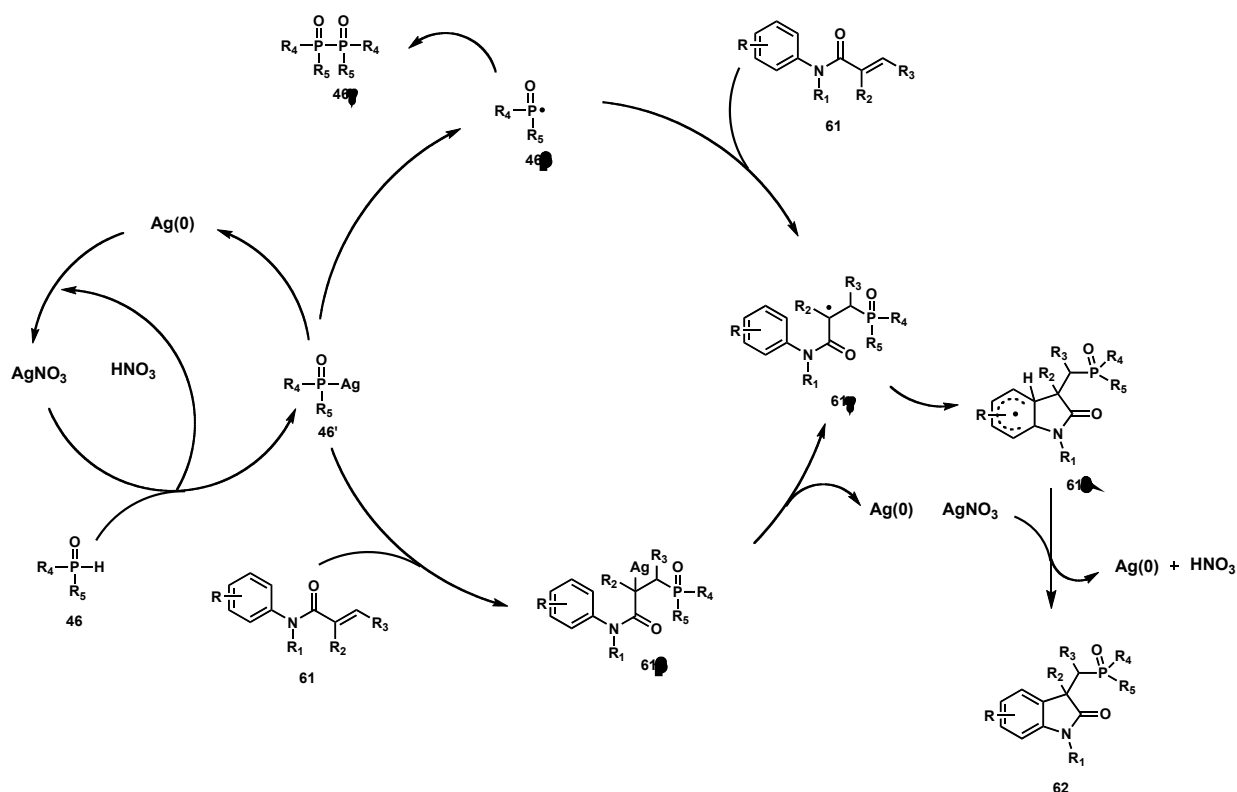


Scheme 4.14. Silver catalyzed phosphorylation of arylacrylamides with secondary phosphine oxides and phosphites

The existence of the radical process was confirmed by the addition in the mixture of 1.0 equivalent of TEMPO that inhibited completely the process. The formation of the phosphinoyl radical was confirmed by ESI/MS spectroscopy revealing a peak corresponding to 46[•], that can proceed *via* two pathways: *i*) either through the formation

¹⁹² Li, Y.-M.; Sun, M.; Wang, H.-L.; Tian, Q.-P.; Yang, S.-D. *Angew. Chem. Int. Ed.* **2013**, *52*, 3972-3976.

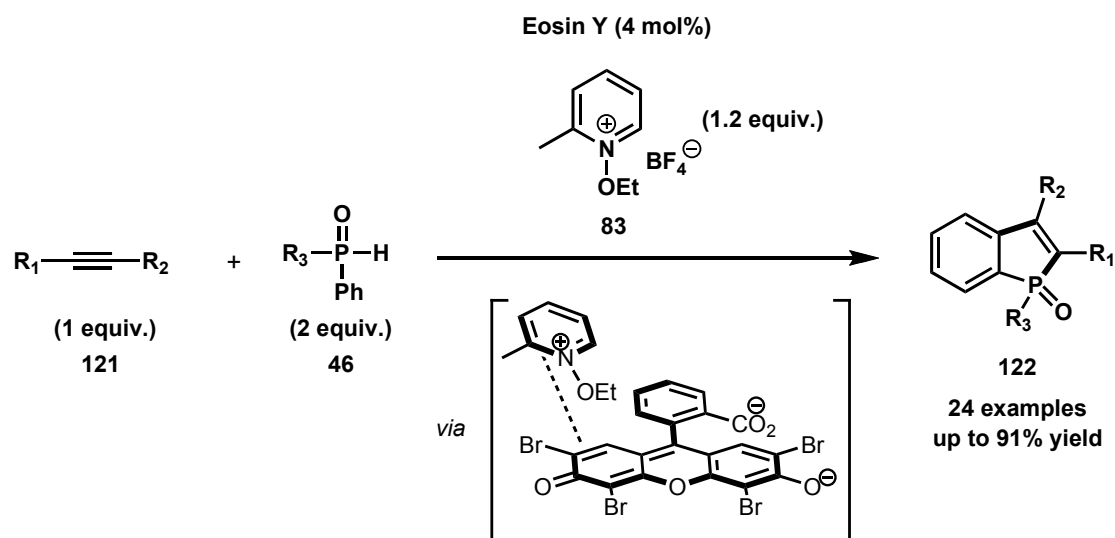
of phosphorus centered radical **46 β** (path A) which can also lead to dimerization product **46 γ** , *ii*) or leading to Ag(I) species **46 β** (path B), followed by oxidation to afford carbon centered radical **61 γ** . The latter is the common intermediate to give rise to radical cyclized intermediate **61 δ** which undergoes single electron transfer reaction (SET) to afford the desired adduct **62** *via* oxidation with Ag(I) (Scheme 4.15).



Scheme 4.15. proposed mechanism for silver-catalyzed phosphorylation of *N*-arylacrylamides with phosphine oxides and phosphites

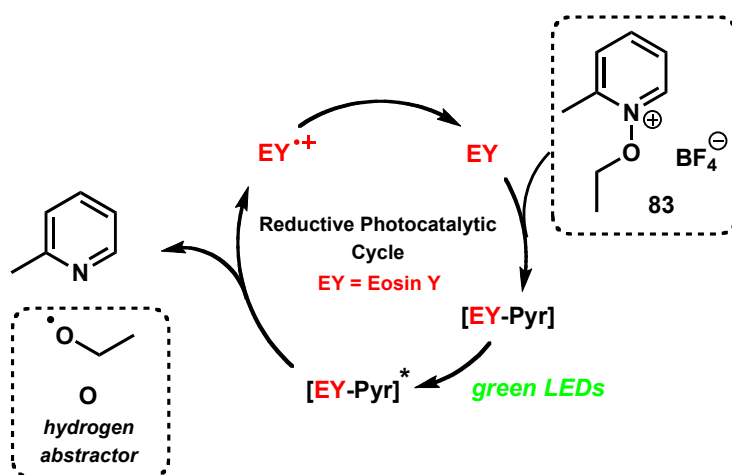
As the reaction mechanism of this process is based on the generation of phosphinoyl radical and the oxidation of the cyclohexadienyl radical formed upon cyclisation, we reasoned that employing our recent approach developed for the formation of benzo[*b*]phospholes¹⁹³ (Scheme 4.16), would offer an efficient approach towards the synthesis of phosphorylated oxindoles.

¹⁹³ Quint, V.; Morlet-Savary, F.; Lohier, J.-F.; Lalevée, J.; Gaumont, A.-C.; Lakhdar, S. *J. Am. Chem. Soc.* **2016**, *138*, 7436-7441.



Scheme 4.16. Visible light photocatalyzed synthesis of benzo[*b*]phosphole oxides

In this work, Lakhdar *et al.* have developed a new metal-free strategy for the formation of benzo[*b*]phosphole oxides under mild conditions combining eosin Y as photocatalyst and *N*-pyridinium oxide as oxidant through formation of a charge transfer complex able to be reduced by irradiation with green LEDs, as shown in Scheme 4.17.



Scheme 4.17. The charge transfer complex [EY-Pyr] can be reduced under light irradiation

On the basis of this work, we wondered if the visible light photocatalyzed annulation reaction leading to phosphorylated 2-oxindoles could proceed at room temperature under mild conditions in the absence of transition metals. With this aim in mind, we decided to develop an innovative methodology employing aryl-secondary phosphine oxides (SPOs) and *N*-arylacrylamides in order to get visible light promoted phosphorylated oxindoles.

4.3. Results and discussion

We investigated the reactivity of diphenylphosphine oxide **46a** (2 equiv.) with acrylamide **61** in the presence of an organic photocatalyst (4 mol%), oxidant **83** or **73** (2 equiv) and a base (1.2 equiv), conditions similar to those previously established.^[8a] As shown in Table 1, when Eosin (**EY**) was employed in combination with the pyridinium salt **83**, the oxindole **61a** has been formed in good conversion (84%) as attested by ³¹P NMR spectroscopy (entry 1). As expected, the reaction proceeded with other organic dyes such as Rhodamine B (**RhB**) (entry 2) or Fluorescein (**Flr**) (entry 3) albeit with modest conversions (42% and 35%), respectively. Substituting the standard base (NaHCO₃) by NaOAc resulted in a drop of conversion to 62% (entry 4). Solvent optimization studies revealed that the reaction works well in DMF and DMSO, yielding the desired product **62a** in good conversions (entry 5, 87% and entry 6, 79%), respectively. However, because these results are comparable to that obtained with acetonitrile (entry 1), the latter has been selected as the solvent of choice.

Interestingly, when diphenyliodonium triflate **73** has been tested as an oxidant instead of **83**, moderate conversion has been observed (Entry 7, 46%). Employing two equivalents of **61a** with respect to diphenylphosphine oxide **46a** (1 equiv.) gave **62a** in about 10% lower conversion (entry 8, 72%) than that obtained under standard conditions (entry 1). The base has been found to be crucial for the reaction as only 24% has been obtained in its absence (entry 9). Control experiments revealed that no reaction occurred in the absence of photocatalyst (entry 10), light (entry 11) and oxidant (entry 12).

Table 4.1. Identification of the optimal reaction conditions

entry	photocatalyst	oxidant	solvent	³¹ P-NMR (%) ^a
1	EY	83	MeCN	84
2	RhB	83	MeCN	42

3	Flr	83	MeCN	35
4	EY ^b	83	MeCN	62
5	EY	83	DMF	87
6	EY	83	DMSO	79
7	EY	73	MeCN	46
8	EY ^c	83	MeCN	72
9	EY ^d	83	MeCN	24
10	-	83	MeCN	3
11	EY ^e	83	MeCN	0
12	EY ^f	-	MeCN	0

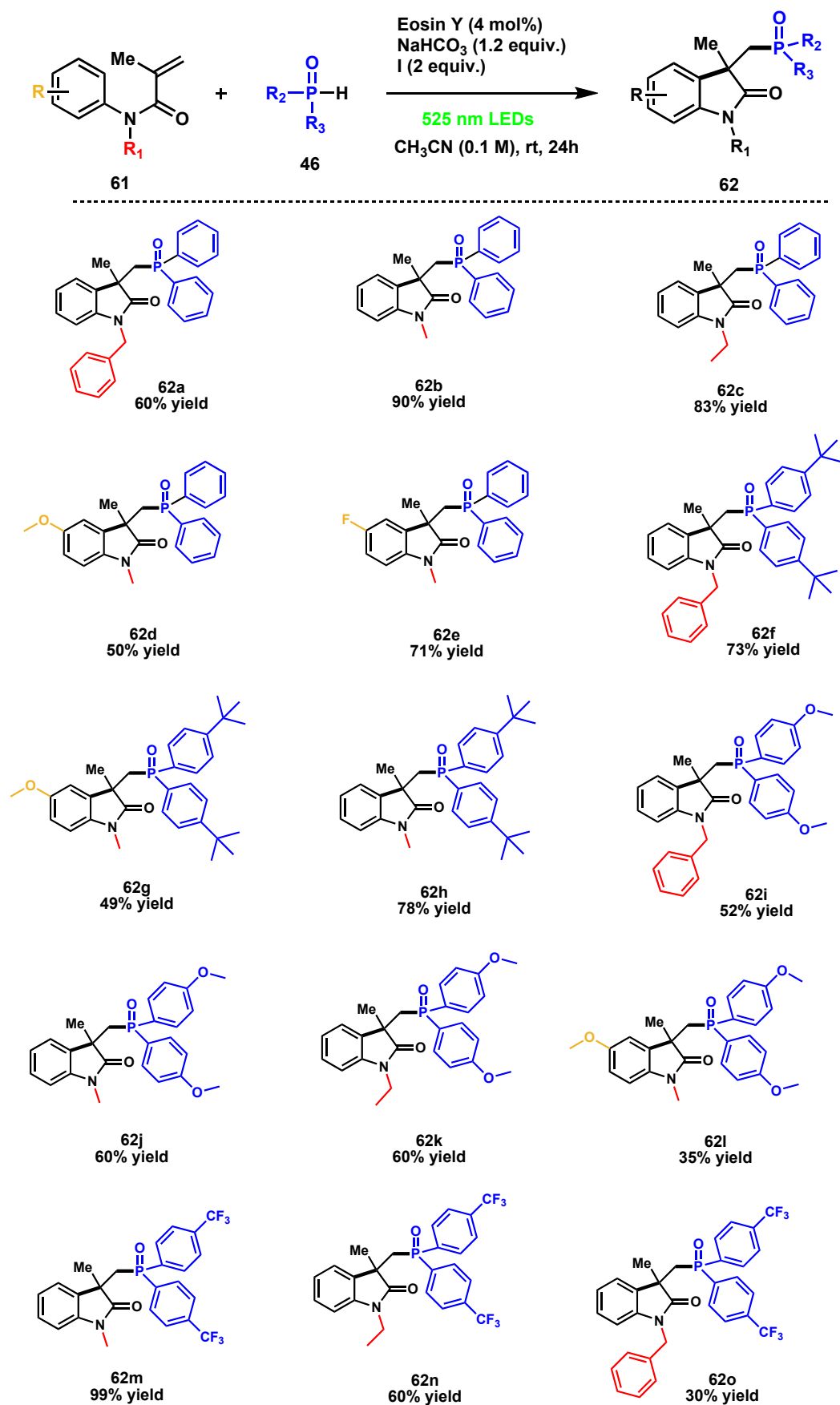
[a] ³¹P NMR spectroscopy using trioctylphosphine oxide as internal standard. [b] NaOac used as a base. [c]. Conditions used: oxidant (1.2 equiv.), **1a** (2 equiv.), and **2a** (1 equiv.) [d] No base used. [e] No light. [f] No oxidant.

With these optimized conditions in hand, we next examined the scope of the reaction. In this regard, we reacted diphenylphosphine oxide **46a** with different *N*-arylacrylamide **3**. As shown in Table 4.2, the reaction proceeds well with acrylamides bearing alkyl groups at the nitrogen, affording the desired oxindoles **62a–c** in good to excellent yields (60–90%). Interestingly, substrates with electron-donating (**61d**) and -withdrawing (**61e**) substituents at the para position of the arylacrylamides reacted also well, yielding **62d,e** in 50 and 70% yields.

Because the scope of the photoredox catalyzed reaction reported by Yu, Lan *et al.* has been studied with only diphenylphosphine oxide, we decided to test the reactivity of other secondary phosphine oxides under our conditions.

As shown in Table 4.2, the diarylphosphine oxide bearing a *tert*-butyl group at the para position **46b** reacts well with the acrylamides **61a** and **61d**, leading to **62f,g** in 73 and 49% yields, respectively. Similarly, *p*-methoxy diarylphosphine oxide **46c** reacts smoothly with arylamides **61**, furnishing **62i–k** in yields ranging from 52 to 60%. Although the heterocycle **62l** has been obtained with good conversion, its isolation turned out to be problematic and only 35% of the final products has been covered after column chromatography. Finally, we have tested the reactivity of the electron withdrawing phosphine oxide **46d** with three arylamides. While the resulting oxindoles **62m,n** have been isolated in excellent (**62m**, 99%) and good (**62n**, 60%) yields, the oxindole **62o** has been obtained in modest 30% yield.

Table 4.2. Scope and limitations of the photocatalyzed annulation reaction of *N*-arylacrylamides with secondary phosphine oxides^a



^aReaction conditions: secondary phosphine oxide **46** (2.0 mmol), *N*-arylacrylamide **61** (1.0 mmol), *N*-ethoxy-methyl pyridinium tetrafluoroborate **83** (2.0 mmol), NaHCO₃ (1.2 mmol), eosin Y (0.04 mmol) in CH₃CN (0.1 M) under green light irradiation.

4.3.1. Mechanistic studies

To get evidences on mechanistic aspects of the photoinduced annulation reaction, EPR studies were carried out.

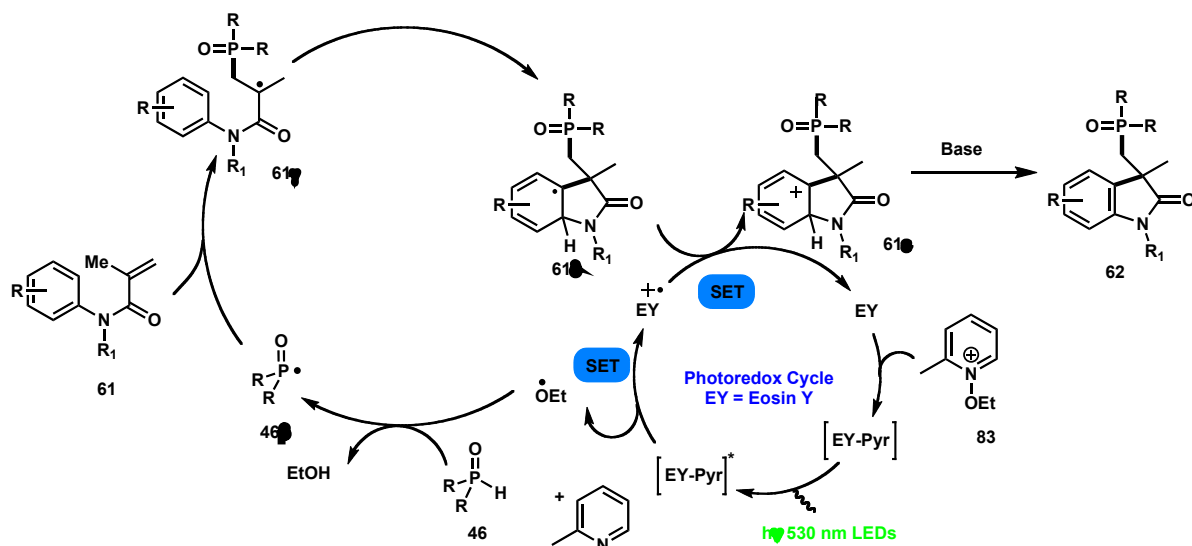
Based on our previous mechanistic studies on EY-photocatalyzed synthesis of benzophospholes,¹⁹³ it has been possible to identify important radical intermediates of our reaction *via* electron paramagnetic resonance (EPR) and to postulate that the current photoreaction proceeds through the same mechanism (Scheme 4.20). Particularly, the reaction of eosin Y with and *N*-methyl-pyridinium oxide **83** in the presence of α -phenyl-*N*-*tert*-butylnitron (PBN) **I** as radical-trap in *tert*-butylbenzene under green irradiation ($\lambda = 530$ nm) allowed determining the formation of ethoxy radical trapped by PBN.

Hyperfine coupling constants ($a_N = 13.6$ G; $a_H = 1.9$ G) are in agreement with literature data.¹⁹⁴

Then, the addition of diphenylphosphine oxide **46a** to this mixture revealed the formation of phosphinoyl radical along remaining ethoxy radical. This result validated our starting hypothesis involving phosphinoyl radical. Furthermore, hyperfine coupling constants ($a_N = 14.18$ G; $a_H = 3.03$ G; $a_P = 18.76$ G) are congruent with those reported in literature.¹⁹⁵

¹⁹⁴ Jenkins, C.A.; Murphy, D.M.; Rowlands, C.C.; Egerton, T.A. *J. Chem. Soc., Perkin Trans. 2* **1997**, 2479-2485.

¹⁹⁵ (a) Morlet-Savary, F.; Klee, J.E.; Pfefferkon, F.; Fouassier, J.P.; Lalevée, J. *Macromol. Chem. Phys.* **2015**, *216*, 2161-2170. (b) Lalevée, J.; Morlet-Savary, F.; Tehfe, M.A.; Graff, B.; Fouassier, J.P. *Macromolecules* **2012**, *45*, 5032-5039.



Scheme 4.18. Proposed mechanism for the photocatalyzed annulation reaction of *N*-arylacrylamides with secondary phosphine oxides

The association of **EY** with the pyridinium salt **83** forms a ground state electron–donor acceptor complex [**EY-Pyr**]. The later undergoes a single electron transfer upon absorption of a green photon to generate the ethoxy radical. This oxygen radical abstracts a hydrogen atom from the secondary phosphine oxide **46** to form the phosphinoyl radical **46β**, which adds at the amide C=C bond to generate the carbon centered radical **61γ**. A subsequent radical cyclization occurs, giving rise to the hexadienyl radical **61δ**, which oxidizes by the radical cation form **EY⁺** to give the arenium cation **61ε** that yields the final adduct **62** after a fast deprotonation with the base.

4.4 Conclusions

In conclusion, we have developed a metal-free, visible light-mediated cascade phosphorylation and cyclization reaction. The reaction combines easily accessible starting materials (secondary phosphine oxides **46** and acrylamides **61**) and requires the use of organic additives under mild conditions. This reaction has a relatively large scope and proceeds with high yields.

Although this procedure has been applied for the generation of phosphorus radicals, one can use this approach for the generation of other radicals derived from precursors possessing low to mild (X-H) bond dissociation energies. Exploration of this chemistry is ongoing on the CALIPSO group.

4.5 Material and methods

4.5.1 General

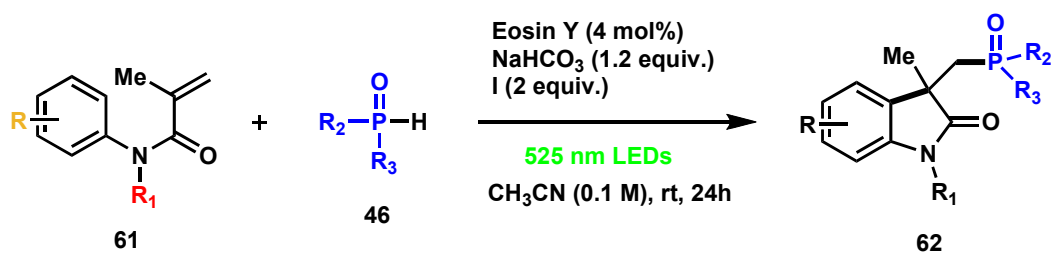
¹H NMR spectra were recorded on a BRUKER AVANCE III 400 MHz spectrometer, the chemical shifts are reported in parts per million (ppm) referenced to residual chloroform (7.26 ppm). Coupling constants are reported in Hertz (Hz). The following abbreviations were used to express the multiplicities: s (singlet), d (doublet), t (triplet), q (quartet), m (multiplet), bs (broad singlet). ¹³C NMR spectra were recorded on the same instrument at 100 MHz, the chemical shifts are expressed in parts per million (ppm), reported from the central chloroform peak (77.2 ppm). ³¹P NMR spectra were recorded on the same instrument at 162 MHz (decoupled ³¹P NMR). High Resolution Mass Spectrometry (HRMS) was performed on a Varian MAT 311 spectrometer or a QTOF Micro WATERS spectrometer.

All reactions were air or water sensitive and set up under an argon atmosphere in dried glassware using Schlenk techniques with dry solvents. Chromatographic purification of products was accomplished using flash chromatography (FC) on silica gel (35-70 mesh). For Thin Layer Chromatography (TLC) analysis throughout this work, Merck precoated TLC plates (silica gel 60 F₂₅₄) were employed. Visualization was performed with UV light and by immersion in anisaldehyde stain (by volume: 93% ethanol, 3.5% sulfuric acid, 1% acetic acid, 2.5% *p*-anisaldehyde) or basic aqueous potassium permanganate solution (KMnO₄) stain followed by heating as developing tool. Organic solutions of products were dried over anhydrous MgSO₄ and concentrated under reduced pressure on a Büchi rotatory evaporator. *N*-arylacrilamides were synthesized according to the literature¹⁹⁶. Acetonitrile was dispensed by PURESOLVTM developed by Innovative Technology Inc. and used without further purification.

¹⁹⁶ (a) Pinto, A.; Jia, Y.; Neuville, L.; Zhu, J. *Chem. Eur. J.* **2007**, *13*, 961-967. (b) Wei, H.; Piou, T.; Dufour, J.; Neuville, L.; Zhu, J. *Org. Lett.* **2011**, *13*, 2244-2247. (c) Mu, X.; Wu, T.; Wang, H.; Guo, Y.; Liu, G. *J. Am. Chem. Soc.* **2012**, *134*, 878-881. (d) C.-W. Chan; P.-Y. Lee; W.-Y. Yu *Tetrahedron Lett.* **2015**, *56*, 2559-2563.

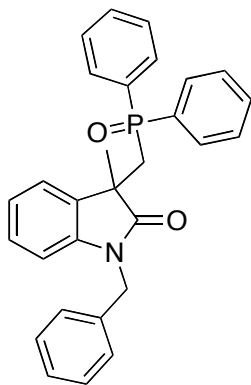
4.6 Annulation Reaction to form Phosphorylated Oxindoles

4.6.1 General Procedure



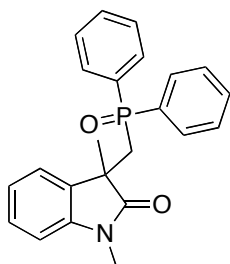
In a oven-dried Schlenk tube, eosin Y (0.01 mmol, 0.04 eq.), sodium hydrogen carbonate (0.3 mmol, 1.2 eq.), *N*-ethoxy-2-methylpyridinium tetrafluoroborate **83** (0.5 mmol, 2 eq.), and secondary phosphine oxide **46** (0.5 mmol, 2 eq.), were mixed. To this solid mixture, *N*-arylacrylamide **61** (1 equiv.) either as solid or viscous oil was finally added and the mixture was dissolved in dry CH₃CN (0.1 M). The clear solution was surrounded by 5W green LEDs and stirred from 24 to 48 hours. Then, the solvent was removed by concentration under reduced pressure on rotavapor to give oil as crude product. The latter was purified by flash column chromatography using ethyl acetate: *n*-pentane, ethyl acetate:acetone or ethyl acetate:dichloromethane to afford the desired product.

1-benzyl-3-((diphenylphosphoryl)methyl)-3-methylindolin-2-one, (62a)



Conditions: (*N*-benzyl-*N*-phenylmethacrylamide: 62 mg, 0.25 mmol, 1 equiv.); (*N*-ethoxy-2-methylpyridinium tetrafluoroborate: 112 mg, 0.5 mmol, 2 equiv.); (diphenylphosphine oxide: 100 mg, 0.5 mmol, 2 equiv.); (eosin Y: 6.5 mg, 0.01 mmol, 0.04 equiv.); (sodium hydrogen carbonate: 25 mg, 0.3 mmol, 1.2 equiv.). The reaction was carried out following the general procedure. The crude product was purified by flash column chromatography (*n*-pentane:EtOAc 30:70). **Yield:** 67 mg, 60%. **¹H-NMR** (400 MHz, CDCl₃) δ (ppm) 7.61-7.51 (m, 5H, Ar-H), 7.43-7.40 (m, 2H, Ar-H), 7.35-7.33 (m, 4H, Ar-H), 7.26-7.24 (m, 4H, Ar-H), 7.17-7.16 (m, 1H, Ar-H), 7.02-6.99 (m, 1H, Ar-H), 6.72-6.69 (m, 1H, Ar-H), 6.54-6.53 (m, 1H, Ar-H), 5.03 (d, ²*J* = 16.0 Hz, 1H), 4.39 (d, ²*J* = 16.0 Hz, 1H), 3.07 (dd, ²*J* = 11.0 Hz, ²*J* = 15.0 Hz, 1H), 2.91 (dd, ²*J* = 9.6 Hz, ²*J* = 15.0 Hz, 1H), 1.47 (s, 3H). **¹³C-NMR** (100 MHz, CDCl₃) δ (ppm) 179.8 (d, *J* = 4.2 Hz), 142.2 (s), 136.6 (s), 133.8 (d, *J* = 98.4 Hz), 133.4 (d, *J* = 98.2 Hz), 131.7 (s), 131.6 (d, ⁴*J* = 2.9 Hz), 131.4 (d, ⁴*J* = 2.9 Hz), 130.9 (d, ³*J* = 9.5 Hz), 130.7 (d, ³*J* = 9.5 Hz), 128.8 (s), 128.6 (d, ²*J* = 11.9 Hz), 128.4 (d, ²*J* = 11.9 Hz), 127.9 (s), 127.5 (s), 127.3 (s), 125.0 (s), 122.3 (s), 109.0 (s), 45.7 (d, *J* = 3.8 Hz), 44.1 (s), 37.5 (d, ¹*J* = 71.5 Hz), 27.1 (d, ³*J* = 11.6 Hz). **³¹P-NMR** (162 MHz, CDCl₃) δ (ppm) 26.2 (s). **HRMS:** calcd for C₂₉H₂₇NO₂P [M+H]⁺ 452.1778, found 452.1779.

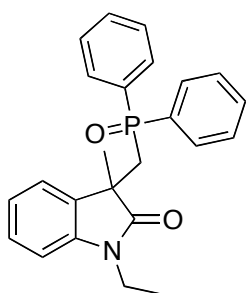
3-((diphenylphosphoryl)methyl)-1,3-dimethylindolin-2-one, (62b)



Conditions: (*N*-methyl-*N*-phenylmethacrylamide: 43 mg, 0.25 mmol, 1 equiv.); (*N*-ethoxy-2-methylpyridinium tetrafluoroborate: 112 mg, 0.5 mmol, 2 equiv.); (diphenylphosphine oxide: 100 mg, 0.5 mmol, 2 equiv.); (eosin Y: 6.5 mg, 0.01 mmol, 0.04 equiv.); (sodium hydrogen carbonate: 25 mg, 0.3 mmol, 1.2 equiv.). The reaction was carried out following the general procedure. The crude product was purified by flash column chromatography (*n*-pentane:EtOAc 30:70). **Yield:** 85 mg, 90%. **M_p** = 94-96° C. **¹H-NMR** (400 MHz, CDCl₃) δ (ppm) 7.69-7.64 (m, 2H, Ar-H), 7.60-7.56 (m, 3H, Ar-H), 7.50-7.41 (m, 5H, Ar-H), 7.26-7.24 (m, 2H, Ar-H), 6.90-6.86 (m, 1H, Ar-H), 6.78-6.76 (m, 1H, Ar-H), 3.11-3.05 (m, 1H), 3.00 (s,

3H), 2.88-2.82 (m, 1H), 1.42 (s, 3H). $^{13}\text{C-NMR}$ (100 MHz, CDCl_3) δ (ppm) 179.6 (d, $^3J = 4.1$ Hz), 143.1 (s), 134.0 (d, $^1J = 93.9$ Hz), 133.0 (d, $^1J = 93.9$ Hz), 132.1 (s), 130.9 (d, $^2J = 9.5$ Hz), 130.6 (d, $^2J = 9.5$ Hz), 128.5 (d, $^3J = 11.7$ Hz), 128.3 (d, $^3J = 11.7$ Hz), 128.0 (s), 124.9 (s), 122.3 (s), 108.0 (s), 46.5 (d, $^3J = 3.8$ Hz), 44.1 (s) 37.6 (d, $^1J = 71.3$ Hz), 27.0 (d, $^2J = 11.2$ Hz). $^{31}\text{P-NMR}$ (162 MHz, CDCl_3) δ (ppm) 25.8 (s). **HRMS:** calcd for $\text{C}_{23}\text{H}_{23}\text{NO}_2\text{P}$ $[\text{M}+\text{H}]^+$ 376.1469, found 376.1466.

3-((diphenylphosphoryl)methyl)-1-ethyl-3-methylindolin-2-one, (62c)

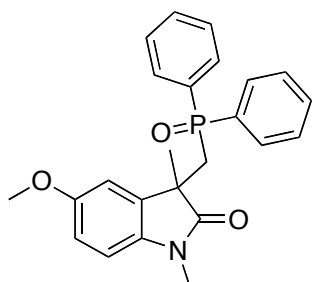


Conditions: (*N*-ethyl-*N*-phenylmethacrylamide: 47 mg, 0.25 mmol, 1 equiv.); (*N*-ethoxy-2-methylpyridinium tetrafluoroborate: 112 mg, 0.5 mmol, 2 equiv.); (diphenylphosphine oxide: 100 mg, 0.5 mmol, 2 equiv.); (eosin Y: 6.5 mg, 0.01 mmol, 0.04 equiv.); (sodium hydrogen carbonate: 25 mg, 0.3 mmol, 1.2 equiv.). The reaction was carried out following the general procedure. The

crude product was purified by flash column chromatography (*n*-pentane:EtOAc 30:70).

Yield: 80 mg, 83%. $^1\text{H-NMR}$ (400 MHz, CDCl_3) δ (ppm) 7.58-7.49 (m, 4H, Ar-H), 7.41-7.31 (m, 6H, Ar-H), 7.17-7.11 (m, 2H, Ar-H), 6.76-6.70 (m, 2H, Ar-H), 3.70-3.62 (m, 1H), 3.51-3.42 (m, 1H), 3.05-2.99 (m, 1H), 2.89-2.82 (m, 1H), 1.40 (s, 3H), 1.21 (t, $^3J = 7.6$ Hz, 3H). $^{13}\text{C-NMR}$ (100 MHz, CDCl_3) δ (ppm) 179.2 (d, $^3J = 5.3$ Hz), 142.1 (s), 133.8 (d, $^1J = 98.5$ Hz), 133.4 (d, $^1J = 98.7$ Hz), 131.9 (s), 131.5 (d, $^4J = 2.9$ Hz), 131.4 (d, $^4J = 2.9$ Hz), 130.8 (d, $^2J = 9.4$ Hz), 130.7 (d, $^2J = 9.4$ Hz), 128.5 (d, $^3J = 11.8$ Hz), 128.4 (d, $^3J = 11.8$ Hz), 127.9 (s), 125.2 (s), 122.1 (s), 108.1 (s), 45.6 (d, $J = 3.8$ Hz), 37.4 (d, $^1J = 71.5$ Hz), 34.9 (s), 26.9 (d, $^3J = 11.4$ Hz), 12.6 (s). $^{31}\text{P-NMR}$ (162 MHz, CDCl_3) δ (ppm) 26.1 (s). **HRMS:** calcd for $\text{C}_{24}\text{H}_{25}\text{NO}_2\text{P}$ $[\text{M}+\text{H}]^+$ 390.1625, found 390.1623.

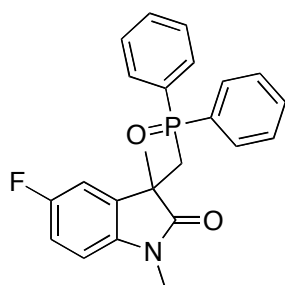
3-((diphenylphosphoryl)methyl)-5-methoxy-1,3-dimethylindolin-2-one, (62d)



Conditions: (*N*-methyl-*N*-*p*-methoxyphenylmethacrylamide: 51 mg, 0.25 mmol, 1 equiv.); (*N*-ethoxy-2-methylpyridinium tetrafluoroborate: 112 mg, 0.5 mmol, 2 equiv.), (diphenylphosphine oxide: 100 mg, 0.5 mmol, 2 equiv.),

(eosin Y: 6.5 mg, 0.01 mmol, 0.04 equiv.), (sodium hydrogen carbonate: 25 mg, 0.3 mmol, 1.2 equiv.). The reaction was carried out following the general procedure. The crude product was purified by flash column chromatography (*n*-pentane:EtOAc 10:90). **Yield:** 50 mg, 50%. **¹H-NMR** (400 MHz, CDCl₃) δ (ppm) 7.55-7.48 (m, 4H, Ar-H), 7.43-7.38 (m, 2H, Ar-H), 7.36-7.30 (m, 4H, Ar-H), 6.74-6.73 (m, 1H, Ar-H), 6.70-6.67 (m, 1H, Ar-H), 6.59-6.57 (m, 1H, Ar-H), 3.62 (s, 3H), 3.10-3.04 (m, 1H), 3.03 (s, 3H), 2.85-2.78 (m, 1H), 1.41 (s, 3H). **¹³C-NMR** (100 MHz, CDCl₃) δ (ppm) 179.3 (d, *J* = 3.8 Hz), 155.6 (s), 136.7 (s), 133.8 (d, ¹*J* = 98.6 Hz), 133.3 (d, ¹*J* = 98.4 Hz), 132.7 (s), 131.6 (d, ⁴*J* = 2.8 Hz), 131.3 (d, ⁴*J* = 2.8 Hz), 130.8 (d, ²*J* = 9.7 Hz), 130.7 (d, ²*J* = 9.7 Hz), 128.5 (d, ³*J* = 7.0 Hz), 128.4 (d, ³*J* = 7.0 Hz), 113.3 (s), 111.6 (s), 108.4 (s), 55.7 (s), 46.1 (d, ²*J* = 4.2 Hz), 37.6 (d, ¹*J* = 71.8 Hz), 26.9 (d, ³*J* = 12.0 Hz), 26.6 (s). **³¹P-NMR** (162 MHz, CDCl₃) δ (ppm) 26.1 (s). **HRMS:** calcd for C₂₄H₂₅NO₃P [M+H]⁺ 406.1572, found 406.1570.

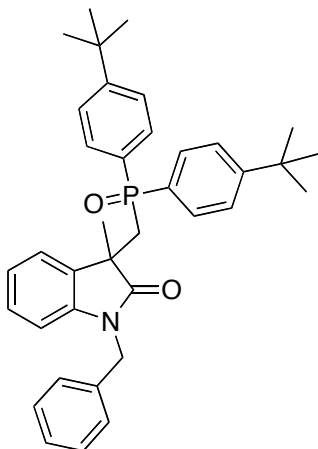
3-((diphenylphosphoryl)methyl)-5-fluoro-1,3-dimethylindolin-2-one, (62e)



Conditions: (*N*-methyl-*N*-*p*-fluorophenylmethacrylamide: 48 mg, 0.25 mmol, 1 equiv.); (*N*-ethoxy-2-methylpyridinium tetrafluoroborate: 112 mg, 0.5 mmol, 2 equiv.); (diphenylphosphine oxide: 100 mg, 0.5 mmol, 2 equiv.); (eosin Y: 6.5 mg, 0.01 mmol, 0.04 equiv.); (sodium hydrogen carbonate: 25 mg, 0.3 mmol, 1.2 equiv.). The reaction was

carried out following the general procedure. The crude product was purified by flash column chromatography (*n*-pentane:EtOAc 10:90). **Yield:** 69 mg, 71%. **M_p** = 86-88°C. **¹H-NMR:** (400 MHz, CDCl₃) δ (ppm) 7.57-7.51 (m, 4H, Ar-H), 7.45-7.41 (m, 2H, Ar-H), 7.36 (m, 4H, Ar-H), 6.87-6.79 (m, 2H, Ar-H), 6.62-6.59 (m, 1H, Ar-H), 3.10-3.07 (m, 1H), 3.05 (s, 3H), 2.85-2.79 (m, 1H), 1.41 (s, 3H). **¹³C-NMR:** (100 MHz, CDCl₃) δ (ppm) 182.1 (s), 159.9 (s), 141.3 (s), 134.1 (s), 133.6 (s), 132.5 (s), 130.7 (d, ²*J* = 12.1 Hz), 130.4 (d, ²*J* = 12.1 Hz), 116.3 (d, ¹*J* = 24.3 Hz), 114.2 (d, ¹*J* = 24.3 Hz), 111.0 (s), 47.8 (s), 38.6 (d, ¹*J* = 72.0 Hz), 28.0 (d, ²*J* = 13.3 Hz), 15.3 (s). **³¹P{¹H}-NMR:** (162 MHz, CDCl₃) δ (ppm) 26.0 (s). **¹⁹F{¹H}-NMR:** (376.5 MHz, CDCl₃) δ (ppm) -122.8, -155.0. **HRMS:** calcd for C₂₃H₂₂FN₂O₂P [M+H]⁺ 394.1374, found 394.1372.

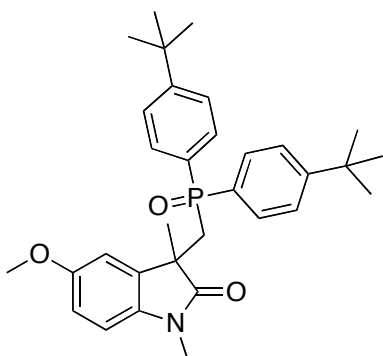
1-benzyl-3-((bis(4-*tert*-butylphenyl)phosphoryl)methyl)-3-methylindolin-2-one, (62f)



Conditions: (*N*-benzyl-*N*-phenylmethacrylamide: 40 mg, 0.16 mmol, 1 equiv.); (*N*-ethoxy-2-methylpyridinium tetrafluoroborate: 72 mg, 0.32 mmol, 2 equiv.), (bis-(4-*tert*butyl)diphenylphosphine oxide: 100 mg, 0.32 mmol, 2 equiv.), (eosin Y: 4 mg, 0.006 mmol, 0.04 equiv.), (sodium hydrogen carbonate: 16 mg, 0.18 mmol, 1.2 equiv.). The reaction was carried out following the general procedure.

The crude product was purified by flash column chromatography (*n*-pentane:EtOAc 10:90). **Yield:** 65 mg, 73%. **¹H-NMR:** (400 MHz, CDCl₃) δ (ppm) 7.63-7.52 (m, 3H, Ar-H), 7.49-7.44 (m, 3H, Ar-H), 7.37-7.35 (m, 4H, Ar-H), 7.30-7.29 (m, 2H, Ar-H), 7.23-7.19 (m, 2H, Ar-H), 7.02-6.98 (m, 1H, Ar-H), 6.73-6.70 (m, 1H, Ar-H), 5.00 (d, ²*J* = 15.8 Hz, 1H), 4.33 (d, ²*J* = 15.8 Hz, 1H), 3.08-2.85 (m, 2H), 1.47 (s, 3H), 1.30 (s, 18H). **¹³C-NMR:** (100 MHz, CDCl₃) δ (ppm) 179.9 (s), 154.8 (d, ⁴*J* = 2.7 Hz), 154.7 (d, ⁴*J* = 2.7 Hz), 142.1 (s), 136.3 (s), 130.8 (d, ²*J* = 9.3 Hz), 130.6 (d, ²*J* = 9.3 Hz), 128.8 (s), 127.8 (s), 127.5 (s), 127.2 (s), 125.6 (d, ³*J* = 12.0 Hz), 125.4 (d, ³*J* = 12.0 Hz), 122.3 (s), 108.9 (s), 45.8 (d, ²*J* = 3.7 Hz), 44.0 (s), 37.9 (d, ¹*J* = 72.3 Hz), 35.0 (s), 31.2 (s), 27.1 (d, ³*J* = 11.8 Hz). **³¹P{¹H}-NMR:** (162 MHz, CDCl₃) δ (ppm) 26.1 (s). **HRMS:** calcd for C₃₇H₄₃NO₂P[M+H]⁺ 564.3031, found 564.3029.

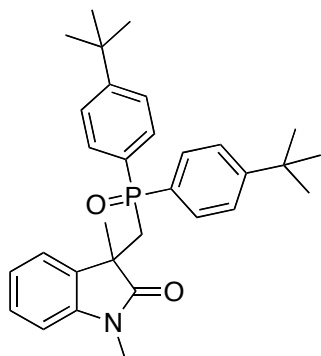
3-((bis(4-*tert*-butylphenyl)phosphoryl)methyl)-5-methoxy-1,3-dimethylindolin-2-one, (62g)



Conditions: (*N*-methyl-*N*-*p*-methoxyphenylmethacrylamide: 33 mg, 0.16 mmol, 1 equiv.); (*N*-ethoxy-2-methylpyridinium tetrafluoroborate: 72 mg, 0.32 mmol, 2 equiv.), (bis-(4-*tert*butyl)diphenylphosphine oxide: 100 mg, 0.32 mmol, 2 equiv.), (eosin Y: 4.1 mg, 0.006 mmol, 0.04 equiv.), (sodium hydrogen carbonate: 16 mg, 0.19 mmol, 1.2

equiv.). The reaction was carried out following the general procedure. The crude product was purified by flash column chromatography (*n*-pentane:EtOAc 10:90). **Yield:** 40 mg, 49%. **¹H-NMR** (400 MHz, CDCl₃) δ (ppm) 7.53-7.48 (m, 2H, Ar-H), 7.45-7.40 (m, 2H, Ar-H), 7.36-7.30 (m, 4H, Ar-H), 6.86-6.85 (m, 1H, Ar-H), 6.69-6.67 (m, 1H, Ar-H), 6.55-6.53 (m, 1H, Ar-H), 3.65 (s, 3H), 3.00 (m, 4H), 2.83-2.77 (m, 1H), 1.41 (s, 3H), 1.29 (s, 9H), 1.27 (s, 9H). **¹³C-NMR** (100 MHz, CDCl₃) δ (ppm) 179.6 (s), 155.7 (s), 154.7 (s), 136.6 (s), 132.6 (d, *J* = 97.4 Hz), 132.5 (d, *J* = 97.6 Hz), 130.7 (d, ²*J* = 9.6 Hz), 130.6 (d, ²*J* = 9.6 Hz), 125.9 (s), 125.8 (s), 125.5 (d, ³*J* = 12.1 Hz), 125.3 (d, ³*J* = 12.1 Hz), 113.4 (s), 111.7 (s), 108.3 (s), 55.8 (s), 46.2 (d, ²*J* = 3.8 Hz), 37.9 (d, ¹*J* = 71.4 Hz), 35.0 (s), 31.2 (s), 26.9 (d, ³*J* = 11.7 Hz), 26.6 (s). **³¹P-NMR** (162 MHz, CDCl₃) δ (ppm) 26.9 (s). **HRMS:** calcd for C₃₂H₄₁NO₃P [M+H]⁺ 518.2824, found 518.2822.

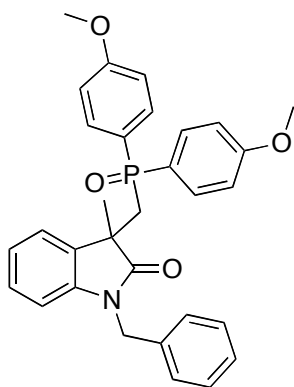
3-((bis(4-*tert*-butylphenyl)phosphoryl)methyl)-1,3-dimethylindolin-2-one, (62h)



Conditions: (*N*-methyl-*N*-phenylmethacrylamide: 28 mg, 0.16 mmol, 1 equiv.); (*N*-ethoxy-2-methylpyridinium tetrafluoroborate: 72 mg, 0.32 mmol, 2 equiv.), (bis-(4-*tert*butyl)diphenylphosphine oxide: 100 mg, 0.32 mmol, 2 equiv.), (eosin Y: 4 mg, 0.006 mmol, 0.04 equiv.), (sodium hydrogen carbonate: 16 mg, 0.18 mmol, 1.2 equiv.). The reaction was carried out following the general procedure.

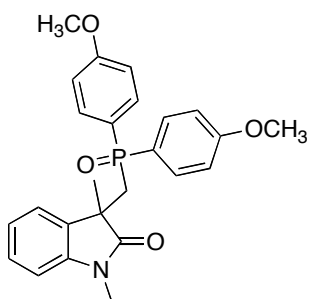
The crude product was purified by flash column chromatography (*n*-pentane:EtOAc 30:70). **Yield:** 60 mg, 78%. **¹H-NMR:** (400 MHz, CDCl₃) δ (ppm) 7.52-7.47 (m, 2H, Ar-H), 7.43-7.38 (m, 2H, Ar-H), 7.35-7.30 (m, 4H, Ar-H), 7.17-7.11 (m, 2H, Ar-H), 6.78-6.74 (m, 1H, Ar-H), 6.62-6.60 (m, 1H, Ar-H), 3.08-3.02 (m, 1H), 2.98 (s, 3H), 2.85-2.78 (m, 1H), 1.41 (s, 3H), 1.29 (s, 9H), 1.26 (s, 9H). **¹³C-NMR:** (100 MHz, CDCl₃) δ (ppm) 179.8 (s), 154.7 (s), 142.9 (s), 130.8 (d, ²*J* = 10.1 Hz), 130.6 (d, ²*J* = 10.1 Hz), 127.9 (s), 127.5 (s), 127.2 (s), 125.5 (d, ³*J* = 12.0 Hz), 125.3 (d, ³*J* = 12.0 Hz), 125.0 (s), 122.3 (s), 107.8 (s), 45.6 (s), 44.0 (s), 38.0 (d, ¹*J* = 71.6 Hz), 35.0 (s), 31.2 (s), 31.2 (s), 27.1 (d, ³*J* = 12.0 Hz), 26.4 (s). **³¹P{¹H}-NMR:** (162 MHz, CDCl₃) δ (ppm) 26.2 (s).

1-benzyl-3-((bis(4-methoxyphenyl)phosphoryl)methyl)-3-methylindolin-2-one, (62i)



Conditions: (*N*-benzyl-*N*-phenylmethacrylamide: 48 mg, 0.19 mmol, 1 equiv.); (*N*-ethoxy-2-methylpyridinium tetrafluoroborate: 86 mg, 0.38 mmol, 2 equiv.); (bis-(4-methoxy)diphenylphosphine oxide: 100 mg, 0.38 mmol, 2 equiv.); (eosin Y: 5 mg, 0.008 mmol, 0.04 equiv.); (sodium hydrogen carbonate: 19 mg, 0.23 mmol, 1.2 equiv.). The reaction was carried out following the general procedure. The crude product was purified by flash column chromatography (*n*-pentane:EtOAc 10:90). **Yield:** 50 mg, 52%. **M_p** = 245°C. **¹H-NMR:** (400 MHz, CDCl₃) δ (ppm) 7.59-7.55 (m, ArH, 2H), 7.39-7.26 (m, ArH, 7H), 7.03-7.00 (m, ArH, 3H), 6.88-6.84 (m, ArH, 3H), 6.69-6.68 (m, ArH, 1H), 6.62-6.59 (m, ArH, 1H), 5.09 (d, ²*J* = 16 Hz, 1H), 4.70 (d, ²*J* = 16 Hz, 1H), 3.86 (s, 3H), 3.82 (s, 3H), 3.16 (d, ²*J* = 10 Hz, 2H), 1.48 (s, 3H). **¹³C-NMR:** (100 MHz, CDCl₃) δ (ppm) 182.6 (s), 164.9 (d, ⁴*J*_{CP} = 3 Hz), 164.6 (d, ⁴*J*_{CP} = 3 Hz), 144.0 (s), 138.4 (s), 134.5 (d, ³*J*_{CP} = 11 Hz), 129.9 (d, ¹*J*_{CP} = 188 Hz), 129.6 (d, ²*J*_{CP} = 39 Hz), 126.1 (s), 124.3 (s), 116.1 (s), 116.0 (s), 115.9 (s), 111.3 (s), 56.8 (s), 56.7 (s), 47.5 (s), 47.5 (s), 45.7 (s), 38.8 (d, ¹*J*_{CP} = 73 Hz), 29.2 (d, ³*J*_{CP} = 14 Hz). **³¹P{¹H}-NMR:** (162 MHz, CDCl₃) δ (ppm) 30.3 (s). **HRMS:** calcd for C₃₁H₃₁NO₄P [M+1]⁺ 512.1987, found 512.1991.

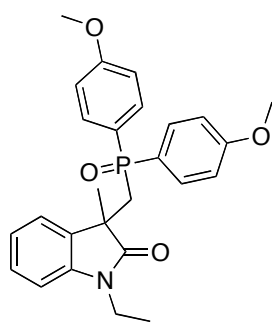
3-((bis(4-methoxyphenyl)phosphoryl)methyl)-1,3-dimethylindolin-2-one, (62j)



Conditions: (*N*-methyl-*N*-phenylmethacrylamide: 33 mg, 0.19 mmol, 1 equiv.); (*N*-ethoxy-2-methylpyridinium tetrafluoroborate: 86 mg, 0.38 mmol, 2 equiv.); (bis-(4-methoxy)diphenylphosphine oxide: 100 mg, 0.38 mmol, 2 equiv.); (eosin Y: 5 mg, 0.008 mmol, 0.04 equiv.); (sodium hydrogen carbonate: 19 mg, 0.23 mmol, 1.2 equiv.). The reaction was carried out following the general procedure. The crude product was purified by flash column chromatography (*n*-pentane:EtOAc 30:70). **Yield:** 50 mg, 60%. **¹H-NMR** (400 MHz, CDCl₃) δ (ppm) 7.51-7.46 (m, 2H, Ar-H), 7.36-7.31 (m, 2H,

Ar-H), 7.24-7.22 (m, 1H, Ar-H) 7.19-7.15 (m, 1H, Ar-H), 6.99-6.96 (m, 1H, Ar-H), 6.87-6.85 (m, 2H, Ar-H), 6.81-6.78 (m, 2H, Ar-H), 6.67-6.65 (m, 1H, Ar-H), 3.81 (s, 3H), 3.78 (s, 3H), 3.07-3.00 (m, 1H), 2.99 (s, 3H), 2.81-2.74 (m, 1H), 1.40 (s, 3H). $^{13}\text{C-NMR}$ (100 MHz, CDCl_3) δ (ppm) 178.6 (d, $J = 3.6$ Hz), 162.1 (s), 143.0 (s), 132.8 (d, $^3J = 11.4$ Hz), 132.5 (d, $^3J = 11.4$ Hz), 131.3 (d, $J = 97.6$ Hz), 130.7 (d, $J = 97.4$ Hz), 128.0 (s), 125.0 (s), 124.3 (d, $J = 2.8$ Hz), 123.9 (d, $J = 2.9$ Hz), 122.3 (s), 114.1 (d, $^2J = 13.0$ Hz), 113.8 (d, $^2J = 13.0$ Hz), 107.9 (s), 55.4 (s), 45.7 (s), 37.9 (d, $^1J = 71.9$ Hz), 27.2 (d, $^3J = 12.0$ Hz), 26.4 (s). $^{31}\text{P-NMR}$ (162 MHz, CDCl_3) δ (ppm) 26.2 (s). **HRMS:** calcd for $\text{C}_{25}\text{H}_{27}\text{NO}_4\text{P}$ $[\text{M}+\text{H}]^+$ 436.1676, found 436.1678.

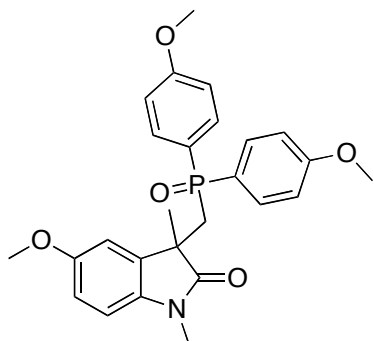
3-((bis(4-methoxyphenyl)phosphoryl)methyl)-1-ethyl-3-methylindolin-2-one, (62k)



Conditions: (*N*-ethyl-*N*-phenylmethacrylamide: 36 mg, 0.19 mmol, 1 equiv.); (*N*-ethoxy-2-methylpyridinium tetrafluoroborate: 86 mg, 0.38 mmol, 2 equiv.), (bis-(4-methoxy)diphenylphosphine oxide: 100 mg, 0.38 mmol, 2 equiv.); (eosin Y: 5 mg, 0.008 mmol, 0.04 equiv.); (sodium hydrogen carbonate: 19 mg, 0.23 mmol, 1.2 equiv.). The reaction was carried out following the general procedure. The

crude product was purified by flash column chromatography (*n*-pentane:EtOAc 30:70). **Yield:** 51 mg, 60%. $^1\text{H-NMR}$ (400 MHz, CDCl_3) δ (ppm) 7.51-7.46 (m, 2H, Ar-H), 7.41-7.36 (m, 2H, Ar-H), 7.24-7.22 (m, 1H, Ar-H), 7.17-7.13 (m, 1H, Ar-H), 6.86-6.79 (m, 4H, Ar-H), 6.71-6.69 (m, 1H, Ar-H), 3.81 (s, 3H), 3.78 (s, 3H), 3.69-3.62 (m, 1H), 3.47-3.42 (m, 1H), 2.99-2.93 (m, 1H), 2.81-2.73 (m, 1H), 1.39 (s, 3H), 1.20 (t, $^3J = 7.3$ Hz, 3H). $^{13}\text{C-NMR}$ (100 MHz, CDCl_3) δ (ppm) 179.3 (d, $^3J = 5.1$ Hz), 162.1 (d, $^4J = 2.9$ Hz), 162.0 (d, $^4J = 2.9$ Hz), 142.0 (s), 132.7 (d, $^3J = 10.9$ Hz), 132.5 (d, $^3J = 10.9$ Hz), 127.9 (s), 125.2 (s), 125.1 (d, $^1J = 106.5$ Hz), 124.8 (d, $^1J = 106.7$ Hz), 122.1 (s), 114.1 (d, $^2J = 12.7$ Hz), 113.9 (d, $^2J = 12.7$ Hz), 108.1 (s), 55.4 (s), 55.4 (s), 45.7 (d, $J = 3.8$ Hz), 37.6 (d, $^1J = 72.0$ Hz), 34.8 (s), 27.1 (d, $^3J = 12.3$ Hz), 12.6 (s). $^{31}\text{P-NMR}$ (162 MHz, CDCl_3) δ (ppm) 26.2 (s). **HRMS:** calcd for $\text{C}_{26}\text{H}_{29}\text{NO}_4\text{P}$ $[\text{M}+\text{H}]^+$ 450.1839, found 450.1834.

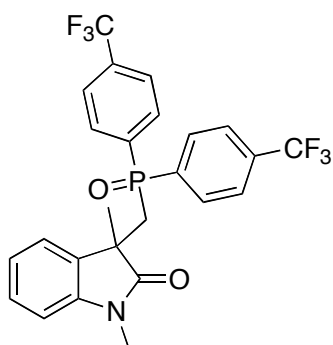
3-((bis(4-methoxyphenyl)phosphoryl)methyl)-5-methoxy-1,3-dimethylindolin-2-one, (62l)



Conditions: (*N*-methyl-*N*-*p*-methoxyphenylmethacrylamide: 39 mg, 0.19 mmol, 1 equiv.); (*N*-ethoxy-2-methylpyridinium tetrafluoroborate: 86 mg, 0.38 mmol, 2 equiv.), (bis-(4-methoxy)diphenylphosphine oxide: 100 mg, 0.38 mmol, 2 equiv.), (eosin Y: 5 mg, 0.008 mmol, 0.04 equiv.), (sodium hydrogen carbonate: 19 mg, 0.23 mmol, 1.2

equiv.). The reaction was carried out following the general procedure. The crude product was purified by flash column chromatography (*n*-pentane:EtOAc 10:90). **Yield:** 30 mg, 35%. **¹H-NMR:** (400 MHz, CDCl₃) δ (ppm) 7.46-7.38 (m, 4H, Ar-H), 7.04-6.94 (m, 1H, Ar-H), 6.85-6.81 (m, 3H, Ar-H), 6.75-6.69 (m, 2H, Ar-H), 6.60-6.58 (m, 1H, Ar-H), 3.82 (s, 3H), 3.79 (s, 3H), 3.66 (s, 3H), 3.04 (s, 3H), 3.02-2.98 (m, 1H), 2.76-2.69 (m, 1H), 1.40 (s, 3H). **HRMS:** calcd for C₂₆H₂₉NO₅P [M+H]⁺ 466.1783, found 466.1785.

3-((bis(4-(trifluoromethyl)phenyl)phosphoryl)methyl)-1,3-dimethylindolin-2-one, (62m)

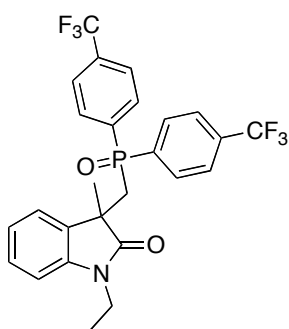


Conditions: (*N*-methyl-*N*-phenylmethacrylamide: 26 mg, 0.15 mmol, 1 equiv.); (*N*-ethoxy-2-methylpyridinium tetrafluoroborate: 68 mg, 0.3 mmol, 2 equiv.); (bis-(4-trifluoromethyl)diphenylphosphine oxide: 100 mg, 0.3 mmol, 2 equiv.); (eosin Y: 4 mg, 0.006 mmol, 0.04 equiv.); (sodium hydrogen carbonate: 15 mg, 0.18 mmol, 1.2 equiv.). The reaction was carried out following the general procedure. The crude product was purified by flash column

chromatography (*n*-pentane:EtOAc 30:70). **Yield:** 75 mg, 99%. **¹H-NMR:** (400 MHz, CDCl₃) δ (ppm) 7.68-7.60 (m, 8H, Ar-H), 7.19-7.16 (m, 1H, Ar-H), 7.03-7.00 (m, 1H, Ar-H), 6.76-6.72 (m, 1H, Ar-H), 6.67-6.65 (m, 1H, Ar-H), 3.23-3.16 (m, 1H), 3.01 (s, 3H), 2.91-2.85 (m, 1H), 1.44 (s, 3H). **¹³C-NMR:** (100 MHz, CDCl₃) δ (ppm) 179.1 (s), 143.1 (s), 138.4 (d, ¹J = 83.3 Hz), 136.5 (d, ¹J = 83.3 Hz), 131.4 (d, ²J = 9.9 Hz), 131.1

(d, $^2J = 9.9$ Hz), 130.9 (d, $^3J = 3.1$ Hz), 128.6 (s), 125.4 (dq, $^4J = 3.7$ Hz, $^2J = 25.7$ Hz), 124.6 (s), 123.6 (dd, $^5J = 5.0$ Hz, $^1J_{CF} = 271.6$ Hz), 123.4 (s), 108.2 (s), 45.4 (d, $^2J = 4.1$ Hz), 37.7 (d, $^1J = 71.1$ Hz), 27.3 (d, $^3J = 14.0$ Hz), 26.5 (s). $^{31}\text{P}\{\text{H}\}$ -NMR: (162 MHz, CDCl_3) δ (ppm) 24.2 (s). $^{19}\text{F}\{\text{H}\}$ -NMR: (376.5 MHz, CDCl_3) δ (ppm) -63.3, -63.2. **HRMS:** calcd for $\text{C}_{25}\text{H}_{21}\text{NO}_2\text{PF}_6$ $[\text{M}+\text{H}]^+$ 512.1219, found 512.1214.

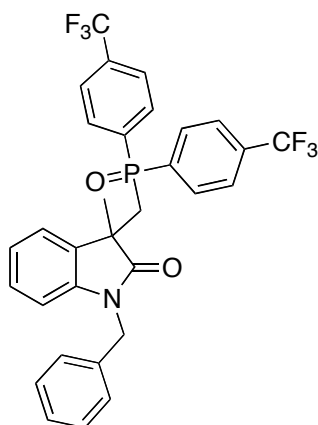
3-((bis(4-(trifluoromethyl)phenyl)phosphoryl)methyl)-1-ethyl-3-methylindolin-2-one, (62n)



Conditions: (*N*-ethyl-*N*-phenylmethacrylamide: 28 mg, 0.15 mmol, 1 equiv.); (*N*-ethoxy-2-methylpyridinium tetrafluoroborate: 66 mg, 0.3 mmol, 2 equiv.); (bis-(4-trifluoromethyl)diphenylphosphine oxide: 100 mg, 0.3 mmol, 2 equiv.); (eosin Y: 4 mg, 0.006 mmol, 0.04 equiv.); (sodium hydrogen carbonate: 215 mg, 0.18 mmol, 1.2 equiv.). The reaction was carried out following the general procedure. The

crude product was purified by flash column chromatography (*n*-pentane:EtOAc:MeOH 30:70:20). **Yield:** 51 mg, 66%. **M_p** = 188°C. ^1H -NMR (400 MHz, CDCl_3) δ (ppm) 7.74-7.66 (m, 4H, Ar-H), 7.64-7.60 (m, 4H, Ar-H), 7.17-7.13 (m, 1H, Ar-H), 6.98-6.97 (m, 1H, Ar-H), 6.72-6.66 (m, 2H, Ar-H), 3.71-3.62 (m, 1H), 3.53-3.42 (m, 1H), 3.19-3.12 (dd, $^2J = 11.0$ Hz, $^2J = 15.2$ Hz, 1H), 2.90-2.84 (dd, $^2J = 11.0$ Hz, $^2J = 15.2$ Hz, 1H), 1.43 (s, 3H), 1.23 (t, $^3J = 7.0$ Hz, 3H). ^{13}C -NMR (100 MHz, CDCl_3) δ (ppm) 178.6 (d, $^3J = 4.1$ Hz), 142.2 (s), 137.2 (d, $^1J = 96.2$ Hz), 136.8 (d, $^1J = 96.4$ Hz), 131.2 (d, $^2J = 10.3$ Hz), 131.0 (d, $^2J = 10.3$ Hz), 128.2 (s), 125.3 (dq, $^4J = 2.9$ Hz, $^2J = 8.3$ Hz), 125.2 (dq, $^4J = 2.8$ Hz, $^2J = 8.5$ Hz), 124.4 (s), 123.7 (d, $^1J = 254.5$ Hz), 123.6 (d, $^1J = 254.6$ Hz), 121.9 (s), 108.2 (s), 45.2 (d, $^4J = 4.3$ Hz), 37.4 (d, $^1J = 73.0$ Hz), 34.8 (s), 27.2 (d, $^3J = 13.7$ Hz), 12.4 (s). ^{31}P -NMR (162 MHz, CDCl_3) δ (ppm) 24.2 (s). ^{19}F -NMR (376.5 MHz, CDCl_3) δ (ppm) -63.3, -63.3. **HRMS:** calcd for $\text{C}_{26}\text{H}_{23}\text{NO}_2\text{PF}_6$ $[\text{M}+\text{H}]^+$ 526.1373, found 526.1371.

1-benzyl-3-((bis(4-(trifluoromethyl)phenyl)phosphoryl)methyl)-3-methylindolin-2-one, (62o)



Conditions: (*N*-benzyl-*N*-phenylmethacrylamide: 37 mg, 0.15 mmol, 1 equiv.); (*N*-ethoxy-2-methylpyridinium tetrafluoroborate: 68 mg, 0.3 mmol, 2 equiv.); (bis-(4-trifluoromethyl)diphenylphosphine oxide: 100 mg, 0.3 mmol, 2 equiv.); (eosin Y: 4 mg, 0.006 mmol, 0.04 equiv.); (sodium hydrogen carbonate: 15 mg, 0.18 mmol, 1.2 equiv.). The reaction was carried out following the general procedure. The crude product was purified by flash column chromatography (*n*-pentane: EtOAc 30:70). **Yield:** 25 mg,

30%. **M_p** = 196-198°C. **¹H-NMR:** (400 MHz, CDCl₃) δ (ppm) 7.98-7.81 (m, 2H, Ar-H), 7.74-7.60 (m, 8H, Ar-H), 7.32-7.29 (m, 3H, Ar-H), 7.05-7.00 (m, 2H, Ar-H), 6.69-6.65 (m, 1H, Ar-H), 6.56-6.54 (m, 1H, Ar-H), 5.10-5.04 (m, 1H), 4.38-4.34 (m, 1H), 3.24-3.18 (m, 1H), 2.97-2.91 (m, 1H), 1.51 (s, 3H). **¹³C-NMR:** (100 MHz, CDCl₃) δ (ppm) 179.3 (d, ³*J* = 4.1 Hz), 142.3 (s), 136.0 (s), 132.3 (d, ³*J* = 11.0 Hz), 131.4 (d, ²*J* = 9.9 Hz), 131.2 (d, ²*J* = 9.9 Hz), 131.0 (s), 129.0 (s), 128.1 (d, ¹*J* = 68.7 Hz), 127.3 (s), 125.5 (dq, ⁴*J* = 4.1 Hz, ²*J* = 26.8 Hz), 124.6 (s), 123.6 (d, ¹*J*_{CF} = 272.0 Hz), 122.4 (s), 109.3 (s), 53.6 (s), 45.5 (d, ²*J* = 3.9 Hz), 44.2 (s), 37.6 (d, ¹*J* = 72.0 Hz), 27.5 (d, ³*J* = 12.9 Hz), 12.5 (s). **³¹P{¹H}-NMR:** (162 MHz, CDCl₃) δ (ppm) 24.4 (s). **¹⁹F{¹H}-NMR:** (376.5 MHz, CDCl₃) δ (ppm) -63.3. **HRMS:** calcd for C₃₁H₂₅NO₂F₆P [M+H]⁺ 588.1528, found 588.1527.

GENERAL CONCLUSIONS

“*Radical chemistry has always taken a backseat to ionic chemistry*”. It was with these words that Phil S. Baran has described the development of radical chemistry during the last decades.¹⁹⁷ Indeed, this research field suffered from the reputation that radical species are highly reactive and thus hardly controllable, which made a large part of organic synthesis community skeptical to employ radical reaction in their synthetic routes.

Although this misconception is still common, the renaissance of the field of visible light photoinduced reactions and especially photoredox catalysis has significantly contributed to improve the image of radical chemistry, which is now used in academia and beyond. This is mainly due to the mild conditions in which numerous radical species can be generated.

The main objective of this work is not only to provide efficient synthetic routes for the synthesis of organophosphorus compounds, but also to understand factors governing those reactions. In this regard, we believe that the combination of mechanistic and synthetic efforts can lead to a deep understanding of this chemistry which will certainly help to develop an efficient synthetic development in this field.

In the first chapter, we attended to help the reader to get an overview of what we consider relevant contributions, in the areas of phosphorus chemistry and visible photoredox catalysis.

The subsequent chapter treats the generation of phosphorus based radicals derived from ethyl and butyl phosphinates and their reactions with unactivated alkenes. Because these radical types have never been generated under photoinduced conditions, we reported in this work an efficient and purely organic route to promote H-phosphinates. Apart from the synthetic importance of these compounds, which can without any doubt be generated *via* other protocols, we have been able to propose a rational mechanism of this reaction. This has been achieved through the combination of different physical organic tools. Firstly, we showed the ability of Fukuzumi photocatalyst to reduce diphenyliodonium (the oxidant) in order to form phenyl radical, which has been characterized by EPR spectroscopy. Further information came also from Fluorescence quenching and photolysis experiments which supported this hypothesis. The intriguing use of toluene as a co-solvent has been deciphered by an independent controlling

¹⁹⁷ Yan, M.; Lo, J. C.; Edwards, J. T.; Baran, P. S. *J. Am. Chem. Soc.* **2016**, *138*, 12692-12741.

experiment, where we showed that the association of the acridinium salt with diphenyliodonium in toluene in the presence of O₂ under blue irradiation leads to the formation of benzaldehyde. This shows the powerful of radical cation form of acridinium salt to oxidize an inert solvent such as toluene. This serendipitous result opens a new avenue in the field of photoredox catalysis because one can now access to highly reactive intermediates *via* the high oxidative potential of Acr^{•+}/Acr. The CALIPSO group is now working to explore further this chemistry.

In the third chapter, we employed another powerful physical organic concept to generate phosphorus radicals. This concept, which has been introduced by Mulliken many decades again postulates that bringing a very well selected electron donor and acceptor components can lead to the formation of what is called electron donor-acceptor complex. This complex is typically colored and can then be excited by visible light to promote SET events. In this context, we questioned whether diphenyliodonium ion can form EDA-complex when it is combined with secondary phosphine oxides.

A joint experimental and theoretical efforts permitted to confirm this hypothesis. Indeed, EPR spectroscopy showed the formation of phenyl and phosphinoyl radicals when Ph₂I⁺ and Ph₂P(O)H are illuminated with blue light. In addition, DFT and TD-DFT calculations showed that the lone pair of phosphorus atom of phosphinous acids interacts with Ph₂I⁺ to form a EDA-complex that is visible light active. When this complex is irradiated, it gives phenyl radical that is a key intermediate to promote the generation of phosphorus radical. As a proof of concept, we applied this approach to hydrophosphination reaction. Interestingly, the reaction works smoothly and has a broad scope. This approach is now used in the laboratory for the synthesis of other phosphorus-based molecules.

The last chapter of this thesis is dedicated to the synthesis of phosphorylated oxindoles through the use of an effective photoredox-mediated tandem phosphorylation/cyclisation of secondary phosphine oxides with acrylamides. Based in previous discovery in the group, we showed that the association of Eosin Y as a photocatalyst and *N*-ethoxypyridinium as an oxidant leads to the formation of a charge transfer complex that become the driving force of the photoredox process. This complex enables efficient generation of the ethoxy radical and thus the phosphinoyl radical. By employing this approach, a large panel of oxindoles has been synthesized under mild

conditions. Because many of these molecules are biologically active, the development of a sustainable method for their synthesis should attract the attention of researchers active in academia and industry as well.

In summary, this thesis provides three complementary approaches for the generation of phosphorus-based radicals. These species have been characterized and used for the synthesis of phosphorus-based molecules.

Giovanni Fausti

☎: +33 782 07 58 21

Permis de conduire B

✉ giovanni.fausti23@gmail.com - Skype: giovafausti



Nationalité: Italienne, **Date de naissance** 23/12/1988, Polla (SA).

Expérience professionnelle

Février 2017 – Present

CRA Trainee - QuintilesIMS

Formation d'attaché de recherche clinique chez QuintilesIMS, Dublin – Saint-Ouen, Paris.

Formation

Novembre 2016-Février 2017

Master Professionnel de Management Pharmaceutique: Marketing, Market Access et Vente

Pharmaceutical Marketing - Pharmaceutical Sales - Coaching and Team managing - Clinical data - Market Access - Regulatory Affairs – Leadership – Direct and Full Costing
Istum, Institut des Etudes de Management, Milan, Italie.
<http://www.istum.it/>

Janvier 2014-Décembre 2016

Doctorat de Chimie Organique

Encadrants: Prof. Annie-Claude Gaumont et Dr. Sami Lakhdar.

Normandie Université, LCMT, ENSICAEN, UNICAEN,
CNRS, 14000-France.

Développement de nouvelles méthodes photocatalytiques pour les synthèses de molécules organiques fonctionnalisées.

Décembre 2014

Diplôme d'Etat de Pharmacien.

Obtention de la License de pharmacien et membre de la Société Italienne de Pharmaciens.

2008-2013

Master de Chimie et Technologie Pharmaceutique.

“Selective Synthesis of α and γ Carbolines: Versatile Intermediates for Medicinal Chemistry and New Materials”. Encadrant: Prof. Stefano Menichetti.

Université de Florence, Viale G. Pieraccini, 24, 50139, Florence.

Mai 2013-Juillet 2013

Programme d'échange inter-universitaire (ERASMUS).

“Synthesis of racemic and enantioenriched alkynylphosphine-boranes by copper-catalysis”.

Encadrants: Prof. Annie-Claude Gaumont et Dr. Carole Alayrac-Witulski.
Normandie Université, LCMT, ENSICAEN, UNICAEN, CNRS, 14000-France.

2001-2008

License de Flûte Traversière.

Conservatoire “Lorenzo Perosi” de Campobasso, Italie.

Parcours et Communications Scientifiques

Septembre 2016

Journées Scientifiques SynOrg, Rouen, Normandie, France

Communication oral: “Visible Light Mediated C-P Bond Forming Reactions”

Septembre 2016

6th EuCheMS Chemistry Congress, Seville, Espagne.

Communication oral: “Visible Light Mediated Hydrophosphinylation of Alkenes with Phosphinic Acid Derivatives: Synthetic and Mechanistic Investigations”

Juin 2016

Journée de l’Ecole Doctorale Normande de Chimie, JEDNC, Caen, Normandie, France.

Membre du comité d’organisation du congrès, communication oral et présentation d’un poster: “Visible Light Mediated Hydrophosphinylation of Alkenes with Phosphinic Acid Derivatives: Synthetic and Mechanistic Investigations”

Juin 2015

ICHAC-11, 11th International Conference on Heteroatom Chemistry, Caen, Normandie.

Membre du comité d’organisation du congrès, présentation d’un poster: “Metal-Free Photoredox Hydrophosphinylation of Alkenes with Phosphinic Acid Derivatives: Scope and Limitations”

Mai 2015

Journées Nord-Ouest Européennes des Jeunes Chercheurs 2015 Normandie.

Communication orale: “C-P bond Formation Via Metal-Free Hydrofunctionalizations to Afford Phosphorylated Olefins”

Octobre 2012-Novembre 2013

Stage de recherche en laboratoire de chimie organique.

Université de Florence, Pôle Scientifique de Sesto Fiorentino, Via della Lastruccia, 3.

“Synthesis of nitrogen-based heterocycles with applications in the field of photovoltaics.”

Publications Scientifiques

Novembre 2016

How Do Phosphinates React with Unactivated Alkenes Under Organic Photocatalyzed Conditions? Substrate Scope and Mechanistic Insights

CHEMISTRY – A EUROPEAN JOURNAL

DOI: 10.1002/chem.201604683

Langues et Informatiques

Langues	Italien, Anglais (Avancé, orale et écrit), Espagnol (Avancé, oral et écrit) et Français (Avancé, oral et écrit).
Systèmes d'exploitation	WINDOWS, MAC OS
Programmes	Pack Office, Adobe suite Reader, ChemDraw, TopSpin.
Web	Réseaux sociaux (Facebook, LinkedIn, Twitter)

Compétences Personnelles

- Travail d'équipe.
- Capacité à résoudre des problèmes.
- Sens de l'organisation
- Forte motivation.

Activités Culturelles et Sportifs

- ✓ Ski alpin
- ✓ Cyclisme
- ✓ Course à pied
- ✓ Football
- ✓ Musique et lecture.

Autorisation du traitement des données personnelles.

How Do Phosphinates React with Unactivated Alkenes Under Organic Photocatalyzed Conditions? Substrate Scope and Mechanistic Insights

Giovanni Fausti,^[a] Fabrice Morlet-Savary,^[b] Jacques Lalevée,^[b] Annie-Claude Gaumont,^[a] and Sami Lakhdar^{*[a]}

Dedicated to the memory of Abdelkader Khemiss

Abstract: The first visible-light-mediated, metal-free hydrophosphinylation of unactivated alkenes with ethyl and butyl phosphinates is described. The reaction works with a low catalyst loading of 9-mesityl-10-methylacridinium perchlorate (Fukuzumi photocatalyst, 0.5 mol%) in the presence of

diphenyliodonium triflate as oxidant. The reaction proceeds smoothly and covers a broad scope of substrates. Detailed mechanistic investigations, including EPR spectroscopy, fluorescence and steady-state photolysis, allowed the mechanism of this photoreaction to be rationalized.

Introduction

Trichlorophosphine (PCl_3) is a cornerstone in phosphorus chemistry from which a large variety of organophosphorus compounds can be synthesized.^[1] However, because significant environmental risks are involved in its preparation, intensive academic and industrial research has focused on identifying PCl_3 surrogates. In this context, phosphinates ($\text{H}_2\text{P(O)OR}$), which are nontoxic and typically produced on a huge industrial scale, have recently emerged as sustainable alternatives to PCl_3 .^[2] This chemistry has extensively been studied by Montchamp et al, who developed elegant methodologies for efficient and selective P–H functionalization of phosphinates and related compounds over the last decade.^[3] For instance, hydrophosphinylation of unactivated alkenes has attracted much attention, as it allows atom-economic access to *H*-phosphinates, which are relevant compounds in pharmaceutical and materials sciences.^[1] In this context, it has been shown that this reaction can be accomplished through transition-metal catalysis or radical activation.^[4] Nevertheless, despite the efficiency of these approaches in terms of reaction yields and chemoselectivity, the use of metals, ligands, and the require-

ment for relatively high temperature raise the need for developing milder processes.

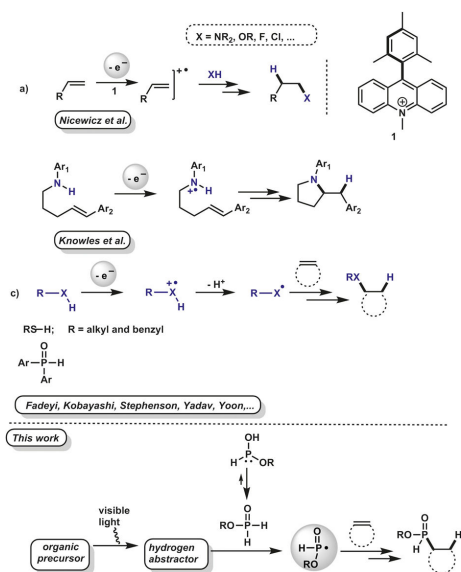
For this purpose, we envisaged using visible-light photoredox catalysis, which has been shown to be a sustainable and efficient approach for the generation of open-shell species.^[5] This technology has previously been applied for various hydrofunctionalizations of alkenes by using the three approaches outlined in Scheme 1.^[6] In the first approach, Nicewicz et al. took advantage of the high reduction potential of the excited state of acridinium salt **1** ($E^* = +2.06$ V vs. SCE) to oxidize a large variety of alkenes, which can then react with numerous nucleophiles (Scheme 1 a).^[6,7] Knowles et al. developed a complementary approach for intramolecular amination. Their concept consists of oxidizing the nitrogen center by an iridium-based photocatalyst to form an aminium radical cation, which then undergoes reduction and proton transfer to yield the desired product (Scheme 1 b).^[8] The third approach, known as “smart initiation technology”,^[9] relies on the use of a visible-light photoredox reaction to promote the initiation step of a classical radical chain process (Scheme 1 c).^[10]

Because phosphinates ($\text{H}_2\text{P(O)OR}$) are known to exist predominantly in their P^{V} form ($K \approx 10^{-8}$),^[11] none of the strategies described above would be compatible with the hydrophosphinylation of alkenes, because the P^{III} lone pair is not available. To circumvent this issue, we hypothesized that the use of an external organic oxidant that forms a highly reactive radical under photoredox conditions would be capable of abstracting a hydrogen atom from secondary P^{V} species to form the corresponding phosphinoyl radical.^[12] In this context, we selected diphenyliodonium salt **2**, which is known to generate the highly reactive phenyl radical under visible-light photoredox conditions and is capable of abstracting PH hydrogen atoms from phosphinates.^[13] This reaction is expected to be thermodynamically feasible, as redox potentials of excited states of

[a] G. Fausti, Prof. A.-C. Gaumont, Dr. S. Lakhdar
Normandie Univ., LCMT, ENSICAEN, UNICAEN, CNRS
6, Boulevard Maréchal Juin, Caen, 14000 (France)
E-mail: sami.lakhdar@ensicaen.fr

[b] Dr. F. Morlet-Savary, Prof. J. Lalevée
Institut de Science des Matériaux de Mulhouse
IS2M-UMR CNRS 7361-UHA
15, rue Jean Starcky, 68057 Mulhouse Cedex (France)

Supporting information and the ORCID identification number(s) for the author(s) of this article can be found under <http://dx.doi.org/10.1002/chem.201604683>.



Scheme 1. Common visible-light-photocatalyzed hydrofunctionalization (previous work) and hydrophosphinylation (this work) of activated alkenes.

common organic photocatalysts^[14,6] can easily reduce **2** ($E^\circ = -0.2$ V/SCE).^[15]

Results and Discussion

To test the above hypothesis, we investigated the hydrophosphinylation of ethyl phosphinate (**3a**) with cyclohexene (**4a**) in the presence of diphenyliodonium triflate (**2**)^[16] and various photocatalysts under visible-light irradiation (Table 1). Ethyl phosphinate was prepared by a previously described method and was used as a 0.5 M stock solution in toluene.^[3] The oxidant loading was first evaluated, and 0.5 equiv of **2** was found to be optimal (see Figure S2, Supporting Information).

As shown in Table 1, the reaction strongly depends on the nature of the organic photocatalyst. For instance, while a moderate conversion of **5a** was obtained with Rhodamine B (40%; Table 1, entry 2), a trace of **5a** or no conversion was observed with common organic dyes (Table 1, entries 1, 3, 4, and 5). In contrast, the photocatalyst 9-mesityl-10-methylacridinium perchlorate (**1**), which is well known to be highly efficient in reductive quenching cycles,^[5g,6,17] was found to be effective in a presumably oxidative cycle furnishing **5a** in 84% conversion (Table 1, entry 6). Remarkably, this high conversion was achieved with a very low catalyst loading (0.5 mol%).

Screening of solvents showed that the photoreaction proceeded in toluene (Table 1, entry 8, 55%) and DMF/toluene (1:1) (Table 1, entry 6, 84%), whereas it did not take place in acetonitrile (Table 1, entry 7) or methanol (Table 1, entry 9).

Table 1. Identification of the optimal reaction conditions.

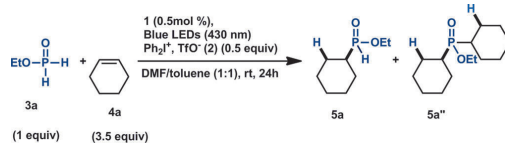
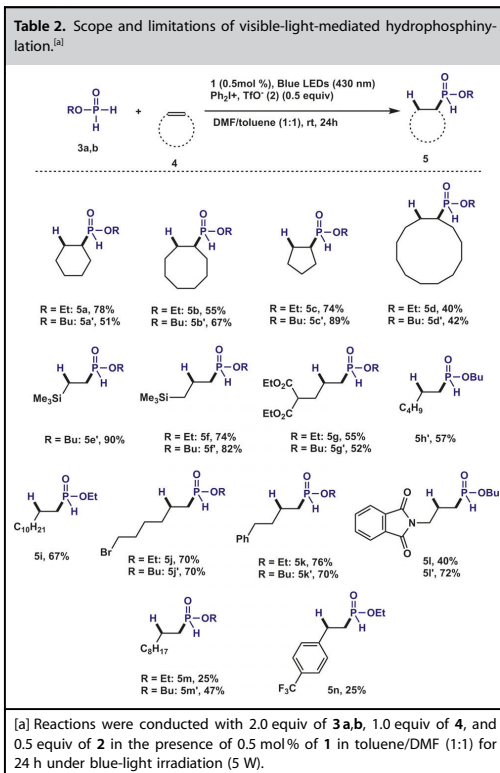
Entry	Photocatalyst	Solvent	Conversion [%] ^[k]
1	Eosin Y ^[a]	DMF/Tol ^[d]	0 ^[e]
2	Rhodamine B ^[a]	DMF/Tol ^[d]	40 ^[e]
3	Fluorescein ^[a]	DMF/Tol ^[d]	≈ 2 ^[f]
4	Methylene Blue ^[b]	DMF/Tol ^[d]	0 ^[f]
5	Rose Bengal ^[b]	DMF/Tol ^[d]	0 ^[e]
6	acridinium salt 1 ^[c]	DMF/Tol ^[d]	84 ^[f]
7	acridinium salt 1 ^[c]	Acetonitrile	0 ^[f]
8	acridinium salt 1 ^[c]	Toluene	55 ^[f]
9	acridinium salt 1 ^[c]	methanol	0 ^[f]
10	acridinium salt 1 ^[c]	DMF/Tol ^[d]	≤ 1 ^[g]
11	acridinium salt 1 ^[c]	DMF/Tol ^[d]	≤ 1 ^[h]
12	–	DMF/Tol ^[d]	18 ^[i]
13	acridinium salt 1 ^[c]	DMF/Tol ^[d]	50 ^[j]

[a] 3 mol% of the photocatalyst. [b] 5 mol% of the photocatalyst. [c] 0.5 mol% of the photocatalyst. [d] DMF/toluene (1:1). [e] Green LEDs (5 W). [f] Blue LEDs (5 W). [g] Without light. [h] Without oxidant. [i] Without photocatalyst and after 72 h. [j] With cutoff UV filter (NaNO₂ solution in water). [k] Derived from ³¹P NMR spectra on integration of all formed species.

Control experiments revealed the essential role of light (Table 1, entry 10) and the oxidant (Table 1, entry 11), as only traces of **5a** were detected in their absence. The photocatalyst was found to be essential for this photoreaction, even though 18% conversion was observed after a long reaction time (72 h, Table 1, entry 12). To exclude possible involvement of UV light, we irradiated the sample through a UV filter (75% w/v NaNO₂ solution, cut-off: $\lambda = 400$ nm). The fair conversion (50%, Table 1, entry 13) of **5a** that was observed thus attests that the reaction is visible-light-mediated. It is noteworthy that our photoreaction does not require inert conditions or degassed solvents (see Supporting Information).

After identifying the optimal reaction parameters, we turned our attention to studying the scope of the reaction with respect to alkenes **5a–n** (Table 2). Fair to good yields, ranging from 50 to 78%, were obtained for the reactions of **3a** with alkenes **4a–d**, **4f,g**, and **4i–n**. The reactions proceed regioselectively, as only anti-Markovnikov adducts were observed in all tested cases. More importantly, the reaction is chemoselective and leads to the exclusive formation of the monosubstituted *H*-phosphinate ester **5**. When an excess of **4a** (3.5 equiv) was combined with *H*-phosphinate **3a** (1 equiv) in the presence of diphenyliodonium triflate (0.5 equiv) under blue irradiation, the bis-addition product **5a''** was detected in a moderate conversion (25%) along with the mono-adduct **5a** (Scheme 2).

As shown in Table 2, the reaction proceeds well with both cyclic **4a–d** and noncyclic **4f,g** and tolerates functional groups such as ester and bromide (**4g** and **4j**, respectively). Though the conversions to phosphinates **5l** and **5n** were higher than 50%, as judged by ³¹P NMR spectroscopy, the yields of isolated



Scheme 2. Reaction of **3a** (1 equiv) with an excess of **4a** (3.5 equiv) in the presence of diphenyliodonium triflate (0.5 equiv) under photoredox conditions.

products dropped significantly to 40 and 25%, respectively. This is presumably due to the sensitivity of *H*-phosphinate esters during the purification process on silica gel.^[4] Unfortunately, our photoredox approach was found to be incompatible with alkynes such as phenylacetylene or diphenylacetylene, as only low ³¹P NMR conversions (around 10 and ≤ 1%, respectively) were detected after a long irradiation time (72 h).

When butyl hypophosphite **3b** was combined with unactivated alkenes (Table 2) under the optimized reaction conditions, the desired adducts **5a'–h'** and **5j'–5m'** were isolated in yields ranging from 47 to 90%. In agreement with previous observations,^[4] yields of isolated butyl phosphinates

5' were higher than those of ethyl phosphinates **5**, clearly due to their higher stability.

To get insights into the mechanism of this visible-light-mediated reaction, mechanistic studies were undertaken. First, quenching fluorescence experiments on the reaction of acridinium salt **1** with diphenyliodonium triflate (**2**) were performed.^[18] A decrease of the emission peak of **1** at 530 nm was observed when different concentrations of **2** were added to **1** in acetonitrile at room temperature (Figure 1). The resulting Stern–Volmer plot yielded a quenching rate of $k_q = 3.2 \times 10^6 \text{ M}^{-1} \text{ s}^{-1}$, consistent with our initial hypothesis that diphenyliodonium salt **2** is reduced by the excited state of photocatalyst **1**.^[19]

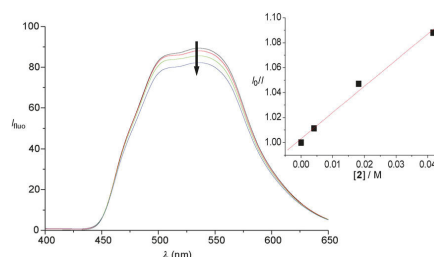


Figure 1. Fluorescence spectra ($\lambda_{\text{ex}} = 530 \text{ nm}$) of acetonitrile solutions of *N*-methyl-9-mesitylacridinium photocatalyst (**1**) ($5 \times 10^{-6} \text{ M}$) containing increasing concentrations of iodonium triflate at 20 °C. Inset: Stern–Volmer quenching plot of photocatalyst **1** in dependence on the concentration of the iodonium salt **2**.

Additional evidence for the reaction of **1*** with **2** comes from the steady-state photolysis of **1** and **2** (Figure 2), which shows an increase of the UV/Vis absorbance above 400 nm when **2** is added to **1** under blue-light irradiation ($\lambda = 430 \text{ nm}$).

To prove the intermediacy of the phenyl radical **6**, EPR experiments on the reaction of diphenyl iodonium salt **2** with photocatalyst **1** in the presence of α -phenyl-*N*-*tert*-butylnitrene

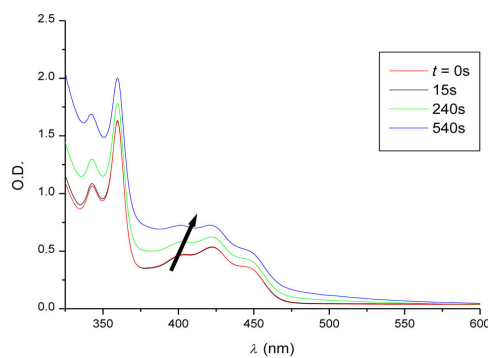


Figure 2. Photolysis of acetonitrile solutions of photocatalyst **1** with diphenyliodonium compound **2** on irradiation (LED at $\lambda_{\text{max}} = 420 \text{ nm}$; from $t = 0$ to 540 s).

(PBN, **7**) as a radical trap were carried out in *tert*-butylbenzene at room temperature. When this mixture was irradiated with blue light ($\lambda = 420$ nm), clean formation of spin adduct **8** was observed (Scheme 3). The hyperfine coupling constants of **8** ($a_N = 14.4$ G and $a_H = 2.2$ G) are in perfect accordance with those reported in the literature (Figure 3).^[20] This strongly supports the formation of the phenyl radical through the reduction of **2** by the excited state of the photocatalyst **1***.

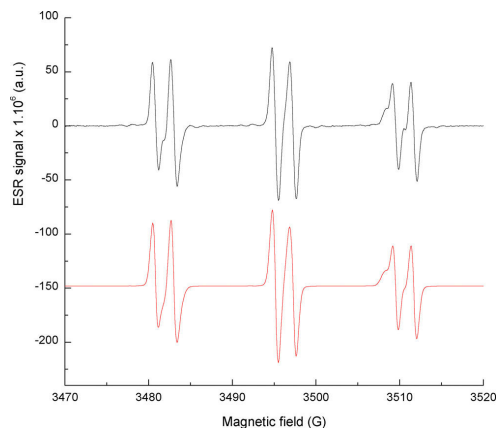
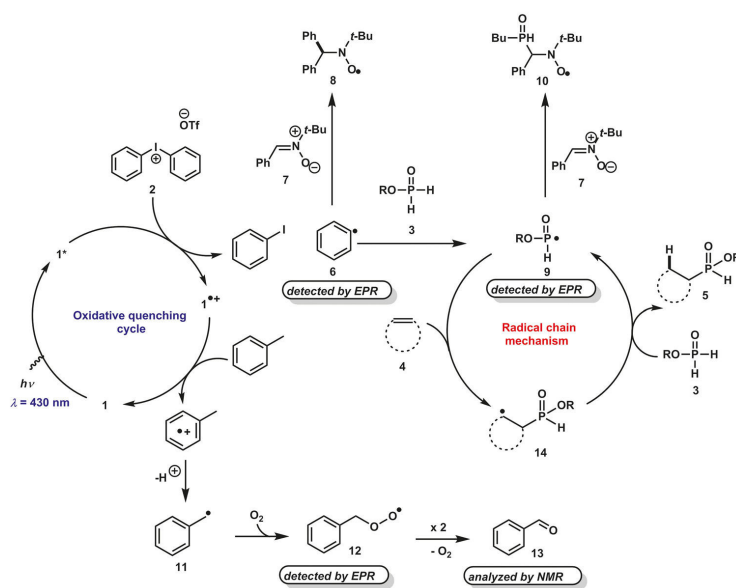


Figure 3. EPR spin-trapping spectra resulting on irradiation ($\lambda = 420$ nm) of 1/2 solution in the presence PBN (**7**) in toluene at room temperature.

The addition of a toluene solution of butyl phosphinate **3b** to this mixture gave a more complex EPR spectrum (Figure S5, Supporting Information, page S17). The simulation of these data indicated the presence of the remaining phenyl radical along with a phosphorus- and an oxygen-centered radicals. While the hyperfine coupling constants of the phosphorus species ($a_N = 15.2$ G, $a_{H1} = 3.3$ G, $a_{H2} = 1.6$ G, and $a_P = 14.3$ G) are consistent with the PBN–phosphinoyl adduct **10**, it was more difficult to assign the structure of the oxygen radical species. However, as the formation of the latter can be due to the presence of residual air in the solvent, we carried out the reaction of diphenyliodonium ion **2** with photocatalyst **1** in toluene under blue-light irradiation and in the presence of O_2 . Interestingly, the 1H NMR spectrum of this mixture revealed the formation of benzaldehyde (**13**). This hypothesis is supported by a recent report of Lei et al., who showed that acridinium salt **1** can catalyze the oxidation of toluene to benzaldehyde in acidic medium in the presence of O_2 .^[21] Importantly, the reaction did not occur in the absence of O_2 , as only diphenyliodonium salt was recovered after 24 h of blue illumination ($\lambda = 420$ nm). Consequently, we postulated that the oxygen-centered radical observed by EPR spectroscopy is the benzo-peroxyl radical **12** ($a_N = 13.7$ G and $a_H = 2.0$ G). Furthermore, the quantum yield of the reaction, which was determined to be $\Phi = 22$, indicates a radical chain process.^[18]

The mechanistic details of the visible-light-mediated hydrophosphinylation reaction are outlined in Scheme 3. The reaction starts with excitation of **1** by blue light to generate **1***, which reduces diphenyliodonium salt **2** to phenyl radical **8**,



Scheme 3. Proposed mechanism for the visible-light-mediated hydrophosphinylation of phosphinates **3a,b** with terminal unactivated alkenes **4** in the presence of 9-mesityl-10-methylacridinium perchlorate (**1**) as photocatalyst.

which abstracts a hydrogen atom from phosphinate **3** to form phosphinoyl radical **9**. This radical adds to alkene **4** to form the carbon-centered radical **14**, which abstracts a hydrogen atom of **3** to yield the hydrophosphinylated adduct **5** and regenerate the phosphinoyl radical **9**. To close the photocatalytic cycle, we assume that toluene donates an electron to the oxidized form of the photocatalyst 1^{*+} to generate the benzyl radical **11** on fast deprotonation. The latter reacts with O_2 , present in the medium, to afford peroxy radical **12**, which is subsequently converted to benzaldehyde **13**.

Conclusion

We have reported the first visible-light, metal-free hydrophosphinylation of ethyl and butyl phosphinates with unactivated alkenes. The reaction proceeds smoothly with perfect regio- and chemoselectivity. The proposed mechanism has been supported by fluorescence, steady-state photolysis, and EPR spectroscopy. Given the importance of phosphinates in various area of chemistry, this mild approach for the generation of phosphinoyl radicals should pave the way to the development of synthetically useful transformations.

Acknowledgements

The authors thank the CNRS, Normandie Université, EU support through FEDER funding, and Labex Synorg (ANR-11-LABX-0029) for financial support.

Keywords: hydrophosphinylation · phosphinates · photochemistry · radical reactions · reaction mechanisms

- [1] a) L. D. Quin, *A Guide to Organophosphorus Chemistry*, Wiley, Hoboken, **2000**; b) J.-L. Montchamp, *Phosphorus Sulfur Silicon Relat. Elem.* **2013**, *188*, 66–75.
 [2] For an excellent review, see: J.-L. Montchamp, *Acc. Chem. Res.* **2014**, *47*, 77–87.
 [3] For selected examples see: a) S. Deprère, J.-L. Montchamp, *J. Org. Chem.* **2001**, *66*, 6745–6755; b) S. Deprère, J.-L. Montchamp, *Org. Lett.* **2004**, *6*, 3805–3808.
 [4] For transition metal catalyzed hydrophosphinylation reactions, see: a) S. Deprère, J.-L. Montchamp, *J. Am. Chem. Soc.* **2002**, *124*, 9386–9387; b) P. Ribière, K. Bravo-Altamirano, M. I. Antczak, J. D. Hawkins, J.-L. Montchamp, *J. Org. Chem.* **2005**, *70*, 4064–4072; c) S. Ortial, H. C. Fisher, J.-L. Montchamp, *J. Org. Chem.* **2013**, *78*, 6599–6608; For radical promoted hydrophosphinylation of alkenes, see: d) M. I. Antczak, J.-L. Montchamp, *Synthesis* **2006**, 3080–3084; e) P. Troupa, P. G. Katsioulari, S. Vassiliou, *Synlett* **2015**, 2714–2719.
 [5] For selected examples, see: a) K. Zeitler, *Angew. Chem. Int. Ed.* **2009**, *48*, 9785–9789; *Angew. Chem.* **2009**, *121*, 9969–9974; b) T. P. Yoon, M. A. Ischay, J. Du, *Nat. Chem.* **2010**, *2*, 527–532; c) J. Xuan, W.-J. Xiao, *Angew. Chem. Int. Ed.* **2012**, *51*, 6828–6838; *Angew. Chem.* **2012**, *124*, 6934–

- 6944; d) L. Shi, W.-J. Xia, *Chem. Soc. Rev.* **2012**, *41*, 7687–7697; e) C. K. Prier, D. A. Rankic, D. W. C. MacMillan, *Chem. Rev.* **2013**, *113*, 5322–5363; f) J. W. Beatty, C. R. J. Stephenson, *Acc. Chem. Res.* **2015**, *48*, 1474–1484; g) N. A. Romero, D. A. Nicewicz, *Chem. Rev.* **2016**, *116*, 10075–10166.
 [6] For a recent review, see: K. A. Margrey, D. A. Nicewicz, *Acc. Chem. Res.* **2016**, *49*, 1997–2006.
 [7] For selected examples of 1-photocatalyzed hydrofunctionalization reactions, see: a) D. S. Hamilton, D. A. Nicewicz, *J. Am. Chem. Soc.* **2012**, *134*, 18577–18580; b) A. J. Perkowski, D. A. Nicewicz, *J. Am. Chem. Soc.* **2013**, *135*, 10334–10337; c) T. M. Nguyen, D. A. Nicewicz, *J. Am. Chem. Soc.* **2013**, *135*, 9588–9591.
 [8] A. J. Musacchio, L. Q. Nguyen, G. H. Beard, R. R. Knowles, *J. Am. Chem. Soc.* **2014**, *136*, 12217–12220.
 [9] The concept of smart initiation has recently been introduced by Curran and Studer: A. Studer, D. P. Curran, *Angew. Chem. Int. Ed.* **2016**, *55*, 58–102; *Angew. Chem.* **2016**, *128*, 58–106.
 [10] a) E. L. Tyson, M. S. Ament, T. P. Yoon, *J. Org. Chem.* **2013**, *78*, 2046–2050; b) M. H. Keylor, J. E. Park, C.-J. Wallentin, C. R. J. Stephenson, *Tetrahedron* **2014**, *70*, 4264–4269; c) W.-J. Yoo, S. Kobayashi, *Green Chem.* **2014**, *16*, 2438–2442; d) T. Keshari, V. K. Yadav, V. P. Srivastava, L. D. S. Yadav, *Green Chem.* **2014**, *16*, 3986–3992; e) O. O. Fadeyi, J. J. Mousseau, Y. Feng, C. Allais, P. Nuhant, M. Z. Chen, B. Pierce, R. Robinson, *Org. Lett.* **2015**, *17*, 5756–5759.
 [11] B. G. Janesko, H. C. Fisher, M. J. Bridle, J.-L. Montchamp, *J. Org. Chem.* **2015**, *80*, 10025–10032 and references therein.
 [12] Selected examples of the generation of phosphorus-centered radicals by photoredox catalysis: a) J. Xuan, T.-T. Zeng, J.-R. Chen, L.-Q. Lu, W.-J. Xiao, *Chem-Eur. J.* **2015**, *21*, 4962–4965; b) V. Quint, F. Morlet-Savary, J.-F. Lohier, J. Lalevée, A.-C. Gaumont, S. Lakhdar, *J. Am. Chem. Soc.* **2016**, *138*, 7436–7441; c) P. Peng, L. Peng, G. Y. Wang, F. Y. Wang, Y. Luo, A. W. Lei, *Org. Chem. Front.* **2016**, *3*, 749–752.
 [13] E. Ay, Z. Raad, O. Dautel, F. Dumur, G. Wantz, D. Gignes, J.-P. Fouassier, J. Lalevée, *Macromolecules* **2016**, *49*, 2124–2134.
 [14] D. A. Nicewicz, T. M. Nguyen, *ACS Catal.* **2014**, *4*, 355–360.
 [15] J.-P. Fouassier, J. Lalevée, *Photoinitiators for Polymer Synthesis: Scope, Reactivity and Efficiency*, Wiley-VCH, Weinheim, **2012**.
 [16] Our choice of diphenyliodonium triflate as an oxidant was based on its low toxicity facile preparation, and high stability: E. A. Merritt, B. Olofsson, *Angew. Chem. Int. Ed.* **2009**, *48*, 9052–9070; *Angew. Chem.* **2009**, *121*, 9214–9234.
 [17] For a recent review on the use of the acridinium salt **1** in photocatalysis, see: S. Fukuzumi, K. Ohkubo, T. Suenobu, *Acc. Chem. Res.* **2014**, *47*, 1455–1464.
 [18] For recent reviews on mechanistic studies of visible-light photoredox reactions, see: a) S. P. Pitre, Ch. D. McTiernan, J. C. Scaiano, *Acc. Chem. Res.* **2016**, *49*, 1320–1330; b) M. A. Cismesia, T. P. Yoon, *Chem. Sci.* **2015**, *6*, 5426–5434.
 [19] The reduction potential E_{red} of **1**^{*} was determined by Fukuzumi et al. to be -0.57 V: H. Kotani, K. Ohkubo, S. Fukuzumi, *J. Am. Chem. Soc.* **2004**, *126*, 15999–16006.
 [20] J. Lalevée, F. Dumur, C. R. Mayer, D. Gignes, G. Nasr, M.-A. Tehfe, S. Téletel, F. Morlet-Savary, B. Graff, J.-P. Fouassier, *Macromolecules* **2012**, *45*, 4134–4141.
 [21] L. Zhang, H. Yi, W. Jue, A. Lei, *Green. Chem.* **2016**, *18*, 5122–5126.

Manuscript received: October 5, 2016

Accepted Article published: November 14, 2016

Final Article published: ■■■■■ 0000

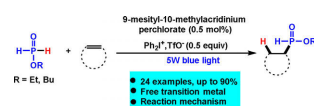
FULL PAPER

Hydrophosphinylation

G. Fausti, F. Morlet-Savary, J. Lalevée,
A.-C. Gaumont, S. Lakhdar*



How Do Phosphinates React with Unactivated Alkenes Under Organic Photocatalyzed Conditions? Substrate Scope and Mechanistic Insights



When visible light meets *H*-phosphinates: Efficient C–P bond-formation reactions of two *H*-phosphinates with unactivated alkenes was achieved by visible-light irradiation under metal-free conditions (see scheme). The scope and limitations of this approach were investigated, and a detailed mechanistic study was carried out.